

Grain boundaries in high- T_c superconductors

H. Hilgenkamp

*Low Temperature Division, Applied Physics Department and MESA+Institute,
University of Twente, P.O. Box 217, 7500 AE Enschede, The Netherlands*

J. Mannhart

*Experimentalphysik VI, Center for Electronic Correlations and Magnetism,
Institute of Physics, Augsburg University, 86135 Augsburg, Germany*

(Published 17 May 2002)

Since the first days of high- T_c superconductivity, the materials science and the physics of grain boundaries in superconducting compounds have developed into fascinating fields of research. Unique electronic properties, different from those of the grain boundaries in conventional metallic superconductors, have made grain boundaries formed by high- T_c cuprates important tools for basic science. They are moreover a key issue for electronic and large-scale applications of high- T_c superconductivity. The aim of this review is to give a summary of this broad and dynamic field. Starting with an introduction to grain boundaries and a discussion of the techniques established to prepare them individually and in a well-defined manner, the authors present their structure and transport properties. These provide the basis for a survey of the theoretical models developed to describe grain-boundary behavior. Following these discussions, the enormous impact of grain boundaries on fundamental studies is reviewed, as well as high-power and electronic device applications.

CONTENTS

I. Introduction	485	IX. Irradiation of Grain Boundaries	518
II. Introduction to Grain Boundaries	486	A. Irradiation with electrons	518
III. Preparation of Single Grain Boundaries	488	B. Irradiation with light	518
A. Bicrystalline junctions	489	C. Irradiation with ions	519
B. Biepitaxial junctions	489	X. Bulk Applications	519
C. Step-edge junctions	491	A. Powder-in-tube method	520
IV. Structural Properties	491	B. Coated conductors	520
V. Transport Properties of Grain Boundaries	496	XI. Applications of Grain Boundaries in Thin Films	522
A. Current-voltage characteristics	496	A. SQUIDs	522
B. Critical current density	498	B. Radiation detectors and spectrometers	524
1. Dependence on grain-boundary angle	498	C. Three-terminal devices	525
2. Temperature dependence of the critical currents	502	D. Superconducting logic circuits	526
3. Magnetic-field dependence of the critical currents	502	E. Research devices	526
C. Current-phase relation	504	XII. Summary and Outlook	528
D. Normal-state resistivity	504	Acknowledgments	529
E. The $I_c R_n$ product	505	References	529
F. Grain-boundary capacitance	506		
G. Microwave properties	507		
H. Grain-boundary noise	507		
I. Self-generated magnetic flux	509		
J. Penetration of magnetic flux into grain boundaries	510		
VI. Effects of Doping	510		
VII. Grain-Boundary Mechanisms	511		
A. Mechanisms based on structural properties	511		
B. Mechanisms based on deviations from ideal stoichiometry	512		
C. Order-parameter symmetry-based mechanisms	514		
D. Interface charging and band bending	515		
E. Mechanisms based on direct suppression of the pairing mechanism	516		
VIII. Control of Grain Boundaries with Electric Fields or Quasiparticle Injection	517		
A. Applied electric fields	517		
B. Quasiparticle injection	518		

I. INTRODUCTION

After the enthusiasm following the discovery of high- T_c superconductivity, it was realized that applications of these materials are exceedingly difficult to achieve. The reasons for these difficulties are rooted in the fundamental physics of high- T_c superconductors, which directly determines the properties of interfaces in these compounds: the ultrashort coherence length of a few angstroms seemed to preclude the realization of high-quality Josephson junctions, and the small critical current density J_c of polycrystalline samples, a few hundred A/cm² at 4.2 K, apparently ruled out the fabrication of useful high- T_c wires.

The properties of polycrystalline high- T_c superconductors are influenced in a complex manner by a large variety of interfaces, such as grain or twin boundaries (see Fig. 1). To understand the behavior of bulk poly-

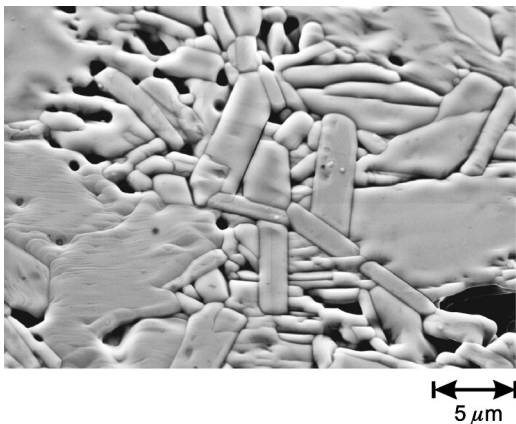


FIG. 1. SEM micrograph of a polycrystalline $\text{YBa}_2\text{Cu}_3\text{O}_{7-\delta}$ sample. The grains and their boundaries are clearly visible.

crystals, information about the properties of individual and well-defined interfaces is required. Owing to the complexity of the problem, however, it is rather challenging to understand the superconducting properties of individual interfaces by analyzing polycrystalline samples. To unveil the basic properties of the interfaces, the bicrystal technology was invented, which allows single, well-defined grain boundaries to be fabricated and analyzed in thin-film samples. Bicrystal experiments readily yielded several intriguing results (see, for example, Mannhart and Chaudhari, 2001): as suspected in the original paper on high- T_c superconductivity (Bednorz and Müller, 1986), grain boundaries generally limit the critical current densities J_c of polycrystalline high- T_c samples. But excitingly, large-angle boundaries also form excellent Josephson junctions. Characterized by these properties, grain boundaries in the high- T_c superconductors differ fundamentally from their counterparts in classical metallic superconductors and in MgB_2 . Those boundaries are electronically much less active and act as pinning sites at most (see, for example, DasGupta *et al.*, 1978). To take advantage of the unusual properties of the boundaries in the high- T_c superconductors, other techniques besides bicrystal technology, such as bi-epitaxial growth or the step-edge technology, have been developed and widely applied.

Owing to their universal, largely compound-independent properties, grain boundaries in high- T_c superconductors are of central importance for numerous applications, ranging from high-current-carrying cables to electronic circuits and sensors, from rf devices operating in the THz range to superconducting quantum interference devices (SQUIDs). For many experiments aimed at elucidating the physics of high- T_c superconductivity, for example, attempts to identify the order-parameter symmetry of the cuprates or to search for time-reversal symmetry breaking, grain boundaries have also been used with outstanding success.

The remarkable behavior of the grain boundaries has been investigated in numerous studies performed on thin films and bulk samples, which led to considerable progress in understanding the grain-boundary mecha-

nisms. With this, it became feasible to optimize and tailor these interfaces and to envisage and develop novel devices. In particular it has been possible to optimize the grain boundaries in high- T_c wires and tapes, which is crucial for the realization of competitive high- T_c cables.

Owing to its importance and appeal, this field is growing with remarkable speed, and the technologies developed for the fabrication of grain boundaries in high- T_c superconductors are now being applied to other material systems such as the ferrates (Scholl *et al.*, 2000), the bismuthates (Kussmaul, Hellman, *et al.*, 1993; Inoue *et al.*, 1994; Takami *et al.*, 1994; Roshchin *et al.*, 1995; Yamamoto *et al.*, 1995), or the manganates showing colossal magnetoresistance (Mathur *et al.*, 1997; Steenbeck *et al.*, 1997; Todd *et al.*, 1999; Westerburg *et al.*, 1999; Höfener *et al.*, 2000).

Because grain boundaries have a critical impact on research and applications of high- T_c superconductivity, the quantity of data published is close to overwhelming. The aim of this review is to provide, without claiming that it be anywhere near complete, an overview of grain boundaries in high- T_c superconductors. We attempt to summarize the available data, to provide references, and to discuss developments. In writing this article we realized that, due to the extent of the field, this review will likely not be free of errors or omissions, for which we apologize.

II. INTRODUCTION TO GRAIN BOUNDARIES

Grain boundaries are usually classified according to the displacement and the rotation of the abutting crystals, as shown schematically in Fig. 2. For rotational grain boundaries a distinction is made between the tilt and twist components of the misorientation. Here, *tilt* refers to a rotation around an axis in the plane of the grain boundary, and *twist* to a rotation of the crystal grains around the axis perpendicular to the grain boundary plane. A 24° [001]-tilt boundary, for example, connects two crystals rotated with respect to each other by 24° around the [001] direction, which is common to both crystals and lies in the grain-boundary plane. Furthermore, combinations of tilt and twist components may occur, leading to so-called mixed boundaries. Grain boundaries with identical misorientations of the grains with respect to the grain-boundary interface are called *symmetric*; otherwise they are *asymmetric*. For the high- T_c superconductors with their layered structure, 90° boundaries are particularly noteworthy. Three of these boundaries, which are commonly present in *a*-axis-oriented high- T_c films, namely, a 90° [010]-twist boundary, a 90° [010]-basal-plane-faced tilt boundary, and a symmetrical 90° [010] tilt boundary, are shown in Fig. 3. The latter two boundaries are also frequently found in step-edge junctions.

In addition to those boundaries associated with a rotation of the crystals, boundaries may also be formed as a result of a translation between the two grains. For standard *c*-axis-oriented $\text{YBa}_2\text{Cu}_3\text{O}_{7-\delta}$ films, such translational boundaries usually extend along the [001]

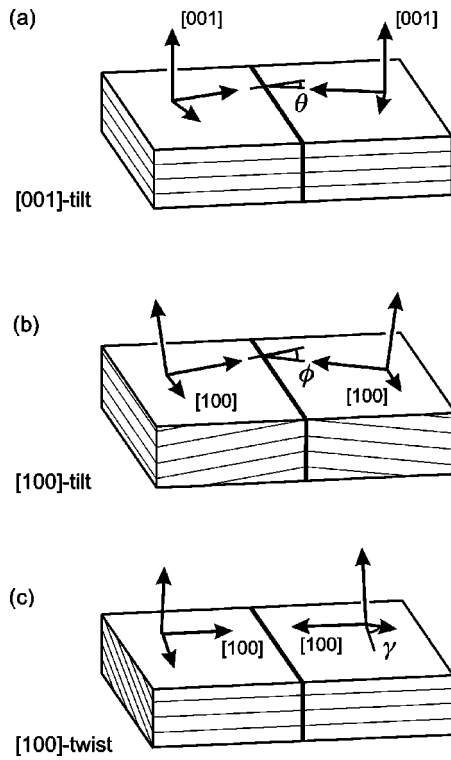


FIG. 2. Schematic diagram showing the crystallography of (a) a [001]-tilt boundary, (b) a [100]-tilt boundary, and (c) a [100]-twist boundary in a cubic material.

direction and comprise a shift over $1/3$ or $2/3$ of the [001] lattice vector, in which case they are referred to as *antiphase* or *out-of-phase boundaries* (Haage *et al.*, 1997; Zandbergen *et al.*, 1988; Bals *et al.*, 2001).

To accommodate the misorientation, along low-angle grain boundaries dislocations are formed, separated by well lattice-matched regions (see Fig. 4). Depending on the symmetry, one or two sets of edge dislocations are usually generated in pure tilt boundaries, and two sets of screw dislocations are created in pure twist boundaries. In mixed boundaries, at least three sets of dislocations are present. In the standard grain-boundary dislocation theory, the distance d between the dislocations of a certain set is given by Frank's formula:

$$d = |\vec{b}| / \sin \theta, \quad (2.1)$$

where $|\vec{b}|$ is the magnitude of the Burgers vector \vec{b} . The Burgers vector is derived from a comparison between a closed contour in the undisturbed crystal and a contour connecting corresponding lattice points around the dislocation, the so-called Burgers circuit. The vector that has to be added to close the Burgers circuit, the *closure failure*, defines the Burgers vector. If more than one set of dislocations is formed, they each have their own Burgers vectors and dislocation spacings.

Whereas the microstructure of dislocations is material dependent, the formation of dislocations at grain boundaries is a consequence of topology and occurs in a common way for grain boundaries in many different materials. Note that the structures of dislocations in metals and ceramics differ strongly due to the different types of

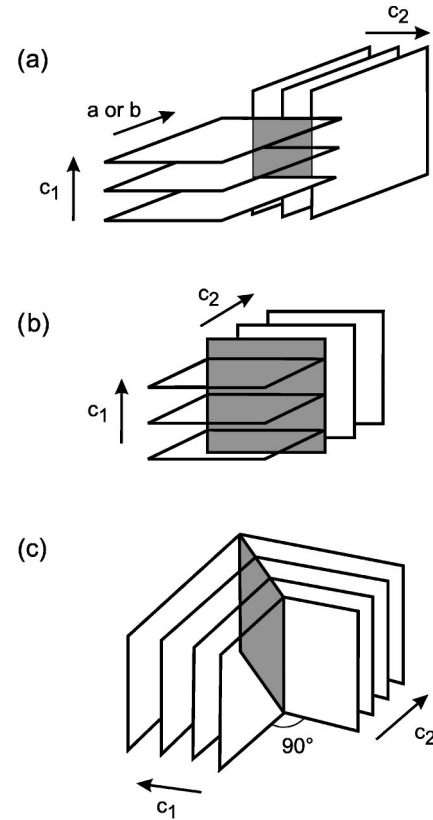


FIG. 3. Schematic diagrams of three types of 90° grain boundaries (drawn in gray); (a) a 90° [010] twist boundary; (b) a 90° [010] basal-plane-faced tilt boundary; (c) a 90° [010] symmetrical tilt boundary. Note that a 90° [010] symmetrical tilt boundary is a (110) twin boundary. Adapted from Eom *et al.* (1992).

chemical bonds present in these materials (Chisholm and Smith, 1989, and references therein). The coordination of the atoms at grain boundaries in elemental metals and semiconductors is generally similar to that in the grains. In ionically bonded compounds, the Coulomb potential plays an important role, potentially leading to the formation of built-in electrostatic potentials at the interfaces.

In materials of which the unit cell is composed of smaller subcells, dissociation of the dislocations into partial dislocations can occur, especially for small misorientations. For these partial dislocations the Burgers vector is given by a base vector of the sub-unit cell, instead of the larger base vectors of the complete cell. This can be the case, for example, for the high- T_c superconductors, the unit cells of which are composed of stacks of perovskite cells.

The interface energy associated with a low-angle grain boundary is approximated by the Read-Shockley equation:

$$\gamma_{gb} = \gamma_0 \theta (A - \ln \theta), \quad (2.2)$$

where γ_0 is the product of the magnitude of the Burgers vector, the elastic modulus, and a geometrical factor, and $A = 1 + \ln(b/2\pi r_0)$, where r_0 is the dislocation core radius (Read and Shockley, 1950; Cottrell, 1964; Chan, 1994).

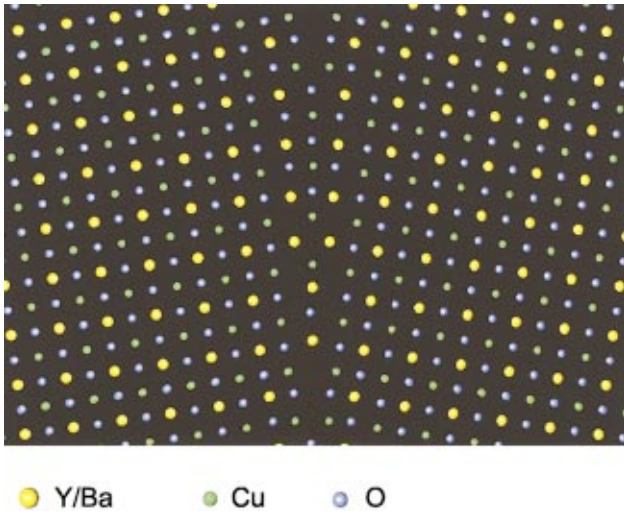


FIG. 4. Schematic drawing of the (001) surface of a $\text{YBa}_2\text{Cu}_3\text{O}_{7-\delta}$ bicrystal containing a symmetric 16° [001]-tilt grain boundary in $\text{YBa}_2\text{Cu}_3\text{O}_{7-\delta}$. Figure courtesy of G. Hammerl, Augsburg University, Germany [Color].

With increasing grain-boundary angle, the dislocations are spaced closer together until they merge into a closed interface layer. This layer may be structurally distorted or composed of well-defined structural units (Browning *et al.*, 1995). For such high-angle grain boundaries, Eqs. (2.1) and (2.2) no longer apply. A convenient model for describing the interface energy of high-angle boundaries makes use of the *coincidence site lattice* (CSL), as described, for example, by Sutton and Baluffi (1995). The CSL is the lattice obtained from superposing the two lattices of the abutting crystals. A key parameter for describing the grain boundaries is their Σ value, defined according to

$$\Sigma = |\vec{C}_1 \cdot (\vec{C}_2 \times \vec{C}_3)| / |\vec{a} \cdot (\vec{b} \times \vec{c})|, \quad (2.3)$$

where \vec{a} , \vec{b} , and \vec{c} are the lattice vectors of the crystal grains and \vec{C}_1 , \vec{C}_2 , and \vec{C}_3 are the primitive vectors of the CSL. A small value of Σ implies that the two grains share many lattice sites at the interface and therefore the boundary is expected to have low energy. Indeed, using freely rotatable grains in MgO smoke, it has been shown that such boundaries are preferentially formed (Chaudhari and Matthews, 1971). These boundaries are referred to as low- Σ , coincidence, or special boundaries. Boundaries for which only a small constraint of the crystal lattice would result in a low- Σ configuration are called near- Σ boundaries. A list of low- Σ misorientations

TABLE I. Low- Σ boundaries in cubic materials.

Grain-boundary angle	Low-index planes aligned	Σ
16.3	(430) (340)	$\Sigma 25$
22.62	(320) (230)	$\Sigma 13$
28.07	(410) (140)	$\Sigma 17$
36.87	(210) (120)	$\Sigma 5$
43.6	(520) (250)	$\Sigma 29$

for materials with a cubic crystal structure is provided in Table I (Singh *et al.*, 1990; Tietz and Carter, 1991). With small adaptations arising from the potential orthorhombicity of the high- T_c compounds, this list also applies to the cuprate superconductors. Indeed, Smith *et al.* (1988) found a preference for the formation of these boundaries in $\text{YBa}_2\text{Cu}_3\text{O}_7$ crystals produced from a melt.

Figure 5 displays a semiquantitative plot of the grain-boundary energy γ versus the misorientation angle for [001]-tilt boundaries in cubic materials (Ravi *et al.*, 1990). For the low-angle regime, γ follows the Read-Shockley relation [Eq. (2.2)]. In the large-angle regime several low- Σ boundaries can be formed with correspondingly small energy. Intergranular phases resulting for example from impurity additions may occur if the interfacial energy of a clean grain boundary γ_{gb} exceeds twice the energy of an interface between a grain and the impurity phase $2\gamma_{\text{gi}}$. In Fig. 5 such a threshold value is indicated. The figure suggests that low-energy boundaries, i.e., low-angle and coincidence boundaries, are the most likely ones to be free of intergranular phases.

Several high- T_c cuprates are orthorhombic and thus characterized by a slight difference between the lattice parameters of the a and b axes. In these materials, possible alternations of the a and b directions define twin boundaries. Twinning occurs along the (110) planes, often as families of parallel lamellae. For $\text{YBa}_2\text{Cu}_3\text{O}_{7-\delta}$, with $|a| \approx 3.82 \text{ \AA}$ and $|b| \approx 3.88 \text{ \AA}$, a twin boundary presents a $\Sigma 64$, 89.1° [001]-tilt boundary. The microstructure of twin boundaries in $\text{YBa}_2\text{Cu}_3\text{O}_{7-\delta}$ has been reviewed extensively by Cai and Zhu (1998).

III. PREPARATION OF SINGLE GRAIN BOUNDARIES

In 1987, the technological potential of high- T_c superconductivity (Bednorz and Müller, 1986; Wu *et al.*, 1987)

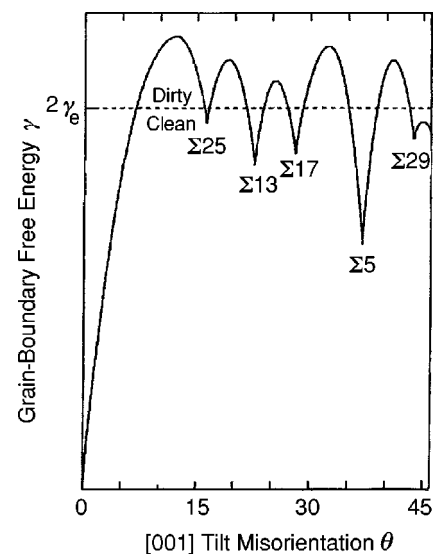


FIG. 5. Semiquantitative plot of the grain-boundary energy γ versus the misorientation angle θ for [001]-tilt boundaries in cubic materials. From Ravi *et al.* (1990); figure courtesy of S.-W. Chan, Bellcore, USA.

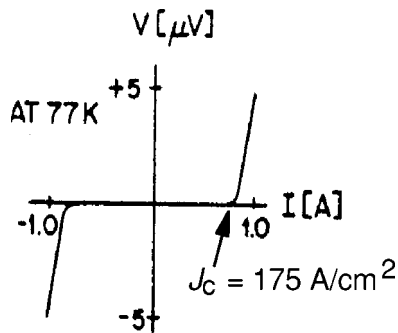


FIG. 6. Current-voltage characteristic of a $\text{YBa}_2\text{Cu}_3\text{O}_{7-\delta}$ wire reflecting the state of the art in 1987. After Jin *et al.* (1987).

was underlined by the growth of the first epitaxial films with critical current densities J_c exceeding 10^5 A/cm² at 77 K under self-field conditions (Chaudhari *et al.*, 1987; for a review see Schlom and Mannhart, 2002). Prior to that, the critical current densities of the best polycrystalline bulk samples (Camps *et al.*, 1987; Cava *et al.*, 1987; Jin *et al.*, 1987) and of polycrystalline films (Koch *et al.*, 1987) were in the range of 10^2 – 10^4 A/cm² at 4.2 K, impractical values for all but a few applications. This is illustrated by Fig. 6, which shows the current-voltage characteristic of a 1987 state-of-the-art wire of $\text{YBa}_2\text{Cu}_3\text{O}_{7-\delta}$, which had a J_c of 175 A/cm² (77 K). As suggested in the original work by Bednorz and Müller, and in further work, e.g., by Ekin and colleagues, the low J_c and the Josephson behavior of polycrystalline samples has mostly been attributed to poor superconducting coupling across the grain boundaries (Bednorz and Müller, 1986; Ekin *et al.*, 1987; Koch *et al.*, 1987; Larbalestier *et al.*, 1988; Peterson and Ekin, 1988), but other contributing factors were also discussed, such as a superconducting glass state (Müller *et al.*, 1987), the anisotropy of the cuprates (Ekin *et al.*, 1987), twin boundaries (Deutscher and Müller, 1987), intragrain weak links (Larbalestier *et al.*, 1988; Küpfer *et al.*, 1989), and metallic cores of the grains (Ginley *et al.*, 1987). To clarify the influence of the grain boundaries on superconducting transport, a series of experiments was undertaken at IBM to measure the properties of well-defined, single grain boundaries by using the thin-film bicrystal technology [see Fig. 7(a)] invented for this purpose (Chaudhari, Dimos, *et al.*, 1988; Chaudhari, Mannhart, *et al.*, 1988; Dimos *et al.*, 1988, 1990; Mannhart *et al.*, 1988; for an overview see Mannhart and Chaudhari, 2001). Soon, with various biepitaxial junction configurations [see Fig. 7(b),(c); Char *et al.*, 1991a; Di Chiara *et al.*, 1997], the step-edge junction technique [Fig. 7(d); Daly *et al.*, 1991] and fabrication procedures involving grain rotation by ion irradiation of the substrate (Chew *et al.*, 1992; Ramos *et al.*, 1993), several other technologies were developed, which do not require bicrystalline substrates to produce well-defined grain boundaries in films. Furthermore, a variety of techniques has been used to fabricate bicrystals for bulk high- T_c materials as well. These include growth by flux techniques (see Fig. 8; Gayle and Kaiser, 1991), the isolation of single grain boundaries in polycrystals (Schindler *et al.*, 1992; Saleh

et al., 1998), melt texturing (Nillson-Mellbin and Salama, *et al.*, 1994a, 1994b; Field *et al.*, 1997), seeded growth (Todt *et al.*, 1996; Delamare *et al.*, 2000), optimized sintering (Tomita *et al.*, 1990; Parikh *et al.*, 1994; Wang *et al.*, 1994) and welding processes (Bradley *et al.*, 1999; Leenders *et al.*, 1999; Delamare *et al.*, 2000). Note, that long before, in 1985, bulk bicrystals of the oxide superconductor $\text{BaPb}_{1-x}\text{Bi}_x\text{O}_3$ were fabricated using spontaneous crystallization of an appropriate melt (Stepankin *et al.*, 1985).

A. Bicrystalline junctions

The principle of the bicrystal technology illustrated in Fig. 7(a) consists of growing a film epitaxially on a bicrystalline substrate, which contains a grain boundary of the desired configuration (Dimos *et al.*, 1988). Owing to epitaxial growth, the substrate grain boundary is replicated in the film. This technique enables one to fabricate well-defined grain boundaries of many misorientations and to analyze their properties in direct comparison to those of the abutting grains (for an overview see Mannhart and Chaudhari, 2001). By using substrates composed of more than two crystals this technique has also been applied to the fabrication of tricrystalline high- T_c films of various configurations (Tsuei *et al.*, 1994, 1996, 1997; Kaplunenko *et al.*, 1995; Kirtley, Tsuei, *et al.*, 1995, 1996; Miller, Ying, *et al.*, 1995; Sugimoto *et al.*, 2001), tetracrystalline films (Tsuei *et al.*, 1997; Schulz *et al.*, 2000), and polycrystalline samples consisting of large grains (Dimos *et al.*, 1988; Mannhart, Huebener, *et al.*, 1990).

Whereas the first bicrystal films were grown on homemade SrTiO_3 bicrystals or polycrystals, bicrystalline substrates of many compounds, including SrTiO_3 , doped SrTiO_3 , MgO, yttria-stabilized zirconia (YSZ), silicon, and sapphire are now commercially available. Furthermore, NdGaO_3 (Quincey, 1993), LaAlO_3 (Kaestner *et al.*, 2000), and Ni films grown on bicrystalline KCl substrates (Thiele *et al.*, 2001) have successfully been used as substrates. As a substrate boundary with a small density of defects such as voids is an obvious prerequisite for a homogenous boundary in the high- T_c film (McDaniel *et al.*, 1997; Jiang *et al.*, 1998), Balbashov and co-workers have developed a floating-zone method to further enhance the quality of boundaries (Balbashov *et al.*, 1997; Vengrus *et al.*, 1997). According to their studies, these boundaries are remarkably clean and homogenous, leading to excellent bicrystal Josephson junctions. The bicrystal technology has been used to fabricate grain boundaries in most high- T_c cuprates, as listed in Sec. V.B.1.

B. Biepitaxial junctions

In an approach pioneered by Char and co-workers at Conductus, a technique was found to freely select the position of the grain boundary (Char *et al.*, 1991a, 1991b). This so-called biepitaxial process utilizes changes in the orientation of high- T_c films induced by

epitaxial growth on structured template layers. Depending on the underlying layers, the high- T_c films are rotated in-plane, resulting in rotational grain boundaries at the edges of the template structures, as shown schematically in Fig. 7(b). Here it should be noted that $\text{YBa}_2\text{Cu}_3\text{O}_{7-\delta}$ grows with $[100]\parallel[100]$ on SrTiO_3 . Various combinations of materials can be employed to induce variations of the in-plane orientation. Char *et al.* (1991a), for example, used a MgO template layer on an r -plane sapphire substrate to rotate a $\text{SrTiO}_3/\text{YBa}_2\text{Cu}_3\text{O}_{7-\delta}$ bilayer by 45° compared to an identical bilayer grown directly on sapphire, making use of the epitaxial relationships: $\text{SrTiO}_3[110]\parallel\text{Al}_2\text{O}_3[11\bar{2}0]$

and $\text{SrTiO}_3[100]\parallel\text{MgO}[100]\parallel\text{Al}_2\text{O}_3[11\bar{2}0]$ [see Fig. 7(b)]. In an extension of that work, the sapphire substrate was replaced by a base layer of SrTiO_3 grown on a variety of substrate materials, and the SrTiO_3 buffer layer by CeO_2 (Char *et al.*, 1991b). In this setup, the epitaxial relations $\text{CeO}_2[110]\parallel\text{SrTiO}_3[100]$ and $\text{CeO}_2[100]\parallel\text{MgO}[100]\parallel\text{SrTiO}_3[100]$ served as the basis for the creation of a 45° [001]-tilt grain boundary in the $\text{YBa}_2\text{Cu}_3\text{O}_{7-\delta}$ film, which in both cases grows with $\text{YBa}_2\text{Cu}_3\text{O}_{7-\delta}[110]\parallel\text{CeO}_2[100]$. The template layer, MgO in the above cases, is usually kept fairly thin, i.e., 3–30 nm (Char *et al.*, 1991a), to minimize the step height at the intended position of the grain boundary.

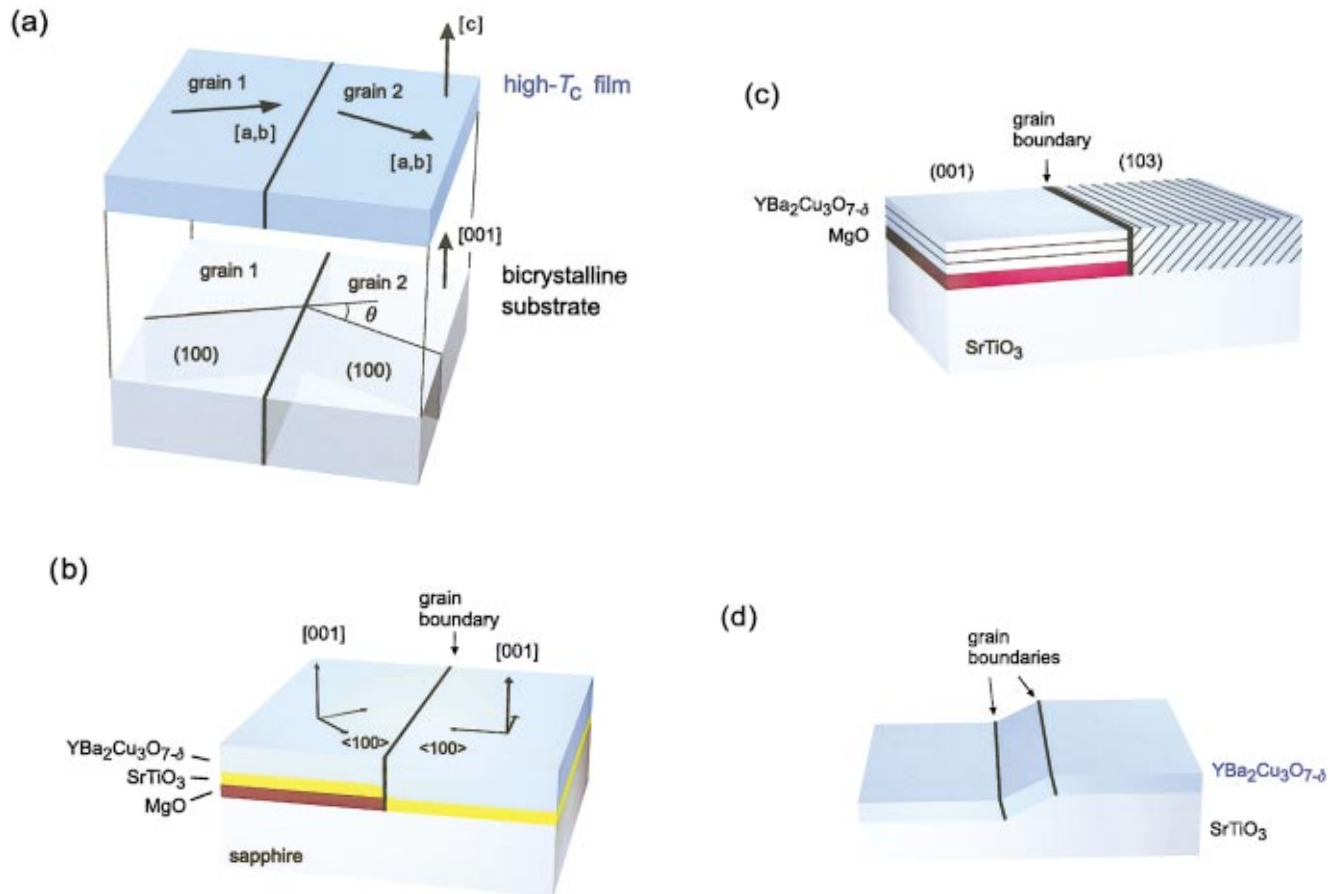


FIG. 7. Technologies developed to fabricate individual, well-defined grain boundaries in epitaxial films: (a) Sketch of the thin-film bicrystal principle using the example of a symmetric [001]-tilt grain boundary with a tilt angle θ . After Dimos *et al.* (1988); Tsuei *et al.* (1989); (b) sketch of the biepitaxial principle as developed by Char *et al.* (1991a). Under suitable conditions, a [001]-oriented $\text{YBa}_2\text{Cu}_3\text{O}_{7-\delta}$ film is grown with $\text{YBa}_2\text{Cu}_3\text{O}_{7-\delta}[110]\parallel\text{SrTiO}_3[110]\parallel\text{Al}_2\text{O}_3[11\bar{2}0]$ and with $\text{YBa}_2\text{Cu}_3\text{O}_{7-\delta}[100]\parallel\text{SrTiO}_3[100]\parallel\text{MgO}[100]\parallel\text{Al}_2\text{O}_3[11\bar{2}0]$. Therefore a 45° grain boundary is formed at the edge of the MgO seed layer. SrTiO_3 may also be used as a substrate; (c) sketch of the biepitaxial principle developed by Di Chiara *et al.* (1997), which uses (110)-oriented MgO seed layers grown on a (110) SrTiO_3 surface to create a 45° boundary at the edge of the seed layer. Note that besides the 45° tilt boundary shown in the figure, 45° twist boundaries can be created by using the edge of the seed layer at the front of the sample, rotated by 90° with respect to the grain-boundary line drawn; (d) sketch of step-edge junctions. At a substrate step, two grain boundaries are nucleated, one at its bottom and one at its top [Color].

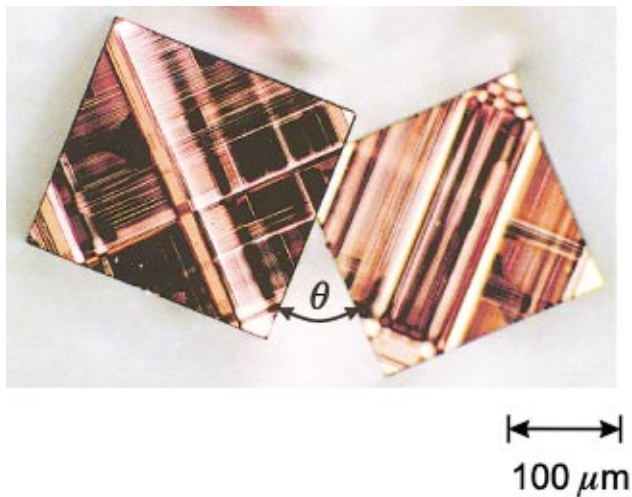


FIG. 8. Polarized light micrograph of a flux-grown $\text{YBa}_2\text{Cu}_3\text{O}_{7-\delta}$ bicrystal. Bands in the crystal result from the twinned microstructure. Horizontal faces imaged in-plane view are parallel to $[001]$. The vertical faces are parallel to (100) and (010) . The bicrystal was grown by D. Kaiser (NIST, Gaithersburg, USA). The figure is from Babcock and Larbalestier (1994), courtesy of S. Babcock and D. C. Larbalestier, University of Wisconsin, USA [Color].

An inventory of possible combinations for creating 45° $[001]$ -tilt biepitaxial template junctions was presented by Wu *et al.* (1992), who studied the in-plane orientational relationships between LaAlO_3 , SrTiO_3 , yttria-stabilized ZrO_2 , MgO , CeO_2 , BaZrO_3 , and SrTiO_3 . In various adaptations of these compounds, several groups have investigated the fabrication and properties of template biepitaxial grain-boundary junctions.¹ Almost all reports on biepitaxial junctions concern $\text{YBa}_2\text{Cu}_3\text{O}_{7-\delta}$. However, 45° $[001]$ -tilt grain-boundary junctions have also been prepared in (001) -oriented $\text{Bi}_2\text{Sr}_2\text{Ca}_2\text{Cu}_3\text{O}_{8+\delta}$ films by Takami *et al.*, (1993). The technique has furthermore been extended to grain-boundary studies in nonsuperconducting perovskites, such as $\text{La}_{0.8}\text{Sr}_{0.2}\text{MnO}_{3-\delta}$ (Lee *et al.*, 1999).

Relying on the occurrence of low- Σ combinations according to the coincidence site lattice model (see Sec. II), one might expect that grain-boundary angles other than 45° are also obtainable in $[001]$ -oriented $\text{YBa}_2\text{Cu}_3\text{O}_{7-\delta}$ films by using the biepitaxial template process. Indeed, some exceptions from a cube-to-cube or a 45° -rotated growth have been reported, e.g., an in-plane rotation of 18° occurring for CeO_2 films grown on MgO substrates (Ijsselsteijn *et al.*, 1993), and in-plane rotations of 9° for $\text{YBa}_2\text{Cu}_3\text{O}_{7-\delta}$ grown on YSZ (Schlom *et al.*, 1996). To date, however, no process has been established to create reproducible $[001]$ -tilt boundaries with angles deviating from 45° .

¹See, for example, Ijsselsteijn *et al.*, 1993, 1994; Vollnhals *et al.*, 1994; Li *et al.*, 1995; Petersen, Stolzel, *et al.*, 1995; Boikov *et al.*, 1997a, 1997b; L. Chen *et al.*, 1997; Y. Chen *et al.*, 1997; Horng *et al.*, 1997; Nicoletti and Villegier, 1997a, 1997b; Tsai *et al.*, 1998.

In an alternative approach, a group at the University of Naples uses (110) -oriented SrTiO_3 substrates and MgO seed layers. With this, asymmetric 45° $[100]$ tilt boundaries and asymmetric $[100]$ twist boundaries with promising properties can be fabricated (Di Chiara *et al.*, 1997; Tafuri *et al.*, 1999, 2000; Testa *et al.*, 1999). Furthermore, using obliquely cut SrTiO_3 substrates and $\text{CeO}_2/\text{Y-ZrO}_2$ template layers, 20° $[010]$ -tilt and twist boundaries were reported by Youm and Kim (1995).

C. Step-edge junctions

As shown first by the TRW group, grain boundaries are also readily nucleated by growing a high- T_c film over a suitable step patterned into the substrate (Daly *et al.*, 1991; Friedl *et al.*, 1991; Herrmann *et al.*, 1991; Edwards *et al.*, 1992; Luine *et al.*, 1992; Reuter *et al.*, 1993; Ramos *et al.*, 1993; Yi *et al.*, 1994). Typically, two grain boundaries are nucleated at one substrate step, one at its bottom and one at its top. These grain boundaries are connected in series [see Fig. 7(d)]. As the required substrate steps are easily defined by photolithography, for example, by using an amorphous carbon mask and ion-beam etching or reactive ion etching, such step-edge junctions can be positioned anywhere on the substrate. This freedom has been exploited to fabricate up to six hundred junctions on one chip (Reuter *et al.*, 1993). Typically, the step height is chosen to be larger than the film thickness, a characteristic value being 200–300 nm. The step angle has been found to be a crucial parameter, as it controls the microstructure and the grain-boundary configuration of the high- T_c film (Jia *et al.*, 1991, 1992; Lombardi *et al.*, 1998). Standard angles are in the range of 50° – 60° . The substrate material is also of importance, because on some materials, e.g., MgO , the high- T_c superconductors tend to grow with the $[001]$ axis parallel to the local substrate normal, giving rise to $[100]$ -tilt boundaries with misorientation angles determined by the slope of the substrate step edge (Ramos *et al.*, 1993), whereas on other materials, e.g., SrTiO_3 and LaAlO_3 , the high- T_c superconductors grow throughout with their $[100]$ or $[001]$ axes parallel to the substrate $[001]$ direction, creating only 90° grain boundaries (Jia *et al.*, 1991, 1992).

As predicted by Hilgenkamp, Mannhart, *et al.* (1996), and measured by Lee *et al.* (2000), the critical current density of the step-edge junctions is also strongly affected by the orientation of the step with respect to the $\langle 100 \rangle$ directions of the superconductor. Whereas step-edge junctions are typically fabricated from $\text{YBa}_2\text{Cu}_3\text{O}_{7-\delta}$ films, TlBaCaCuO has also been used without further specification of the composition being given (Martens *et al.*, 1992a, 1992b). We are not aware of step-edge junctions fabricated with BSCCO compounds.

IV. STRUCTURAL PROPERTIES

The microstructure of grain boundaries in high- T_c superconductors has been investigated by several means, of which transmission electron microscopy (TEM)

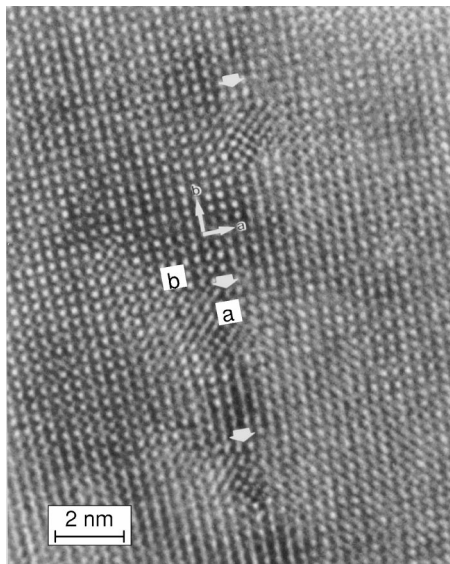


FIG. 9. Transmission electron micrograph of a 3.5° [001]-tilt bicrystal grain boundary in an $\text{YBa}_2\text{Cu}_3\text{O}_{7-\delta}$ film. Three dislocations, which are indicated by arrows, are visible. From Gao *et al.* (1991); micrograph courtesy of K. L. Merkle, Argonne National Laboratory, USA.

proved to be particularly useful. From the earliest TEM studies revealing detailed information about the interface atomic structure of rotational grain boundaries in high- T_c superconductors,² an example of which is given in Fig. 9, it soon became clear that low-angle grain boundaries consist of arrays of separate dislocations. As suggested by standard dislocation theory, these dislocations merge into a continuous interface layer in large-angle grain boundaries. A particularly important conclusion from the initial microscopy studies was that the weak-link nature of the grain boundaries in the high- T_c cuprates does not result from coarse defects in the grain boundaries, such as voids or impurity layers, but that it is characteristic of clean and structurally well-defined boundaries. A beautiful example of such a boundary is given in Fig. 10. In this flux-grown $\text{YBa}_2\text{Cu}_3\text{O}_{7-\delta}$ bicrystal containing a 31° [001]-tilt grain boundary, the structure of the grains appears unaltered right up to the boundary.

Complementing such microstructural investigations, various techniques were employed to analyze the chemical composition of the grain boundaries. Some of the initial studies reported impurity segregation at grain boundaries, in particular of silicon (Camps *et al.*, 1987) or carbon (Nakahara *et al.*, 1987). Insulating segregation layers have been found in $\text{Ba}_{1-x}\text{K}_x\text{BiO}_3$ grain boundaries (Chan *et al.*, 1998). Thanks to advances in the pro-

²These included, for example, the work of Nakahara *et al.*, 1987, 1988; Babcock *et al.*, 1988, 1990; Dimos *et al.*, 1988; Zandbergen and Thomas, 1988; Zandbergen, Gronsky, and Thomas, 1988; Chisholm and Smith, 1989; Chan *et al.*, 1989; Chisholm and Pennycook, 1991; Gao *et al.*, 1991; Marshall and Eom, 1993; and Alarco *et al.*, 1993.

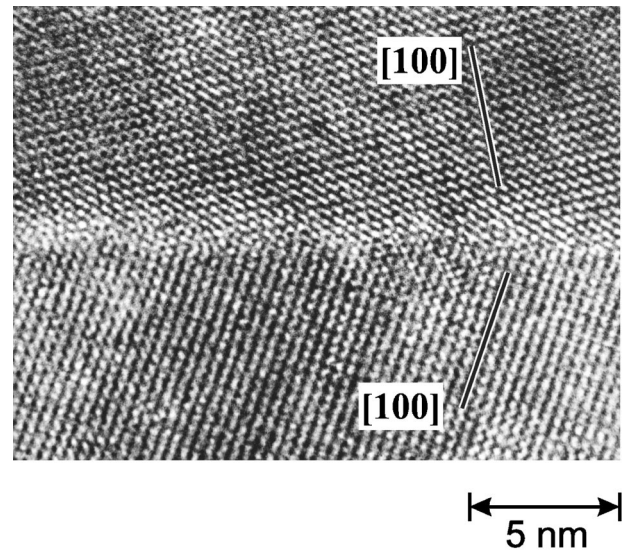


FIG. 10. High-resolution TEM image of a 31° [001]-tilt grain boundary in a flux-grown $\text{YBa}_2\text{Cu}_3\text{O}_{7-\delta}$ bicrystal. From Babcock *et al.* (1994); figure courtesy of S. Babcock and D. C. Larbalestier, University of Wisconsin, USA.

cessing procedures of high-temperature superconductors, such segregation could later be ruled out. While free from measurable levels of impurities, the dislocation cores are generally found to differ in stoichiometry from the bulk. X-ray photoemission spectroscopy (Stucki *et al.*, 1988), Auger electron spectroscopy (Kroeger *et al.*, 1988) and energy-dispersive x-ray microanalysis (Babcock *et al.*, 1988, 1989; Vargas *et al.*, 1997) revealed that the dislocations of $\text{YBa}_2\text{Cu}_3\text{O}_{7-\delta}$ grain boundaries are typically Cu rich. An example can be seen in Fig. 11, which shows the results of an x-ray microanalysis, revealing an enhanced concentration of Cu along a 7° and a 31° [001]-tilt $\text{YBa}_2\text{Cu}_3\text{O}_{7-\delta}$ bicrystal grain boundary (Vargas *et al.*, 1997).

The findings of the early grain-boundary microscopy studies were confirmed and extended by additional high-resolution TEM investigations of grain boundaries in $\text{YBa}_2\text{Cu}_3\text{O}_{7-\delta}$ and BSCCO polycrystalline films, in bulk samples (Ravi *et al.*, 1990), and in biepitaxial films grown on bicrystalline substrates (Alarco *et al.*, 1993; Browning *et al.*, 1993, 1998; Trøholt *et al.*, 1994; Seo *et al.*, 1995; Wang *et al.*, 1996; Yu *et al.*, 1997; Takagi *et al.*, 1999; Wen *et al.*, 1999; Carmody *et al.*, 2000a), on substrate steps (Tanaka *et al.*, 1993; Alarco *et al.*, 1994), on ion-treated substrate surfaces (Vuchic *et al.*, 1995, 1996), or on template structures (Tanimura *et al.*, 1993). Atomic-resolution TEM studies have further been carried out for $\text{YbBa}_2\text{Cu}_3\text{O}_{7-x}$ grain boundaries (Kogure *et al.*, 1988), for bulk $\text{Bi}_2\text{Sr}_2\text{CaCu}_2\text{O}_{8+\delta}$ bicrystals (Tsu *et al.*, 1998; Zhu *et al.*, 1998), and for grain boundaries formed by different phases of BSCCO (Zakharov *et al.*, 1998).

As mentioned, to accommodate the lattice mismatch, dislocations separated by well lattice-matched regions are formed at small-angle boundaries. This is beautifully illustrated by the TEM micrograph (Fig. 12) from

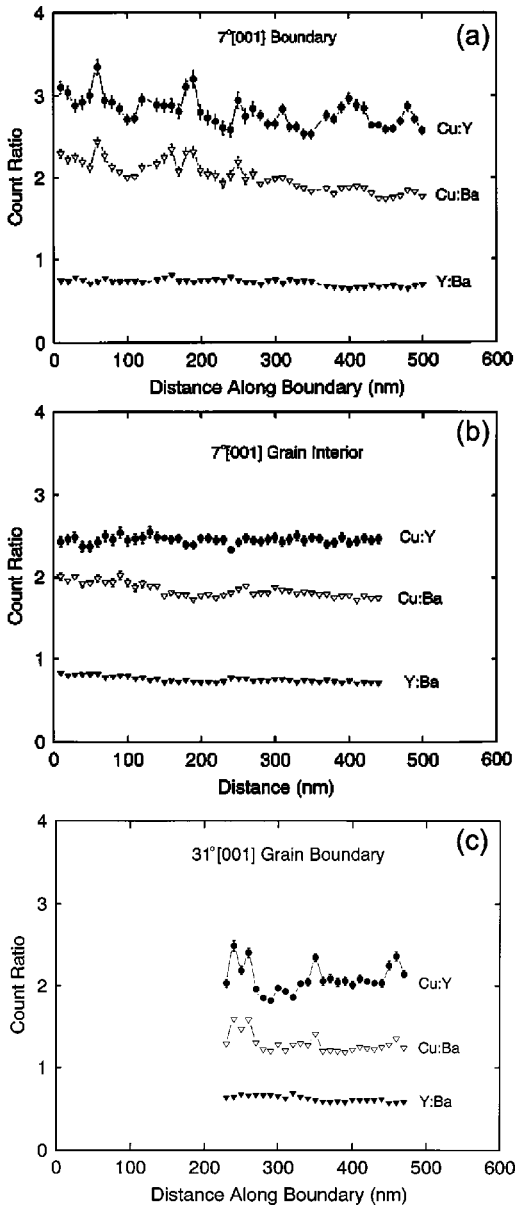


FIG. 11. X-ray intensity ratios (Cu:Y), (Cu:Ba), and (Y:Ba) as a function of position: (a) along a 7° [001] tilt grain boundary; (b) inside a grain of a 7° bicrystal, and (c) along a 31° [001]-tilt grain boundary of a $\text{YBa}_2\text{Cu}_3\text{O}_{7-\delta}$ bulk bicrystal, grown by a flux method. The spectra taken at points with the same x coordinate in (a) and (b) refer nominally to the same thickness. The x -coordinate value in (c) denotes the position relative to an arbitrary zero. From Vargas *et al.* (1997); figure courtesy of S. Babcock, University of Wisconsin, USA.

Chisholm and Smith (1989), showing dislocations along a 5° [100]-tilt boundary. Periodic defects, which in this two-dimensional projection have a triangular shape and which are separated by well-ordered crystalline material, are clearly visible. For these defects, a Burgers vector with $|\vec{b}| = 1.17$ nm, the $\text{YBa}_2\text{Cu}_3\text{O}_{7-\delta}$ c -axis unit cell length, was found. The spacing between the defects is ~ 15 nm. Enlargements of these images (Chisholm and Smith, 1989) suggest that the dislocations are dissociated into three partials (see also Gutkin and Ovid'ko, 2001). Chisholm and Smith also show a TEM image of a 1°

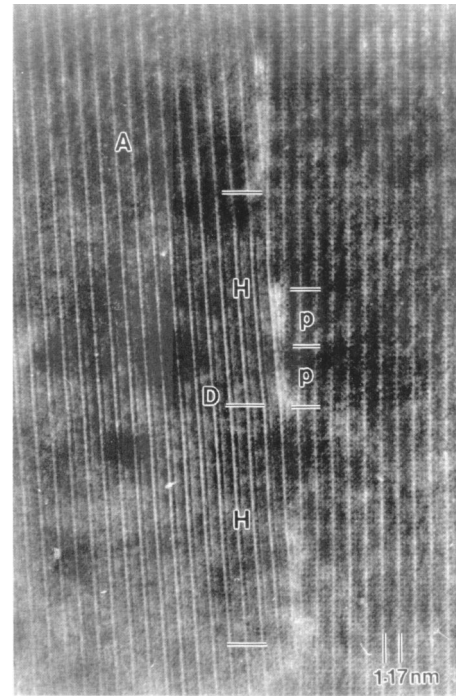


FIG. 12. Transmission electron micrograph of a 5° [100]-tilt grain boundary in bulk-processed $\text{YBa}_2\text{Cu}_3\text{O}_{7-\delta}$. The boundary is parallel to the [001] plane of grain A and contains an array of dislocations with a spacing H . Each dislocation appears to have dissociated into three partials separated by a distance p . From Chisholm and Smith (1989); micrograph courtesy of M. F. Chisholm, Oak Ridge National Laboratory, USA.

[001]-tilt boundary, the dislocations of which exhibit a closure failure of $|\vec{b}| = 0.389$ nm. Interestingly, the widths of the structurally distorted regions in this boundary are similar to those in the [100] boundaries. Based on their TEM studies, Gao *et al.* report a typical radius of 1 nm for dislocations along a 3.5° [001]-tilt boundary (Gao *et al.*, 1991).

With increasing grain-boundary angle, the separation between dislocations decreases and for a given angle the dislocation cores merge, forming a continuous layer along the grain-boundary interface. For $\text{YBa}_2\text{Cu}_3\text{O}_{7-\delta}$ boundaries this transition angle was reported to be 7.5° (Chisholm and Smith, 1989). Based on atomic-resolution TEM studies (see Fig. 13), it was pointed out by Browning *et al.* (1998), that this interface layer consists of well-defined structural units, which supposedly comprise the same core structures as seen in isolated dislocations (Browning *et al.*, 1996). This group further applied a bond-valence sum analysis based on the atomic arrangements of the ions in the structural units, and from this they estimated the widths of the nonsuperconducting zones adjacent to the interfaces. These were found to increase linearly from ≈ 0.2 nm to ≈ 0.9 nm for an increase of the misorientation angle from 11° to 45° (Browning *et al.*, 1998).

Boundaries with a 90° misorientation, which frequently appear in a -axis and mixed a/c -axis-oriented

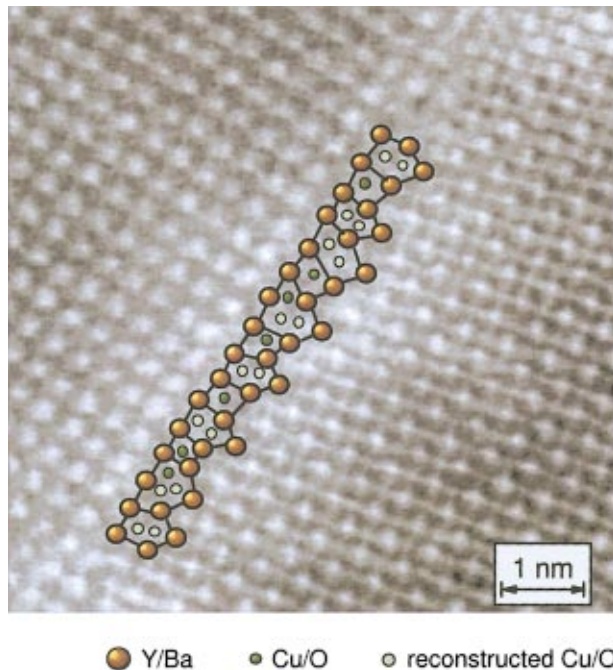


FIG. 13. Planar view, Z-contrast TEM image of a 30° [001] tilt $\text{YBa}_2\text{Cu}_3\text{O}_{7-\delta}$ thin-film bicrystal grain boundary. Indicated in this image are also the structural units of which the grain boundary is composed. From Browning *et al.* (1998); micrograph courtesy of N. Browning, Oak Ridge National Laboratory and University of Illinois at Chicago, USA [Color].

films, are particularly interesting, as some of them, such as 90° twist boundaries, have been found to support large critical currents as described in Sec. V.B.1. Figure 14 displays the structure of these boundaries formed in an a -axis-oriented $\text{YBa}_2\text{Cu}_3\text{O}_{7-\delta}$ film, showing the occurrence of 90° [010] basal-plane-faced boundaries and symmetrical 90° [010]-tilt boundaries in the same sample.

Ninety-degree boundaries can also be induced at substrate step edges. For most substrate materials, $\text{YBa}_2\text{Cu}_3\text{O}_{7-\delta}$ films are grown c -axis-oriented on the substrate plane and with the c axis parallel to the substrate's [100] direction on the flank of the step. As a result, two 90° boundaries are formed, the microstructure of which is clearly visible in Fig. 15.

The charge-carrier concentration at grain-boundary interfaces has been investigated by various groups with spatially resolved electron-energy-loss spectroscopy (EELS).³ Most EELS measurements demonstrate the presence of a layer with a reduced density of holes, i.e., missing electrons, at the boundary, an example of which is shown in Fig. 16. The reported widths of these layers range from 0.2 to 20 nm. This spread may reflect the challenges faced in sample preparation and imaging, in particular concerning oxygen loss. Usually, EELS inves-

³For EELS studies, see Browning *et al.*, 1993; Dravid *et al.*, 1993; Wang *et al.*, 1993; Babcock and Larbalestier, 1994; Zhu *et al.*, 1994; Babcock and Vargas, 1995; Zhu and Suenaga, 1995; Vargas *et al.*, 1997.

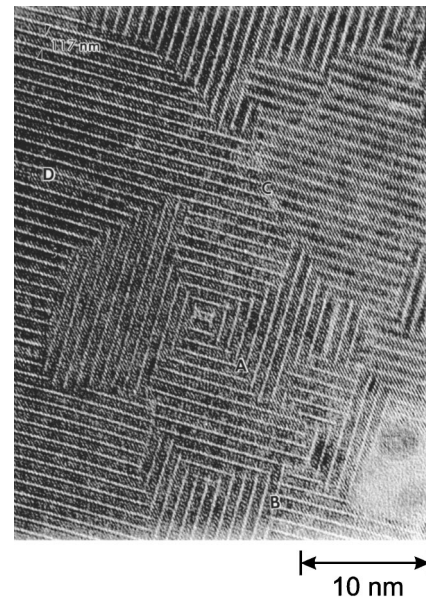


FIG. 14. Planar-view TEM image of an a -axis-oriented $\text{YBa}_2\text{Cu}_3\text{O}_{7-\delta}$ film. The 90° boundaries exhibit basal-plane-faced facets and symmetrical facets. From Eom *et al.* (1990), figure courtesy of C.B. Eom, Bell Laboratories, USA.

tigations study the magnitude of the pre-edge peak of the oxygen $1s$ absorption K edge. Although a reduction of this peak is often interpreted as an indication of a locally reduced oxygen concentration, it is rather a signature of the reduced density of charge carriers (Nücker *et al.*, 1988, 1989; Zhu *et al.*, 1994; Babcock and Vargas, 1995; Zhu and Suenaga, 1995), which need not necessarily be due to an oxygen deficiency. It is an intriguing question whether the carrier density reduction does not occur for symmetric boundaries, as suggested by Fig. 16, because these boundaries are also known to have a limited critical current density (see Sec. V.B.1.).

Most grain boundaries in high- T_c films are composed of facets with typical lengths of less than 100 nm, as was shown for $\text{YBa}_2\text{Cu}_3\text{O}_{7-\delta}$ and BSCCO by TEM,⁴ by scanning electron microscopy (SEM) (Ayache *et al.*, 1998), by atomic force microscopy (AFM) (Mannhart, Hilgenkamp, *et al.*, 1996; Nesher and Ribak, 1997; Ayache *et al.*, 1998; Hawley, 2000), by scanning near-field optical microscopy (McDaniel *et al.*, 1997), and by laser scanning microscopy (Shadrin *et al.*, 1999). Grain-boundary faceting is clearly visible in the TEM images in Figs. 14 and 17, as well as in the AFM micrograph in Fig. 18. The facet orientations and dimensions depend on the grain-boundary configuration, the high- T_c compound, the substrate (Trøholt *et al.*, 1994; Jiang *et al.*, 1997, 1998; McDaniel *et al.*, 1997), and the conditions used for the film deposition. Faceting, which takes place in all

⁴TEM studies include those of Gao *et al.*, 1991; Jia *et al.*, 1992; Rosner *et al.*, 1992; Alarco *et al.*, 1993; Marshall and Eom, 1993; Kabius *et al.*, 1994; Trøholt *et al.*, 1994; Miller, Roberts, *et al.*, 1995; Seo *et al.*, 1995; Vuchic *et al.*, 1996; Ayache *et al.*, 1998; Li *et al.*, 1999c; Verbist *et al.*, 1999.

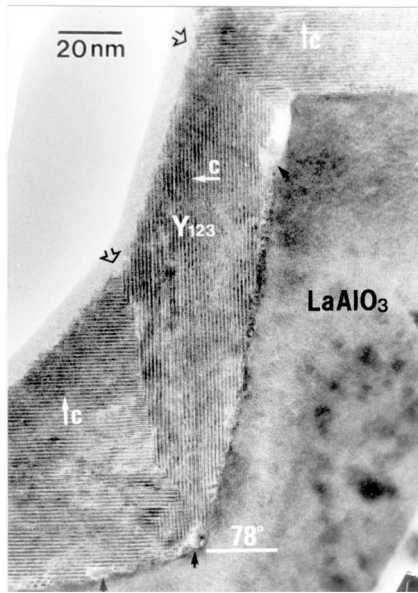


FIG. 15. Lattice fringe TEM image of a $\text{YBa}_2\text{Cu}_3\text{O}_{7-\delta}$ film grown over an ion-milled 78° step on a LaAlO_3 substrate. Two 90° boundaries are formed in the $\text{YBa}_2\text{Cu}_3\text{O}_{7-\delta}$ film, as indicated by the open arrows. Part of the step-edge $\text{YBa}_2\text{Cu}_3\text{O}_{7-\delta}$ film was etched away in the TEM preparation process. From Jia *et al.* (1992); figure courtesy of C.L. Jia and J. Schubert, Forschungszentrum Jülich, Germany.

three dimensions (Træholt *et al.*, 1994; Ayache *et al.*, 1998), is a consequence of the growth modes of the cuprates and is observed for grain boundaries fabricated with the bicrystal, biepitaxial, and step edge techniques. Several studies report that boundaries in cuprate thin

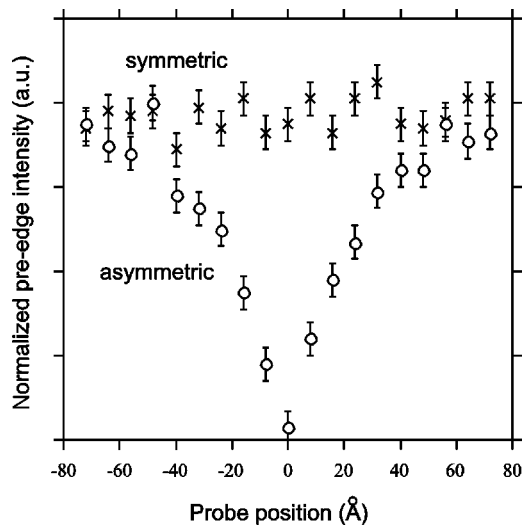


FIG. 16. Result of a high-resolution electron-energy-loss spectroscopy (EELS) measurement of the local hole concentration of a symmetric 36° near $\Sigma 5$ boundary and of an asymmetric 29° near $\Sigma 17$ boundary in a polycrystalline $\text{YBa}_2\text{Cu}_3\text{O}_{7-\delta}$ film. The figure shows the pre-edge intensity of the oxygen K edge for scans perpendicular to the grain boundary located at the zero position. From Browning *et al.* (1993); figure courtesy of N. Browning, Oak Ridge National Laboratory, USA.

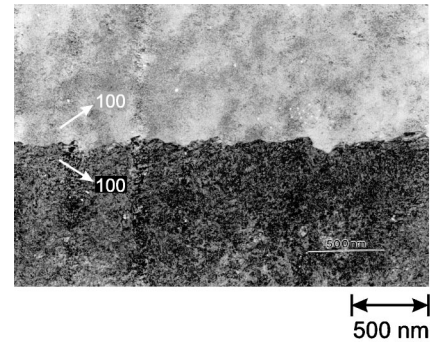


FIG. 17. Low-magnification plane-view image of a symmetric 67° [001]-tilt boundary in an $\text{YBa}_2\text{Cu}_3\text{O}_{7-\delta}$ film. The viewing direction is slightly tilted to improve the contrast between the two sides. From Træholt *et al.* (1994).

films grown on bicrystalline substrates largely consist of facets corresponding to the bicrystal misorientation and of facets associated with a low-index plane of one of the grains, such as (100), (010), or (110) (Gao *et al.*, 1991; Alarco *et al.*, 1993; Kabius *et al.*, 1994; Træholt *et al.*, 1994; Seo *et al.*, 1995; Tsu *et al.*, 1998). Owing to the faceting, at the surface of the high- T_c film the grain boundary meanders over a width that is usually comparable to the film thickness. Also, considerable deviations from the substrate grain-boundary position have been observed at the film-substrate interface (Træholt *et al.*, 1994).

Successful experiments have been undertaken to fabricate single-facet thin-film grain boundaries. It has been shown by a group at Argonne that larger facet dimensions are achieved by reducing the film deposition rate

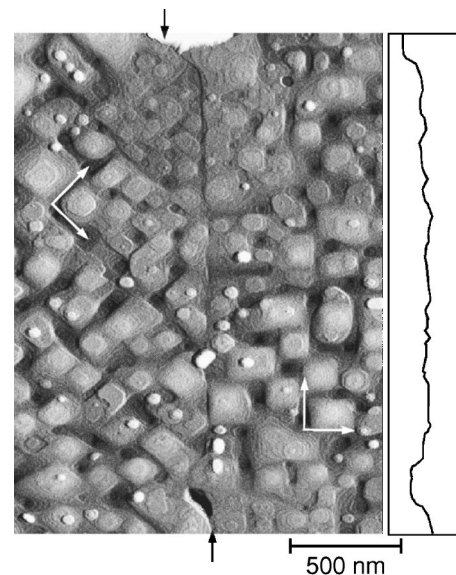


FIG. 18. Atomic force microscopy image of the surface of a ≈ 150 -nm-thick $\text{YBa}_2\text{Cu}_3\text{O}_{7-\delta}$ film with an asymmetric 45° [001]-tilt grain boundary. The orientation of the grains is revealed by the orientation of the growth islands. The location of the grain boundary is indicated by arrows. For clarity, the meandering path of the grain boundary has been redrawn at the right. From Mannhart, Hilgenkamp, *et al.* (1996).

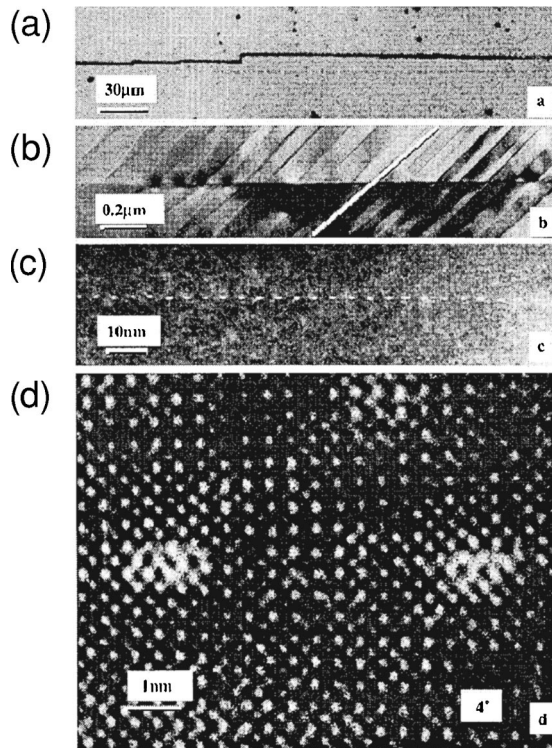


FIG. 19. Planar-view images of 4° [001]-tilt grain boundaries of a $\text{YBa}_2\text{Cu}_3\text{O}_{7-\delta}$ film grown by liquid-phase epitaxy: (a) optical micrograph; (b)–(d) TEM images. From Koshizuka *et al.* (2000); figure courtesy of N. Koshizuka, ISTE, Tokyo, Japan.

(Zhang, Miller, *et al.*, 1996). Impressive results have been reported from ISTE (Takagi *et al.*, 1999; Wen *et al.*, 1999; Koshizuka *et al.*, 2000), where single-facet grain boundaries over $50 \mu\text{m}$ are obtained in films grown by liquid-phase epitaxy on bicrystalline substrates (see Fig. 19). Furthermore, bulk bicrystals have been fabricated with amazingly flat grain boundaries by various techniques (St. Louis-Weber *et al.*, 1996; Todt *et al.*, 1996; Field *et al.*, 1997; Gray *et al.*, 1998).

It has been reported by a group at Brookhaven that [001]-twist boundaries in $\text{Bi}_2\text{Sr}_2\text{CaCu}_2\text{O}_{8+\delta}$ bicrystals can be microscopically flat and clean without impurities (Li *et al.*, 1999a, 1999b, 1999c). Figure 20 shows an example of such a boundary. The boundary interface plane was found to be the BiO layer, and this double BiO layer at the boundary appears to be the same as those in single crystals (Li *et al.*, 1999a).

V. TRANSPORT PROPERTIES OF GRAIN BOUNDARIES

A. Current-voltage characteristics

Figure 21 shows the current-voltage $I(V)$ characteristic of a 24° [001]-tilt boundary of $\text{YBa}_2\text{Cu}_3\text{O}_{7-\delta}$ at various temperatures, and Fig. 22 those of a 36.8° [001]-tilt boundary of $\text{Bi}_2\text{Sr}_2\text{Ca}_2\text{Cu}_3\text{O}_{10+\delta}$. These characteristics, which for all high- T_c compounds are typical for short [001]-tilt grain boundaries with misorientation angles between 15° and 45° , are those of strongly coupled, SNS-type Josephson junctions (Mannhart *et al.*, 1988).

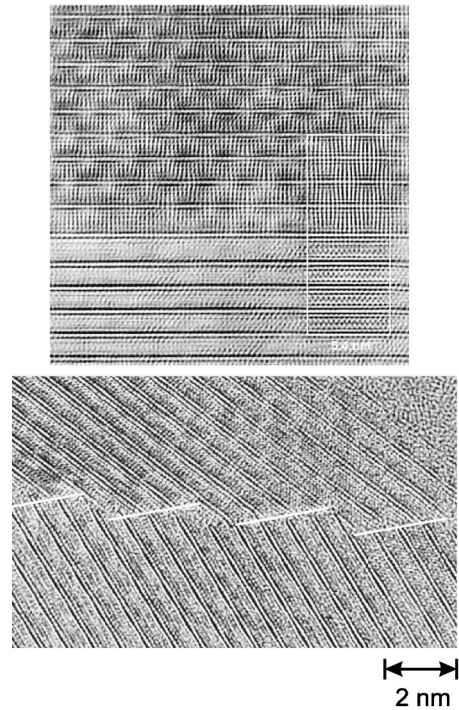


FIG. 20. Cross-section TEM images of bulk $\text{Bi}_2\text{Sr}_2\text{CaCu}_2\text{O}_{8+\delta}$ bicrystals: (a) 37.45° [001]-twist grain boundary. The top crystal is viewed along the a axis. (b) 30° non-basal-plane-faced tilt grain boundary with facets along the grain-boundary plane. The saw-toothed line is a guide for the eye to indicate the facets. The double Bi-O layer spacing shown is 15.3 \AA . From Li *et al.* (1999c); figure courtesy of Y. Zhu, Brookhaven National Laboratory, USA.

For long junctions, or for boundaries with large current densities, excess currents are frequently seen, but usually the characteristics follow the resistively shunted junction model (Gross, Chaudhari, *et al.*, 1990b). They also have been described quantitatively with the time-dependent Ginzburg-Landau equations (Andoh *et al.*,

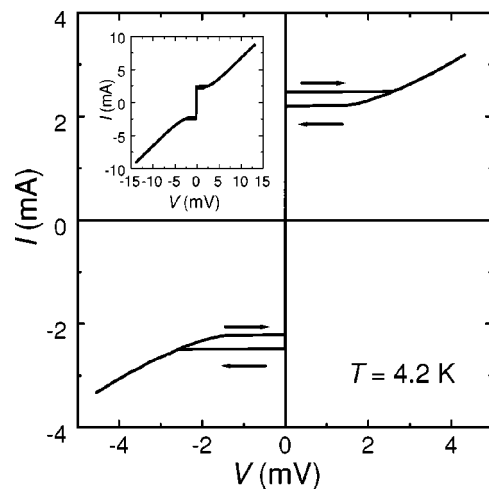


FIG. 21. Current-voltage characteristic of a $2.3\text{-}\mu\text{m}$ -wide bridge straddling a 24° [001]-tilt grain boundary in a 120-nm -thick $\text{YBa}_2\text{Cu}_3\text{O}_{7-\delta}$ film. The data were taken at 4.2 K . Figure courtesy of C. W. Schneider, Augsburg University, Germany.

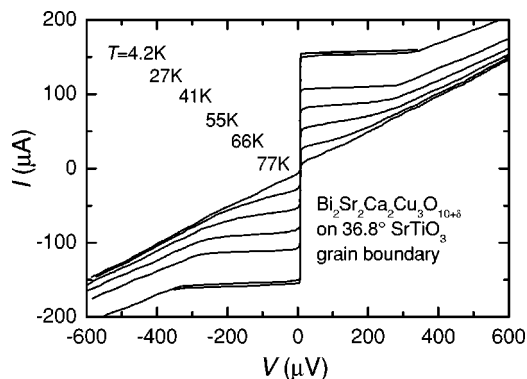


FIG. 22. $I(V)$ curves of a 36.8° [001]-tilt grain boundary in a $\text{Bi}_2\text{Sr}_2\text{Ca}_2\text{Cu}_3\text{O}_{10+\delta}$ film measured at various temperatures. From Frey *et al.* (1997); figure courtesy of H. Adrian and J.C. Martinez, Johannes Gutenberg-Universität, Mainz, Germany.

2000). Step-edge junctions and biepitaxial junctions show similar $I(V)$ dependencies (Lombardi *et al.*, 2000).

At voltages above 10 mV, various types of dependencies have been observed for the $I(V)$ characteristics of large-angle bicrystals. The conductance $\sigma(V) = dI/dV(V)$ has been found to increase linearly or quadratically with applied voltage V for well-oxidized (Mannhart, Gross, *et al.*, 1990; Ivanov *et al.*, 1996) and oxygen-deficient samples (Froehlich *et al.*, 1997a 1997b), respectively. Conductances that are constant up to voltages beyond 100 mV have been measured for doped and undoped grain boundaries in oxidized films (Ivanov, Stepansov, *et al.*, 1994; Hammerl *et al.*, 2000).

In the voltage range of a few millivolts, Fiske resonances are frequently found, as shown in Fig. 23 (Mannhart, Gross, *et al.*, 1989; Winkler *et al.*, 1994; Doderer *et al.*, 1995; Médiçi *et al.*, 1995; Moeckly *et al.*, 1995; Yi *et al.*, 1995; Elly *et al.*, 1997), which have been used to derive the grain-boundary capacitance (Tarte

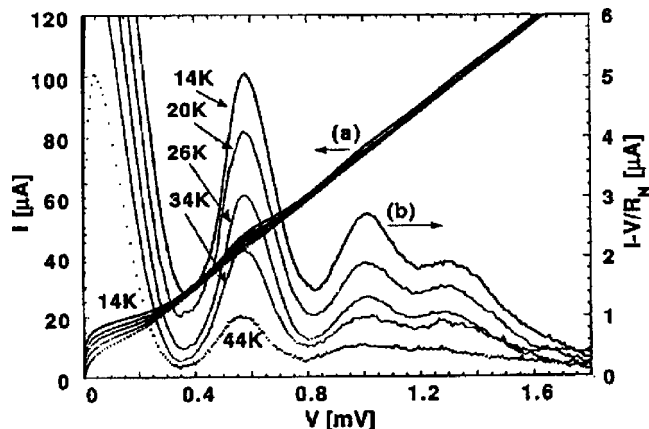


FIG. 23. Current-voltage characteristics of a 32° [001]-tilt $\text{YBa}_2\text{Cu}_3\text{O}_{7-\delta}$ bicrystal junction measured in a magnetic field of ~ 0.1 G for various temperatures: (a) the raw data; (b) data with the normal conductance subtracted. The characteristic shows clear Fiske resonances. From Winkler *et al.* (1994); figure courtesy of D. Winkler, Chalmers University of Technology, Göteborg, Sweden.

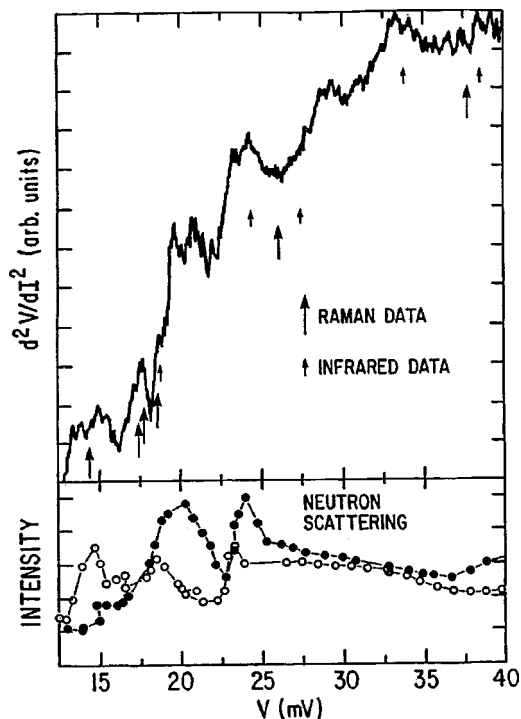


FIG. 24. The second derivative, d^2V/dI^2 , of the $I(V)$ characteristic of a 45° [001]-tilt grain-boundary junction in a $\text{YBa}_2\text{Cu}_3\text{O}_{7-\delta}$ film measured at 4.2 K. Shown for comparison are phonon data obtained by other techniques; the larger arrows indicate the positions of Raman lines, the smaller arrows infrared reflection lines and inelastic neutron data. From Chaudhari *et al.*, 1993; figure courtesy of P. Chaudhari and E. Sarnelli, IBM T.J. Watson Research Center, USA.

et al., 1997). The Fiske resonances suggest the presence of an insulating interface layer at large-angle [001]-tilt boundaries (Winkler *et al.*, 1994). The $I(V)$ characteristics have been discovered to show a rich and intriguing fine structure in the millivolt range, part of which has been attributed to phonon excitations, as displayed by Fig. 24 (Chaudhari, Dimos, and Mannhart, 1989; Chaudhari, Sarnelli, *et al.*, 1993). At very small voltages, anomalous conductance peaks centered at zero voltage, the so-called zero-bias anomalies, are observable in many high- T_c compounds. These anomalies are clearly shown by Fig. 25 (Froehlich *et al.*, 1997a, 1997b; Alff, Kleefisch, *et al.*, 1998). After initially being ascribed to Kondo scattering at magnetic impurities following the Anderson-Appelbaum mechanism (Froehlich *et al.*, 1997a, 1997b), these anomalies are now attributed to zero-energy states formed by Andreev-bound states caused by the predominantly $d_{x^2-y^2}$ pairing symmetry of the cuprates (Hu, 1994; Tanaka and Kashiwaya, 1995, 1996; Alff, Beck, *et al.*, 1998, for overviews see Kashiwaya and Tanaka, 2000 and Löfwander *et al.*, 2001). For $\text{Nd}_{1.85}\text{Ce}_{0.15}\text{CuO}_{4-y}$ such zero-bias anomalies have not been observed (see Fig. 25). The lack of the anomaly has been interpreted as evidence that the order parameter of $\text{Nd}_{1.85}\text{Ce}_{0.15}\text{CuO}_{4-y}$ has an s -wave symmetry (Schoop *et al.*, 1999), but could also be caused by other effects, such as strong disorder at the barrier layer.

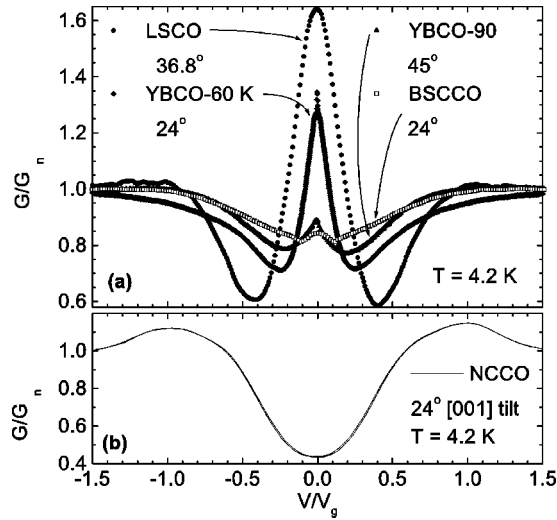


FIG. 25. Normalized conductance as a function of normalized voltage of [001]-tilt grain boundaries with various misorientations formed by the 60-K and 90-K phases of (a) $\text{YBa}_2\text{Cu}_3\text{O}_{7-\delta}$, $\text{Bi}_2\text{Sr}_2\text{CaCu}_2\text{O}_{8+\delta}$, $\text{La}_{1.85}\text{Sr}_{0.15}\text{CuO}_4$, and (b) $\text{Nd}_{1.85}\text{Ce}_{0.15}\text{CuO}_{4-y}$ at 4.2 K. From Alff, Beck, *et al.* (1998); figure courtesy of L. Alff, Universität zu Köln, Germany.

For misorientation angles below a transition angle of about 8° – 10° (Dimos *et al.*, 1988, 1990; Sarnelli, Testa, and Esposito, 1993; Heinig *et al.*, 1996; Redwing *et al.*, 1999), the exact value of which depends slightly on grain-boundary configuration, temperature, and compound, the $I(V)$ characteristics are determined by the flow of Abrikosov vortices along the grain boundaries (Dimos *et al.*, 1990; Heinig *et al.*, 1996; Díaz *et al.*, 1998b; Hogg *et al.*, 2001). This crossover in transport properties is clearly visible in Fig. 26, which shows the $I(V)$ characteristic of a 10° [001]-tilt $\text{YBa}_2\text{Cu}_3\text{O}_{7-\delta}$ grain boundary with Josephson behavior above 77 K and flux flow at lower temperatures.

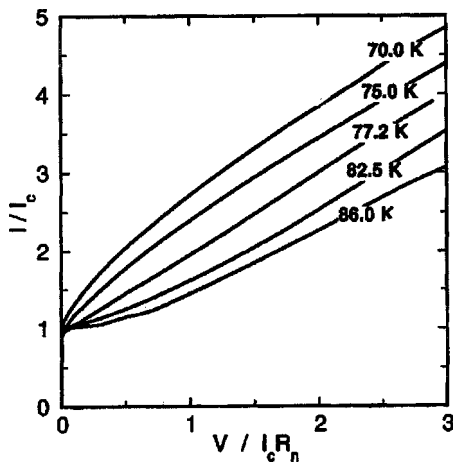


FIG. 26. Normalized current-voltage characteristic of a $10\text{-}\mu\text{m}$ -wide and 250-nm -thick 10° [001]-tilt grain boundary in an $\text{YBa}_2\text{Cu}_3\text{O}_{7-\delta}$ film at several temperatures. Note the change in curvature associated with the crossover from flux flow to Josephson junction behavior between 75 and 77.2 K. From Redwing *et al.* (1999); figure courtesy of M.S. Rzchowski, University of Wisconsin, USA.

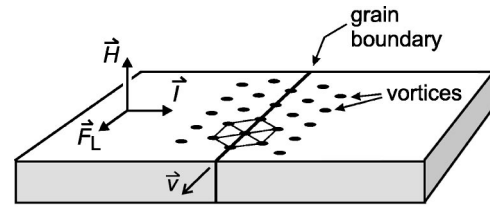


FIG. 27. Sketch of the hexagonal vortex lattice in the vicinity of a [001]-tilt grain boundary. For an applied field H within the plane of the grain boundary, vortices are pinned by dislocation cores in the boundary. However, when a current in excess of the critical one is applied, vortices in the grain boundary start to move with the velocity v due to the Lorentz force F_L directed along the grain boundary. After Díaz *et al.* (1998b).

In applied magnetic fields in the Tesla range, the $I(V)$ characteristics have been observed to be curved (Heinig *et al.*, 1996, 1999; Field *et al.*, 1997) or linear with residual currents (Díaz *et al.*, 1998b; Verebelyi *et al.*, 2000; Hogg *et al.*, 2001), the latter being referred to as non-Ohmic, linear differential (NOLD) behavior (Verebelyi *et al.*, 1999, 2000). In some cases even kinking of the $V(I)$ curves has been found (Hogg *et al.*, 2001). In this regime the critical current densities of long junctions are controlled by pinning of vortices at the facets of the boundaries, at the dislocations, and in large applied magnetic fields by the vortex lattice in the grains as illustrated in Fig. 27 (Gurevich and Cooley, 1994; Kasatkin *et al.*, 1997; Cai, Gurevich, *et al.*, 1998; Díaz *et al.*, 1998a; Gray *et al.*, 1998, 2000; Gurevich, 1999; Kim *et al.*, 2000; Hogg *et al.*, 2001). By using magneto-optical techniques, pinning of vortices has also been observed at antiphase boundaries (Jooss *et al.*, 1999; Jooss, Warthmann, *et al.*, 2000; Jooss, Warthmann, and Kronmüller, 2000).

B. Critical current density

1. Dependence on grain-boundary angle

One of the most intriguing aspects of grain boundaries is the strong dependence of their critical current density on the boundary misorientation angle θ . Already the first measurements on bicrystalline $\text{YBa}_2\text{Cu}_3\text{O}_{7-\delta}$ films revealed for [001]-tilt boundaries a pronounced decrease of J_c as θ was increased from 0° to 45° ; see Fig. 28 (Dimos *et al.*, 1988). In bicrystalline films, for a given grain-boundary symmetry, this reduction closely follows an exponential dependence (Ivanov *et al.*, 1991; Alarco *et al.*, 1994; Heinig *et al.*, 1996; Klushin *et al.*, 1997; Hilgenkamp and Mannhart, 1998b; Holzapfel *et al.*, 2000): This is shown by Fig. 29, which presents the data of Ivanov *et al.* (1991), and by Fig. 30, in which a collection of data published in the literature is compiled. Data showing an exponential $J_c(\theta)$ dependence and critical current densities of [100]-tilt and [100]-twist boundaries have also been published by Gross and Mayer (1991) and Gross (1994). It seems that many of these data are reproductions of data given by Dimos *et al.* (1990) and Ivanov *et al.* (1991). As is obvious from Fig. 30, which comprises data from symmetric and asymmetric boundaries in films

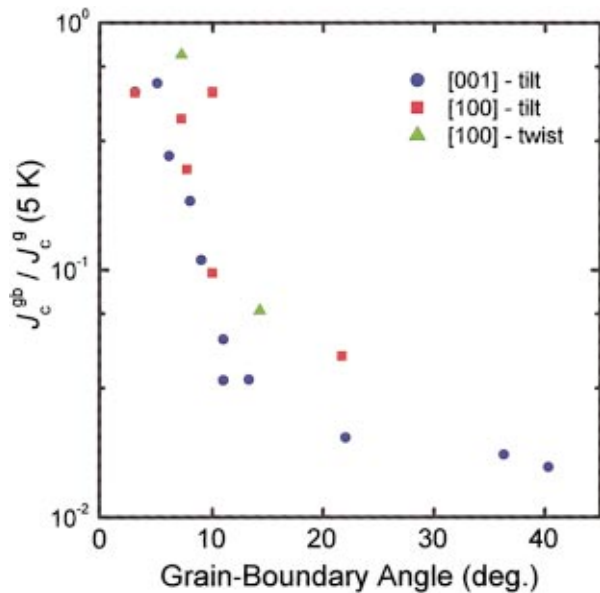


FIG. 28. Ratio of the intergrain and intragrain critical current densities of grain boundaries in bicrystalline $\text{YBa}_2\text{Cu}_3\text{O}_{7-\delta}$ films as a function of the misorientation angle. The various symbols distinguish the primary component of the misorientation. From Dimos *et al.* (1990) [Color].

grown under different conditions and on various substrates, the critical current densities show a significant spread (see also Shadrin *et al.*, 2001). For films grown under identical conditions, this spread is considerably smaller. Remarkably, the critical current densities of low- Σ [001]-tilt boundaries were also found to follow the exponential $J_c(\theta)$ dependence closely. This dependence was found in studies of single-faceted grain boundaries

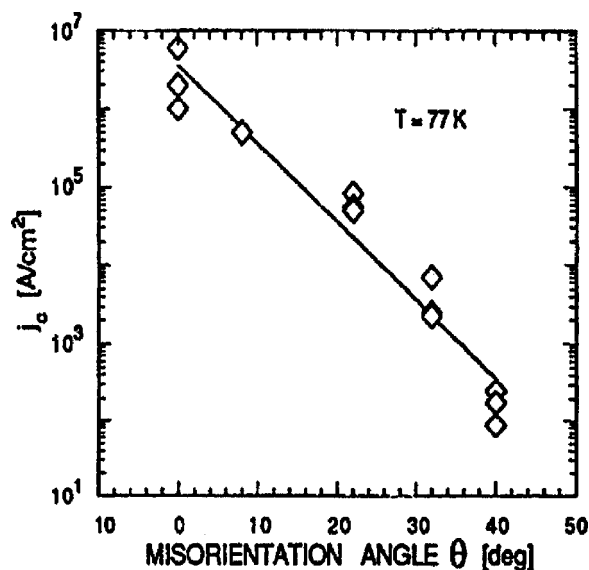


FIG. 29. Critical current densities of asymmetric [001]-tilt grain boundaries in $\text{YBa}_2\text{Cu}_3\text{O}_{7-\delta}$ films grown on Y-ZrO_2 bicrystal substrates as a function of grain-boundary angle. The data were measured at 77 K. From Ivanov *et al.* (1991); figure courtesy of Z. G. Ivanov and T. Claeson, Chalmers University of Technology, Göteborg, Sweden.

(Wen *et al.*, 2000) and in experiments with polycrystalline samples (Strikovsky *et al.*, 1992). Recently, a saturation of the critical current density has been reported for tilt angles below $\sim 2^\circ$ (Verebelyi *et al.*, 2000), which has been associated with the twin boundaries in the grains, across which the crystal main axes are misaligned by 0.9° (Christen, 2000). Bicrystalline $\text{YBa}_2\text{Cu}_3\text{O}_{7-\delta}$ films grown by liquid phase epitaxy displayed a saturation for misorientation angles of less than $\sim 12^\circ$, which has been attributed to reduced pinning of vortices in the grains, which have an unusually small dislocation density (Koshizuka *et al.*, 2000). Also it was found that close to T_c the critical current density of a 4° boundary in a submicron-wide bridge approached the pair-breaking limit of $\text{YBa}_2\text{Cu}_3\text{O}_{7-\delta}$ films (Ivanov, Fogel, *et al.*, 1994).

Similar angular dependencies of the grain boundary J_c have been reported for all other high- T_c superconductors of which grain-boundary properties have been analyzed.⁵ For bicrystalline $\text{Bi}_2\text{Sr}_2\text{CaCu}_2\text{O}_{8+\delta}$ and $\text{YBa}_2\text{Cu}_3\text{O}_{7-\delta}$ films it has been explicitly noted that the angular dependencies of J_c normalized to the intragrain critical current density are identical, as depicted in Fig. 31 (Amrein *et al.*, 1995). Bicrystalline samples of $\text{YBa}_2\text{Cu}_4\text{O}_8$ have apparently not been fabricated yet. Magnetic susceptibility measurements and local chemical analyses of the grain boundaries in polycrystalline $\text{YBa}_2\text{Cu}_4\text{O}_8$ have revealed that in this compound the grain boundaries form weak links as well (Wang *et al.*, 1993). As already noted, for the electron-doped $\text{Nd}_{2-x}\text{Ce}_x\text{CuO}_4$ superconductors, an exponential angular dependence of J_c has also been reported, which is illustrated by Fig. 32. The measured critical current densities and characteristic voltages are, however, considerably lower than those reported for the other high- T_c cuprates. Frequently, J_c is even immeasurably small. This may reflect the fact that it is difficult to fabricate $\text{Nd}_{2-x}\text{Ce}_x\text{CuO}_4$ grain boundaries with the desired oxygen concentration or small defect density.

Ivanov and co-workers revealed that in addition to the misorientation angle θ , the orientation of the main crystal axes with respect to the grain boundary has a decisive influence on the critical current density (Ivanov *et al.*, 1998). Experiments with $\theta=32^\circ$ [001]-tilt boundaries performed at 4.2 K displayed a reduction of J_c by a

⁵These superconductors include doped La_2CuO_4 (Kawasaki *et al.*, 1993; Beck *et al.*, 1996), Ag-doped $\text{YBa}_2\text{Cu}_3\text{O}_{7-\delta}$ (Holzapfel *et al.*, 2000), $\text{NdBa}_2\text{Cu}_3\text{O}_{7-\delta}$ (Romans *et al.*, 2001), $\text{Bi}_2\text{Sr}_2\text{CaCu}_2\text{O}_{8+\delta}$ (Tomita *et al.*, 1990; Mayer *et al.*, 1993; Amrein *et al.*, 1995; K. Lee *et al.*, 1996), $\text{Bi}_2\text{Sr}_2\text{Ca}_2\text{Cu}_3\text{O}_{10+\delta}$ (Ohbayashi *et al.*, 1995; Yan *et al.*, 1995; Frey *et al.*, 1996b; Takami *et al.*, 1996; Yoshida *et al.*, 1997; Attenberger *et al.*, 2001), $\text{Tl}_2\text{Ba}_2\text{CaCu}_2\text{O}_{8+x}$ (Cardona *et al.*, 1993; Sarnelli *et al.*, 1994; Y. F. Chen *et al.*, 1996; Weaver *et al.*, 1996), $\text{Tl}_1\text{Ba}_2\text{Ca}_2\text{Cu}_3\text{O}_x$ (Nabatame *et al.*, 1994), $\text{HgBa}_2\text{CaCu}_2\text{O}_{6+\delta}$ (Gupta *et al.*, 1994; Tsukamoto *et al.*, 1998; Yu *et al.*, 1999; Inoue *et al.*, 2000; Adachi *et al.*, 2001), and $\text{Nd}_{2-x}\text{Ce}_x\text{CuO}_4$ (Kawasaki *et al.*, 1993; Kussmaul, Tedrow, and Gupta, 1993; Kleefisch *et al.*, 1998; Schoop *et al.*, 1999; Woods *et al.*, 1999).

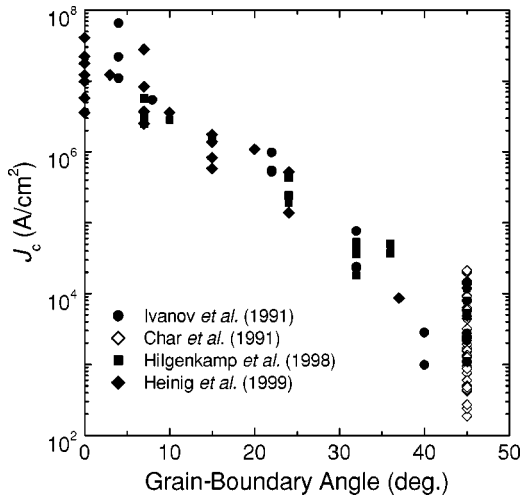


FIG. 30. Critical current densities of [001]-tilt grain boundaries in $\text{YBa}_2\text{Cu}_3\text{O}_{7-\delta}$ films as a function of tilt angle. The data, compiled from the literature as indicated, were measured at 4.2 K, except for those of Ivanov *et al.* (1991). As the latter were measured at 77 K, these current densities were multiplied by a factor of 10.9, which was obtained from the temperature dependence of I_c (see Fig. 36). The data of Char *et al.* were measured with biepitaxial junctions, the others with bicrystalline junctions.

factor of 1000 below the exponential limit if the grain-boundary orientation was altered, which is presented in Fig. 33. Similar results were obtained by the Naples group, who report a variation of J_c and of the $I_c R_n$ product by two orders of magnitude for a change of the in-plane orientation of biepitaxial 45° [100]-tilt boundaries (Tafari *et al.*, 2000; Sarnelli *et al.*, 2001; Sarnelli and Testa, 2001), by a group at Korea University, who measured a J_c variation by a factor of 3 for step-edge junctions (Lee and Hwang, 2000; S. G. Lee *et al.*, 2000), and by a Columbia-IBM-Houston collaboration studying grain-boundary transport by scanning SQUID microscopy (Chan, 2000; Tsai *et al.*, 2001). The critical current densities of nominally symmetric and asymmetric [001]-tilt boundaries were also measured as a function of the boundary angle (Klushin *et al.*, 1997; Hilgenkamp *et al.*, 1998a, 1998b). These measurements revealed that the J_c of symmetric boundaries slightly exceeds the J_c of the asymmetric ones.

Film grain boundaries with misorientations other than [001] tilt or with misorientation angles greater than 45° have been investigated in only a few cases. Bicrystals with [100]-twist and [100]-tilt boundaries were explored by Dimos *et al.* (1990), who found that their critical current density, normalized to the one of the adjacent grains, shows the same angular dependence as the one of the [001]-tilt boundaries. These early measurements were recently repeated by Goetz *et al.*, who confirmed that the misorientation dependence of J_c of low-angle [100]- and [001]-tilt boundaries are identical if the CuO_2 planes of the [100]-tilt boundaries are tilted with positive ϕ values. Here we use the notation of Fig. 2 (Götz, 2000; Goetz *et al.*, 2001). These data are displayed in Fig. 34. As also disclosed by this figure, for [100]-twist bound-

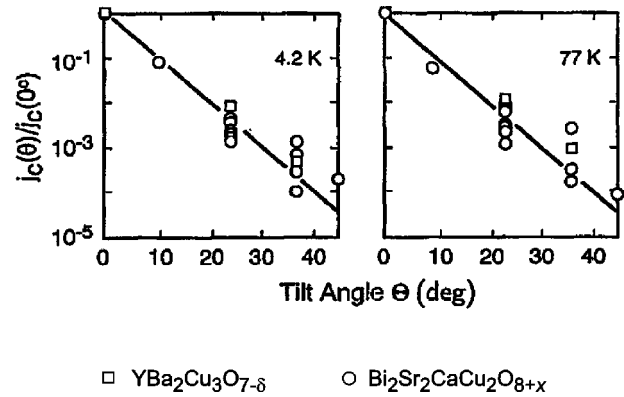


FIG. 31. Ratio of the intergrain and intragrain critical current densities as a function of misorientation angle for bicrystalline [001]-tilt $\text{Bi}_2\text{Sr}_2\text{CaCu}_2\text{O}_{8+x}$ (circles) and $\text{YBa}_2\text{Cu}_3\text{O}_{7-\delta}$ films (squares). From Amrein *et al.* (1995); figure courtesy of L. Schultz, Siemens, Germany.

aries the exponential reduction of J_c with γ was found to be even stronger (Götz, 2000; Goetz *et al.*, 2001). Poppe and co-workers reported that symmetric 24° [100]-tilt bicrystals with “negative” tilt angles ϕ have a smaller reduction of J_c , reaching 2×10^6 A/cm 2 at 4.2 K (Poppe *et al.*, 2001).

The first investigations of 90° grain boundaries were performed by Chan and colleagues at Bellcore (Chan *et al.*, 1989, 1990; Chan, 1994), who explored $\text{YBa}_2\text{Cu}_3\text{O}_{7-\delta}$ layers grown on (014) SrTiO_3 and discovered that the 90° boundaries formed in the polycrystalline films have critical current densities as high as 2×10^6 A/cm 2 at 77 K. Similar experiments were performed by the Stanford group (Eom *et al.*, 1991; Lew *et al.*, 1994), who reported that 90° [010]-twist grain boundaries provided strong coupling with critical current densities exceeding 10^6 A/cm 2 at 4.2 K, while 90° [010] basal-plane-faced tilt boundaries had weak-

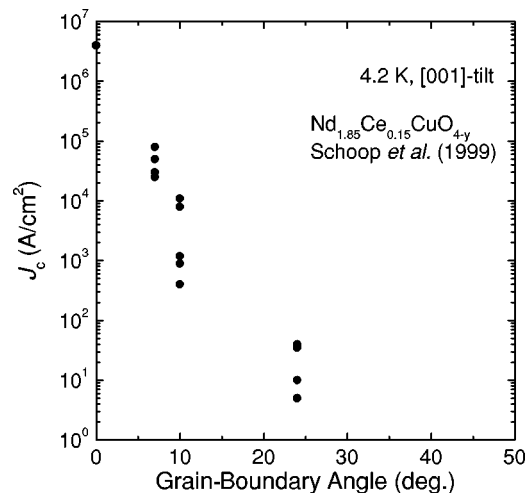


FIG. 32. Critical current densities of 2–20- μm -wide symmetric [001]-tilt grain boundaries in bicrystalline $\text{Nd}_{1.85}\text{Ce}_{0.15}\text{CuO}_{4-y}$ films as a function of tilt angle. The data were measured at 4.2 K. After Schoop *et al.* (1999).

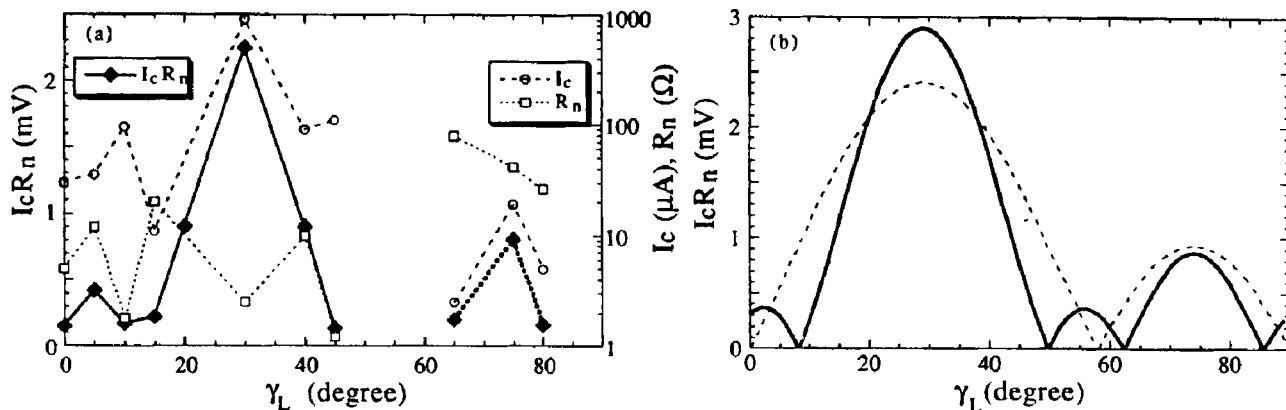


FIG. 33. Critical current I_c , normal-state resistance R_n , and characteristic voltage $I_c R_n$ plotted as a function of the fan angle γ_l for 7- μm -wide 32° [001]-tilt bicrystalline grain boundaries in 240-nm-thick $\text{YBa}_2\text{Cu}_3\text{O}_{7-\delta}$ films measured at 4.2 K. The angle γ_l is defined as the angle between the [110] direction of one grain and the grain-boundary normal. From Ivanov *et al.* (1998); figure courtesy of Z.G. Ivanov, Chalmers University of Technology, Göteborg, Sweden.

link character with a J_c of about 3×10^4 A/cm² at 4.2 K. Extended studies of basal-plane-faced tilt boundaries have also been carried out by using polycrystalline films (Moeckly and Buhrman, 1994; Ishimaru *et al.*, 1995, 1997; Yang *et al.*, 1999). Using a modified biepitaxial technology, the Naples group fabricated 45° [100]-tilt and twist junctions in $\text{YBa}_2\text{Cu}_3\text{O}_{7-\delta}$ films and found current densities of $\sim 10^2$ A/cm² and 10^3 A/cm²– 3×10^4 A/cm², respectively, at 4.2 K (Di Chiara *et al.*, 1997; Sarnelli, Carillo, *et al.*, 2001).

A large number of careful J_c measurements were performed on bulk bicrystals as well. $\text{YBa}_2\text{Cu}_3\text{O}_{7-\delta}$ grain boundaries were explored by the groups working in Madison (Babcock, Cai, *et al.*, 1990; Larbalestier *et al.*, 1991; Wang *et al.*, 1994; Field *et al.*, 1997), Houston

(Nilsson-Mellbin and Salama, 1994a, 1994b; Parikh *et al.*, 1994; Du *et al.*, 1998; Salama *et al.*, 2000), Columbia (Chan, 1994), Argonne (St. Louis-Weber *et al.*, 1996; Todt *et al.*, 1996; Field *et al.*, 2001), and Paris (Laval *et al.*, 1996). Detailed studies of [001]-twist $\text{Bi}_2\text{Sr}_2\text{CaCu}_2\text{O}_{8+\delta}$ grain boundaries were done at the Brookhaven National Laboratory (Zhu *et al.*, 1998; Li *et al.*, 1999a). In some of these experiments the measured angular dependence of J_c differed significantly from the angular dependence of film bicrystals. In several cases strong coupling or high critical current densities were reported for large-angle grain boundaries (Babcock, Cai, *et al.*, 1990; Hwang *et al.*, 1990; Babcock and Larbalestier, 1994; Chan, 1994; Parikh *et al.*, 1994; Wang *et al.*, 1994; Du *et al.*, 1998; Salama *et al.*, 2000), as were critical current densities comparable for intergrain and intragrain transport (Laval *et al.*, 1996; Zhu *et al.*, 1998; Li *et al.*, 1999a, 1999b), or intergrain critical currents independent of the misorientation angle (Zhu *et al.*, 1998; Li *et al.*, 1999b). To the best of our knowledge, in all these experiments the critical current densities in absolute numbers were limited to values well below those that had been achieved in the corresponding film boundaries. Therefore it is suggested that, at least in some studies of bulk samples, self-field effects or very small intragrain critical current densities prohibit the measurement of the grain boundary J_c . That this is the case for the $\text{Bi}_2\text{Sr}_2\text{CaCu}_2\text{O}_{8+\delta}$ twist boundaries described above (Zhu *et al.*, 1998; Li *et al.*, 1999b) has been confirmed by Li *et al.* (1999a, 1999c). Recent cross-whisker studies revealed indeed a strongly angular-dependent J_c for BiSrCaCuO [001]-twist boundaries (Tachiki and Machida, 2001).

Owing to its relevance to the fabrication of wires and tapes, the field of grain-boundary critical current densities in bulk samples is very active and developing rapidly. Review articles of the work on bulk bicrystals have been provided by Babcock and Larbalestier (1994), Chan (1994), Babcock and Vargas (1995), Cai and Zhu (1998), and Gray *et al.* (2000).

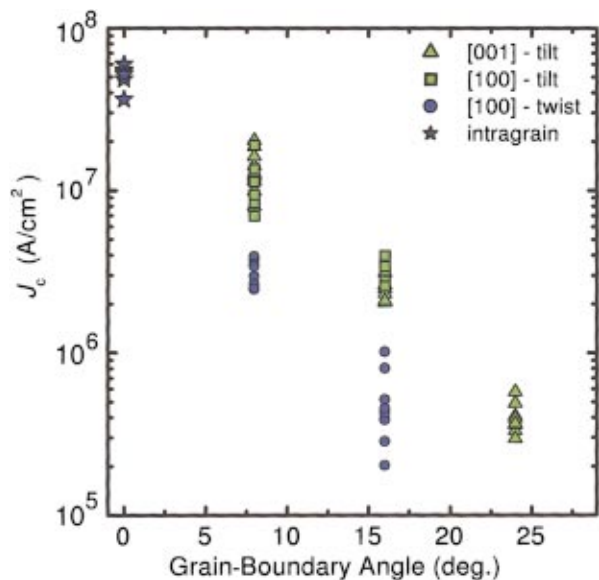


FIG. 34. Critical current densities of bicrystalline grain boundaries in $\text{YBa}_2\text{Cu}_3\text{O}_{7-\delta}$ films with various configurations as a function of the misorientation angle. The data were measured at 4.2 K. From Götz (2000); figure courtesy of B. Götz, Augsburg University, Germany [Color].

In the early days of high- T_c superconductivity, twin boundaries were suspected of forming intragranular weak links. As epitaxial $\text{YBa}_2\text{Cu}_3\text{O}_{7-\delta}$ films are highly twinned but not weakly linked, it is obvious that these twin boundaries are not Josephson junctions but can be crossed by supercurrents with densities of several 10^6 A/cm² at 77 K. Using low-temperature scanning tunneling spectroscopy, the critical current density along a twin boundary has also been measured. These studies, performed by analyzing the difference in vortex density of the domains forming the twin boundary (see Fig. 35; Maggio-Aprile *et al.*, 1997), revealed that the local critical current density for current flow along the twin boundary even approaches the depairing limit.

2. Temperature dependence of the critical currents

As a function of temperature, J_c changes almost linearly over a wide range (see Fig. 36) (Mannhart *et al.*, 1988). Typically, for $\text{YBa}_2\text{Cu}_3\text{O}_{7-\delta}$, at 77 K the critical current density is a factor of 10 smaller than at 4.2 K. The Chalmers group has discovered that the J_c of some asymmetric 45° grain boundaries (0°/45°) shows a pronounced maximum of the critical current density below 4.2 K. For asymmetric 32° boundaries (37°/−5°), a minimum was seen at even lower temperatures (Alarco *et al.*, 1994; Claeson, 1999). This intriguing behavior follows naturally from superconducting/semiconducting/superconducting junction models (Ivanov *et al.*, 1993). To explain this temperature dependence it has been further suggested that part of the grain-boundary current tunnels via midgap states. For symmetric 45° boundaries, Il'ichev *et al.* (2001) observed a minimum of I_c at a temperature of about 10 K, below which a strong second harmonic of the current-phase relation was measured.

At higher temperatures, for large-angle grain boundaries operated close to T_c , the thermal energy exceeds the Josephson coupling energy, causing thermally activated phase-slip processes (Tinkham, 1989), as described in the Ambegaokar-Halperin model (Ambegaokar and Halperin, 1969). This model has been used to describe the foot of the $R(T)$ curve displayed by grain-boundary junctions just below T_c and to deduce the value of I_c , as if it were unaffected by thermal noise (Gross, Chaudhari, *et al.*, 1990a; Lin *et al.*, 1996). Similar results were obtained in measurements of the current-voltage characteristics close to T_c performed over four decades (Steel *et al.*, 1996). Differing from the conventional SIS Josephson tunneling behavior, the critical current varied as $I_c(T) \sim (1 - T/T_c)^2$, complying with an SNS model (Steel *et al.*, 1996).

3. Magnetic-field dependence of the critical currents

The critical current of a grain boundary exhibits an intriguing magnetic-field behavior, which strongly depends on the misorientation angle, as shown in Fig. 37. In low-angle grain boundaries, which are limited by flux creep, I_c is rather insensitive to an applied field—these boundaries are strongly coupled. For [001]-tilt film bicrystals with boundary angles of $\sim 8^\circ$ or a little higher,

Fraunhofer-like magnetic-field dependencies with only small distortions are observed (Humphreys and Edwards, 1993; Neshor and Ribak, 1997). With increasing misorientation angle the distortions become more pronounced and, as illustrated in Fig. 37, develop for faceted asymmetric 45° boundaries into highly anomalous patterns (Copetti *et al.*, 1995; Hilgenkamp, Mannhart, and Mayer, 1996; Mannhart, Mayer, and Hilgenkamp, 1996; Neils and Van Harlingen, 2002). This characteristic behavior is caused by the grain-boundary microstructure and the $d_{x^2-y^2}$ -wave-pairing symmetry of the high- T_c cuprates. Unfaceted, asymmetric 45° boundaries ($\{100\}/\{110\}$ interfaces) grown by liquid-phase epitaxy were found to have fairly regular Fraunhofer patterns (Eltsev *et al.*, 2001). For such 45° $\{100\}/\{110\}$ boundaries, the $I_c(H)$ dependencies were also calculated. Calculations based on the assumption that the predominant component of the tunneling current flows via d -wave symmetry-induced midgap states, the energies of which shift as a function of applied magnetic field, also predict anomalous $I_c(H)$ characteristics for unafaceted boundaries (Yan and Hu, 1999).

For faceted boundaries with J_c alternating along the grain-boundary line, the $I_c(H)$ dependence and the behavior of Josephson vortices has been analyzed by Mints and Kogan (1997), Mints (1998), and Mints and Papiashvili (2000, 2001). Intriguingly, these authors foresee the existence of fractional Josephson vortices at long grain boundaries. Within a given 45° [001]-tilt junction two types of these fractional vortices may exist, with magnetic flux Φ_i complying with $\Phi_1 + \Phi_2 = \Phi_0$ (Mints, 1998; Mints and Papiashvili, 2001).

Neils and Van Harlingen (2002) used the $I_c(H)$ dependence of 45° $\{100\}/\{110\}$ boundaries to deduce the order-parameter symmetry of $\text{YBa}_2\text{Cu}_3\text{O}_{7-\delta}$ close to the boundary and found a pure $d_{x^2-y^2}$ component with no measurable complex admixture.

Carmody and collaborators developed a phase-retrieval algorithm to determine the spatial dependence of J_c from experimentally observed $I_c(H)$ dependencies (Carmody *et al.*, 1999, 2000a, 2000b). Depending on the grain boundary analyzed, highly nonuniform critical current densities along the boundaries were found in these studies.

At field strengths above several hundred Gauss, the $I_c(H)$ behavior of the grain boundaries becomes hysteretic due to flux trapping inside the grains and pinning of grain-boundary vortices by these flux lines (Dimos *et al.*, 1990; Däumling *et al.*, 1992; Gurevich and Cooley, 1994; Hinaus *et al.*, 1997; Gray *et al.*, 2000; Kim *et al.*, 2000). The reported results, which seem to be sample-dependent, differ in details. Studying bicrystalline films, the IBM group found a small but relatively constant J_c in fields up to 5 T for 25° and 37° grain boundaries (Däumling *et al.*, 1992; Sarnelli, Chaudhari, and Lacay, 1993), which in some cases even increased for larger fields as presented in Fig. 38 (Däumling *et al.*, 1992). A relatively constant $I_c(H)$ dependence of 15° and 24° boundaries at high fields was also found by the Oak

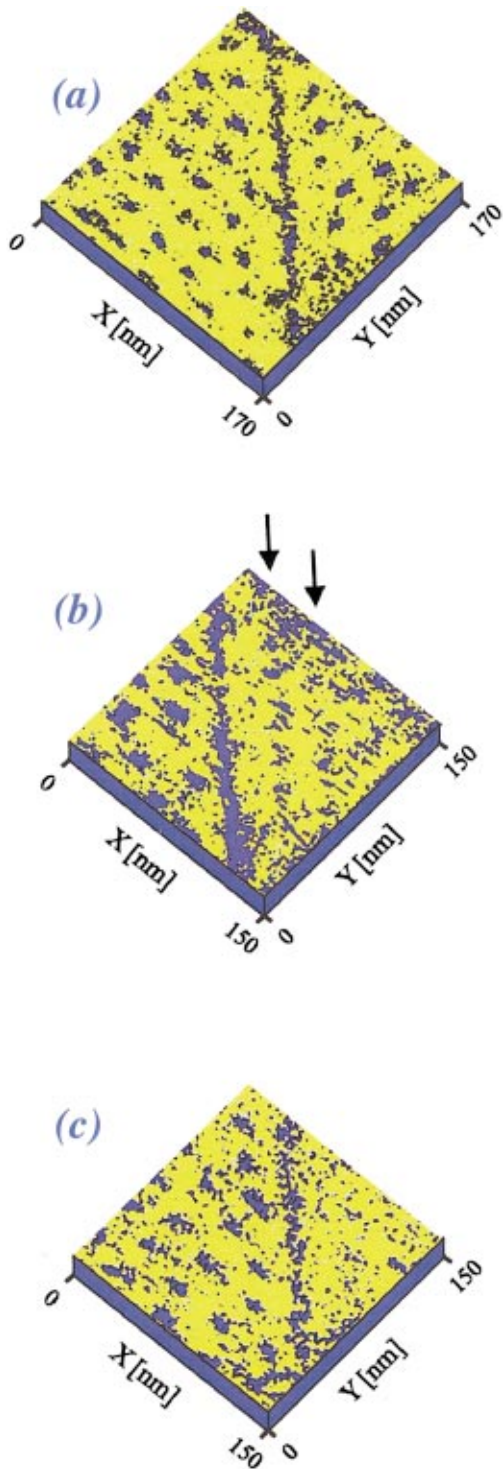


FIG. 35. Spectroscopic scanning tunneling microscopy images of the vortex lattice on the (001) surface of a YBa₂Cu₃O_{7-δ} single crystal, with magnetic field applied parallel to the c axis. One twin boundary extends through the micrographs from top to bottom, separating two crystal domains. (a) Image taken at 3 T (field cooled). Both domains of the crystal are filled with a nearly equal density of flux lines. The 90° rotation of the ab -plane anisotropy is observed across the twin boundary. (b) Same area taken 12 h after the field was reduced from 3 to 1.5 T. The arrows indicate the vortex movements observed in the domain to the right. (c) Three days after the field reduction, no more flux lines can be detected throughout the domain to the right over at least 80 nm. The images give clear evidence of a large pinning strength for motion of vortices perpendicular across a twin boundary. From Maggio-Aprile *et al.* (1997); figure courtesy of I. Maggio-Aprile and Ø. Fischer, Université de Genève [Color].

Ridge group, as shown by Fig. 39 (Verebelyi *et al.*, 1999). This group furthermore reported that at 77 K and for fields applied parallel to the c axes, the grain boundary J_c and the grain J_c become indistinguishable for misorientation angles smaller than $\sim 4.5^\circ$ and fields above 3 T, as also displayed in Fig. 39 (Verebelyi *et al.*, 2000). Peaks in the $I_c(H)$ dependence and hysteretic behavior were reported for bulk bicrystals, too (Kim *et al.*, 2000). For 24° [001]-tilt film boundaries, a continuously decreasing I_c was measured at fields up to 12 T (Froehlich *et al.*, 1995; Holzapfel *et al.*, 2000).

It should be pointed out that due to flux focusing by the abutting grains, the local flux density at the grain boundary exceeds the macroscopic flux density by the flux focusing factor, as has been analyzed in detail by Rosenthal *et al.* (1991) and Humphreys *et al.* (1993). This flux focusing factor may easily reach values of 5 to 10, depending in a complicated way on temperature and magnetic field, and leads to an inhomogeneous flux distribution along the junction. Therefore the local value of the applied magnetic field is well known only in exceptional cases, creating difficulties for experiments that re-

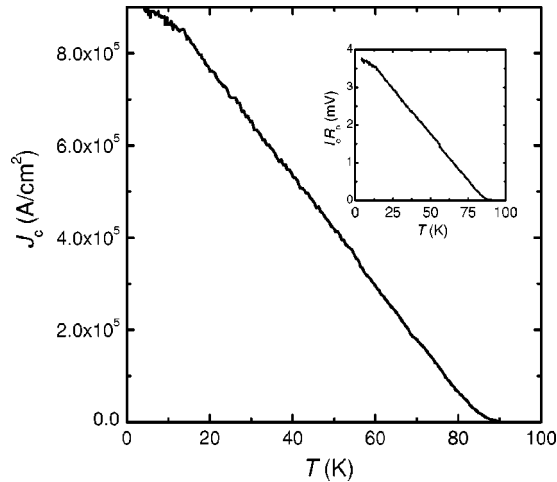


FIG. 36. Temperature dependence of the critical current of the 2.3- μm -wide bridge straddling a 24° [001]-tilt grain boundary in a 120-nm-thick $\text{YBa}_2\text{Cu}_3\text{O}_{7-\delta}$ film shown in Fig. 21. Figure courtesy of C. W. Schneider, Augsburg University, Germany.

quire knowledge of its exact number (see, for example, Froehlich *et al.*, 1994, 1996).

C. Current-phase relation

The relation between the Josephson current and the phase difference across the junction $I(\varphi)$, which is arguably the most fundamental property of any Josephson junction, has been measured by using rf SQUIDS (Il'ichev *et al.*, 1998). According to these studies, the current-phase relation of $\text{YBa}_2\text{Cu}_3\text{O}_{7-\delta}$ [001]-tilt grain boundaries with a misorientation of 24° is essentially sinusoidal, as is also reported in other work (Ovsyannikov *et al.*, 2000). In contrast, as shown by Fig. 40, for 45° [001]-tilt boundaries nonsinusoidal current-phase relations are found, which may show a π -periodic component (Il'ichev *et al.*, 1998, 1999a, 2001). In some asymmetric 45° [001]-tilt junctions, the π component has been observed to be dominant (Il'ichev *et al.*, 1999b, 2000). All these studies were performed on grain boundaries in $\text{YBa}_2\text{Cu}_3\text{O}_{7-\delta}$ films.

D. Normal-state resistivity

Figure 41 displays the normal-state interface resistivities $R_n A$ measured for bicrystal junctions of various high- T_c superconductors at 4.2 K as a function of misorientation angle θ . Here, R_n refers to the resistance shown by the grain boundaries biased with a current far exceeding I_c , and A is the cross-sectional area of the junction. The resistivities are similar at 77 K, with variations of $R_n A$ in the 10% range being observed as a function of temperature (Ijsselsteijn *et al.*, 1994; Nicoletti *et al.*, 1997a; Redwing *et al.*, 1999; Verebelyi *et al.*, 1999). If θ is enhanced from 15° to 45°, the specific interface resistivity rises by a factor of about 20. These values are typical for grain boundaries in films (Dimos *et al.*, 1990; Hilgenkamp and Mannhart, 1998b; Mannhart and

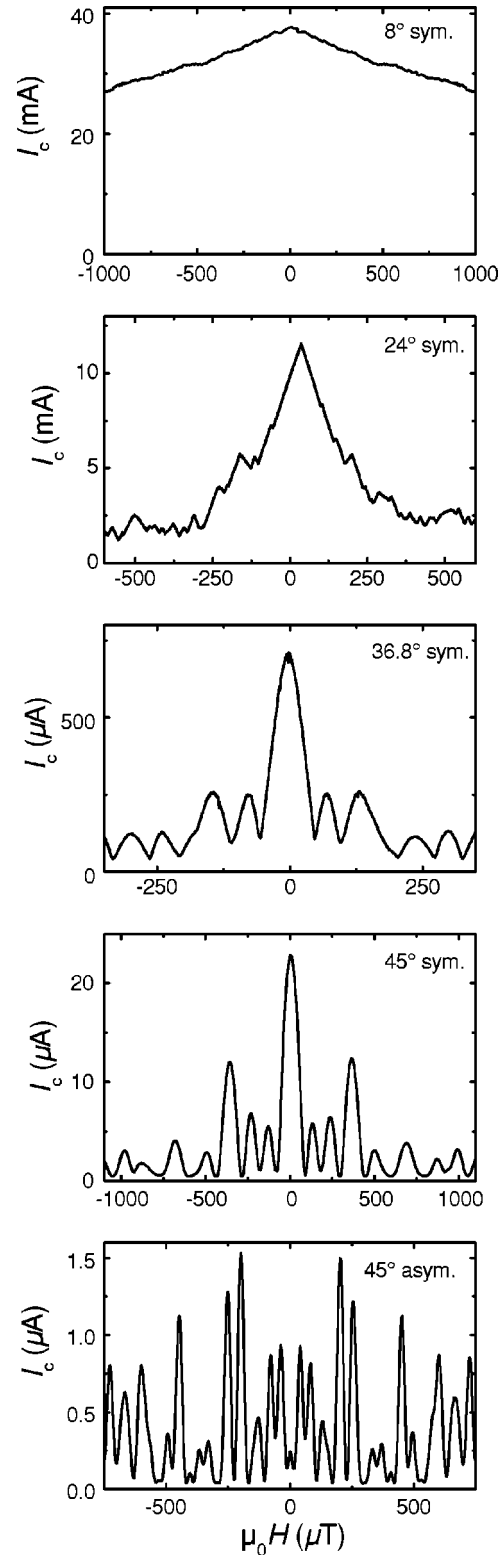


FIG. 37. Critical currents of five [001]-tilt grain-boundary junctions of various misorientations in ~ 120 -nm-thick (top four) and ~ 40 -nm-thick (bottom, 45° asym.) $\text{YBa}_2\text{Cu}_3\text{O}_{7-\delta}$ films plotted as a function of applied magnetic field. The magnetic field is oriented in the grain-boundary plane parallel to the c axis of both grains, and its value has not been corrected for demagnetization effects. The junctions had widths between 3 and 6 μm , and were measured at 4.2 K. Figure courtesy of C. W. Schneider, Augsburg University, Germany.

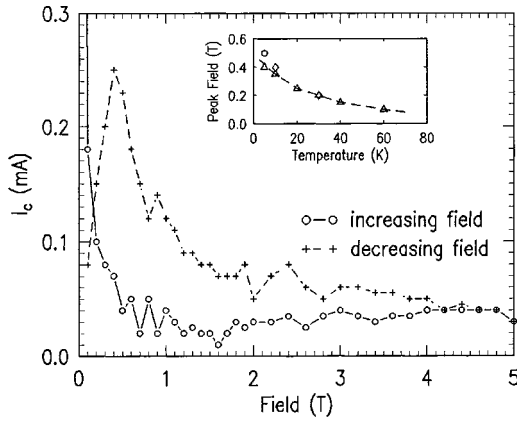


FIG. 38. Critical current at 5 K as a function of applied field for a 100- μm -wide, 25° [001]-tilt $\text{YBa}_2\text{Cu}_3\text{O}_{7-\delta}$ bicrystalline film. The magnetic field was applied in the boundary plane, along the c axis of both grains. The inset shows the position of the I_c peak in decreasing magnetic field as a function of temperature. From Däumling *et al.* (1992); figure courtesy of P. Chaudhari and E. Sarnelli, IBM T.J. Watson Research Center, USA.

Hilgenkamp, 1998) and in bulk materials (Larbalestier *et al.*, 1991; Nilsson-Mellbin and Salama, 1994a; St. Louis-Weber *et al.*, 1996; Field *et al.*, 1997; Mannhart and Hilgenkamp, 1998). As shown by Fig. 41, in most of the high- T_c superconductors for which they have been measured, the $R_n A$ values are very similar if the boundaries are clean. The values reported for grain boundaries

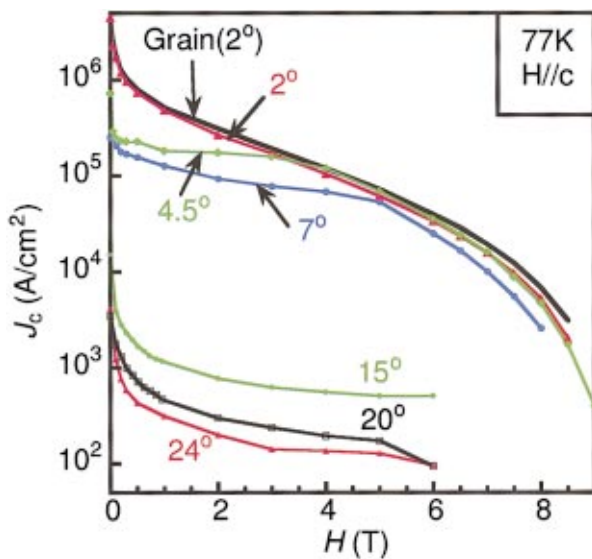


FIG. 39. Magnetic-field dependence of the critical current density of various [001]-tilt grain boundaries in $\text{YBa}_2\text{Cu}_3\text{O}_{7-\delta}$ bicrystalline films. The magnetic field was applied in the boundary plane, along the c axis of both grains. Above 4°, grain boundaries have a reduced J_c and at large fields are less sensitive to field than their adjacent grains. For small θ and at large applied magnetic fields, J_c is limited by the grains, not by the grain boundaries. From Verebelyi *et al.* (2000); figure courtesy of D. Verebelyi and D. K. Christen, Oak Ridge National Laboratory, USA [Color].

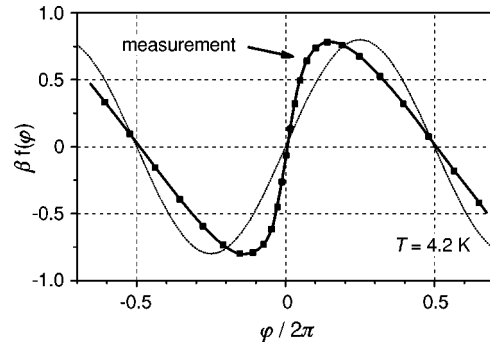


FIG. 40. Normalized current through a symmetric 45° [001]-tilt grain boundary in a bicrystalline $\text{YBa}_2\text{Cu}_3\text{O}_{7-\delta}$ film measured at 4.2 K as a function of the phase difference across the junction. A sinusoidal function is plotted for comparison. From Il'ichev *et al.* (1998).

in $\text{Nd}_{2-x}\text{Ce}_x\text{CuO}_4$ films are exceptionally high and amount to several $10^{-6} \Omega \text{ cm}^2$ for 24° junctions (Klee-fisch *et al.*, 1998), which may be attributed to the difficulties in adjusting the oxygen concentration at these boundaries, as described in Sec. V.B.1. It seems surprising that the standard $R_n A$ values of the high- T_c grain boundaries are comparable to the typical resistivities of other types of high- T_c Josephson junctions, such as ramp-type junctions or superconductor/normal-metal contacts (Mannhart and Hilgenkamp, 1999).

E. The $I_c R_n$ product

For applications of Josephson junctions the characteristic voltage $I_c R_n$ is of great relevance, as it is proportional to the characteristic Josephson frequency of the junction and thereby provides an upper limit for its

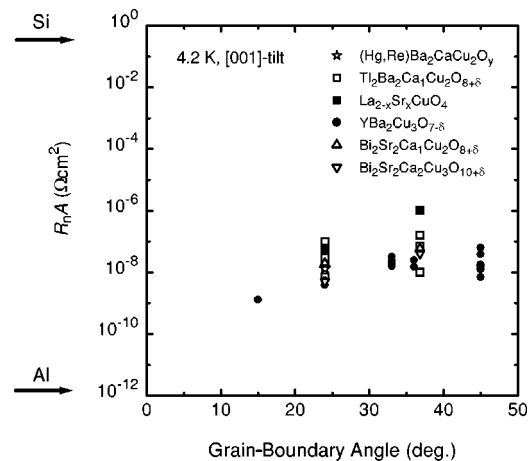


FIG. 41. Grain-boundary resistivities of various high- T_c superconductors plotted as a function of the grain-boundary misorientation angle. The data were compiled from the following sources: $(\text{Hg,Re})\text{Ba}_2\text{CaCu}_2\text{O}_y$: Tsukamoto *et al.* (1998); $\text{Tl}_2\text{Ba}_2\text{Ca}_1\text{Cu}_2\text{O}_{8+\delta}$: Weaver *et al.* (1996); $\text{La}_{2-x}\text{Sr}_x\text{CuO}_{4+\delta}$: Beck *et al.* (1996); $\text{YBa}_2\text{Cu}_3\text{O}_{7-\delta}$: Hilgenkamp and Mannhart (1998b); $\text{Bi}_2\text{Sr}_2\text{Ca}_1\text{Cu}_2\text{O}_{8+\delta}$: Mayer *et al.* (1993); $\text{Bi}_2\text{Sr}_2\text{Ca}_1\text{Cu}_2\text{O}_{8+\delta}$: Frey *et al.* (1996b).

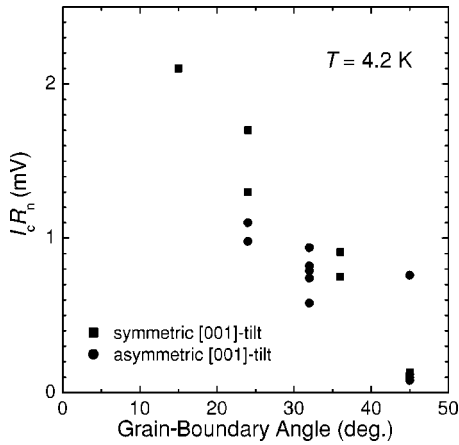


FIG. 42. Dependence of the $I_c R_n$ product for symmetric and asymmetric [001]-tilt grain boundaries in $\text{YBa}_2\text{Cu}_3\text{O}_{7-\delta}$ films on the misorientation angle θ at 4.2 K. From Hilgenkamp and Mannhart (1998b).

speed of operation. For most applications one wants the $I_c R_n$ product to be as large as possible. For 24° [001]-tilt bicrystal junctions in $\text{YBa}_2\text{Cu}_3\text{O}_{7-\delta}$ films, $I_c R_n$ values are approximately 2 mV at 4.2 K (see Fig. 42). As noted by Poppe *et al.* (2001), for [100]-tilt boundaries the $I_c R_n$ product can be significantly greater, with best reported values of 8 mV at 4.2 K and 1.2 mV at 77 K for 24° junctions, consistent with expectations based on the $d_{x^2-y^2}$ -wave order-parameter symmetry and the grain-boundary microstructure (see Sec. VII.C). Assuming an isotropic s -wave order parameter, it was noted already in very early work that the $I_c R_n$ values of [001]-tilt bicrystals are significantly lower than expected from the bulk gap value Δ and the Ambegaokar-Baratoff equation (Ambegaokar and Baratoff, 1963) $I_c R_n = \pi\Delta/2e$ for ideal tunnel junctions (Mannhart *et al.*, 1988; Bungre *et al.*, 1989; Dimos *et al.*, 1990). The small $I_c R_n$ products were taken as an indication of gap suppression at the boundary (Mannhart *et al.*, 1988), of inhomogeneous supercurrent flow across the boundary (Bungre *et al.*, 1989), or of an internal shunt within the boundaries caused by resonant tunneling states (Halbritter, 1992; Gross, 1994). In hindsight it is obvious that the anisotropy and the phase changes of the $d_{x^2-y^2}$ order parameter are partially responsible for the reduction of the $I_c R_n$ product, as discussed in Sec. VII.C.

The behavior of the $I_c R_n$ product of 45° [001]-tilt grain boundaries in $\text{YBa}_2\text{Cu}_3\text{O}_{7-\delta}$ films was investigated in experiments in which the grain boundaries were altered by depleting them of oxygen with thermal anneals (Russek *et al.*, 1990). These experiments showed that upon oxygen depletion the characteristic voltage of the junctions scales with the normal-state conductivity $\sigma_n = (R_n A)^{-1}$ as $I_c R_n \propto \sigma_n^{0.85}$, or, equivalently, as $I_c R_n \propto J_c^q$ with $q=0.46$ (Russek *et al.*, 1990). For 90° basal-plane-faced tilt boundaries it was reported later that $q=0.3$ (Moeckly *et al.*, 1995).

Extending this work, Gross and co-workers suggested that the scaling behavior is universal with $q=0.5 \pm 0.1$ (Gross, Chaudhari, *et al.*, 1990b; Gross, Alff, *et al.*, 1997;

Marx, Alff, and Gross, 1997; Marx and Gross, 1997), for all grain boundaries as a function of oxygen depletion, change of misorientation angle, or variation of deposition conditions (Gross, 1994). This universal scaling has been proposed to be applicable to boundaries in all high- T_c cuprates (Gross, 1994; Kleefisch *et al.*, 1998) with the possible exception of $\text{Nd}_{2-x}\text{Ce}_x\text{CuO}_4$, for which both $q \sim 0.5$ (Kleefisch *et al.*, 1998) and $q \sim 0.3$ have been reported (Schoop *et al.*, 1999), as well as to high- T_c Josephson junctions with artificial barriers in general (Gross, Alff, *et al.*, 1997; Marx and Gross, 1997). Such a universal scaling behavior has been reported to be in line with the expectations following from the intrinsically shunted junction model (see Sec. VII.A). It has also been attributed to effects resulting from the short coherence lengths of the high- T_c superconductors (Deutscher and Chaudhari, 1991).

Various experiments do not support such a universal scaling law, e.g., the studies by Ivanov *et al.*, who varied the orientation of the boundary with respect to the grains for a fixed misorientation angle (Ivanov, Stepantsov, *et al.*, 1998). Sarnelli (1993) carried out calculations of the $I_c R_n(J_c)$ relation for realistic grain-boundary junctions consisting of alternating superconducting and nonsuperconducting regions, and found an $I_c R_n \propto J_c^{0.5}$ behavior only in the limit of large misorientation angles (see also Sarnelli and Testa, 2001).

A number of studies have been carried out specifically to investigate the existence of a universal scaling law. Sydow *et al.* (1999a, 1999b) modified $\text{YBa}_2\text{Cu}_3\text{O}_{7-\delta}$ bicrystals by ozone treatments and electromigration and concluded that only for considerable oxygen depletion do the grain boundaries follow the scaling behavior, consistent with earlier reports from the same group (Russek *et al.*, 1990). For well-oxygenated boundaries the $I_c R_n$ product remained constant with variations of J_c . Neither did the results of studies on grain boundaries doped with calcium or cobalt support a universal scaling law (Schneider *et al.*, 1999), as was the case for boundaries annealed in argon (Redwing *et al.*, 1999). A comparison of boundaries with varying misorientation angles showed a decrease of $I_c R_n$ with decreasing J_c , as the misorientation angle was increased. This decrease, which did not follow an obvious scaling law (Hilgenkamp and Mannhart, 1998b), arises naturally from the angular-dependent influences of the $d_{x^2-y^2}$ order-parameter symmetry (see Sec. VII.C), which are not taken into account in the intrinsically shunted junction models. Considering further the spread of the data presented, for example, by Gross *et al.* (1997), especially if only the grain boundary junctions are considered, the authors of the present review conclude that the proposed universal scaling law does not exist for well-oxygenated grain boundaries, but only for grain boundaries that have been artificially depleted of oxygen.

F. Grain-boundary capacitance

Important information about the boundary barrier has been obtained from studies of the Fiske resonances

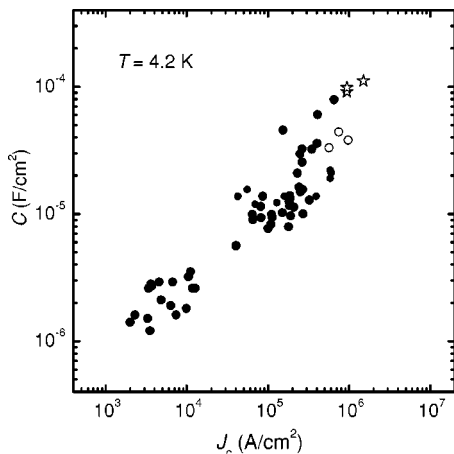


FIG. 43. Capacitance of grain-boundary junctions plotted as a function of critical current density for $\text{YBa}_2\text{Cu}_3\text{O}_{7-\delta}$ (solid circles) and $\text{Y}_{1-x}\text{Ca}_x\text{Ba}_2\text{Cu}_3\text{O}_{7-\delta}$ films with $x=0.1$ (open circles), and $x=0.3$ (stars). The data, from Yi *et al.* (1996) and Tarte *et al.* (2001), were measured at 4.2 K. After Tarte *et al.* (2001); figure courtesy of E. Tarte and J. Ransley, Cambridge University, UK.

(Alarco *et al.*, 1994; Winkler *et al.*, 1994; Médicini *et al.*, 1995; Tarte *et al.*, 2001). The presence of Fiske resonances suggests the existence of a dielectric layer at the grain boundaries investigated and shows that the grains superconduct well within 5–20 nm from the boundary interface. From these investigations and from studies of Josephson flux-flow resonances (Zhang *et al.*, 1996), the average ratio of the effective grain-boundary width t and the dielectric constant ϵ_r of the boundary was derived to be $t/\epsilon_r \cong 0.3\text{--}0.4$ nm. This value corresponds to a specific capacitance of the boundaries of $C/A \cong 3 \times 10^{-6}$ F/cm². In other work, the hysteresis appearing in the current-voltage characteristic has been analyzed (Winkler *et al.*, 1994; Beck *et al.*, 1995; Moeckly and Buhrman, 1995; Tarte *et al.*, 1997, 2001; McBrien *et al.*, 1999, 2000). In general, capacitance values of $C/A \cong 10^{-7}\text{--}10^{-4}$ F/cm² have been reported, measured for a range of grain boundaries differing in structure, configuration, and misorientation (Tarte *et al.*, 2001). For SrTiO_3 substrates, in particular, the capacitance has been attributed to the stray capacitance of the substrate (Gross, Chaudhari, *et al.*, 1991; Gross and Mayer, 1991; Gross 1994; Tarte *et al.*, 1997). Remarkably, as illustrated in Fig. 43, the capacitance increases strongly with the critical current density. It drops as a function of resistance, following a $C/A \sim (R_n A)^{-1}$ dependence over three orders of magnitude (Moeckly and Buhrman, 1995; McBrien *et al.*, 2000; Tarte *et al.*, 2001).

G. Microwave properties

When grain-boundary Josephson junctions are irradiated by rf fields, their $I(V)$ characteristics show well-pronounced Shapiro steps, which in many aspects agree with the theoretical expectations following from the resistively shunted junction (RSJ) model (Häuser *et al.*,

1989; Divin *et al.*, 1992, 1993; Early *et al.*, 1993, 1994; Terpstra *et al.*, 1994; Boikov *et al.*, 1997a; Borisenko *et al.*, 2001). The sensitivity of the $I(V)$ characteristics to irradiation extends to high frequencies. This is demonstrated by Fig. 44, which shows the response of a 25° [001]-tilt $\text{YBa}_2\text{Cu}_3\text{O}_{7-\delta}$ grain boundary to 72-GHz radiation. In several cases, as shown in Fig. 45, subharmonic Shapiro steps have been found, which have been attributed to an inhomogeneous, filamentary current flow across the boundaries (Early *et al.*, 1993, 1994; Boikov *et al.*, 1997a) or to the motion of phase-locked Josephson vortices along the junctions (Terpstra *et al.*, 1994).

The microwave surface resistance of grain boundaries has been investigated with special interest, as grain boundaries have been found to increase the surface resistance of high- T_c films substantially (Hylton *et al.*, 1988; Pinto *et al.*, 1993; Hein *et al.*, 1994; Herd *et al.*, 1997; Kusunoki *et al.*, 1999). Moreover, it was measured that at microwave frequencies the rf losses depend on the boundary angle. Experiments performed by an MIT/NIST collaboration showed that in agreement with the dc behavior of $J_c(\theta)$, grain boundaries with small misorientation angles have power-handling capabilities superior to those at greater misorientations (Habib *et al.*, 1998). For fixed microwave frequencies, the grain boundaries display well-defined microwave absorption lines as a function of applied magnetic field (Wosik *et al.*, 1995). Similarly, in other experiments peaks in the microwave losses have been observed at well-defined magnetic dc fields, which are attributed to individual Josephson vortices penetrating the grain-boundary junctions (Xin *et al.*, 2000). Reduction of the surface resistance of $\text{YBa}_2\text{Cu}_3\text{O}_{7-\delta}$ films at a given reduced temperature T/T_c has been reported in studies in which the $\text{YBa}_2\text{Cu}_3\text{O}_{7-\delta}$ films were covered with $\text{Y}_{1-x}\text{Ca}_x\text{Ba}_2\text{Cu}_3\text{O}_{7-\delta}$ capping layers (Obara *et al.*, 2001). This reduction has been attributed to a reduction of the grain-boundary losses due to Ca doping (Hammerl *et al.*, 2000; Obara *et al.*, 2001); see Sec. VI.

H. Grain-boundary noise

The noise of single grain boundaries is a topic of obvious interest,⁶ not only because of its relevance for applications, but also because it provides clues about the grain-boundary mechanisms. The noise-generating processes include thermal effects, fluctuations of the critical current and of the normal-state resistance due to charge trapping at the barrier, as well as thermally activated flux motion at the boundary and in nearby areas of the film (Hao *et al.*, 1994). Like other junctions involving high- T_c cuprate interfaces, the grain-boundary junctions display

⁶See, for example, Gross and Mayer, 1991; Lathrop *et al.*, 1991; Divin *et al.*, 1992; Kawasaki *et al.*, 1992; Miklich *et al.*, 1992; Hammond *et al.*, 1993; Koelle *et al.*, 1993a; Hao *et al.*, 1994, 1996, 1997; MacFarlane *et al.*, 1995, 1997; Marx *et al.*, 1995a, 1995b, 1997; Fischer *et al.*, 1997; Marx and Gross, 1997; Selvam *et al.*, 1997; Enpuku *et al.*, 1999; Sarnelli *et al.*, 1999.

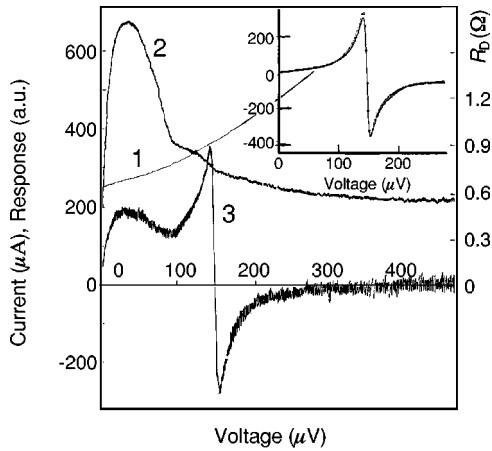


FIG. 44. $I(V)$ characteristic (1), differential resistance (2), and response to 72 GHz radiation (3) of a 16- μm -wide, 25° $\text{YBa}_2\text{Cu}_3\text{O}_{7-\delta}$ bicrystalline grain-boundary junction at 78 K. The inset shows the measured and calculated normalized response $(\Delta V/R_n)/IV$ to the irradiation. From Divin *et al.* (1992); figure courtesy of J. Mygind and N. F. Pedersen, the Technical University of Denmark.

a strong $1/f$ noise up to high frequencies, as shown clearly in Fig. 46. The first work on noise in bicrystalline Josephson junctions revealed that the $1/f$ noise decreases after oxygen anneals, and it was observed that in many cases the ratio $|\delta I_c/I_c|/|\delta R_n/R_n|$ equals about 2.5 (Kawasaki *et al.*, 1992). This is illustrated by Fig. 47, which presents the current and voltage noise of a 25° [001]-tilt $\text{YBa}_2\text{Cu}_3\text{O}_{7-\delta}$ bicrystalline junction at 77 K as measured by Kawasaki *et al.* (1992). It was shown further in this work that the $1/f$ noise arises from critical-current fluctuations if the boundaries are biased close to I_c , and from resistance fluctuations for large-bias currents. Based on this, the noise was suggested to originate from trapping and detrapping of charge carriers (Kawasaki *et al.*, 1992). This interpretation is consistent with the observation of telegraph noise caused by grain

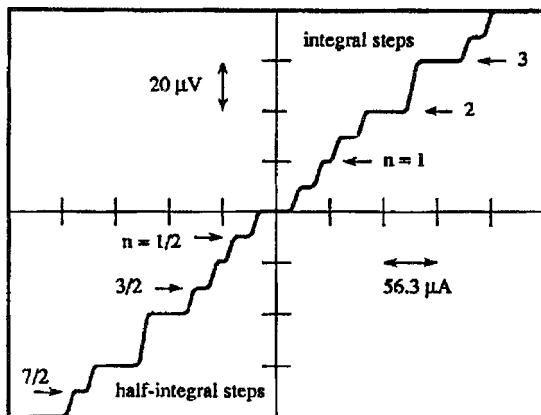


FIG. 45. $I(V)$ curves of a 50- μm -wide $\text{YBa}_2\text{Cu}_3\text{O}_{7-\delta}$ biepitaxial junction at 4.2 K in a microwave field of 9.311 GHz. Both integral and half-integral constant voltage steps are indicated by arrows and indexed by n . From Early *et al.* (1993); figure courtesy of K. Char, Conductus, Sunnyvale, USA.

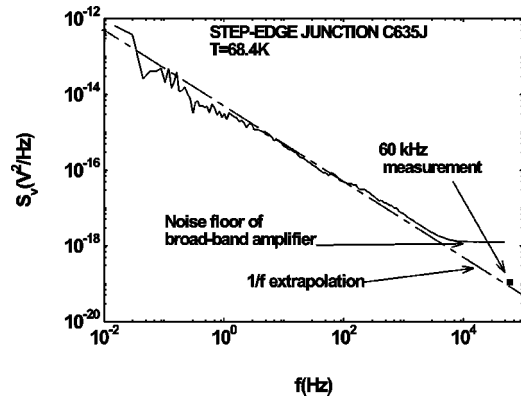


FIG. 46. Spectral density of the voltage noise as a function of frequency for a $\text{YBa}_2\text{Cu}_3\text{O}_{7-\delta}$ step-edge junction measured at 68.4 K. The noise was measured with a broadband fast-Fourier-transform technique (solid curve) and with a highly sensitive spot measurement at 60 kHz. The two techniques are in agreement and show a $1/f$ behavior. From Hao *et al.* (1996); figure courtesy of J. C. Macfarlane, University of Strathclyde, UK.

boundaries (Chaudhari, Dimos, and Mannhart, 1989; Miklich *et al.*, 1992; Gross, 1994). In the work performed by Marx *et al.*, charge trapping in the dielectric barrier was also reported to be the source of the $1/f$ noise, and the trapping time was found to decay exponentially with increasing bias voltage (Marx *et al.*, 1995a, 1995b; Marx, Alff, and Gross, 1997; Herbristrit *et al.*, 2001).

The dependence of the voltage noise on the current bias of 45° grain boundaries in $\text{YBa}_2\text{Cu}_3\text{O}_{7-\delta}$ films as measured by Hammond *et al.* is shown in Fig. 48. In these studies, the fluctuations of the critical current and of the resistance have been found to be not correlated, supporting the view that the normal current and supercurrent components are carried through these junctions

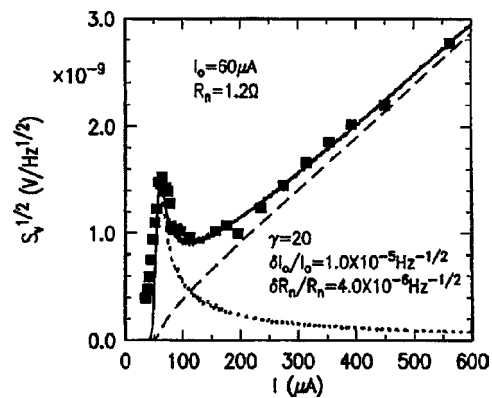


FIG. 47. Voltage noise as a function of bias current of a 10- μm -wide, 25° [001]-tilt $\text{YBa}_2\text{Cu}_3\text{O}_{7-\delta}$ bicrystalline junction measured at 77 K. Calculated results based on the resistivity shunted junction model are also shown. The dotted line was calculated by assuming only I_c fluctuations, the dashed line by considering only R_n fluctuations. The calculations leading to the solid line consider both types of fluctuations. From Kawasaki *et al.* (1992); figure courtesy of P. Chaudhari and M. Kawasaki, IBM T. J. Watson Research Center, USA.

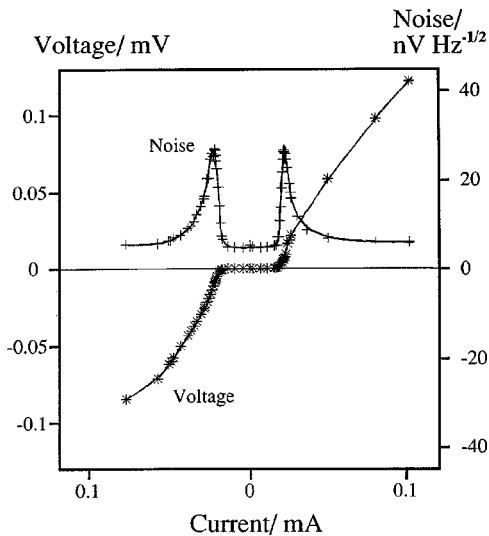


FIG. 48. Current-voltage characteristic and voltage noise of a $\text{YBa}_2\text{Cu}_3\text{O}_{7-\delta}$, biepitaxial 45° [001]-tilt junction measured at 25 K and 10 Hz. For current biases above several hundred μA the voltage noise increases approximately linearly with the bias current (not shown). From Hammond *et al.* (1993); figure courtesy of C. M. Muirhead, University of Birmingham, UK, and K. Char, Conductus, Sunnyvale, USA.

in different channels (Hammond *et al.*, 1993). In other work, in which the $1/f$ noise in $\text{YBa}_2\text{Cu}_3\text{O}_{7-\delta}$ and $\text{Bi}_2\text{Sr}_2\text{CaCu}_2\text{O}_{8+\delta}$ grain boundaries with 24° and 36.8° misorientation was investigated, it was pointed out that in these junctions the fluctuations of the critical current $\delta I_c/I_c$ and of the normal-state resistance, $\delta R_n/R_n$, are anticorrelated, and that $|\delta I_c/I_c|/|\delta R_n/R_n| \cong 1/(1-q)$, where $q=0.5$ is the coefficient of the asserted universal scaling law (see Sec. V.E; Marx *et al.*, 1995b; Gross *et al.*, 1997). It has been noted that due to the d -wave symmetry and the faceting of the boundaries, the supercurrent and the normal current will be distributed differently over the grain boundary (Hilgenkamp, Mannhart, and Mayer, 1996). As this difference increases with grain-boundary angles, the noise correlations are expected to decrease with the misorientation, in keeping with the experimental observations (Hilgenkamp, Mannhart, and Mayer, 1996).

The effective noise temperature of grain-boundary junctions was measured in the range of 4.5 to 90 K (Divin *et al.*, 1992; Fischer *et al.*, 1997). The noise temperature can be as low as the physical temperature of the sample (see Fig. 49), which demonstrates the applicability of grain-boundary junctions for radiation spectroscopy, even at 77 K. A comparison and discussion of the noise in various types of grain-boundary junctions is given by Hao *et al.* (1996).

I. Self-generated magnetic flux

In a surprising set of scanning SQUID microscopy studies, unquantized magnetic flux was observed at biepitaxial grain boundaries. These boundaries were formed by triangular or hexagonal $\text{YBa}_2\text{Cu}_3\text{O}_{7-\delta}$ is-

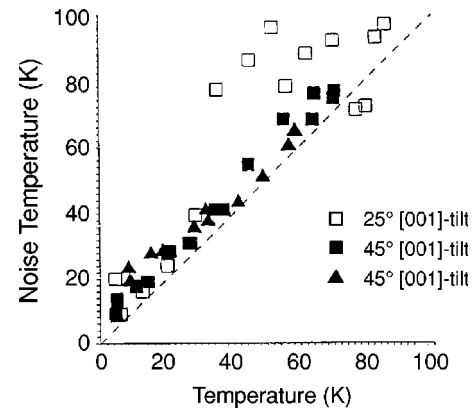


FIG. 49. Noise temperature vs physical temperature of various $\text{YBa}_2\text{Cu}_3\text{O}_{7-\delta}$ bicrystalline grain-boundary junctions derived from measured values of the millimeter wave irradiation-induced Josephson linewidth. From Divin *et al.* (1992); figure courtesy of J. Mygind and N. F. Pedersen, the Technical University of Denmark.

lands embedded in films rotated by 45° with respect to the grains (Kirtley, Chaudhari, *et al.*, 1995). It has been argued that these fractional vortices provide evidence of time-reversal symmetry breaking at the grain boundaries (Sigrist *et al.*, 1995; Bailey *et al.*, 1997; Zhu *et al.*, 1999; Amin *et al.*, 2001). Unquantized magnetic flux was also observed at bicrystalline, asymmetric 45° grain boundaries in $\text{YBa}_2\text{Cu}_3\text{O}_{7-\delta}$ films, but not in boundaries with smaller misorientation angles (Mannhart, Hilgenkamp, *et al.*, 1996). As discussed in Sec. VII.C, this flux, like the anomalous $I_c(H)$ patterns, is apparently generated by the $d_{x^2-y^2}$ -wave pairing symmetry of $\text{YBa}_2\text{Cu}_3\text{O}_{7-\delta}$ and the faceted microstructure of the boundaries. Detailed modeling of these effects has recently been provided (Mints and Papiashvili, 2000). Walker (1996) further proposed that twin boundaries may play an important role in the flux generation.

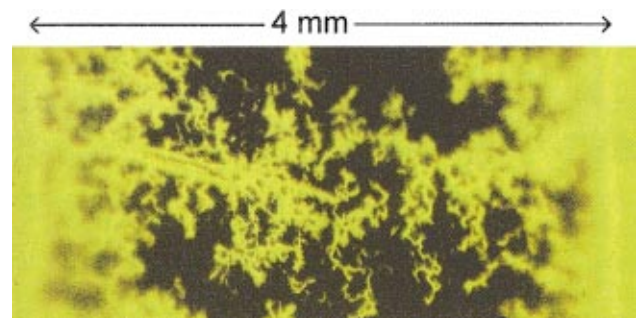


FIG. 50. Magneto-optical image of the whole width of a RABiTS-type $4 \times 10\text{-mm}^2$ -large and $0.6\text{-}\mu\text{m}$ -thick $\text{YBa}_2\text{Cu}_3\text{O}_{7-\delta}$ film grown on a deformation-textured Ni substrate. The image was taken after cooling the sample in zero magnetic field to 15 K and then applying a field of 60 mT. Bright areas indicate magnetic-flux penetration, dark areas flux shielding. Magnetic flux enters the sample from the edges and propagates preferentially along weaker-linked regions such as grain boundaries. From Feldmann *et al.* (2000); figure courtesy of S. E. Babcock, M. Feldmann, and D. C. Larbalestier, University of Wisconsin, USA [Color].

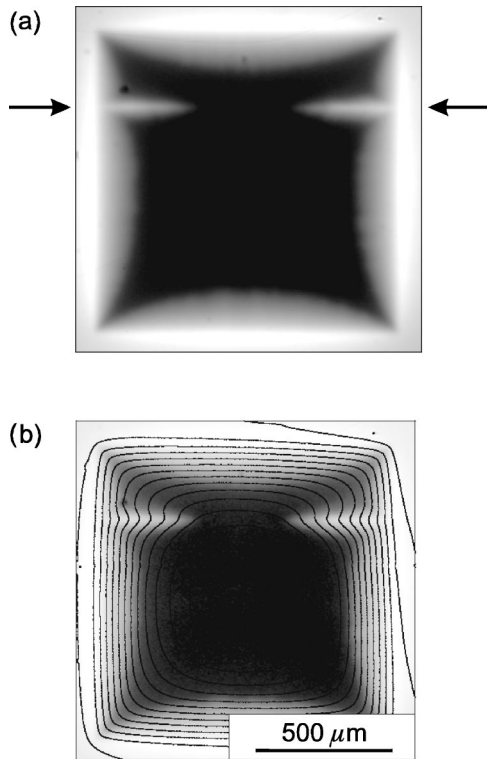


FIG. 51. Magneto-optical investigation of a bicrystal boundary: (a) Grayscale plot of the magnetic-flux density distribution of a bicrystalline $\text{YBa}_2\text{Cu}_3\text{O}_{7-\delta}$ film at 5 K containing a 3° [001]-tilt grain boundary, the location of which is indicated by arrows. Bright parts refer to high flux densities. The image was obtained after zero-field cooling the sample and then applying a flux density of 48 mT perpendicular to the film surface; (b) distribution of the current density distribution calculated from (a) and plotted as current stream lines overlaid on the flux density distribution. From Albrecht *et al.* (2000a); figures courtesy of J. Albrecht and H. Kronmüller, Max-Planck-Institut für Metallforschung, Stuttgart, Germany.

J. Penetration of magnetic flux into grain boundaries

In polycrystalline samples, applied magnetic fields usually enter or leave the samples via the grain boundaries, preferably along those with large misorientation angles, as has been imaged directly in magneto-optical studies, an example of which is given by Fig. 50 (Forkl *et al.*, 1990; Nakamura *et al.*, 1992; Dorosinskii *et al.*, 1993; Schuster *et al.*, 1993; Koblischka *et al.*, 1994; Turchinskaya *et al.*, 1994; Vlasko-Vlasov *et al.*, 1994; Polyanskii *et al.*, 1996; Jooss *et al.*, 1999; Albrecht *et al.*, 2000a, 2000b; Feldmann *et al.*, 2000; Jooss, Bringmann, *et al.*, 2000; Jooss, Warthmann, and Kronmüller, 2000; Jooss, Warthmann, *et al.*, 2000; Kawano *et al.*, 2000) and in scanning SQUID microscopy investigations (Tsai *et al.*, 2001). With the field profile known, the supercurrent distributions can be derived by inversion techniques (Polyanskii *et al.*, 1996; Jooss *et al.*, 1999; Albrecht *et al.*, 2000a; Jooss, Warthmann, and Kronmüller, 2000; Jooss, Warthmann, *et al.*, 2000; Kawano *et al.*, 2000; Jooss, Albrecht, *et al.*, 2001). This is demonstrated by Fig. 51, which shows the magnetic-flux density distribution of a

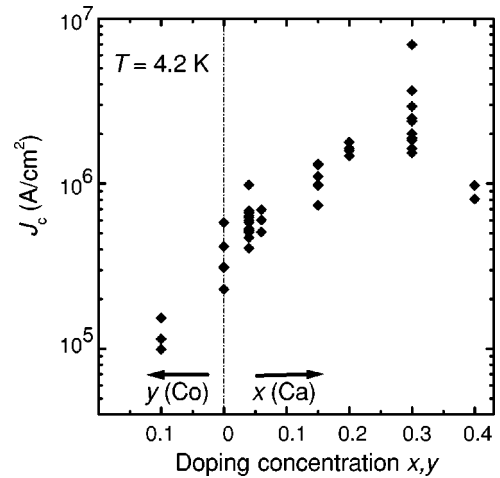


FIG. 52. Dependence of the critical current density of symmetric 24° [001]-tilt grain boundaries in $\text{Y}_{1-x}\text{Ca}_x\text{Ba}_2\text{Cu}_3\text{O}_{7-\delta}$ and in $\text{YBa}_2\text{Cu}_{3-y}\text{Co}_y\text{O}_{7-\delta}$ films on the Ca and Co concentrations x and y at $T=4.2$ K; After Schmehl *et al.* (1999).

bicrystalline $\text{YBa}_2\text{Cu}_3\text{O}_{7-\delta}$ film at 5 K containing a 3° [001]-tilt grain boundary and the corresponding spatial dependence of the supercurrent. Furthermore, magneto-optic imaging has been used for the analysis of the critical current density and the pinning properties of antiphase boundaries (Jooss, Bringmann, *et al.*, 2000; Jooss, Warthmann, and Kronmüller, 2000; Jooss, Warthmann, *et al.*, 2000; Jooss, Albrecht, *et al.*, 2001) in analogy with the study of twin boundaries by scanning tunneling spectroscopy (see Fig. 35; Maggio-Aprile *et al.*, 1997; see also Gyorgy *et al.*, 1990; Kwok *et al.*, 1990; Swartzendruber *et al.*, 1990; Herbsommer *et al.*, 2000).

VI. EFFECTS OF DOPING

For high- T_c Josephson junctions, appropriate doping of the boundary layer as well as doping of the superconductor were expected to provide a means for a controlled adjustment of the junction parameters. In the first of these studies, optimization of the grain boundaries was attempted by enhancing their oxygen content, in particular by electromigration (Russek *et al.*, 1990) or by anneals in an ozone atmosphere (Kawasaki *et al.*, 1992; Sarnelli, Chaudhari, and Lacey, 1993). Remarkably, although the noise properties of the grain boundaries were affected by some of these treatments, it was impossible to significantly increase the critical current densities. Various groups have also studied the modification of grain-boundary properties by chemical doping of the grains, for example, for $\text{YBa}_2\text{Cu}_3\text{O}_{7-\delta}$ by addition of silver (Wen and Abe, 1996; Bolaños *et al.*, 1997; Selvam *et al.*, 1997), calcium (Dong *et al.*, 1995; Wakao *et al.*, 1995; Sung *et al.*, 1997; Holzapfel *et al.*, 2000), cobalt (Sung *et al.*, 1997), or nickel (Odagawa and Enomoto, 1995). Local doping of the boundaries has been done with silver (Chaudhari *et al.*, 1988), iron (Ivanov, Stepantsov, *et al.*, 1994), and platinum (Ivanov,

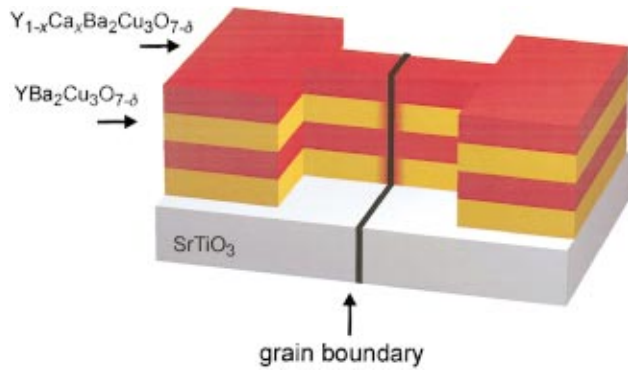


FIG. 53. Illustration of the local doping of grain boundaries intended by the use of grain-boundary diffusion in doping heterostructures. After Hammerl *et al.* (2001) [Color].

Stepantsov, *et al.*, 1994). In all these cases, doping degraded the grain-boundary properties.

As the band-bending model, of which a more detailed description will be given in Sec. VII.D, predicts that doping improves the grain-boundary properties, the possibility of interface doping was explored by Schmehl *et al.*, who investigated the effects of partially substituting Ca^{2+} for Y^{3+} in $\text{YBa}_2\text{Cu}_3\text{O}_{7-\delta}$ films, thereby significantly increasing the critical current density and reducing the normal-state resistance of [001]-tilt boundaries with a range of misorientation angles (Schmehl *et al.*, 1999; Mannhart *et al.*, 2000a). As shown in Fig. 52, when 30% of the Y^{3+} was replaced by Ca^{2+} , the critical current density of 24° grain boundaries was enhanced by almost one order of magnitude to $\sim 7 \times 10^6 \text{ A/cm}^2$ at 4.2 K. For 5° boundaries at 11 K, the group of Larbalestier at the University of Wisconsin-Madison observed a doubling of J_c to $\sim 6 \times 10^6 \text{ A/cm}^2$ (Daniels *et al.*, 2000; Larbalestier, 2000). For 8° grain boundaries the University of Göttingen group also reported an enhancement by a factor of 2 to up to $\sim 1.2 \times 10^7 \text{ A/cm}^2$ at 4.2 K (Jooss, 2000; see also Guth *et al.*, 2001). Moreover, doping was found to decrease the grain-boundary normal-state resistivity by even greater factors (Schmehl *et al.*, 1999; Schneider *et al.*, 1999). Furthermore, doping was reported to enhance the critical current density in large magnetic fields (Daniels *et al.*, 2000).

As a homogenous doping of the entire superconductor not only strengthens the grain-boundary coupling but also decreases the T_c of the grains, the attainable J_c enhancement is only marginal at 77 K. To achieve enhanced grain-boundary coupling together with a large intragrain T_c , local doping of the grain boundaries on the length scale of the coherence length and the electrical screening length is required. Selectively doping the grain boundaries is possible by benefiting from grain-boundary diffusion in doping heterostructures, as sketched in Fig. 53 (Hammerl *et al.*, 2000, 2001; see also Grant, 2000 and Delamare *et al.*, 2002). Relevant diffusion coefficients for this procedure have been reported by Berenov *et al.* (Berenov, Farvacque, *et al.*, 2001; Berenov, Marriott, *et al.*, 2001). With such heterostructures, for 24° grain boundaries in $\text{YBa}_2\text{Cu}_3\text{O}_{7-\delta}$ films, critical

current densities as high as $3.3 \times 10^5 \text{ A/cm}^2$ have been obtained at 77 K. These values equal the usual current densities measured for 7° boundaries at 77 K, or the typical current densities of 24° boundaries at 4.2 K (Hammerl *et al.*, 2000, 2001; for J_c increases see also Berenov, Farvacque, *et al.*, 2001).

Obara *et al.* (2001) reported that the surface resistance of $\text{YBa}_2\text{Cu}_3\text{O}_{7-\delta}$ films is reduced by covering the films with $\text{Y}_{1-x}\text{Ca}_x\text{Ba}_2\text{Cu}_3\text{O}_{7-\delta}$ capping layers. This reduction has been attributed to a reduction of the grain-boundary losses due to Ca doping (Hammerl *et al.*, 2000; Obara *et al.*, 2001); see Sec. V G.

VII. GRAIN-BOUNDARY MECHANISMS

The key issues to be explained by the grain-boundary models are the presence of the experimentally observed insulating layer at the boundary, which causes the characteristic boundary resistivity of $10^{-9} - 10^{-7} \Omega \text{ cm}^2$, and the strongly angular dependent J_c . To account for these properties, many mechanisms have been suggested, which in the following are grouped for clarity into five families. It is understood that these mechanisms are not mutually exclusive but that several interacting mechanisms control grain-boundary transport simultaneously. The influence of microstructural effects on J_c , for example, is enhanced by the short coherence length of the cuprates (Deutscher and Müller, 1987), the presence of the metal-insulator phase transition, and the $d_{x^2-y^2}$ -wave pairing symmetry.

Grain boundaries are structural defects which, by definition, interrupt the lattice structure of the adjacent crystals and thereby affect most of the properties of the correlated electron system. Therefore a microscopically accurate description of the superconducting pairing at the grain boundaries has to be based on a quantitative description of pairing in the cuprates with modified, spatially dependent parameters of the electron system and of the crystal lattice. As at present our understanding of the pairing mechanism(s) in the cuprates is incomplete, any description of the superconducting properties of interfaces or surfaces of the superconductors must also be incomplete and has to be guided by intuition.

A. Mechanisms based on structural properties

TEM studies have confirmed that at low-angle grain boundaries the grain misorientation is accommodated by arrays of separated, periodic dislocations (see Secs. II and IV). With increasing grain-boundary angle the dislocations merge into a perturbed layer, which has been found to consist of structural units (Chisholm and Smith, 1989; Chaudhari, Dimos, and Mannhart, 1990; Dimos *et al.*, 1990; Babcock and Larbalestier, 1990; Gao *et al.*, 1991; Browning *et al.*, 1998; Merkle *et al.*, 2001). Therefore low-angle grain boundaries are composed of an array of alternating superconducting and nonsuperconducting regions, as described in the so-called Dayem

bridge model and related theories.⁷ Various effects arise from the structural distortions associated with the boundary, which also include the accompanying stress fields:⁸ the electronic structure of the superconductor is modified, the pairing interactions are suppressed, and quasiparticles are scattered. These effects lower the superconducting order parameter at the grain-boundary interface and thereby also the critical current density.⁹ A detailed quantitative analysis of this process has been carried out by Gurevich and Pashitskii (1998). Considering these phenomena, the transition from low-angle boundaries to large-angle ones has frequently been offered as an explanation for the onset of the Josephson behavior at misorientation angles of $\sim 8^\circ - 10^\circ$.¹⁰ Sarnelli and Testa (2001) presented an analysis showing that their model based on filamentary current flow (Sarnelli, Chaudhari, and Lacey, 1993; Sarnelli, Testa, and Esposito, 1993) successfully describes various aspects of grain-boundary transport properties, including the behavior of the $I_c R_n$ -product and noise characteristics.

With increasing misorientation, the width of the disordered layer at large-angle boundaries increases linearly as found by Browning *et al.* (1998). This behavior has been recognized as one reason for the angular dependence of J_c . With the assumption that the height of the tunneling barrier caused by the disordered layer is not influenced by the misorientation angle, an exponential $J_c(\theta)$ dependence is readily obtained from this (Browning *et al.*, 1998).

It was suggested early on that grain boundaries are charged (Chaudhari, Dimos, and Mannhart, 1990). Such charging is expected to arise, for example, from an ionic charge surplus in the dislocation cores or in the structural units as observed by TEM (Browning *et al.*, 1999), as well as from migration to the boundary, e.g., of point defects in the boundary's stress field. It has further been noted that the charging may be indirectly induced by the antiferromagnetism of the CuO_2 planes (Chaudhari, Dimos, and Mannhart, 1990). Charging will considerably

enhance scattering of carriers and will give rise to space-charge layers that reach into the adjacent grains, as discussed in Sec. VII.D.

It has been suggested that the disorder associated with the grain boundary reduces the hybridization of the $\text{CuO } p-d$ bonds and thereby also the carrier density at the interface (Halbritter, 1992, 1993). Accordingly, an intrinsically insulating zone with localized states of a density of $\leq 10^{21} \text{ cm}^{-3}$ was proposed to be formed at the interface (Halbritter, 1992).

Electron-structure calculations based on TEM images of grain boundaries in bulk $\text{YBa}_2\text{Cu}_3\text{O}_{7-\delta}$ show that at the interface Cu-O bonds are broken, which modifies the local density of states of the $\text{Cu } d$ electrons. Considering the implications of this for the superconducting order parameter, the Houston group has developed a model to describe the grain-boundary properties (Salama *et al.*, 2000; Stolbov *et al.*, 2001). In this work it is pointed out that grain boundaries containing (001) planes have the smallest J_c reduction.

On a more macroscopic level, the influence of a twist misorientation on grain-boundary properties in layered superconductors has been examined (Fletcher *et al.*, 1997). In this model, the current flows along the junction in helical paths, which is considered to cause inductances and magnetic fields generated at the boundaries.

Taking into consideration the anisotropy of high- T_c superconductors, the superconducting behavior of grain boundaries has been calculated based on a generalized London model (Kogan, 1989). According to this work, a reduction of J_c at the grain boundary is expected for anisotropic superconductors, independent of microstructural properties.

In contrast to these effects, which have all been proposed to decrease J_c , the inhomogeneous structure of the boundaries provided by the facets or by defects also enhances flux pinning and thereby J_c (Dimos *et al.*, 1990; Gray *et al.*, 1998, 2000). Indeed, the separated dislocation cores of low-angle boundaries are appreciated particularly good pinning sites (Díaz *et al.*, 1998a).

B. Mechanisms based on deviations from ideal stoichiometry

Gross deviations of a superconductor's stoichiometry at the boundaries or formation of second phases have been regarded a possible cause of weak-link behavior. Such effects, which seem to control the grain-boundary properties in the bismuthates, can be ruled out as controlling factors for the cuprates, as it was shown that boundaries with excellent cation composition are also weak links (Chisholm and Smith, 1989; Dimos *et al.*, 1990; Chisholm and Pennycook, 1991; Wang *et al.*, 1993; Chan, 1994; Babcock and Vargas, 1995). However, defects in the oxygen sublattice, which may be caused by the mechanical stress fields of the boundaries, will depress the superconducting order parameter (Chaudhari, Dimos, and Mannhart, 1990; Kawasaki *et al.*, 1992; Moeckly *et al.*, 1993; Betouras and Joynt, 1995; Luine and Kresin, 1998, 2001), and, if the oxygen concentration be-

⁷See, for example, Dimos *et al.*, 1988; Chisholm and Pennycook, 1991; Dravid *et al.*, 1993; Sarnelli, 1993; Sarnelli, Chaudhari, and Lacey, 1993; Sarnelli, Testa, and Esposito, 1993; Alarco and Olsson, 1995; Field *et al.*, 1997; Redwing *et al.*, 1999; Verebelyi *et al.*, 1999; Sarnelli and Testa, 2001.

⁸Some of these distortion effects are studied by Campbell, 1989; Dimos *et al.*, 1990; Chisholm and Pennycook, 1991; Jagannadham and Narayan, 1992; Redwing *et al.*, 1993; Sarnelli, Chaudhari, and Lacey, 1993; Meilikhov, 1994, 1996; Agassi *et al.*, 1995; Alarco and Olsson, 1995; Field *et al.*, 1997; Boyko *et al.*, 1998; Gurevich and Pashitskii, 1998; Sarnelli and Testa, 2001.

⁹For further discussion, see Chaudhari *et al.*, 1990; Dimos *et al.*, 1990; Chisholm and Pennycook, 1991; Jagannadham and Narayan, 1992; Sarnelli, Chaudhari, and Lacey, 1993; Meilikhov, 1994; Alarco and Olsson, 1995; Redwing *et al.*, 1999.

¹⁰See, for example, Dimos *et al.*, 1990; Chisholm and Pennycook, 1991; Gao *et al.*, 1991; Sarnelli, Chaudhari, and Lacey, 1993; Babcock and Vargas, 1995; Heinig *et al.*, 1996, 1999; Field *et al.*, 1997; Redwing *et al.*, 1999.

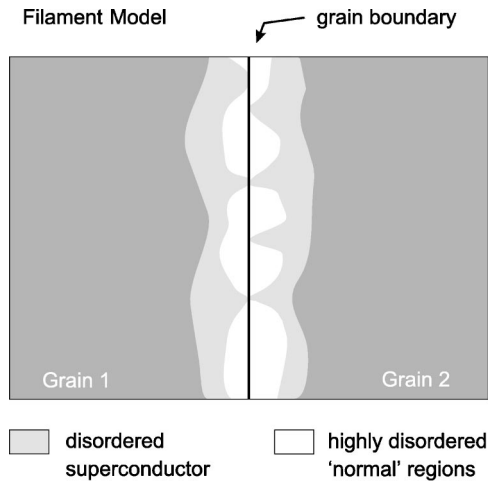


FIG. 54. Sketch of the phenomenological model of a high-angle tilt grain-boundary in $\text{YBa}_2\text{Cu}_3\text{O}_{7-\delta}$ according to Moeckly *et al.* (1993). Filaments of superconducting material sufficiently disordered to have a suppressed T_c , but with otherwise bulklike properties, are distributed on both sides of the grain boundary represented by the solid line. If two such filaments abut each other, a contact supporting a finite I_c is formed. After Moeckly *et al.* (1993).

comes low enough, will render the material insulating. Similar effects occur if the mobile carrier density is reduced for other reasons, such as carrier depletion associated with band bending (see Sec. VII.D). It has been pointed out that local carrier depletion at the grain boundaries may produce a local pseudogap there, and therefore cause a reduction of J_c (Tallon *et al.*, 2000).

As the oxygen concentration or the carrier density may be nonuniform, grain boundaries may be highly inhomogeneous, so that supercurrent flows in filaments across them, as suggested by Moeckly *et al.* (1993; Moeckly and Buhrman, 1995). It has been shown that this filament model, which is illustrated in Fig. 54, consistently describes the resistance, capacitance and $I_c R_n$ products of grain-boundary Josephson junctions, the boundary behavior in electromigration experiments (Moeckly and Buhrman, 1995), and the occurrence of half-integral voltage steps in their $I(V)$ characteristics under microwave irradiation, as presented in Fig. 45 (Early *et al.*, 1994). Deviation of the oxygen stoichiometry from the ideal value is also suggested to be an important factor controlling the exceptionally small critical current densities and characteristic voltages of grain boundaries in the $\text{Nd}_{2-x}\text{Ce}_x\text{CuO}_4$ films produced up to now.

In the intrinsically shunted junction (ISJ) models (Gross and Mayer, 1991; Halbritter, 1992, 1993; Gross, 1994), transport properties of the boundaries are described by presuming the presence of a layer with oxygen defects or oxygen disorder (Gross and Mayer, 1991; Halbritter, 1993), which is supposed to be insulating and include electronlike, localized states (Gross and Mayer, 1991), for which densities of 10^{17} – 10^{18} cm^{-3} have been derived (Froehlich *et al.*, 1997a, 1997b; Gross *et al.*, 1997), as illustrated in Figs. 55 and 56. Whereas quasi-

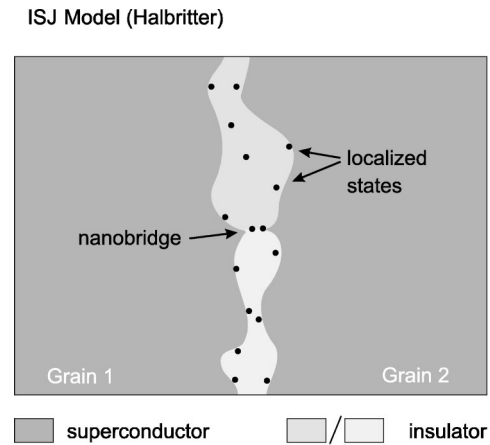


FIG. 55. Sketch of a small part of a grain-boundary with localized states in the insulator, which mediate tunnel channels simulating nanoshorts according to the intrinsically shunted junction model, as presented by Halbritter (1993).

particles are supposed to tunnel resonantly across this layer, predominantly via one localized state, Cooper pairs are supposed to tunnel directly (see Fig. 56). In the ISJ model, spatial inhomogeneities of J_c are accounted for by variations of the barrier width (Gross, Alff, *et al.*, 1995). The results of several experimental studies are in

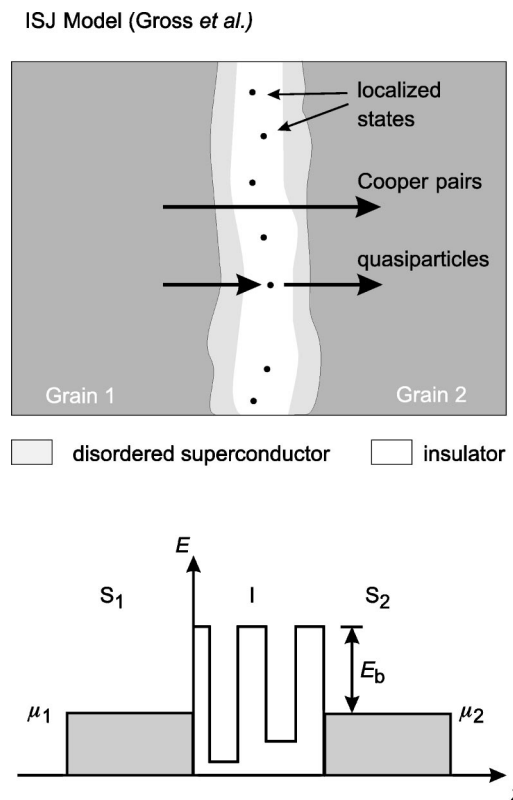


FIG. 56. The intrinsically shunted junction (ISJ) model, as presented by Gross, Alff, *et al.* (1995): upper panel, sketch of the current flow across a grain boundary; lower panel, corresponding energy profile showing a superconductor-insulator-superconductor junction with a barrier layer containing a high density of localized defect states. After Gross (1994, 1995).

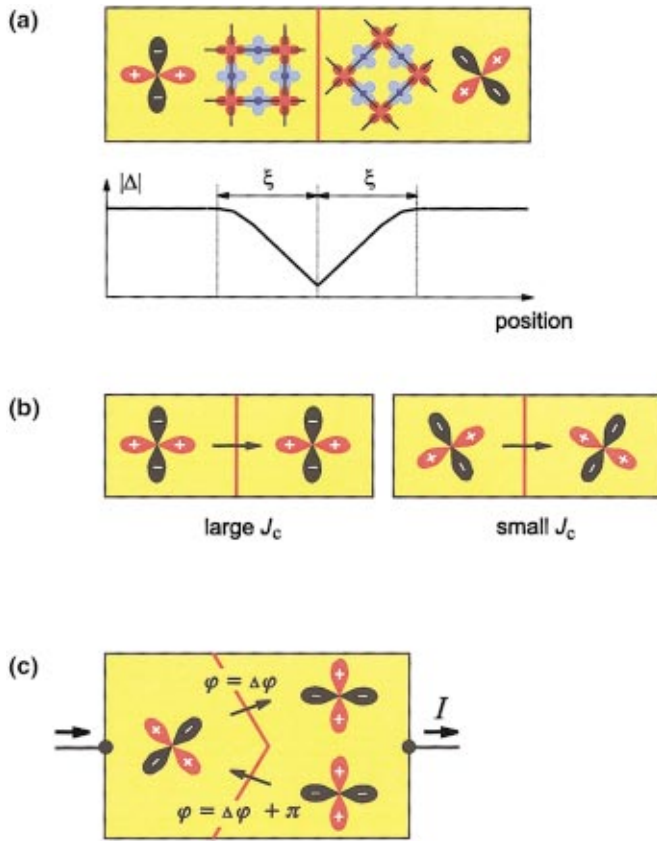


FIG. 57. Illustration of three mechanisms, by which the critical current density of grain boundaries is reduced due to the $d_{x^2-y^2}$ -wave-dominated order-parameter symmetry of the high- T_c superconductors: (a) at the interface layer the order parameter is depressed over a distance of the coherence length ξ due to frustration caused by the misorientation of the CuO_2 planes; (b) the value of the order parameter controlling the tunneling process is affected by the grain-boundary misorientation; (c) due to the phase difference of adjacent lobes of the $d_{x^2-y^2}$ -wave order parameter and grain-boundary faceting, the Josephson current flows across some facets in the direction opposite to the bias current I . From Mannhart *et al.* (2000b) [Color].

disagreement with the implications of the ISJ model (see, for example, Hilgenkamp and Mannhart, 1998b; Mannhart *et al.*, 2000b). According to the ISJ model the $I_c R_n$ product of the grain boundaries is expected to show a universal scaling behavior, which has been the subject of debate, as described in Sec. V.E. Furthermore, according to the model, grain-boundary properties are supposed to differ substantially among the high- T_c superconductors due to the different oxygen kinetics and chemistry of the various high- T_c cuprate families, which is clearly not the case. Finally, the ISJ models do not consider the influences of d -wave order-parameter symmetry. Especially for the $I_c R_n(J_c)$ dependence with varying grain-boundary angle and for the angular-dependent correlation between noise in the critical current and that in the normal-state resistance, d -wave symmetry is considered to be of central importance, as is discussed in the following section.

C. Order-parameter symmetry-based mechanisms

The high- T_c cuprates are characterized by a predominant $d_{x^2-y^2}$ symmetry of the order parameter describing the superconducting condensate as was reviewed by Van Harlingen (1995) and Tsuei and Kirtley (2000). The order-parameter symmetry affects the transport properties of grain boundaries in the high- T_c cuprates in various ways, as described below and depicted in Fig. 57. For film boundaries, the $d_{x^2-y^2}$ -wave-dominated symmetry together with the microstructure of the grain boundaries has been found to cause a depression of J_c by one to two orders of magnitude, as the [001]-tilt angle is increased from 0° to 45° (Hilgenkamp, Mannhart, and Mayer, 1996).

First, owing to the spatial coherence of the wave function describing the superconducting state, a boundary region with a depressed order parameter is expected at the interface between $d_{x^2-y^2}$ -wave superconductors, which form a contact at a misorientation angle θ (Hilgenkamp and Mannhart, 1997). Typically, such a boundary region stretches over a distance of the order of the coherence length ξ from the boundary. The depression of the order parameter is due to the frustration caused by the different crystallographic orientations of the superconductors on either side of the boundary and by the nonzero value of ξ . It is expected that this depression gives rise to quasiparticle states bound by Andreev reflections at the boundary plane, comparable to the quasiparticle states occurring in vortex cores. The magnitude of this depression depends among other parameters on θ , on the boundary symmetry and configuration, on temperature, and on the materials involved. For [001]-tilt boundaries it is expected to be strongest for the maximal obtainable misalignment angle, 45° , for which the superconductor's order-parameter maxima on one side of the grain boundary coincide with the nodes in the gap function of the other side.

Second, the critical current density of a grain-boundary junction increases with increasing values of the order-parameter component perpendicular to the grain-boundary plane. For a grain-boundary junction formed by two $d_{x^2-y^2}$ -wave-dominated grains, this implies a strong dependence of J_c on the orientations of the $d_{x^2-y^2}$ electrodes (Chaudhari, Dimos, and Mannhart, 1990; Dimos *et al.*, 1990). This has been worked out in a first approximation for the case of a highly directional tunneling process (Sigrist and Rice, 1995).

Third, depending on their trajectories, quasiparticles may experience a change of sign in the pair potential when they are reflected at interfaces or when they are transmitted through a grain boundary in a $d_{x^2-y^2}$ superconductor (Hu, 1994). This effect can give rise to bound quasiparticle states at midgap energy (zero-energy states), which are regarded as zero-bias anomalies in tunneling spectroscopy, as discussed above and presented in Fig. 25 (Leseur *et al.*, 1992; Alff *et al.*, 1997). These bound states are expected to reduce the order parameter (Tanaka and Kashiwaya, 1995, 1996; Barash

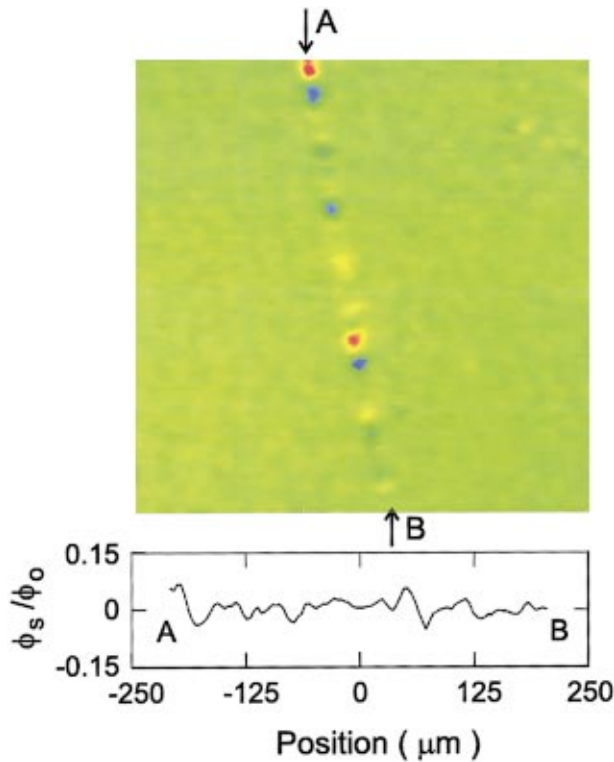


FIG. 58. Scanning SQUID microscope image of a $400 \times 400 \mu\text{m}^2$ area including an asymmetric 45° [001]-tilt $\text{YBa}_2\text{Cu}_3\text{O}_{7-\delta}$ bicrystal grain boundary (film thickness ~ 180 nm). The boundary is marked by arrows A and B. Self-generated magnetic flux is apparent along the grain boundary. The bottom section shows a cross section through the data along the grain boundary measured in units of Φ_0 penetrating the SQUID's pickup loop. The measurements were done at 4.2 K. From Mannhart, Hilgenkamp, *et al.* (1996) [Color].

et al., 1996; Kashiwaya and Tanaka, 2000), and thus to influence current flow. A review has been given by Löfwander *et al.* (2001).

Fourth, independent of the details of the current transfer across the junction (such as the degree of directionality of the charge-transfer process) the order-parameter orientations in specific configurations cause a π -phase shift across the junction. This is, for example, the principle underlying the spontaneous generation of half-flux quanta in specially designed tricrystal rings (Tsuei *et al.*, 1994). Because of the faceted microstructure of thin-film grain boundaries, such π -phase shifts play an important role for individual grain boundaries. Faceting, in combination with the $d_{x^2-y^2}$ symmetry, leads to an inhomogeneous distribution of the Josephson current (Hilgenkamp, Mannhart, and Mayer, 1996), including regions with a supercurrent counterflow (“negative” J_c). This inhomogeneity, which is most prominent for asymmetric 45° [001]-tilt grain boundaries, causes anomalous magnetic-field dependencies of the critical current, as depicted in Fig. 37. It also leads to spontaneously generated magnetic fluxes being observed for asymmetric 45° grain-boundary junctions, as presented in Fig. 58 (Mannhart, Hilgenkamp, *et al.*, 1996; see also Suzuki *et al.*, 2000) and to deviations of the current-

phase relation from the standard sinusoidal dependence as discussed in Sec. V.C (see Fig. 40). The effect of π facets on the grain-boundary critical current is evident from the small value of I_c of 45° [001]-tilt boundaries in zero applied magnetic field. Frequently, much higher critical currents are observed in fields of a few Gauss (Copetti *et al.*, 1995; Humphreys *et al.*, 1995; Hilgenkamp, Mannhart, and Mayer, 1996; Mannhart, Mayer, and Hilgenkamp, 1996). The π facets have also been proposed to improve flux pinning for facet lengths < 300 nm and therefore to enhance the grain boundary I_c (Tuohimaa and Paasi, 1999; Tuohimaa *et al.*, 1999). Based on the combined effects of the $d_{x^2-y^2}$ symmetry of the order parameter and the faceted microstructure of the grain boundaries, a model has been developed that is able to account for all experimental observations concerning the magnetic-field dependence of the critical current, such as its dependence on grain-boundary misorientation and its insensitivity to grain-boundary oxygenation (Hilgenkamp *et al.*, 1997).

The electronic properties of interfaces between d -wave superconductors have been calculated by several groups, considering a range of values for transparency and roughness of the barrier.¹¹ In part of this work, the misorientation-induced order-parameter depression, the amount of s -wave admixture, and the respective local quasiparticle density of states are considered.

To explain the misorientation-independent critical current densities of c -axis-coupled 45° [001]-twist boundaries measured by the Brookhaven group (Zhu *et al.*, 1998; Li *et al.*, 1999a, 1999b), they argue that $\text{Bi}_2\text{Sr}_2\text{CaCu}_2\text{O}_{8+\delta}$ has pure s -wave symmetry, which, however, seems to disagree with a large body of other experimental data. As its validity would have far-reaching consequences for the understanding of high- T_c superconductivity, corroboration of its theoretical and experimental foundations is desirable.

Additional discussions of the effect of grain-boundary and twin behavior in d -wave superconductors are given, for example, by Tsuei and Kirtley (2000).

D. Interface charging and band bending

Pairing symmetry does not significantly affect the normal-state resistivity $R_n A$ of the interfaces. The high $R_n A$ values of typically $10^{-8} \Omega \text{cm}^2$, which correspond to resistivities of the order of $10^{-1} \Omega \text{cm}$ for an assumed effective thickness of a resistive region of ~ 1 nm (Chaudhari, Dimos, and Mannhart, 1990), are indicative

¹¹See, for example, Millis, 1994; Barash *et al.*, 1995; Bruder *et al.*, 1995; Deutscher and Maynard, 1995; Tanaka and Kashiwaya, 1995, 1996; Tang *et al.*, 1996; Walker and Luettmmer-Strathmann, 1996; Fogelström *et al.*, 1997; Hurd, 1997; Fogelström and Yip, 1998; Löfwander, Johansson, *et al.*, 1998; Löfwander, Shumeiko, and Wendin, 1998; Östlund, 1998; Golubov and Kupryyanov, 1999; Hogan-O’Neill *et al.*, 1999; Golubov and Tafuri, 2000; Kashiwaya and Tanaka, 2000; Burkhardt, 2001; Löfwander *et al.*, 2001.

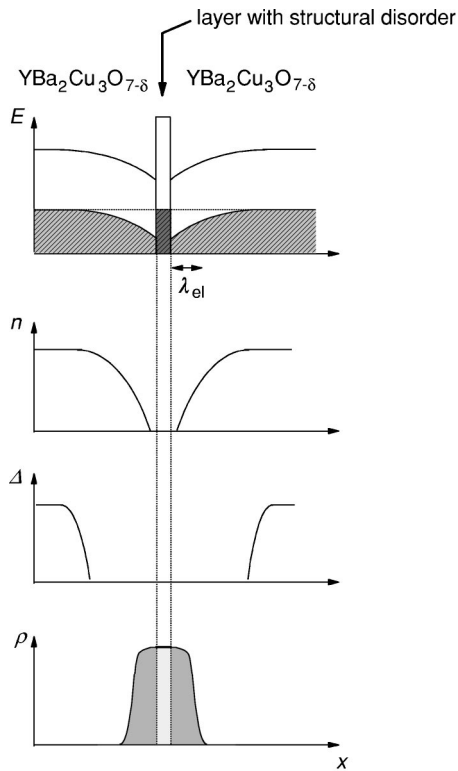


FIG. 59. Sketch of a possible scenario for bending the electronic band structure of high- T_c cuprates at a grain-boundary. In the example shown, depletion layers are formed at the grain-boundary interface, which cause a depression of the superconducting order parameter and a transition of the cuprate into the insulating state in the region at the interface. From Mannhart *et al.* (2000b).

of the presence of an insulating zone at the interfaces. Such an insulating layer would also be in accordance with EELS studies, which have revealed a reduction of mobile charge carriers at grain boundaries (Babcock and Vargas, 1995; Browning *et al.*, 1998), and with Fiske resonance measurements of the Swihart velocity (Winkler *et al.*, 1994). Therefore the question arises whether other mechanisms besides those discussed make the grain boundaries insulating.

Recently it has been pointed out (Mannhart and Hilgenkamp, 1997, 1998; Hilgenkamp and Mannhart, 1998a) that bending of the electronic band structure can occur at interfaces in high- T_c cuprates, causing depletion or enhancement layers (Browning *et al.*, 1993; Babcock, Cai, *et al.*, 1994) next to the interface (Fig. 59). This is in contrast to grain boundaries or other interfaces in conventional superconductors and in MgB_2 , in which the large carrier densities prohibit band bending. Similar space-charge layers occur at grain boundaries in dielectric or ferroelectric oxides (Ravikumar *et al.*, 1995; Sutton and Balluffi, 1995; Chiang *et al.*, 1997; Vollmann *et al.*, 1997) and in semiconductors (Taylor *et al.*, 1952; Werner, 1985; Greuter and Blatter, 1990). In contrast to these more conventional materials, in the high- T_c cuprates, the electrostatic screening length λ_{el} of several Å to about 1 nm and the distance between the mobile charge carriers are comparable, so that the conventional

band-bending models based on a continuum description of the charge distribution are not applicable. Despite this, it is clear that in the layers of modified carrier density the order parameter is reduced, and, for strong enough depletion, the cuprates undergo a phase transition into the antiferromagnetic insulating state. The space-charge layers are easily induced by charges present at the boundaries and stretch on both sides over distances of the order of λ_{el} into the grains. Thereby the influence of the interfaces is extended far beyond the structurally distorted region. In Fig. 59, a possible scenario is sketched for band bending at a high- T_c grain boundary. An exact quantitative description of the effects of band bending on the electronic properties of interfaces is difficult to provide. Such a description requires detailed knowledge of the microscopic electronic properties, including the pairing mechanism, which is not available. For low-angle grain boundaries it has been shown that band bending can explain the reduction of J_c (Gurevich and Pashitskii, 1998). A further indication of its importance can be obtained from its contribution to $R_n A$. Treating the grain boundaries as back-to-back Schottky barriers, $R_n A$ values of the order of $10^{-8} \Omega \text{ cm}^2$ have been estimated, which increase with increasing width of the dislocation layer formed at the grain-boundary interface (Hilgenkamp and Mannhart, 1998a, 1998b; Mannhart and Hilgenkamp, 1998). For the grain-boundary capacitance $C/A \approx 1 \times 10^{-5} \text{ F/cm}^2$ was obtained (Mannhart and Hilgenkamp, 1998). Both values agree well with measured data (Tarte *et al.*, 1997). Furthermore, the band-bending model successfully predicted Ca doping of the $\text{YBa}_2\text{Cu}_3\text{O}_{7-\delta}$ grains to increase the grain-boundary critical current density (Schmehl *et al.*, 1999). The most detailed assessment of band bending has been provided by Nikolic *et al.* (2002; see also Freericks *et al.*, 2001), who reported a self-consistent microscopic study of the effects of screened dipole layers on the characteristic properties of SINIS junctions. The space-charge layers were found to depress the order parameter near the SN boundary, the junction critical current, and, to a lesser extent, its normal-state resistance.

It should be noted that this model of band bending and induced phase transitions does not hold exclusively for high- T_c superconductors, but is of general importance in oxide electronics (Hilgenkamp and Mannhart, 1998a; Mannhart and Hilgenkamp, 1998). With this understanding it has, for example, been suggested that the band-bending mechanism provides a basis for the intriguing grain-boundary behavior of the manganates showing colossal magnetoresistance (Hilgenkamp and Mannhart, 1998a; Klein *et al.*, 1999).

E. Mechanisms based on direct suppression of the pairing mechanism

Depending on the pairing mechanism, the misorientation and the interruption of the periodic lattice structure depress the pairing interaction in different ways, for example, by interrupting the antiferromagnetic order of

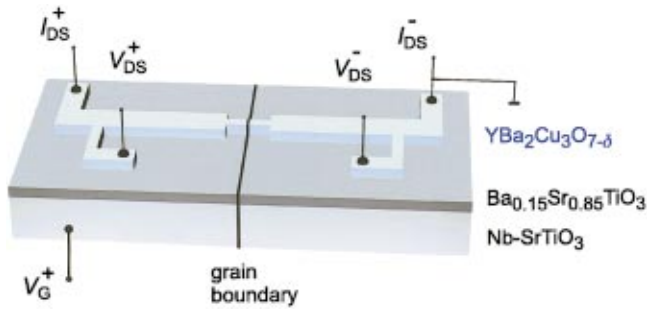


FIG. 60. Sketch of an electric-field-effect device using a bicrystalline $\text{YBa}_2\text{Cu}_3\text{O}_{7-\delta}$ film. The transistor is built in an inverted geometry: the conducting, Nb-doped SrTiO_3 substrate is used as a gate electrode, and the electric field is applied across the $\text{Ba}_{0.15}\text{Sr}_{0.85}\text{TiO}_3$ gate insulator to the $\text{YBa}_2\text{Cu}_3\text{O}_{7-\delta}$ drain-source channel. After Mayer *et al.* (1996) [Color].

the CuO_2 planes (Chaudhari *et al.*, 1990). Analogously, a preferred direction of the spins of the charge carriers forming a Cooper pair, caused possibly by finite spin-orbit coupling, may lead to spin-flip processes, which lower the order parameter of all boundaries except for the [001]-tilt ones (Mannhart and Hilgenkamp 1997, 1998).

VIII. CONTROL OF GRAIN BOUNDARIES WITH ELECTRIC FIELDS OR QUASIPARTICLE INJECTION

A. Applied electric fields

How do electric fields applied in the grain-boundary plane perpendicular to the film surface affect grain-boundary transport? The application of large electric fields in field-effect devices is unfortunately impeded by a problem of epitaxial growth: the bicrystal grain bound-

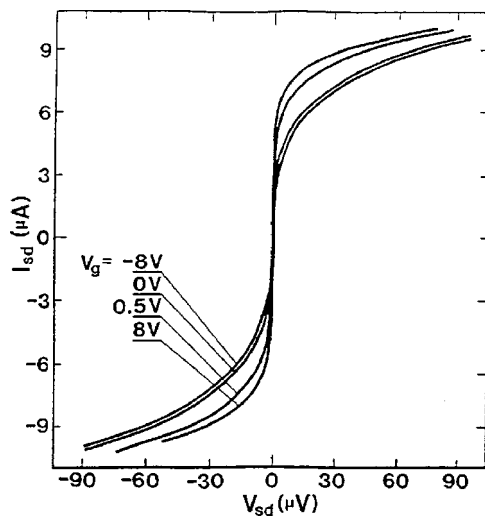


FIG. 61. Current-voltage characteristics of a three-terminal device based on a bicrystal grain-boundary junction with $\theta = 45^\circ$, measured at 4.2 K for different gate voltages V_g . From Ivanov *et al.* (1993); figure courtesy of Z. G. Ivanov and T. Claeson, Chalmers University of Technology, Göteborg, Sweden.

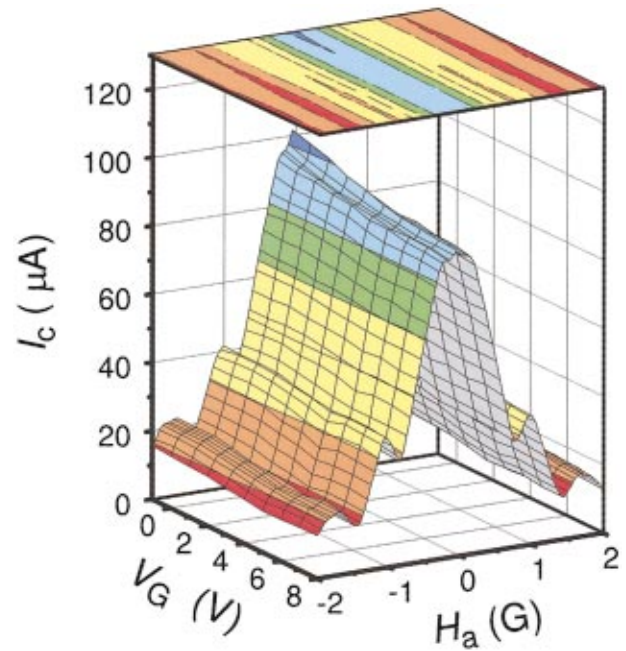


FIG. 62. Critical current of the Josephson field-effect transistor shown in Fig. 60, with a drain-source channel consisting of a $\text{YBa}_2\text{Cu}_3\text{O}_{7-\delta}$ film containing a 36° [001]-tilt grain-boundary. The critical current, which was measured at 4.2 K, is shown as a function of gate voltage V_g and applied magnetic field H_a . From Mayer *et al.* (1996) [Color].

ary is usually inherited into the gate insulator (see Fig. 60), where it acts as a leakage path for the gate current (Frey *et al.*, 1996a). This effect, which may be exploited in an elegant way for quasiparticle injection experiments as described below, has been partially circumvented in various ways. In one set of devices, for example, a bicrystal substrate dimpled to a thickness of $\sim 50 \mu\text{m}$ was used as a gate insulator, which allowed polarizations of $\sim 0.5 \mu\text{C}/\text{cm}^2$ to be applied, resulting in changes of I_c by +6% (Nakajima *et al.*, 1993, 1994). A complete thin-film configuration was used by Ivanov and co-workers, who employed an amorphous SrTiO_3 layer as a gate insulator. Using an amorphous layer allowed all grain-boundary problems to be avoided, but also decreased the permittivity of the gate dielectric. Nevertheless, this group observed an I_c shift of an asymmetric 45° [001]-tilt $\text{YBa}_2\text{Cu}_3\text{O}_{7-\delta}$ bicrystal junction of 40% for a gate voltage of 0.5 V, as shown by Fig. 61 (Ivanov *et al.*, 1993). These researchers observed an increase in the grain boundary I_c for positive voltages applied to the gate. Dong *et al.* (1995) investigated a similar device, using overdoped $\text{Sm}_{1-x}\text{Ca}_x\text{Ba}_2\text{Cu}_3\text{O}_{7-\delta}$ films. They also observed large electric-field effects, but of opposite polarity, as did other groups (Nakajima *et al.*, 1994; Petersen, Takeuchi, *et al.*, 1995; Mayer *et al.*, 1996; Suh *et al.*, 1997). The field-induced changes have been reported to increase with the grain-boundary misorientation angle, being largest for asymmetric 45° grain boundaries (Mayer *et al.*, 1996). The critical current of a 36° Josephson junction as a function of applied electric and magnetic fields is presented in Fig. 62. It came as a surprise

that the field-induced changes in the grain boundaries' normal-state resistances observed in all experiments were very small.

Various models have been proposed to explain the effects of electric fields on grain-boundary transport. Using a Ginzburg-Landau-based model it was shown that the I_c changes observed by Dong and collaborators are consistent with a field-induced change in the carrier density in the Josephson junction (Betouras *et al.*, 1996). As the measured I_c changes were found to scale with the field-dependent, nonlinear dielectric constant of the gate insulator ϵ_r , it was proposed that the effects were caused by an assumed giant piezoelectric effect of the epitaxial SrTiO₃ gate layer (Petersen, Takeuchi, *et al.*, 1995; Windt *et al.*, 1999; see also Grupp and Goldman, 1997). As this hypothesis accounts for neither the small values of the field-induced changes of R_n nor the proportionality of the I_c changes with ϵ_r , it seems more likely that the electric fringe fields arising from charges embedded in the grain boundaries are affected by the gate field-induced change of ϵ_r (Hilgenkamp and Mannhart, 1999). Like the quasiparticle injection effects described in the next section, these field effects have been investigated intensively for use in three-terminal devices (see Sec. XI.C).

B. Quasiparticle injection

Configurations like the one shown in Fig. 60 can also be used to inject quasiparticles into grain boundaries. Injection current densities of 20–140 A/cm² have been reported to cause a nonthermal suppression of the critical current of 24° YBa₂Cu₃O_{7- δ} [001]-tilt boundaries at 4.2 K, attributed to nonequilibrium effects (Iguchi *et al.*, 1994). Quasiparticle injection can also lead to displacement effects in the $I_{DS}(V_{DS})$ characteristics occurring above well-defined voltages V_{DS} , as has been measured in experiments in which quasiparticles were injected from Au contacts into YBa₂Cu₃O_{7- δ} step-edge junctions (Lombardi *et al.*, 2000). Although quasiparticle injection into Josephson junctions causes surprising phenomena and may provide a better understanding of nonequilibrium phenomena in high- T_c superconductors, this work has not been taken up by other groups, and the effects of injection on grain-boundary transport have only begun to be explored.

IX. IRRADIATION OF GRAIN BOUNDARIES

A. Irradiation with electrons

Using low-temperature scanning electron microscopy (Huebener, 1988, 2000), it is possible to image the distribution of the current flow across grain boundaries as illustrated by the example shown in Fig. 63 (Mannhart, Gross, *et al.*, 1989; Fischer *et al.*, 1994; Doderer *et al.*, 1995; Mayer *et al.*, 1995). The spatial resolution of low-temperature SEM is given by the thermal healing length of the sample under investigation and in most cases equals about 1 μ m. Low-temperature SEM, which oper-

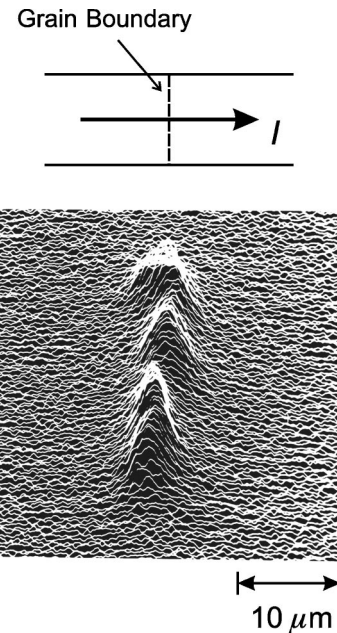


FIG. 63. Image of the voltage response signal of a 38° [001]-tilt grain boundary in a bicrystalline YBa₂Cu₃O_{7- δ} film obtained by low-temperature scanning electron microscopy. The 20- μ m-wide and 0.5- μ m-thick bridge crossing the grain-boundary was biased at 14 K with a current of 39 mA. The signal images the voltage state of the grain boundary, which shows up because the bias current exceeds the critical current of the grain boundary but not of the grains. After Mannhart, Gross, *et al.* (1989).

ates with electron energies of the order of 20–30 keV, has been shown to be an outstanding technology for imaging and analyzing magnetic-flux structures in grain boundaries (Fischer *et al.*, 1994), as well as rf resonances (Mannhart, Gross, *et al.*, 1989; Doderer *et al.*, 1995) and the transport properties of grain-boundary networks (Mannhart, Huebener, *et al.*, 1990).

Electron beams with much higher energies, typically 120 keV, have been used to alter bicrystalline grain boundaries (Tafari *et al.*, 1997, 1998). The electron irradiation causes not only a reduction of J_c and enhancement of R_n , but also a change in the ratio of the barrier thickness to the dielectric constant, signalled by a shift of Fiske steps. These effects are presumably caused by oxygen disorder induced by the electron irradiation.

B. Irradiation with light

The electric response of single grain boundaries to irradiation with light has been investigated extensively by several groups (Kaplan *et al.*, 1991; Bhattacharya *et al.*, 1993; Tanabe *et al.*, 1994; Elly *et al.*, 1997; Hoffmann *et al.*, 1997; Adam *et al.*, 1999; Gilibert *et al.*, 1999; Médicci *et al.*, 2000). To light pulses, nonbolometric responses were observed, with reported time scales as short as 1 ps (Adam *et al.*, 1999, 2000). Irradiation of light was shown to lead to photoinduced hole doping, typically reducing R_n and increasing both I_c and the $I_c R_n$ product (Tanabe *et al.*, 1994; Hoffmann *et al.*, 1997; Gilibert *et al.*, 1999; Médicci *et al.*, 2000). The doping be-

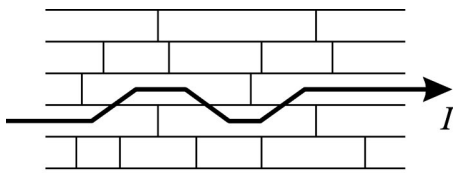


FIG. 64. Sketch of a polycrystal with a large effective grain-boundary area. From Mannhart (1990).

havior was interpreted as resulting from holes being added to grain-boundary layers depleted of charge. Without further evidence this depletion was generally attributed to a reduced oxygen concentration at the boundary. The data are also consistent, however, with depletion layers being caused by band bending (see Sec. VII.D).

Like irradiation with electrons, light irradiation was also found to shift the position and intensity of the Fiske steps, which was accounted for by a doping-induced shift of the ratio of the barrier thickness to the dielectric constant (Elly *et al.*, 1997).

In low-temperature laser scanning microscopy, thermoelectric or bolometric voltages induced in the samples by irradiation with a scanned laser beam are utilized to image the transport properties of the grain boundaries, with submicrometer resolution at best (Divin *et al.*, 1991; Shadrin *et al.*, 1998, 1999; Korolev *et al.*, 2000).

C. Irradiation with ions

Implantation of bicrystalline $\text{YBa}_2\text{Cu}_3\text{O}_{7-\delta}$ films with He^+ ions has been investigated as a tool to modify grain-boundary properties after growth (Navacerrada *et al.*, 2000, 2001). By irradiating the samples with 80 keV He^+ ions delivered in doses of $10^{13}/\text{cm}^2$, grain-boundary critical current densities were increased by about 10%, attributed to rearrangements in the oxygen sublattice. Higher doses, however, irreversibly degraded J_c .

X. BULK APPLICATIONS

In most cases, large critical currents are the key requirement for bulk applications. One approach to obtaining large critical currents is to avoid grain boundaries by using quasi-single-crystalline samples, fabricated, for example, by melt texturing (Cardwell *et al.*, 1998; Murakami, 1999). The other approach is to optimize the structure and the stoichiometry of the grain boundaries in polycrystalline samples. Whereas melt texturing is an appropriate technique for fabrication of samples with length scales of a fraction of a meter, which may be used, for example, to produce magnetic bearings or fault current limiters, for wires with high critical currents one necessarily deals with polycrystalline structures. The critical currents can be enhanced by biaxially aligning the grains (Dimos *et al.*, 1990) and by selecting

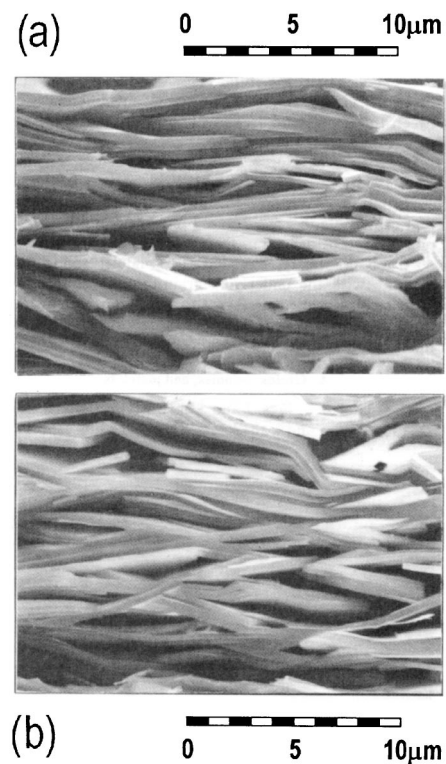


FIG. 65. SEM images of the (a) transverse and (b) longitudinal fracture surfaces of a Bi/Pb (2223) filament with $J_c(77\text{ K}, 0\text{ T}) = 2.5 \times 10^4\text{ A/cm}^2$. The fractures were taken in the middle of the filament and span approximately half of the total filament thickness. From Hensel *et al.* (1995); figure courtesy of R. Flükiger, Université de Genève, Switzerland.

microstructures with large effective grain-boundary areas (Mannhart and Tsuei, 1989).

The critical current of a polycrystalline sample usually differs substantially from the product of the grain-boundary critical current density and the cross-sectional area of the sample. The current flow through polycrystalline high- T_c superconductors provides a fascinating percolation problem, which has been studied with intense interest theoretically,¹² as well as experimentally (see, for example, Mannhart, Huebener, *et al.*, 1990; Larbalestier *et al.*, 1994). As proposed by Mannhart and Tsuei (1989), an optimized grain arrangement, for example, of grains with large aspect ratios in a brick-wall manner, provides large effective grain-boundary areas for the percolating current, resulting in high critical current densities (see Fig. 64; Mannhart and Tsuei, 1989; Mannhart, 1990; Bulaevskii *et al.*, 1992, 1993). In the so-called railway-switch model developed to describe current flow in $(\text{Bi,Pb})_2\text{Sr}_3\text{Ca}_3\text{Cu}_3\text{O}_{10+\delta}$ tapes, the current

¹²Theoretical work on the problem includes that of Mannhart and Tsuei, 1989; Rhyner and Blatter, 1989; Mannhart, Huebener, *et al.*, 1990; Nichols and Clarke, 1991; Bulaevskii *et al.*, 1992, 1993; Cai and Welch, 1992; Hensel *et al.*, 1993, 1995; Kroeger *et al.*, 1994; Goyal, Specht, *et al.*, 1996; Malozemoff *et al.*, 1997; Evetts *et al.* 1999; Rutter *et al.*, 2000; Holzapfel *et al.*, 2001.

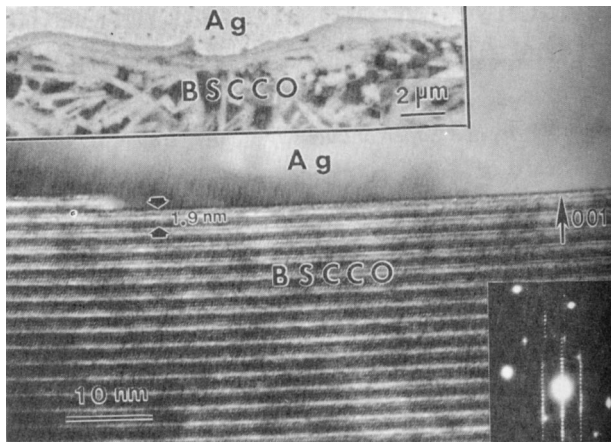


FIG. 66. High-resolution TEM image of an Ag-sheathed Ag-(Bi,Pb) $_2$ Sr $_2$ Ca $_2$ Cu $_3$ O $_x$ tape. The SEM image shows the platelike phase at the Ag interface. From Feng *et al.* (1993); figure courtesy of Y. Feng and D. C. Larbalestier, University of Wisconsin, USA.

is considered to flow predominantly through low-angle [100]-tilt boundaries. As shown by Fig. 65, such boundaries are frequently found in these conductors and tend to form colony structures (Hensel *et al.*, 1993, 1995; Grindatto *et al.*, 1996). In the freeway model (Malozemoff *et al.*, 1997), boundaries between colonies of aligned grains (Feng *et al.*, 1993) are recognized as bottlenecks in (Bi,Pb) $_2$ Sr $_3$ Ca $_3$ Cu $_3$ O $_{10+\delta}$ tapes. Within the colonies, plateletlike grains are well aligned along the c axis. This provides large grain-boundary areas which support high critical currents.

The strategies described to enhance the J_c of polycrystals, namely, the use of large-area grain boundaries and alignment of the grains, are followed by both classes of technologies employed for the fabrication of high- T_c wires: the powder-in-tube technique (Heine *et al.*, 1989; Q. Li *et al.*, 1997) and the coated-conductor technologies (Iijima *et al.*, 1992, 1993; Wu *et al.*, 1994, 1995; Goyal, Norton, *et al.*, 1996; Norton *et al.*, 1996). With these techniques the critical current densities have been increased from the original value of a few hundred A/cm 2 (77 K) for unaligned wires (see Fig. 6; Jin *et al.*, 1987) to several million A/cm 2 (77 K) today (see, for example, Park *et al.*, 1998), corresponding to an increase in the engineering critical current densities from ~ 100 A/cm 2 to $\sim 2 \times 10^4$ A/cm 2 . The wires and tapes fabricated by these techniques have also been characterized in detail by a variety of microscopic techniques, and an extensive literature is available on this topic (see, for example, Vase *et al.*, 2000). Here, it is only possible to describe these technologies briefly with reference to grain-boundary properties.

A. Powder-in-tube method

In the powder-in-tube technology (Heine *et al.*, 1989), the BSCCO phases Bi $_2$ Sr $_2$ CaCu $_2$ O $_{8+\delta}$ or (Bi,Pb) $_2$ Sr $_2$ Ca $_2$ Cu $_3$ O $_{10+\delta}$ are formed in silver tubes by appropriate heat treatment with oxide or calcite pow-

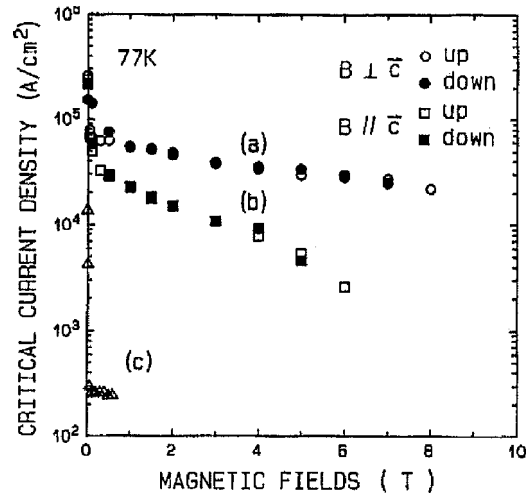


FIG. 67. Critical current density as a function of magnetic field for polycrystalline YBa $_2$ Cu $_3$ O $_{7-\delta}$ films: (a,b) YBa $_2$ Cu $_3$ O $_{7-\delta}$ grown on IBAD-deposited biaxially aligned yttrium-stabilized zirconia (YSZ) layers with $B \perp c$ and $B \parallel c$; (c) YBa $_2$ Cu $_3$ O $_{7-\delta}$ grown on an rf-sputtered YSZ layer with $B \perp c$. This measurement originally demonstrated the benefits of IBAD. After Iijima *et al.* (1992); figure courtesy of Y. Iijima, Fujikura Ltd., Tokyo, Japan.

ders. Similarly, superconductors may be grown by melt-solidification methods on Ag tapes (Muroga *et al.*, 1998). By mechanical deformations and heat treatments of the tubes prior to final anneal, strong texturing is achieved, and densely stacked, platelet-like BSCCO crystals are obtained, oriented with their ab planes parallel to the BSCCO-silver interface (Feng *et al.*, 1992, 1993; Liu *et al.*, 1994; Hensel *et al.*, 1995; Muroga *et al.*, 1998; Q. Y. Hu *et al.*, 1999), as shown in Fig. 66 and analyzed in detail by Cai and Zhu (1998). A large fraction of low-angle grain boundaries has been observed, in particular close to the BSCCO-silver interface (Kumakura *et al.*, 1999). For (Bi,Pb) $_2$ Sr $_2$ Ca $_2$ Cu $_3$ O $_{10+\delta}$, for example, it has been reported that more than 40% of the boundaries have misorientation angles of less than 15° (Goyal *et al.*, 1995) and 30% less than 10°. The grains have been observed to form colonies, with low-angle grain boundaries dominating inside the colonies, and large-angle boundaries being present at their intersection (Liu *et al.*, 1994).

In those wires in which sufficiently strong grain-boundary coupling has been achieved, the current densities are controlled by thermally activated flux motion (Huang *et al.*, 1998). Tönies *et al.* (2001) investigated the transition from grain-boundary-limited J_c to flux-flow-limited behavior as a function of applied magnetic fields for Bi $_2$ Sr $_2$ Ca $_2$ Cu $_3$ O $_{10+\delta}$ tapes, finding a temperature-dependent crossover field between both regimes, the grain boundaries limiting I_c at small fields.

B. Coated conductors

In the coated-conductor technology, YBa $_2$ Cu $_3$ O $_{7-\delta}$ films, typically of micrometer thickness, are deposited on flexible substrates for cable applications, or on cheap,

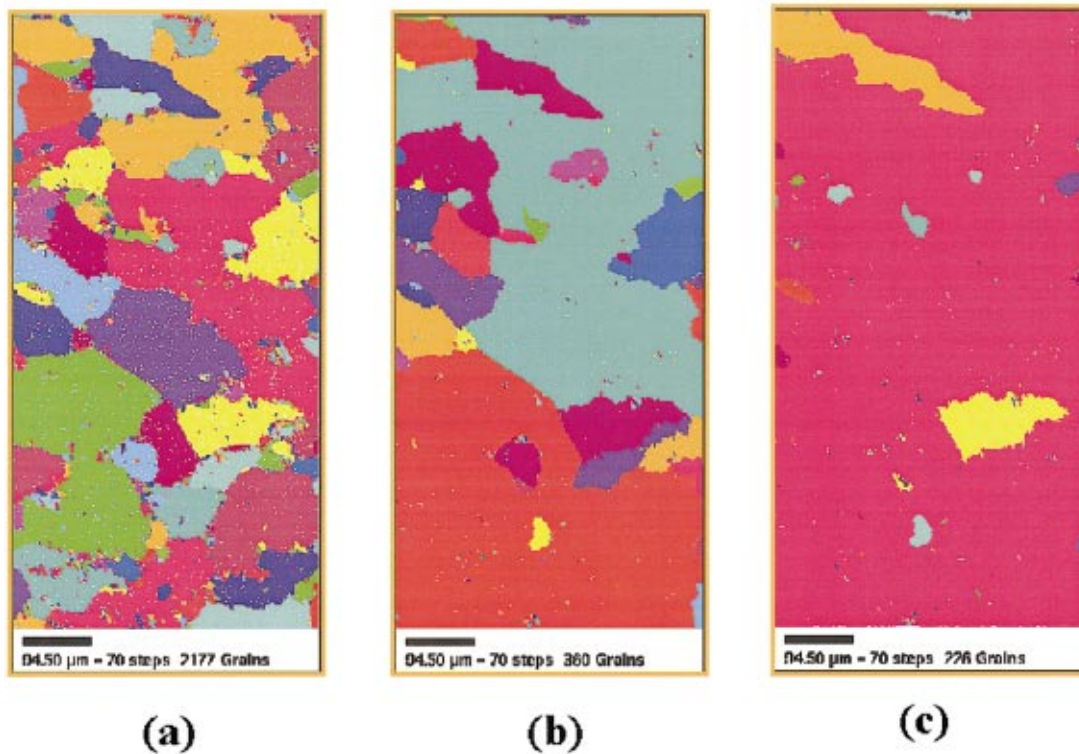


FIG. 68. Orientation image obtained by indexing electron-diffraction patterns of a RABiTS-type sample consisting of a $\text{Nd}_{1+x}\text{Ba}_{2-x}\text{Cu}_3\text{O}_{7-\delta}$ film grown on textured Ni substrates with a YSZ/CeO₂ buffer-layer architecture. The image has been drawn with the criterion that a given color represents a contiguous region without grain-boundary, or regions connected by grain boundaries with angles smaller than (a) 1°, (b) 2°, and (c) 3°. From Cantoni *et al.* (2001); figure courtesy of C. Cantoni and D. K. Christen, Oak Ridge National Laboratory, USA [Color].

large-area, polycrystalline substrates, for example, for use in fault current limiters. It has been found that the grain boundaries present in these layers behave in many ways like bicrystal grain boundaries (Verebelyi *et al.*, 2000). To biaxially align the grains, four technologies are used.

In the ion-beam-assisted deposition (IBAD) process (Iijima *et al.*, 1992, 1993, 2000; Reade *et al.*, 1992; Wu *et al.*, 1994, 1995; Usoskin *et al.*, 2000), the substrate tape, typically made of Inconel or Hastelloy, is covered with an IBAD layer, which usually is a Y-ZrO₂ film grown to a thickness of 0.5–1 μm, while being textured by bombardment with an inclined beam of Ar ions. The Y-ZrO₂ film may be covered by much thinner buffer layers of Y₂O₃ or CeO₂ with a characteristic thickness of 20–30 nm. Alternatively a MgO film, which may have a thickness as small as ≈10 nm and thus can be grown much faster, may be used as an IBAD layer (Willis *et al.*, 2000). Onto this or similar structures, the YBa₂Cu₃O_{7-δ} is grown epitaxially, so that the ion-beam-induced texture is transferred to the superconductor. At present, average in-plane misorientations of ~10° and ~4° are achieved in best cases for ~1 μm yttria-stabilized zirconia (YSZ) and MgO layers on Hastelloy, respectively (Willis *et al.*, 2000). This results in a major portion of low-angle tilt boundaries, with θ in the range of 2°–7° (Kung *et al.*, 1999) for YSZ IBAD layers and correspondingly large J_c values in magnetic fields (see Fig. 67).

In the rolling-assisted, biaxially textured, substrate process (RABiTS; Norton *et al.*, 1996; Goyal, Norton, *et al.*, 1996; Hawsey *et al.*, 1999), a flexible Ni tape is usually employed as a substrate. This tape is biaxially textured by rolling and annealing processes. On this tape, epitaxial buffer layers consisting, for example, of CeO₂(~30 nm)/YSZ(~500 nm)/CeO₂(~30 nm) are deposited before the high- T_c film is grown, again to a typical thickness of 0.5–1 μm. The standard superconductor is YBa₂Cu₃O_{7-δ}, but successful work has also been reported for HgBa₂CaCu₂O₆ (Xie *et al.*, 2000). The texture achieved by the RABiTS process is in the range of 6°–10° (full width at half maximum of the ω and ϕ scans). With diameters of several micrometers to several hundreds of micrometers, the grains are considerably larger than in IBAD samples. Detailed grain orientation and percolation maps have been published (Feldmann *et al.*, 2000; Holzapfel *et al.*, 2001), an example of which is shown in Fig. 68. These studies showed that the mosaic spreads of the YBa₂Cu₃O_{7-δ} films are at least as good as those of the Ni tapes. They may be even smaller, because the out-of plane misorientation of the Ni grains is not necessarily transferred to the YBa₂Cu₃O_{7-δ} film. It was reported that all Ni grain boundaries with misorientation angles exceeding 4° initiate a barrier in the YBa₂Cu₃O_{7-δ} film and may thereby cause percolative current flow (Feldmann *et al.*, 2000).

In the inclined substrate deposition process the texture is induced in a PLD-grown Y-ZrO₂ film or in an

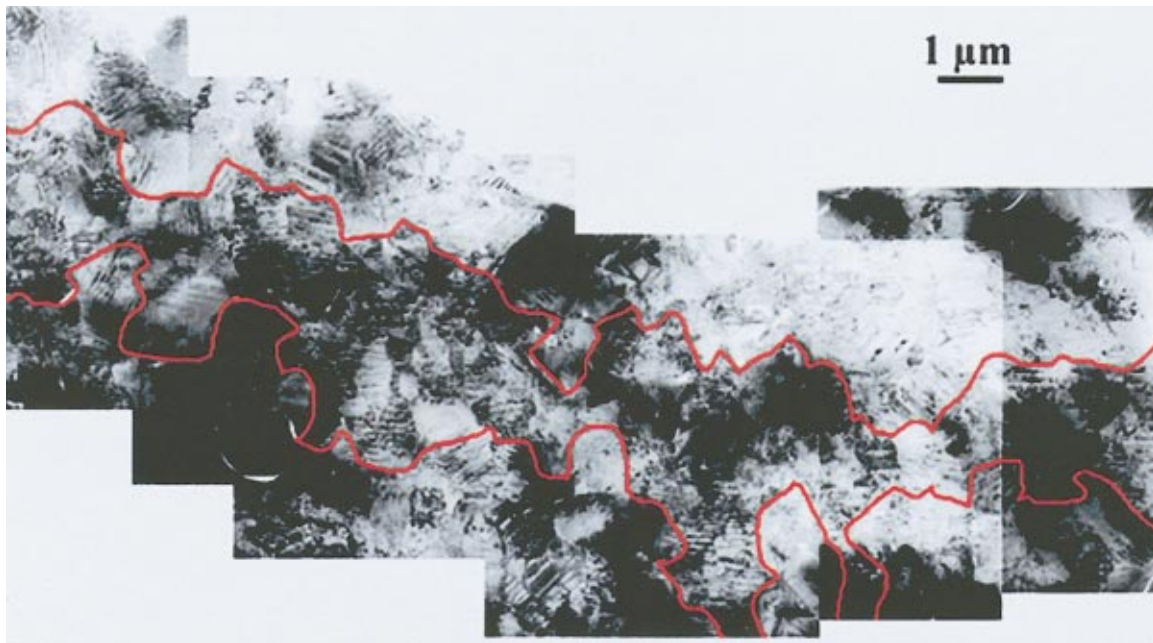


FIG. 69. Low-magnification, TEM-image montages depicting the colony structures of well-aligned grains in a 1- μm -thick $\text{YBa}_2\text{Cu}_3\text{O}_{7-\delta}$ film grown by pulsed laser deposition on a polycrystalline Ni-based substrate. The linkage of the colonies, shown by the outlined regions, provides a percolation pathway for the transport supercurrent. From Kung *et al.* (1999); figure courtesy of H. Kung, Los Alamos National Laboratory, USA [Color].

e -beam-deposited MgO layer by tilting the substrate during growth with respect to the beam of arriving adatoms (Hasegawa *et al.*, 1996; Bauer *et al.*, 1999). The $\text{YBa}_2\text{Cu}_3\text{O}_{7-\delta}$ film is grown with a thickness of up to 2 μm on top of this package. Texturing with a spread of 7° has been reported (Bauer *et al.*, 2000).

To texture $\text{YBa}_2\text{Cu}_3\text{O}_{7-\delta}$ films grown by metal-organic chemical vapor deposition on polycrystalline silver substrates, Ma *et al.* (2000), applied magnetic fields up to 8 T during film growth. The magnetic field was reported to improve the texturing and J_c of the superconducting films.

With the induced texture, the current densities of the $\text{YBa}_2\text{Cu}_3\text{O}_{7-\delta}$ films fabricated by IBAD, RABiTS, or inclined substrate deposition routinely exceed $5 \times 10^5 \text{ A/cm}^2$ for short samples, with best values surpassing $2 \times 10^6 \text{ A/cm}^2$ at 77 K in self-field. As the metallic substrates have thicknesses of 50–100 μm , engineering current densities of $2 \times 10^4 \text{ A/cm}^2$ are obtained. Because the grains may form colonies as shown in Fig. 69, for any of these three processes the effective average grain-boundary angle may be smaller than the texture observed (see also Fig. 68). The main challenges these processes face today are cost, maintaining a high J_c in thick films to meet practical I_c requirements, and fabricating wires of sufficient length. Clearly, for the coated-conductor technology, which exploits the whole potential of high- T_c superconductors, further significant progress may be expected.

XI. APPLICATIONS OF GRAIN BOUNDARIES IN THIN FILMS

Grain boundaries with misorientations greater than 10° – 15° are excellent Josephson contacts (Dimos *et al.*,

1988) and are used accordingly in a variety of practical applications. It is impossible to provide a complete overview of all this work within the limitations of this review. Instead, we shall briefly discuss a few selected applications, namely, SQUID-based sensing devices, high-frequency radiation detectors and spectrometers, three-terminal devices, superconducting logic circuits, and some research devices.

A. SQUIDS

The most widespread application of grain-boundary junctions is probably as high- T_c superconducting quantum interference devices (SQUIDS; Koelle *et al.*, 1999). A favored configuration for bicrystal dc SQUIDS is shown schematically in Fig. 70. By using modulation techniques and appropriate flux-coupling structures, one can operate SQUIDS as highly sensitive sensors for all quantities that can be transduced to a change of magnetic flux, such as magnetic fields, electrical currents, voltages, and position.

Following the early demonstration of dc SQUID behavior by superconducting ring structures in polycrystalline films (Koch *et al.*, 1987), the IBM group at Yorktown Heights fabricated the first single grain-boundary and bicrystal SQUIDS, by using epitaxial $\text{YBa}_2\text{Cu}_3\text{O}_{7-\delta}$ films grown on large-grain polycrystalline and bicrystalline substrates (Chaudhari, Mannhart, *et al.*, 1988; Hagerhorst *et al.*, 1989; Koch *et al.*, 1989; Tsuei *et al.*, 1989) (Fig. 71). These SQUIDS already operated at 77 K. Since then, many groups have further developed, with great success, single-layer, and multilayer high- T_c rf and dc SQUID devices, in particular based on grain-

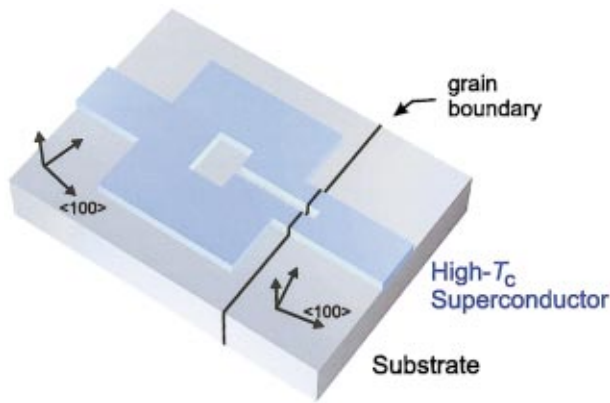


FIG. 70. Schematic presentation of a “square washer” dc SQUID based on bicrystal Josephson junctions [Color].

boundary Josephson junctions.¹³ Figure 71 illustrates the rapid increase in the level of complexity achieved in the early years of high- T_c superconductivity, from the first bicrystal dc SQUID (Hagerhorst *et al.*, 1989) to complex multilayer SQUID magnetometers, as exemplified here by a bicrystal dc SQUID with integrated flux transformer (Hilgenkamp *et al.*, 1994). Although the multilayer devices operate as sensitive magnetometers, their fabrication is very challenging, often resulting in reduced critical temperatures of the SQUIDs, disallowing their practical use at 77 K. For this reason, more popular implementations of the flux-coupling structure have been to couple a multiturn flux transformer on a different substrate to the SQUID in a flip-chip arrangement, or to apply a large inductive shunt to the SQUID. The latter allows the fabrication of a complete device by depositing and structuring only one superconducting film, e.g., on a bicrystalline substrate. The central part of such an inductively shunted, or “directly coupled” SQUID is shown in Fig. 72. Here, the two horizontal leads are connected to a larger pickup circuit.

Most bicrystal high- T_c dc SQUIDs fabricated to date are based on 24° [001]-tilt boundaries. SrTiO₃ bicrystal substrates with this misorientation angle, as well as with a 36.8° [001]-tilt misorientation, were among the first in high quality available commercially. An interesting question arises concerning the optimal misorientation angle for practical applications of grain-boundary junctions. As most applications benefit from a high- $I_c R_n$ product, it appears that lower misorientation angles, in the range of 15° – 20° , are the most promising, provided the boundaries still function as Josephson junctions. As analyzed by Enpuku and co-workers, for the particular

¹³See, for example, Gross, Chaudhari, *et al.*, 1990c, 1990d; Ivanov *et al.*, 1991; Kawasaki *et al.*, 1991; Olsson *et al.*, 1992; Zhang *et al.*, 1992; Koelle *et al.*, 1993a; Kroman *et al.*, 1993; Hilgenkamp *et al.*, 1994; David *et al.*, 1995; Ludwig *et al.*, 1995; Drung, Dantsker, *et al.*, 1996; Glyantsev *et al.*, 1996; Schmidl *et al.*, 1998; Matsuda *et al.*, 1999. For SQUIDs based on natural grain boundaries in the borocarbides see Khare *et al.*, 1996 and Khare and Gupta, 1999.

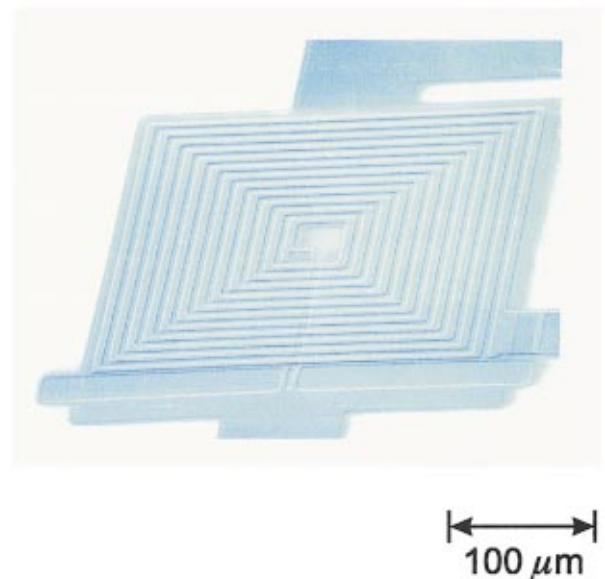
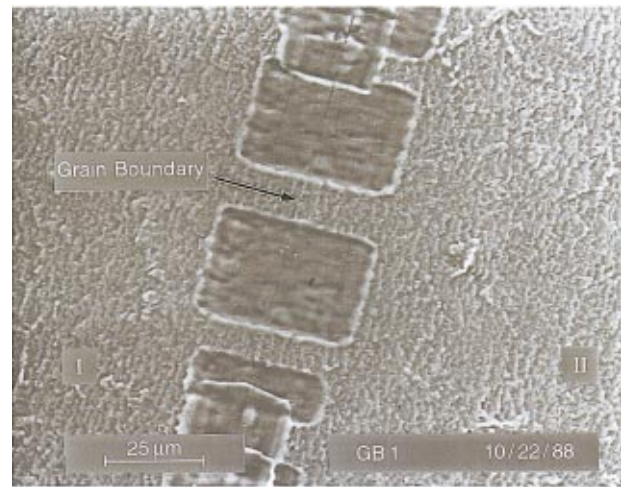


FIG. 71. Scanning electron micrographs of (a) the first bicrystal dc SQUID operating at 77 K (Hagerhorst *et al.*, 1989) and (b) a monolithic flux transformer-coupled dc SQUID magnetometer fabricated on a bicrystal substrate (Hilgenkamp *et al.*, 1994) [Color].

case of dc SQUIDs, a sufficiently large junction normal-state resistance is of additional importance (Enpuku *et al.*, 1995). Considering the limitations imposed on the junction dimensions by standard photolithography (a linewidth of a few μm) they propose that a 30° [001]-tilt is the most favorable grain-boundary misorientation (Minotani *et al.*, 1997; Enpuku *et al.*, 1999).

Many applications of SQUIDs concern the frequency range below 1 kHz. At these frequencies the $1/f$ noise originating from fluctuations of the critical currents of the junctions, discussed in Sec. V.H, strongly limits the attainable resolution unless special precautions are taken. For dc SQUIDs a modulation technique employing bias-current reversal has proved to be very effective

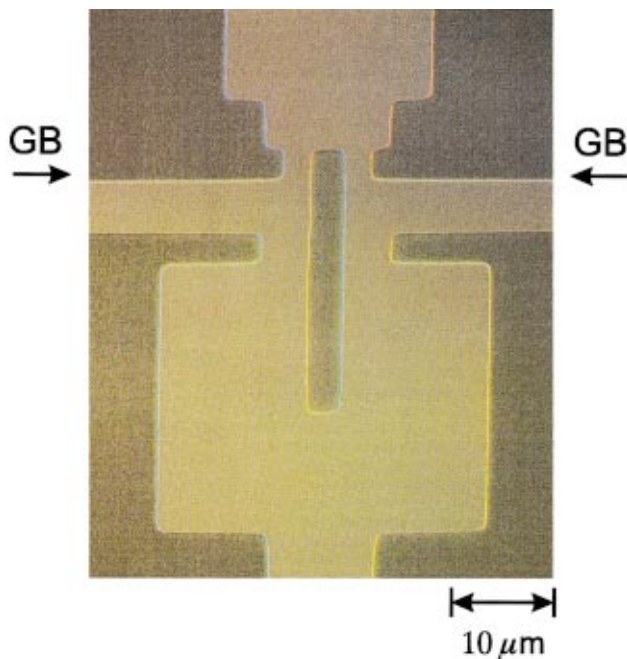


FIG. 72. Optical micrograph of the central part of a single-layer inductively shunted dc SQUID magnetometer based on bicrystal grain-boundary junctions. The vertical stripes connect to the current and voltage leads, the horizontal ones to a large pickup loop. The bicrystal grain boundary, which cannot be seen in this image, extends from the left to the right as indicated by the arrows. Figure courtesy of J. Clarke, University of California, Berkeley, and Lawrence Berkeley Laboratory, Berkeley, USA [Color].

in averaging out this noise signal, as can be seen in Fig. 73. For rf SQUIDs the situation is more convenient, because in their standard mode of operation the $1/f$ noise due to critical current fluctuations is already excluded (Mück *et al.*, 1994).

High- T_c SQUIDs using grain-boundary junctions are fabricated nowadays with equivalent flux-noise values as low as a few $\mu\phi_0/\sqrt{\text{Hz}}$ (white noise). With appropriate flux-transformer circuits, which in some cases have even been made on $20 \times 20 \text{ mm}^2$ bicrystals (Cantor *et al.*, 1995), the effective magnetic-field noise can be as low as $10\text{--}20 \text{ fT}/\sqrt{\text{Hz}}$ (white noise).

Prototype high- T_c SQUID systems are being developed and used for a variety of applications. Traditionally, SQUIDs have been employed as extremely sensitive magnetic-field sensors in biomagnetometry, e.g., magnetoencephalography and magnetocardiography. Whereas the former has already been demonstrated successfully with high- T_c SQUIDs (Curio *et al.*, 1996; Drung, Dantsker, *et al.*, 1996), there is particularly strong interest in employing high- T_c SQUIDs in the latter (Tanaka *et al.*, 1994; Burghoff *et al.*, 1996; Drung, Dantsker, *et al.*, 1996; Drung, Ludwig, *et al.*, 1996). An appealing prospect is the use of high- T_c bicrystal SQUIDs for fetal magnetocardiography (Rijpma *et al.*, 1999). Grain-boundary-junction-based high- T_c SQUIDs are further implemented in systems for nondestructive evaluation, e.g., of aircraft parts (Hohmann *et al.*, 1997;

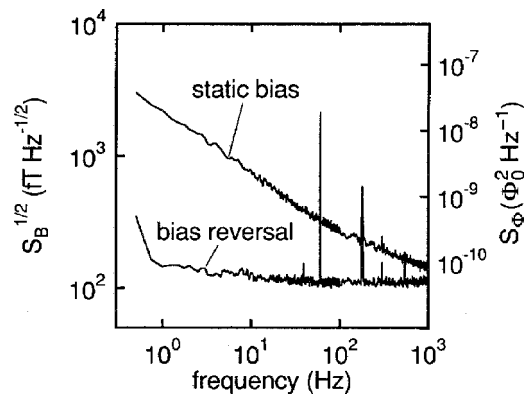


FIG. 73. Spectral density of the effective flux and field noise for an inductively coupled bicrystal high- T_c dc SQUID, showing the effective cancellation of the $1/f$ noise by bias current modulation. From Koelle *et al.* (1993b); figure courtesy of J. Clarke, University of California, Berkeley, and Lawrence Berkeley Laboratory, Berkeley, USA.

Krause *et al.*, 1997; Kreuzbruck *et al.*, 1997; Mück *et al.*, 1997) or reinforcing rods in concrete structures, for the detection of fine magnetic particles in copper wire (Nagaishi *et al.*, 1997), in biology, and for geophysical surveying. Scanning SQUID microscopy is an enticing extension of these applications (see, for example, Mathai *et al.*, 1992, 1993; Kirtley *et al.*, 1994), which in high- T_c versions employing bicrystal grain-boundary junctions was introduced by the groups of Wellstood at the University of Maryland (Black *et al.*, 1993) and of Clarke at UC Berkeley (T. S. Lee *et al.*, 1996, 1997). Even though these microscopes are based on cryogenic sensors, they allow investigations of samples kept at room temperature. Scanning SQUID microscopes fabricated by Neocera Inc. are industrially employed to analyze integrated semiconductor devices (Chatrathorn *et al.*, 2000); see Fig. 74. As mentioned, SQUIDs provide an ultrasensitive tool for various other small-signal measurements as well. Using grain-boundary junctions, this was demonstrated, for example, by their operation in picovoltmeters (Miklich *et al.*, 1995) and in low-field NMR spectroscopy (Kumar *et al.*, 1997; Schlenga *et al.*, 1999).

B. Radiation detectors and spectrometers

The potentially fast response and high output impedance of high- T_c Josephson junctions, both resulting from large $I_c R_n$ products, have motivated interest in using these junctions as detectors for high-frequency radiation, for example, in telecommunications or in high-frequency spectrometers. Using grain boundaries in polycrystalline films, millimeter-wave signal detection was demonstrated in early experiments with $\text{YBa}_2\text{Cu}_3\text{O}_7$ (Kita *et al.*, 1988; Matsui and Ohta, 1993) and with TlBaCaCuO films (Ruggiero *et al.*, 1991). Subsequently, (sub)millimeter-wave detection with artificial grain boundaries was attained, employing $\text{YBa}_2\text{Cu}_3\text{O}_{7-\delta}$ step-edge junctions on MgO substrates (Fukumoto *et al.*, 1993) and using series arrays of bicrys-

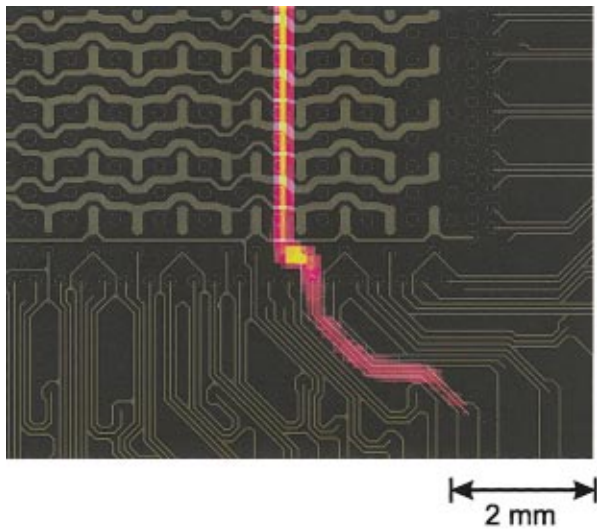


FIG. 74. Current path (orange) in an SRAM die with a short between a bitline and ground measured with a commercial MAGMA-C1 scanning SQUID microscope using a bicrystalline SQUID. The current path, which has been derived by numerically inverting the magnetic-field image as measured by the scanning SQUID at a distance of $375 \mu\text{m}$, is overlaid on the package-level CAD layout of the SRAM. From Knauss (2000); figure courtesy of L. Knauss and T. Venkatesan, Neocera, Inc., Beltsville, USA [Color].

tal and step-edge junctions (Huang *et al.*, 1997). Utilizing $\text{YBa}_2\text{Cu}_3\text{O}_{7-\delta}$ grain-boundary junctions on NdGaO_3 bicrystal substrates, Divin *et al.* (1999, 2000, 2001) demonstrated Hilbert transform spectrometers operating from 60 GHz to 2.25 THz. In a similar configuration, shown in Fig. 75, THz spectroscopy was also accomplished using more readily available LaAlO_3 bicrystals (Kaestner *et al.*, 2000). Further developments related to high-frequency radiation detectors and spectrometers employing high- T_c grain boundaries can be found, for example, in the work of Edstam *et al.* (1993), Hong *et al.* (1993), Kang *et al.* (1993), Tarasov *et al.* (1993), Nakajima *et al.* (1997), Kume *et al.* (1999), Mashnikov *et al.* (1999), and Shimakage *et al.* (1999).

C. Three-terminal devices

In various approaches, grain boundaries are used in high- T_c superconducting transistorlike three-terminal devices, as reviewed by Mannhart (1996). In Josephson field-effect transistors (JoFET's), an example of which is shown in Fig. 60, the sensitivity of grain boundaries to applied electric fields (Moore, 1989; Chen *et al.*, 1991) is exploited. The first operational device was fabricated by Ivanov *et al.* (1993), who used an $\text{YBa}_2\text{Cu}_3\text{O}_{7-\delta}$ bicrystal grain-boundary junction covered with an amorphous SrTiO_3 gate insulator. Based on asymmetric 45° [001]-tilt grain boundaries in a 250-nm $\text{YBa}_2\text{Cu}_3\text{O}_7$ film, remarkably strong enhancements of I_c with applied gate voltage were observed. These enhancements were as high as 40%, as illustrated in Fig. 61.

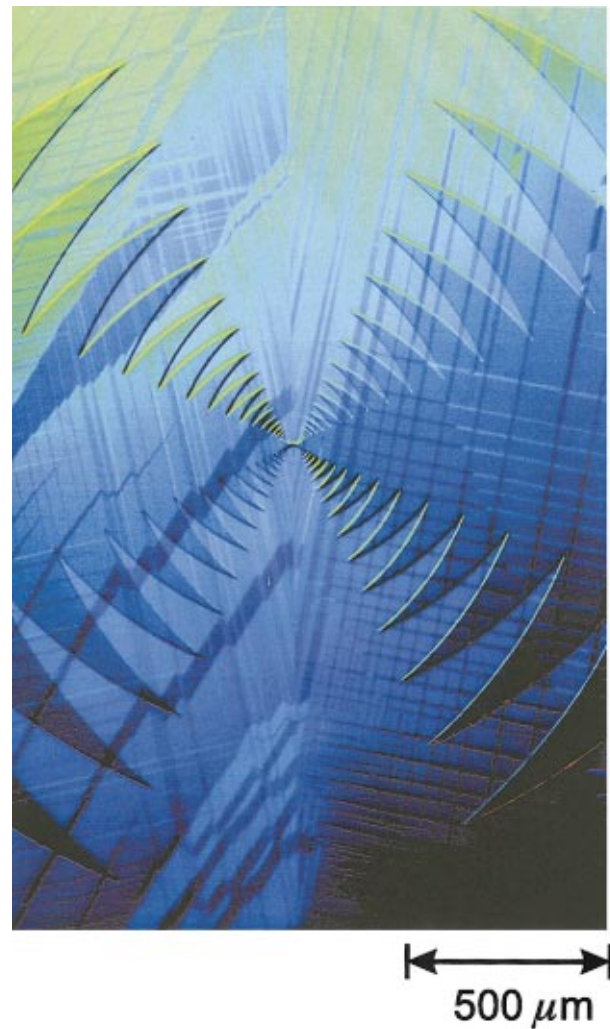


FIG. 75. Phase contrast micrograph of a Josephson junction with a logarithmic-periodic antenna on a LaAlO_3 bicrystal substrate. The vertical grain boundary in the middle of the picture and the twin boundaries in the substrate can be clearly seen. The size of the image is $2370 \times 1550 \mu\text{m}^2$. From Kaestner *et al.* (2000); figure courtesy of M. Schilling, Universität Hamburg, Germany [Color].

Applied electric fields penetrate high- T_c superconductors only over small length scales determined roughly by the Thomas-Fermi or Debye lengths, which typically are of the order of one nanometer. Therefore the use of ultrathin superconducting films is expected to promote a high transconductance $\Delta I_c / \Delta V_g$. Based on 10–30 nm $\text{YBa}_2\text{Cu}_3\text{O}_{7-\delta}$ films, relative changes of the critical current $\Delta I_c / I_c$ of 8% were reported by Petersen, Takeuchi, *et al.* (1995), who studied metal-insulator-superconductor structures on 24° and 36° [001]-tilt bicrystals. The magnitude of the field effects depends on the grain-boundary angle. This was found by Mayer *et al.*, using an inverted metal-insulator-superconductor structure based on a conducting Nb doped SrTiO_3 substrate. They observed an increase in the gate-voltage-induced relative change of I_c with increasing [001]-tilt angle θ from 24° to 45° (Mayer *et al.*, 1996). Other Josephson field-effect devices have been developed

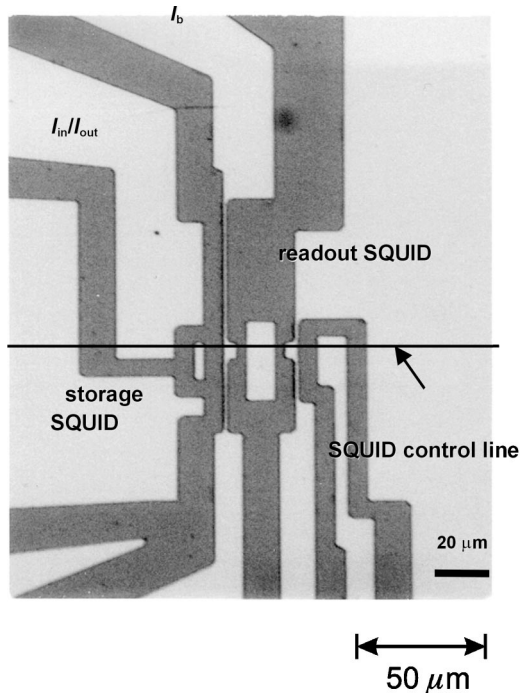


FIG. 76. Optical micrograph of an RSFQ circuit containing four $\text{YBa}_2\text{Cu}_3\text{O}_{7-\delta}$ bicrystal Josephson junctions. The circuit includes a storage SQUID, a readout SQUID, and a SQUID control line. From Sung *et al.* (1999); figure courtesy of S. G. Lee and G. Y. Sung, Korea University and Electronics and Telecommunications Research Institute, Korea.

that employ hole-overdoped bicrystalline $\text{Ca}_x\text{Sm}_{1-x}\text{Ba}_2\text{Cu}_3\text{O}_{7-\delta}$ drain-source channels (Dong *et al.*, 1995), as well as devices based on locally thinned bicrystal substrates used as gate insulators (Nakajima *et al.*, 1993) and devices using 90° grain boundaries (Suh *et al.*, 1997). Additional studies on bicrystal JoFET's have been reported, e.g., by Haensel *et al.* (1997) and Windt *et al.* (1999; see also Sec. VIII.A).

In an alternative mode of operation, the injection of quasiparticles by the application of a gate voltage is utilized to vary the transport characteristics of the Josephson junction. This approach was taken for $\text{YBa}_2\text{Cu}_3\text{O}_{7-\delta}$ bicrystal grain boundaries by Iguchi *et al.* (1994) and Joosse *et al.* (1995), and for $\text{Bi}_2\text{Sr}_2\text{Ca}_{n-1}\text{Cu}_n\text{O}_{2(n+2)}$ by Frey *et al.* (1997).

Vortex-flow devices are a third variety of three-terminal device. They are based on the controlled motion of magnetic-flux quanta through superconducting drain-source channels. In these devices, it has turned out to be advantageous to incorporate Josephson junctions to enhance gain, speed, and output impedance. The first high- T_c Josephson vortex-flow transistors were presented by Satchell *et al.* (1992, 1993), who used step-edge junctions. Most of the subsequent work was based on bicrystal junctions. See, for example, Zhang *et al.* (1994, 1995, 1996), Gerdemann *et al.* (1995), Koelle *et al.* (1995), Isaac *et al.* (1997), Nguyen *et al.* (1999), Tavares *et al.* (1999).

Although still far from market applications, three-terminal structures are successfully being used to ex-

plore the basic physics of high- T_c superconductivity and have led to various developments in materials science (Mannhart and Hilgenkamp, 2002).

D. Superconducting logic circuits

Josephson junctions can be switched at sub-picosecond speeds, offering the prospect of electronic devices operating at frequencies not attainable with semiconductor circuitry. Based on the (rapid) single-flux-quantum (RSFQ) architecture (Likharev and Semenov, 1991), logic circuits are being developed with projected operation speeds exceeding 1 THz. The high speeds are combined with low dissipation levels of the RSFQ elements, which are in the μW range. Examples of prototype circuitry include set-reset triggers, RS flip-flops, shift register circuits, and analog-to-digital converters. Based on bicrystal grain boundaries, various properly operating RSFQ circuits have been demonstrated (Ivanov, Kaplunenko, *et al.*, 1994; Kaplunenko *et al.*, 1994, 1995, 1997; Oelze *et al.*, 1996; Chong *et al.*, 1998; Kim *et al.*, 1999; Sung *et al.*, 1999; Zhang *et al.*, 1997). An example of an RSFQ element containing a storage SQUID, a readout SQUID, and a control line is shown in Fig. 76. In some of the RSFQ devices, 25 bicrystal Josephson junctions are operated simultaneously. Likewise, several hundreds of junctions are used for Josephson voltage standards, prototypes of which have been realized in bicrystal technology (Klushin *et al.*, 1996). A problem faced by such applications is the spread in transport characteristics of the junctions encountered up to now (Alff *et al.*, 1993; Burkhardt *et al.*, 1999). Interesting ways have been developed to circumvent the requirement of the present bicrystal technology that all the Josephson junctions be located along a single line, defined by the substrate grain-boundary. The Chalmers group fabricated RSFQ circuits on Y-ZrO_2 substrates, which incorporated two grain boundaries placed only $10 \mu\text{m}$ apart (Kaplunenko *et al.*, 1995). Other ways to achieve more complex circuits are being explored, for example, the stacking of junctions vertically, as demonstrated by a group at NIST (H. Q. Li *et al.*, 1997) or the use of eutectic substrates, which contain many parallel grain boundaries (Santiso *et al.*, 2000).

E. Research devices

Grain boundaries are excellent Josephson junctions, which can be fabricated with ease and therefore have been exploited very successfully as research devices. Bicrystalline junctions have been found to be particularly fruitful for this purpose, because by choosing the grain-boundary angle, one can freely select the alignment between the lobes of the $d_{x^2-y^2}$ -wave order parameters of both crystals.

Bicrystalline grain boundaries have been used for a variety of basic research experiments, including spectroscopic studies of the cuprates (Chaudhari *et al.*, 1993), studies of the temperature-dependent London penetra-

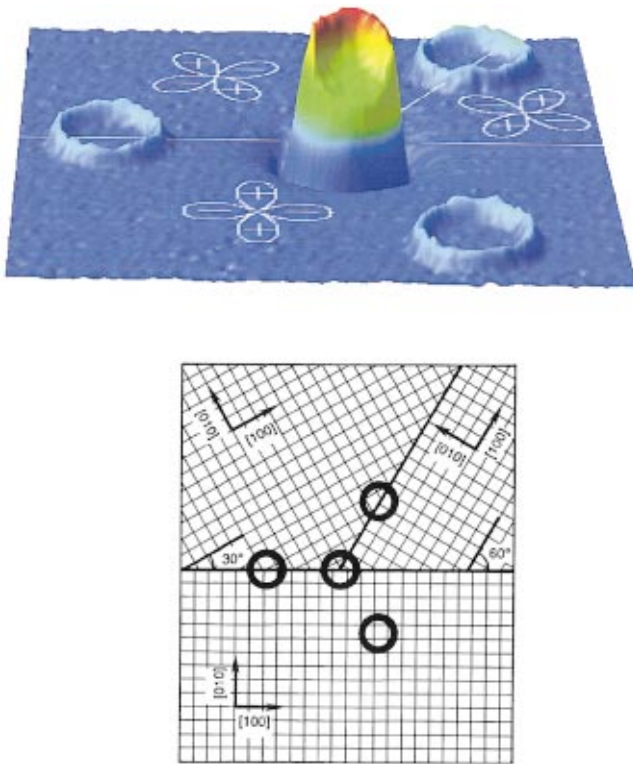


FIG. 77. Scanning SQUID microscopy image of four superconducting rings with inner diameters of $48 \mu\text{m}$ and widths of $10 \mu\text{m}$ patterned into a tricrystalline $\text{YBa}_2\text{Cu}_3\text{O}_{7-\delta}$ film. As shown in the lower half of the figure, the middle ring is centered on the tricrystal point of the substrate. In this ring, a supercurrent generating half of a magnetic flux quantum $h/4e$ is generated. The sample was cooled in a field of $<2 \text{ mG}$ and imaged at 4.2 K . From Kirtley, Tsuei, *et al.* (1995); figure courtesy of J. R. Kirtley and C. C. Tsuei, IBM T. J. Watson Research Center, USA [Color].

tion depth (Froehlich *et al.*, 1994, 1996; Elly *et al.*, 1995; Alff *et al.*, 1999), measurements of the order-parameter symmetry in the high- T_c cuprates (Chaudhari and Lin, 1994; Tsuei *et al.*, 1994, 1996, 1997; Kirtley, Chaudhari, *et al.*, 1995; Kirtley, Tsuei, *et al.*, 1995, 1996; Miller, Ying, *et al.*, 1995; Hilgenkamp, Mannhart, and Mayer, 1996; Ivanov *et al.*, 1996, 1998; Neils and Van Harlingen, 2002), and studies of time-reversal symmetry breaking and fractional vortices (Kirtley, Chaudhari, *et al.*, 1995; Mannhart, Hilgenkamp, *et al.*, 1996; Tafuri *et al.*, 2000; see also Walker, 2000). Particularly impressive experiments have been performed by Tsuei and Kirtley on the symmetry of the superconducting order parameter. Using scanning SQUID microscopy, they investigated spontaneous generation of half-flux magnetic quanta, created by rings structured in tricrystalline and tetracrystalline epitaxial films (Fig. 77) or by these films themselves (Fig. 78). These experiments, confirmed by the group of I. Iguchi at the Tokyo Institute of Technology (Sugimoto *et al.*, 2001), provided clear evidence of a dominating $d_{x^2-y^2}$ order-parameter symmetry in many of the cuprates. This field has been reviewed by Tsuei and Kirtley (2000).

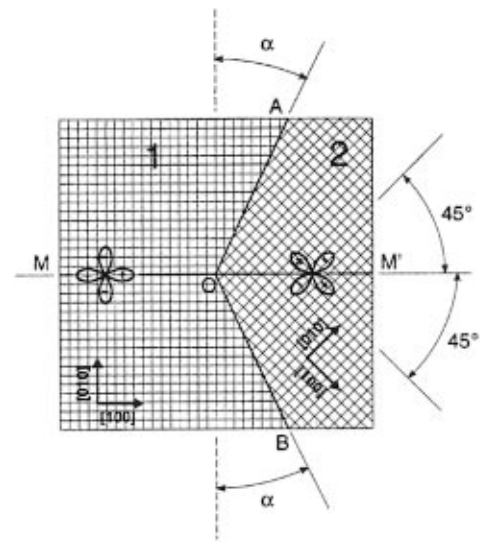
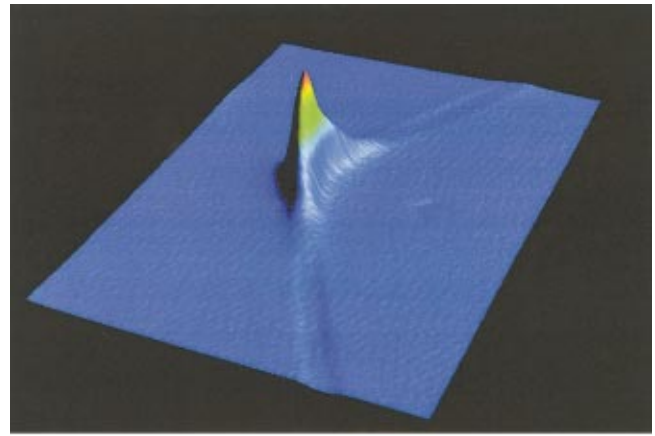


FIG. 78. Scanning SQUID microscopy image of a Josephson vortex comprising half a flux quantum $h/4e$, generated at the wedge tip in a $\text{Tl}_2\text{Ba}_2\text{CuO}_{6+\delta}$ film deposited on a tetracrystal (100) SrTiO_3 substrate of the geometry shown in the lower half of the figure. The sample was cooled in a field of $<1 \text{ mG}$ and imaged at 4.2 K . The length of the short sides of the scanning SQUID image is $100 \mu\text{m}$. From Tsuei *et al.* (1997); figure courtesy of J. R. Kirtley and C. C. Tsuei, IBM T. J. Watson Research Center, USA [Color].

Grain boundaries also provide an opportunity to construct novel superconducting electronic devices by exploiting the $d_{x^2-y^2}$ -wave order-parameter symmetry, as was demonstrated, for example, by the realization of high- T_c dc π SQUIDs (Schulz *et al.*, 2000). Such a device is illustrated in Fig. 79. It consists of one standard junction and one junction with a π phase shift, which causes a shift of the $I_c(H)$ characteristics of the SQUID (see Fig. 80). These devices are useful for quantitative measurements of potential complex admixtures to the $d_{x^2-y^2}$ -wave component of the order parameter and furthermore fulfill the requirements for the realization of complementary Josephson electronics (Terzioglu and Beasley, 1998). Their ground state is degenerated, which may provide the basis for implementation in circuits used for quantum computation.

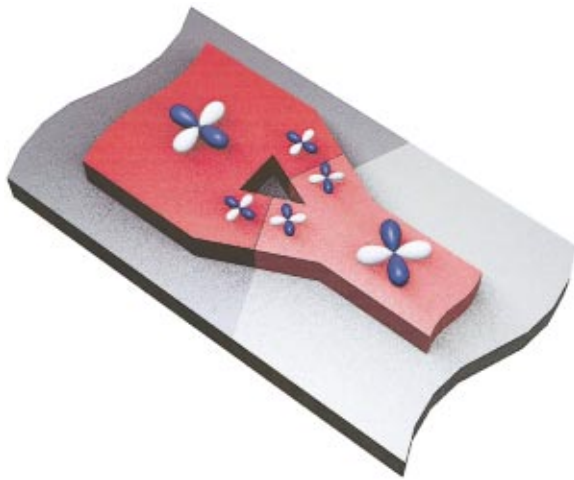


FIG. 79. Schematic rendition of a high- T_c dc π -SQUID fabricated on a tetracrystalline substrate. Resulting from the orientations of the abutting crystals, one of the junctions is biased with an additional π phase shift, leading to characteristics complementary to those of standard SQUID, as presented by Schulz *et al.* (2000), and shown in Fig. 80 [Color].

XII. SUMMARY AND OUTLOOK

Ever since the very first experiments performed by Bednorz and Müller, the high- T_c superconductors have been recognized as fascinating and highly promising materials. At first their usefulness was severely limited by the grain boundaries, which caused weak-link behavior and small critical currents in all polycrystalline samples. It was particularly disappointing that the insufficient critical currents seemed to preclude the fabrication of useful high- T_c wires. Many considered the grain-

boundary problem to be insoluble, because the weak-link behavior was seen as a direct consequence of the cuprates' nonalterable, ultrashort coherence lengths.

In the 15 years since then, our understanding of grain boundaries has improved considerably. As we now know, their behavior is indeed rooted in fundamental properties of the cuprates and is controlled by basic mechanisms. These mechanisms, however, differ considerably from those originally anticipated. We have learned, for example, that due to the unconventional order-parameter symmetry and the large electric screening length, grain-boundary physics is much richer than anybody had foreseen. In the course of investigating grain boundaries, we have also gained important information about the behavior of other interfaces involving cuprates and their surfaces, with further exciting interface phenomena expected even for nonsuperconducting oxides. However, despite the intense effort invested in the grain-boundary problem, our understanding has yet to reach a level that could be considered satisfactory. Further progress and surprises can be anticipated.

Although grain boundaries are not yet understood in full detail, various technologies have been developed to make them accessible and to turn them into useful devices. With these technologies, valuable high- T_c Josephson junctions can be fabricated with ease, which formerly seemed an unrealistic dream. With the bicrystal technology, the fabrication of a good junction is as straightforward as the growth of a superconducting film. These Josephson junctions have been used with remarkable success in several key experiments elucidating the physics of high- T_c superconductivity, such as the tricrystal, half-flux-quanta experiments revealing the $d_{x^2-y^2}$ order-parameter symmetry in many cuprates, or other experiments investigating time-reversal symmetry breaking.

Besides providing the key to basic studies, the grain-boundary Josephson junctions are employed with great success in rf devices reaching the THz range and in basic RSFQ circuits with operation temperatures of 50–60 K. Grain boundaries are the active components of excellent SQUIDs operating at 77 K, which are already in use or are envisaged for a host of applications, such as fetal heart monitoring or the inspection of devices in semiconductor fabrication lines.

Most intriguingly, the original high- T_c wire problem has almost been solved, as a promising way to high- T_c cables with large critical currents has been found: the optimal microstructure is achieved by biaxially aligning the grains to within a few degrees and by selecting grain geometries that provide large effective grain-boundary areas. The composition of the grain boundaries has been improved to yield larger critical currents by selective grain-boundary doping. Technologies that exploit these principles have been developed and the current densities of the superconductors have now reached millions of A/cm² at 77 K.

The authors anticipate that the engineering of grain boundaries by interface doping or other techniques will advance high-power applications and electronic devices.

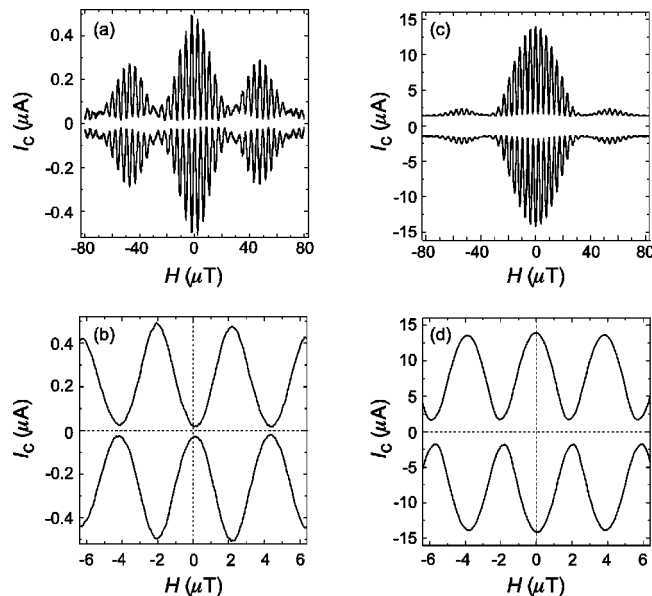


FIG. 80. Measured dependencies of the critical current on applied magnetic field of (a) and (b) a dc π -SQUID and of (c) and (d) a standard SQUID at $T=77$ K. From Schulz *et al.* (2000).

The next few years may see surprising developments in the physics of interfaces of complex oxides, out of which we can expect both a better understanding of grain boundaries in the cuprates and viable new applications.

ACKNOWLEDGMENTS

While writing this manuscript, we had valuable discussions and interactions with many colleagues, in particular with L. Alff, S. Babcock, Y. S. Barash, D. H. A. Blank, P. Chaudhari, D. K. Christen, J. Clarke, U. Eckern, R. Feenstra, J. K. Freericks, H. Freyhardt, B. Goetz, A. Golubov, A. Goyal, P. Grant, L. Greene, G. Hammerl, M. Hein, P. Hirschfeld, B. Holzapfel, E. Il'ichev, Z. G. Ivanov, Ch. Jooss, S. Kashiwaya, J. R. Kirtley, A. M. Klushin, T. Kopp, D. C. Larbalestier, T. Lueck, R. Mints, D. Norton, U. Poppe, J. Ransley, G. Rijnders, H. Rogalla, E. Sarnelli, D. G. Schlom, A. Schmehl, C. W. Schneider, R. R. Schulz, P. Seidel, F. Tafuri, E. Tarte, C. C. Tsuei, D. van Harlingen, D. Winkler, and Y. Zhu, for which we are very thankful. To R. Feenstra, Z. G. Ivanov, C. W. Schneider, E. Tarte, and D. Winkler we are especially grateful for reading parts of the manuscript and for supplying us with their constructive comments. Furthermore, we thank H. Adrian, J. Albrecht, L. Alff, S. Babcock, N. Browning, C. Cantoni, S. W. Chan, K. Char, P. Chaudhari, M. F. Chisholm, D. K. Christen, T. Claeson, J. Clarke, C. B. Eom, M. Feldmann, Y. Feng, Ø. Fischer, R. Flükiger, B. Goetz, Y. Iijima, Z. G. Ivanov, C. L. Jia, M. Kawasaki, J. R. Kirtley, L. Knauss, N. Koshizuka, H. Kronmüller, H. Kung, D. C. Larbalestier, S. G. Lee, I. Maggio-Aprile, J. C. Martinez, J. C. Macfarlane, K. L. Merkle, C. M. Muirhead, J. Mygind, N. F. Pedersen, M. S. Rzchowski, E. Sarnelli, M. Schilling, C. W. Schneider, J. Schubert, L. Schultz, G. Y. Sung, E. Tarte, C. C. Tsuei, T. Venkatesan, D. Verebelyi, D. Winkler, H. W. Zandbergen, and Y. Zhu for providing us with figures. G. Hammerl, A. Herrnberger, S. Leitenmeier, and F. Samtleben-Spleiss we thank with pleasure for their assistance. This work was supported by the BMBF (project number 13N6918), and by the Royal Dutch Academy of Arts and Sciences.

REFERENCES

Adachi, S., N. Inoue, T. Sugano, T. Ugawa, and K. Tanabe, 2001, "Preparation and properties of (Hg,Re)-1212 Josephson junctions using STO and LSAT bicrystal substrates," *Physica C* (in press).
 Adam, R., M. Currie, R. Sobolewski, O. Harnack, and M. Darula, 1999, "Picosecond response of optically driven Y-Ba-Cu-O microbridge and Josephson-junction integrated structures," *IEEE Trans. Appl. Supercond.* **9**, 4091–4094.
 Adam, R., M. Currie, C. Williams, R. Sobolewski, O. Harnack, and M. Darula, 2000, "Direct observation of subpicosecond single-flux-quantum generation in pulse-driven Y-Ba-Cu-O Josephson junctions," *Appl. Phys. Lett.* **76**, 469–471.
 Agassi, D., C. S. Pande, and R. A. Masumura, 1995, "Superconductor superlattice model for small-angle grain boundaries in Y-Ba-Cu-O," *Phys. Rev. B* **52**, 16 237–16 245.

Alarco, J., Y. Boikov, G. Brorsson, T. Claeson, G. Daalmans, J. Edstam, Z. Ivanov, V. K. Kaplunenko, P. Å. Nilsson, E. Olsson, H. K. Olsson, J. Ramos, E. Stepantsov, A. Tzalenchuk, D. Winkler, and Y-M. Zhang, 1994, "Engineered grain boundary junctions—characteristics, structure, applications," in *Materials and Crystallographic Aspects of HT_c -Superconductivity*, edited by E. Kaldis (Kluwer Academic, Dordrecht), pp. 471–490.
 Alarco, J. A., and E. Olsson, 1995, "Analysis and prediction of the critical current density across [001]-tilt $YBa_2Cu_3O_{7-\delta}$ grain boundaries of arbitrary misorientation angles," *Phys. Rev. B* **52**, 13 625–13 630.
 Alarco, J. A., E. Olsson, Z. G. Ivanov, P. Å. Nilsson, D. Winkler, E. A. Stepantsov, and A. Y. Tzalenchuk, 1993, "Microstructure of an artificial grain boundary weak link in a $YBa_2Cu_3O_{7-\delta}$ thin film grown on a [100][110], [001]-tilt Y-ZrO₂ bicrystal," *Ultramicroscopy* **51**, 239–246.
 Albrecht, J., S. Leonhardt, and H. Kronmüller, 2000a, "Influence of vortex-vortex interaction on critical currents across low-angle grain boundaries in $YBa_2Cu_3O_{7-\delta}$ thin films," *Phys. Rev. B* **63**, 014507.
 Albrecht, J., R. Warthmann, S. Leonhardt, and H. Kronmüller, 2000b, "Current densities in low-angle grain boundaries of YBCO," *Physica C* **341-348**, 1459–1460.
 Alff, L., A. Beck, R. Gross, A. Marx, S. Kleefisch, Th. Bauch, H. Sato, M. Naito, and G. Koren, 1998, "Observation of bound surface states in grain-boundary junctions of high-temperature superconductors," *Phys. Rev. B* **58**, 11 197–11 200.
 Alff, L., R. Gerdemann, K. D. Husemann, A. Beck, T. Träuble, B. Mayer, and R. Gross, 1993, in *Applied Superconductivity*, Proceedings EUCAS '93, edited by H. C. Freyhardt (DGM Informationsgesellschaft mbH, Oberursel, Germany), pp. 1199–1202.
 Alff, L., S. Kleefisch, U. Schoop, M. Zittartz, T. Kemen, T. Bauch, A. Marx, and R. Gross, 1998, "Andreev bound states in high-temperature superconductors," *Eur. Phys. J. B* **5**, 423–438.
 Alff, L., S. Meyer, S. Kleefisch, U. Schoop, A. Marx, H. Sato, M. Naito, and R. Gross, 1999, "Anomalous low-temperature behavior of superconducting $Nd_{1.85}Ce_{0.15}CuO_{4-y}$," *Phys. Rev. Lett.* **83**, 2644–2647.
 Alff, L., H. Takashima, S. Kashiwaya, N. Terada, H. Ihara, Y. Tanaka, M. Koyanagi, and K. Kajimura, 1997, "Spatially continuous zero-bias conductance peak on [110] $YBa_2Cu_3O_{7-\delta}$ surfaces," *Phys. Rev. B* **55**, 14 757–14 760.
 Ambegaokar, V., and A. Baratoff, 1963, "Tunneling between superconductors," *Phys. Rev. Lett.* **10**, 486–489; **11**, 104(E)–105(E).
 Ambegaokar, V., and B. I. Halperin, 1969, "Voltage due to thermal noise in the dc Josephson effects," *Phys. Rev. Lett.* **22**, 1364–1366.
 Amin, M. H. S., A. N. Omelyanchouk, and A. M. Zagorskii, 2001, "Mechanisms of spontaneous current generation in an inhomogeneous d -wave superconductor," *Phys. Rev. B* **63**, 212502.
 Amrein, T., L. Schultz, B. Kabius, and K. Urban, 1995, "Orientation dependence of grain-boundary critical current densities in high- T_c bicrystals," *Phys. Rev. B* **51**, 6792–6795.
 Andoh, H., O. Harnack, M. Darula, and H. Kohlstedt, 2000, "Dynamics of order parameter and microwave emission for a $YBa_2Cu_3O_{7-\delta}$ bicrystal junction," *Physica C* **339**, 237–244.

- Attenberger, A., J. Hänisch, B. Holzapfel, and L. Schultz, 2001, "Electrical transport properties of Bi2223 [001] tilt grain boundary junctions" (proceedings of EUCAS 2001), Physica C (in press).
- Ayache, J., A. Thorel, J. Lesueur, and U. Dahmen, 1998, "Characterization of three-dimensional grain boundary topography in a $\text{YBa}_2\text{Cu}_3\text{O}_{7-\delta}$ thin film bicrystal grown on a SrTiO_3 substrate," J. Appl. Phys. **84**, 4921–4928.
- Babcock, S. E., X. Y. Cai, D. L. Kaiser, and D. C. Larbalestier, 1990, "Weak-link-free behavior of high-angle $\text{YBa}_2\text{Cu}_3\text{O}_{7-\delta}$ grain boundaries in high magnetic fields," Nature (London) **347**, 167–169.
- Babcock, S. E., X. Y. Cai, D. C. Larbalestier, D. H. Shin, N. Zhang, H. Zhang, D. L. Kaiser, and Y. Gao, 1994, "A TEM-EELS study of hole concentrations near strongly and weakly coupled grain boundaries in electromagnetically characterized $\text{YBa}_2\text{Cu}_3\text{O}_{7-\delta}$ bicrystals," Physica C **227**, 183–196.
- Babcock, S. E., T. F. Kelly, P. J. Lee, J. M. Seuntjens, L. A. LaVanier, and D. C. Larbalestier, 1988, "Investigation of composition variations near grain boundaries in high quality sintered samples of $\text{YBa}_2\text{Cu}_3\text{O}_{7-\delta}$," Physica C **152**, 25–38.
- Babcock, S. E., and D. C. Larbalestier, 1989, "Evidence for local composition variations within $\text{YBa}_2\text{Cu}_3\text{O}_{7-\delta}$ grain boundaries," Appl. Phys. Lett. **55**, 393–395.
- Babcock, S. E., and D. C. Larbalestier, 1990, "Observation and implications of grain boundary dislocation networks in $\text{YBa}_2\text{Cu}_3\text{O}_{7-\delta}$ high angle grain boundaries," J. Mater. Res. **5**, 919–927.
- Babcock, S. E., and D. C. Larbalestier, 1994, "Bicrystal studies of high transition temperature superconductors," J. Phys. Chem. Solids **55**, 1125–1136.
- Babcock, S. E., and J. L. Vargas, 1995, "The nature of grain boundaries in the high- T_c superconductors," Annu. Rev. Mater. Sci. **25**, 193–222.
- Bailey, D. B., M. Sigrist, and R. B. Laughlin, 1997, "Fractional vortices on grain boundaries: the case for broken time-reversal symmetry in high-temperature superconductors," Phys. Rev. B **55**, 15 239–15 247.
- Balbashov, A. M., I. Y. Parsegov, E. K. Kov'ev, I. I. Vengrus, M. Y. Kupriyanov, S. N. Polyakov, and O. V. Snigirev, 1997, "HTSC Josephson junctions and dc SQUIDs in SrTiO_3 bicrystal substrates grown by floating zone method," IEEE Trans. Appl. Supercond. **7**, 2335–2337.
- Bals, S., G. Rijnders, D. H. A. Blank, and G. van Tendeloo, 2001, "TEM of ultrathin $\text{DyBa}_2\text{Cu}_3\text{O}_{7-x}$ films deposited on TiO_2 terminated SrTiO_3 ," Physica C **355**, 225–230.
- Barash, Y. S., H. Burkhardt, and D. Rainer, 1996, "Low-temperature anomaly in the Josephson critical current of junctions in d -wave superconductors," Phys. Rev. Lett. **77**, 4070–4073.
- Barash, Y. S., A. V. Galaktionov, and A. D. Zaikin, 1995, "Charge transport in junctions between d -wave superconductors," Phys. Rev. B **52**, 665–682.
- Bauer, M., R. Metzger, R. Semerad, P. Berberich, and H. Kinder, 2000, "Inclined substrate deposition by evaporation of magnesium oxide for coated conductors," in *Substrate Engineering—Paving the Way to Epitaxy*, edited by D. P. Norton, D. G. Schlom, N. Newman, and D. H. Matthiesen, MRS Symp. Proc. No. 587 (Materials Research Society, Pittsburgh), O2.2.1.
- Bauer, M., R. Semerad, and H. Kinder, 1999, "YBCO films on metal substrates with biaxially aligned MgO buffer layers," IEEE Trans. Appl. Supercond. **9**, 1502–1505.
- Beck, A., O. M. Froehlich, D. Koelle, R. Gross, H. Sato, and M. Naito, 1996, " $\text{La}_{1.85}\text{Sr}_{0.15}\text{CuO}_{4-\delta}$ bicrystal grain boundary Josephson junctions," Appl. Phys. Lett. **68**, 3341–3343.
- Beck, A., A. Stenzel, O. M. Froehlich, R. Gerber, R. Gerdemann, L. Alff, B. Mayer, R. Gross, A. Marx, J. C. Villegier, and H. Moriceau, 1995, "Fabrication and superconducting transport properties of bicrystal grain boundary Josephson junctions on different substrates," IEEE Trans. Appl. Supercond. **5**, 2192–2195.
- Bednorz, J. G., and K. A. Müller, 1986, "Possible high- T_c superconductivity in the Ba-La-Cu-O system," Z. Phys. B: Condens. Matter **64**, 189–193.
- Berenov, A., C. Farvacque, X. Qi, J. L. MacManus-Driscoll, D. MacPhail, and S. R. Foltyn, 2001, "Ca-doping of YBCO grain boundaries" (Proceedings of EUCAS 2001), Physica C (in press).
- Berenov, A. V., R. Marriott, S. R. Foltyn, and J. L. MacManus-Driscoll, 2001, "Effect of Ca-doping on grain boundaries and superconducting properties of $\text{YBa}_2\text{Cu}_3\text{O}_{7-\delta}$," IEEE Trans. Appl. Supercond. **11**, 3780–3783.
- Betouras, J., and R. Joynt, 1995, "Theoretical study of the critical current of $\text{YBa}_2\text{Cu}_3\text{O}_{7-\delta}$ bicrystals with hole-deficient grain boundaries," Physica C **250**, 256–264.
- Betouras, J. J., and R. Joynt, 1996, "Ginzburg-Landau theory of Josephson field effect transistors," Appl. Phys. Lett. **69**, 2432–2434.
- Bhattacharya, S., X. X. Xi, M. Rajeswari, C. Kwon, S. N. Mao, Q. Li, and T. Venkatesan, 1993, "Optical response of an ultrathin film and a large-angle grain boundary in superconducting $\text{YBa}_2\text{Cu}_3\text{O}_{7-\delta}$," Appl. Phys. Lett. **62**, 3510–3512.
- Black, R. C., A. Mathai, F. C. Wellstood, E. Dantsker, A. H. Miklich, D. T. Nemeth, J. J. Kingston, and J. Clarke, 1993, "Magnetic microscopy using a liquid nitrogen cooled $\text{YBa}_2\text{Cu}_3\text{O}_7$ superconducting quantum interference device," Appl. Phys. Lett. **62**, 2128–2130.
- Boikov, Yu. A., Z. G. Ivanov, and T. Claeson, 1997a, "Electromagnetic radiation induced current steps in biepitaxial $\text{YBa}_2\text{Cu}_3\text{O}_{7-\delta}$ Josephson junctions," Supercond. Sci. Technol. **10**, 801–806.
- Boikov, Y. A., Z. G. Ivanov, and T. Claeson, 1997b, "Weak-link bi-epitaxial Josephson junctions in a $\text{YBa}_2\text{Cu}_3\text{O}_{7-\delta}$ film on $\text{BaZrO}_3/\text{CeO}_2/\text{SrTiO}_3$," Phys. Solid State **39**, 1542–1547.
- Bolaños, G., G. den Ouden, M. Chacón, W. Lopera, M. E. Gómez, A. Pulzara, J. Heiras, and P. Prieto, 1997, "Grain boundary junctions with Ag-doped $\text{YBa}_2\text{Cu}_3\text{O}_{7-x}$ epitaxial thin films," Physica C **282-287**, 2419–2420.
- Borisenko, I. V., P. B. Mozhaev, G. A. Ovsyannikov, K. Y. Constantinian, and E. A. Stepantsov, 2002, "Superconducting current-phase relation in high- T_c symmetrical bicrystal junction," Physica C **368**, 328–331.
- Boyko, V. S., J. Malinsky, N. Abdellatif, and V. V. Boyko, 1998, "The estimation of the thickness of the nonsuperconducting layer at the interfaces in $\text{YBa}_2\text{Cu}_3\text{O}_{7-\delta}$," Phys. Lett. A **244**, 561–564.
- Bradley, A. D., R. A. Doyle, D. Charalambous, W. Lo, D. A. Cardwell, A. M. Campbell, and Ph. Vanderbemden, 1999, "Transport properties of bulk-bicrystal grain boundaries in artificially joined large-grain YBCO," IEEE Trans. Appl. Supercond. **9**, 2038–2041.

- Browning, N. D., J. P. Buban, H. O. Moltaji, S. J. Pennycook, G. Duscher, K. D. Johnson, R. P. Rodrigues, and V. P. Dravid, 1999, "The influence of atomic structure on the formation of electrical barriers at grain boundaries in SrTiO_3 ," *Appl. Phys. Lett.* **74**, 2638–2640.
- Browning, N. D., J. P. Buban, P. D. Nellist, D. P. Norton, M. F. Chisholm, and S. J. Pennycook, 1998, "The atomic origins of reduced critical currents at [001] tilt grain boundaries in $\text{YBa}_2\text{Cu}_3\text{O}_{7-\delta}$ thin films," *Physica C* **294**, 183–193.
- Browning, N. D., M. F. Chisholm, S. J. Pennycook, D. P. Norton, and D. H. Lowndes, 1993, "Correlation between hole depletion and atomic structure at high-angle grain boundaries in $\text{YBa}_2\text{Cu}_3\text{O}_{7-\delta}$," *Physica C* **212**, 185–190.
- Browning, N. D., and S. J. Pennycook, 1996, "Direct experimental determination of the atomic structure at internal interfaces," *J. Phys. D* **29**, 1779–1798.
- Browning, N. D., S. J. Pennycook, M. F. Chisholm, M. M. McGibbon, and A. J. McGibbon, 1995, "Observation of structural units at symmetric [001] tilt boundaries in SrTiO_3 ," *Interface Sci.* **3**, 397–423.
- Bruder, C., A. van Otterlo, and G. T. Zimanyi, 1995, "Tunnel junctions of unconventional superconductors," *Phys. Rev. B* **51**, 12 904–12 907.
- Bulaevskii, L. N., J. R. Clem, L. I. Glazman, and A. P. Malozemoff, 1992, "Model for low-temperature transport of Bi-based high-temperature superconducting tapes," *Phys. Rev. B* **45**, 2545–2548.
- Bulaevskii, L. N., L. L. Daemen, M. P. Maley, and J. Y. Coulter, 1993, "Limits to the critical current in high- T_c superconducting tapes," *Phys. Rev. B* **48**, 13 798–13 816.
- Bungre, S. S., R. Meisels, Z. X. Shen, and A. D. Caplin, 1989, "Are classical weak-link models adequate to explain the current-voltage characteristic in bulk $\text{YBa}_2\text{Cu}_3\text{O}_7$?" *Nature (London)* **341**, 725–727.
- Burghoff, M., L. Trahms, Y. Zhang, H. Bousack, and J. Borgmann, 1996, "Diagnostic application of high-temperature SQUIDs," *J. Clin. Eng.* **21**, 62.
- Burkhardt, H., 2001, "The effect of interface roughness on the Josephson critical current," unpublished.
- Burkhardt, H., O. Brüggemann, A. Rauther, F. Schnell, and M. Schilling, 1999, "Very large $\text{YBa}_2\text{Cu}_3\text{O}_7$ -Josephson-junction arrays," *IEEE Trans. Appl. Supercond.* **9**, 3153–3156.
- Cai, X. Y., A. Gurevich, I. Fei Tsu, D. L. Kaiser, S. E. Babcock, and D. C. Larbalestier, 1998, "Large enhancement of critical-current density due to vortex matching at the periodic facet structure in $\text{YBa}_2\text{Cu}_3\text{O}_{7-\delta}$ bicrystals," *Phys. Rev. B* **57**, 10 951–10 958.
- Cai, X. Z., and Y. Zhu, 1998, *Microstructure and Structural Defects in High-Temperature Superconductors* (World Scientific, Singapore).
- Cai, Z. X., and D. O. Welch, 1992, "Simulation study of the critical current density of $\text{YBa}_2\text{Cu}_3\text{O}_7$ ceramics," *Phys. Rev. B* **45**, 2385–2390.
- Campbell, A. M., 1989, "Ginzburg-Landau calculations of the critical current densities of grain boundaries," *Physica C* **162-164**, 273–274.
- Camps, R. A., J. E. Evetts, B. A. Glowacki, S. B. Newcomb, R. E. Somekh, and W. M. Stobbs, 1987, "Microstructure and critical current of superconducting $\text{YBa}_2\text{Cu}_3\text{O}_{7-x}$," *Nature (London)* **329**, 229–232.
- Cantoni, C., D. P. Norton, D. K. Christen, A. Goyal, D. M. Kroeger, D. T. Verebelyi, and M. Paranthaman, 1999, "Transport and structural characterization of epitaxial $\text{Nd}_{1+x}\text{YBa}_{2-x}\text{Cu}_3\text{O}_{7-x}$ thin films grown on LaAlO_3 and Ni metal substrates by pulsed-laser deposition," *Physica C* **324**, 177–186.
- Cantor, R., L. P. Lee, M. Teepe, V. Vinetskiy, and J. Longo, 1995, "Low-noise, single-layer $\text{YBa}_2\text{Cu}_3\text{O}_{7-x}$ dc SQUID magnetometers at 77 K," *IEEE Trans. Appl. Supercond.* **5**, 2927–2930.
- Cardona, A. H., H. Suzuki, T. Yamashita, K. H. Young, and L. C. Bourne, 1993, "Transport characteristics of $\text{Tl}_2\text{Ba}_2\text{CaCu}_2\text{O}_8$ bicrystal grain boundary junctions at 77 K," *Appl. Phys. Lett.* **62**, 411–413.
- Cardwell, D., K. Salama, and M. Murakami, 1998, Proceedings of the International Workshop on the Processing and Applications of Superconducting (RE)BCO Large Grain Materials, special issue of *Mater. Sci. Eng. B* **53** (Elsevier, New York/Amsterdam).
- Carmody, M., E. Landree, L. D. Marks, and K. L. Merkle, 1999, "Determination of the current density distribution in Josephson junctions," *Physica C* **315**, 145–153.
- Carmody, M., K. L. Merkle, Y. Huang, L. D. Marks, and B. H. Moeckly, 2000a, "The relation between barrier structure and current uniformity in YBCO Josephson junctions," *Interface Sci.* **8**, 231–242.
- Carmody, M., B. H. Moeckly, K. L. Merkle, and L. D. Marks, 2000b, "Spatial variation of the current in grain boundary Josephson junctions," *J. Appl. Phys.* **87**, 2454–2459.
- Cava, R. J., B. Batlogg, R. B. van Dover, D. W. Murphy, S. Sunshine, T. Siegrist, J. P. Remeika, E. A. Rietman, S. Zahurak, and G. P. Espinosa, 1987, "Bulk superconductivity at 91 K in single-phase oxygen-deficient perovskite $\text{Ba}_2\text{YCu}_3\text{O}_{9-\delta}$," *Phys. Rev. Lett.* **58**, 1676–1679.
- Chan, S. W., 1994, "Nature of grain boundaries as related to critical currents in superconducting $\text{YBa}_2\text{Cu}_3\text{O}_{7-x}$," *J. Phys. Chem. Solids* **55**, 1415–1432.
- Chan, S. W., 2000, presentation at the Topical Workshop on Grain Boundaries and Interfaces in High Temperature Superconductors, Williamsburg (VA, USA), Sept. 2000.
- Chan, S. W., D. M. Hwang, and L. Nazar, 1989, "Microstructure of $\text{YBa}_2\text{Cu}_3\text{O}_{7-x}$ thin films grown on SrTiO_3 ," *J. Appl. Phys.* **65**, 4719–4722.
- Chan, S. W., D. M. Hwang, R. Ramesh, S. M. Sampere, L. Nazar, R. Gerhardt, and P. Pruna, 1990, in *High- T_c Superconducting Thin Films: Processing, Characterization, and Applications*, edited by R. Stockbauer, S. V. Krishnaswamy, and R. L. Kurtz, AIP Conf. Proc. No. 200 (AIP, New York), pp. 172–185.
- Chan, S. W., A. Kussmaul, E. S. Hellman, and E. H. Hartford, Jr., 1998, "High resolution transmission electron microscopy of $\text{Ba}_{1-x}\text{K}_x\text{BO}_3$ superconductor-insulator-superconductor grain boundary tunnel junctions," *J. Mater. Res.* **13**, 1774–1779.
- Char, K., M. S. Colclough, S. M. Garrison, N. Newman, and G. Zaharchuk, 1991a, "Biepitaxial grain boundary junctions in $\text{YBa}_2\text{Cu}_3\text{O}_7$," *Appl. Phys. Lett.* **59**, 733–735.
- Char, K., M. S. Colclough, L. P. Lee, and G. Zaharchuk, 1991b, "Extension of the bi-epitaxial Josephson junction process to various substrates," *Appl. Phys. Lett.* **59**, 2177–2179.
- Chatrathorn, S., E. F. Fleet, F. C. Wellstood, L. A. Knauss, and T. M. Eiles, 2000, "Scanning SQUID microscopy of integrated circuits," *Appl. Phys. Lett.* **76**, 2304–2306.

- Chaudhari, P., D. Dimos, J. Mannhart, and C. C. Tsuei, 1988, unpublished.
- Chaudhari, P., D. Dimos, and J. Mannhart, 1989, "Critical current measurements in single crystals and single-grain boundaries in $\text{YBa}_2\text{Cu}_3\text{O}_7$ films," *IBM J. Res. Dev.* **33**, 299–306.
- Chaudhari, P., D. Dimos, and J. Mannhart, 1990, in *Earlier and Recent Aspects of Superconductivity*, edited by J. G. Bednorz and K. A. Müller (Springer-Verlag, Heidelberg), pp. 201–207.
- Chaudhari, P., R. H. Koch, R. B. Laibowitz, T. R. McGuire, and R. J. Gambino, 1987, "Critical-current measurements in epitaxial films of $\text{YBa}_2\text{Cu}_3\text{O}_{7-x}$ compound," *Phys. Rev. Lett.* **58**, 2684–2686.
- Chaudhari, P., and S. Y. Lin, 1994, "Symmetry of the superconducting order parameter in $\text{YBa}_2\text{Cu}_3\text{O}_{7-\delta}$ epitaxial films," *Phys. Rev. Lett.* **72**, 1084–1087.
- Chaudhari, P., J. Mannhart, D. Dimos, C. C. Tsuei, J. Chi, M. M. Oprysko, and M. Scheuermann, 1988, "Direct measurement of the superconducting properties of single grain boundaries in $\text{Y}_1\text{Ba}_2\text{Cu}_3\text{O}_{7-\delta}$," *Phys. Rev. Lett.* **60**, 1653–1656.
- Chaudhari, P., and J. W. Matthews, 1971, "Coincident twist boundaries between crystalline smoke particles," *J. Appl. Phys.* **42**, 3063–3066.
- Chaudhari, P., E. Sarnelli, J. R. Kirtley, and J. Lacey, 1993, "Conductance spectroscopy of high- T_c single-grain-boundary junctions in the $\text{YBa}_2\text{Cu}_3\text{O}_{7-\delta}$ system," *Phys. Rev. B* **48**, 1175–1179.
- Chen, J., T. Yamashita, H. Sasahara, H. Suzuki, H. Kurosawa, and Y. Hirotsu, 1991, "Possible three-terminal devices with YBCO angle grain boundaries," *IEEE Trans. Appl. Supercond.* **1**, 102–107.
- Chen, L. F., J. Yang, H. W. Gu, P. Ma, G. S. Yuan, S. A. Chang, L. Li, L. Chen, and T. Yang, 1997, "Epitaxial deposition and performance of the high T_c biepitaxial grain boundary junctions," *Physica C* **282**, 2413–2414.
- Chen, Y. F., Z. G. Ivanov, L. G. Johansson, R. I. Kojouharov, I. M. Angelov, E. Olsson, V. A. Roddatis, E. A. Stepantsov, A. Ya. Tzalenchuk, A. L. Vasiliev, and T. Claeson, 1997, " $\text{Ti}_2\text{Ba}_2\text{CaCu}_2\text{O}_8$ films: growth and applications in dc SQUIDs and microwave devices," *IEEE Trans. Appl. Supercond.* **7**, 2498–2501.
- Chen, Y. F., Z. G. Ivanov, E. A. Stepantsov, A. Ya. Tzalenchuk, S. Zarembinski, and T. Claeson, 1996, "Transport properties of $\text{Ti}_2\text{Ba}_2\text{CaCu}_2\text{O}_8$ weak links on LaAlO_3 bicrystal substrates," *J. Appl. Phys.* **79**, 9221–9223.
- Chew, N. G., S. W. Goodyear, R. G. Humphreys, J. S. Satchell, J. A. Edwards, and M. N. Keene, 1992, "Orientation control of $\text{YBa}_2\text{Cu}_3\text{O}_7$ thin films on MgO for epitaxial junctions," *Appl. Phys. Lett.* **60**, 1516–1518.
- Chiang, Y. M., D. P. Birnie III, and W. D. Kingery, 1997, *Physical Ceramics. Principles for Ceramic Science and Engineering* (Wiley, New York).
- Chisholm, M. F., and S. J. Pennycook, 1991, "Structural origin of reduced critical currents at $\text{YBa}_2\text{Cu}_3\text{O}_{7-\delta}$ grain boundaries," *Nature (London)* **351**, 47–49.
- Chisholm, M. F., and D. A. Smith, 1989, "Low-angle tilt grain boundaries in $\text{YBa}_2\text{Cu}_3\text{O}_7$ superconductors," *Philos. Mag. B* **59**, 181–197.
- Chong, Y., B. Ruck, R. Dittmann, C. Horstmann, A. Engelhardt, G. Wahl, B. Oelze, and E. Sodtke, 1998, "Measurements of the static error rate of a storage cell for single magnetic flux quanta, fabricated from high- T_c multilayer bicrystal Josephson junctions," *Appl. Phys. Lett.* **72**, 1513–1515.
- Christen, D., 2000, "Characteristic of current transport across low-angle YBCO grain boundaries," presentation at the Topical Workshop on Grain Boundaries and Interfaces in High Temperature Superconductors, Williamsburg (VA, USA), Sept. 2000.
- Claeson, T., 1999, presentation at EUCAS 1999, Sitges, Spain, Sept. 1999.
- Copetti, C. A., F. Rüdgers, B. Oelze, Ch. Buchal, B. Kabius, and J. W. Seo, 1995, "Electrical properties of 45° grain boundaries of epitaxial YBaCuO , dominated by crystalline microstructure and d-wave symmetry," *Physica C* **253**, 63–70.
- Cottrell, A. H., 1964, *Theory of Crystal Dislocations* (Gordon and Breach, New York).
- Curio, G., D. Drung, H. Koch, W. Müller, U. Steinhoff, L. Trahms, Y. Q. Shen, P. Vase, and T. Frelhoft, 1996, "Magnetometry of evoked fields from human peripheral nerve, brachial plexus and primary somatosensory cortex using a liquid nitrogen cooled superconducting quantum interference device," *Neurosci. Lett.* **206**, 204–206.
- Daly, K. P., W. D. Dozier, J. F. Burch, S. B. Coons, R. Hu, C. E. Platt, and R. W. Simon, 1991, "Substrate step-edge $\text{YBa}_2\text{Cu}_3\text{O}_7$ rf SQUIDs," *Appl. Phys. Lett.* **58**, 543–545.
- Daniels, G. A., A. Gurevich, and D. C. Larbalestier, 2000, "Improved strong magnetic field performance of low angle grain boundaries of calcium and oxygen overdoped $\text{YBa}_2\text{Cu}_3\text{O}_x$," *Appl. Phys. Lett.* **77**, 3251–3253.
- DasGupta, A., C. C. Koch, D. M. Kroeger, and Y. T. Chou, 1978, "Flux pinning by grain boundaries in niobium bicrystals," *Philos. Mag. B* **38**, 367–380.
- Däumling, M., E. Sarnelli, P. Chaudhari, A. Gupta, and J. Lacey, 1992, "Critical current of a high- T_c Josephson grain boundary junction in high magnetic field," *Appl. Phys. Lett.* **61**, 1355–1357.
- David, B., D. Grundler, S. Krey, V. Doormann, R. Eckart, J. P. Krumme, G. Rabe, and O. Doessel, 1995, "High- T_c SQUID magnetometers for biomagnetic measurements," *Supercond. Sci. Technol.* **9**, 96–99.
- Delamare, M.-P., K. R. Schöppl, J. D. Pedarnig, and D. Bäuerle, 2002, "Influence of $(\text{Y}_{0.8}\text{Ca}_{0.2})\text{Ba}_2\text{Cu}_3\text{O}_{7-\delta}$ top layer on the transport properties of a-axis oriented $\text{YBa}_2\text{Cu}_3\text{O}_{7-\delta}$ thin films," *Physica C* (in press).
- Delamare, M. P., H. Walter, B. Bringmann, A. Leenders, and H. C. Freyhardt, 2000, "Characterization of natural and artificial low-angle boundaries in YBCO TSMG samples," *Physica C* **329**, 160–177.
- Deutscher, G., and P. Chaudhari, 1991, "Scaling behavior of the critical current of grain-boundary junctions," *Phys. Rev. B* **44**, 4664–4665.
- Deutscher, G., and R. Maynard, 1995, "On the symmetry of the superconducting order parameter and the critical current," *Europhys. Lett.* **30**, 361–366.
- Deutscher, G., and K. A. Müller, 1987, "Origin of superconductive glassy state and extrinsic critical currents in high- T_c oxides," *Phys. Rev. Lett.* **59**, 1745–1747.
- Díaz, A., L. Mechin, P. Berghuis, and J. E. Evetts, 1998a, "Evidence for vortex pinning by dislocations in $\text{YBa}_2\text{Cu}_3\text{O}_{7-\delta}$ low-angle grain boundaries" *Phys. Rev. Lett.* **80**, 3855–3858.
- Díaz, A., L. Mechin, P. Berghuis, and J. E. Evetts, 1998b, "Observation of viscous flux flow in $\text{YBa}_2\text{Cu}_3\text{O}_{7-\delta}$ low-angle grain boundaries," *Phys. Rev. B* **58**, 2960–2963.

- Di Chiara, A., F. Lombardi, F. M. Granozio, U. S. di Uccio, F. Tafuri, and M. Valentino, 1997, "Y₁Ba₂Cu₃O_{7-x} grain boundary Josephson junctions with a MgO seed layer," *IEEE Trans. Appl. Supercond.* **7**, 3327–3330.
- Dimos, D., P. Chaudhari, and J. Mannhart, 1990, "Superconducting transport properties of grain boundaries in YBa₂Cu₃O₇ bicrystals," *Phys. Rev. B* **41**, 4038–4049.
- Dimos, D., P. Chaudhari, J. Mannhart, and F. K. LeGoues, 1988, "Orientation dependence of grain-boundary critical currents in YBa₂Cu₃O_{7-δ} bicrystals" *Phys. Rev. Lett.* **61**, 219–222.
- Divin, Y. Y., J. Mygind, N. F. Pedersen, and P. Chaudhari, 1992, "Josephson oscillations and noise temperature in YBa₂Cu₃O_{7-x} grain boundary junctions," *Appl. Phys. Lett.* **61**, 3053–3055.
- Divin, Y. Y., J. Mygind, N. F. Pedersen, and P. Chaudhari, 1993, "Linewidth of Josephson oscillations in YBa₂Cu₃O_{7-x} grain-boundary junctions," *IEEE Trans. Appl. Supercond.* **3**, 2337–2340.
- Divin, Y. Y., F. Ya. Nad', V. Ya. Pokrovski, and P. M. Shadrin, 1991, "Laser probing of high- T_c superconducting thin films," *IEEE Trans. Magn.* **27**, 1101–1104.
- Divin, Y. Y., U. Poppe, K. Urban, O. Y. Volkov, V. V. Shiroto, V. V. Pavlovskii, P. Schmueser, K. Hanke, M. Geitz, and M. Tonutti, 1999, "Hilbert-transform spectroscopy with high- T_c Josephson junctions: First spectrometers and first applications," *IEEE Trans. Appl. Supercond.* **9**, 3346–3349.
- Divin, Y. Y., U. Poppe, O. Y. Volkov, and V. V. Pavlovskii, 2000, "Frequency-selective incoherent detection of terahertz radiation by high- T_c Josephson junctions," *Appl. Phys. Lett.* **76**, 2826–2828.
- Divin, Y., O. Volkov, V. Pavlovskii, U. Poppe, and K. Urban, 2001, "Terahertz spectral analysis by ac Josephson effect in high- T_c bicrystal junctions," *IEEE Trans. Appl. Supercond.* **11**, 582–585.
- Doderer, T., Y. M. Zhang, D. Winkler, and R. Gross, 1995, "Imaging of electromagnetic resonances in an YBa₂Cu₃O_{7-δ} bicrystal grain-boundary Josephson junction," *Phys. Rev. B* **52**, 93–96.
- Dong, Z. W., V. C. Matijasevic, P. Hadley, S. M. Shao, and J. E. Mooij, 1995, "Electric field effect in Sm_{1-x}Ca_xBa₂Cu₃O_y bicrystal junctions," *IEEE Trans. Appl. Supercond.* **AS-5**, 2879–2882.
- Dorosinskii, L. A., M. V. Indenbom, V. I. Nikitenko, A. A. Polyanskii, R. L. Prozorov, and V. K. Vlasko-Vlasov, 1993, "Magneto-optic observation of the Meissner effect in YBa₂Cu₃O_{7-x} single crystals," *Physica C* **206**, 360–366.
- Dravid, V. P., H. Zhang, and Y. Y. Wang, 1993, "Inhomogeneity of charge carrier concentration along the grain boundary plane in oxide superconductors," *Physica C* **213**, 353–358.
- Drung, D., E. Dantsker, F. Ludwig, H. Koch, R. Kleiner, J. Clarke, S. Krey, D. Reimer, B. David, and O. Dössel, 1996, "Low noise YBa₂Cu₃O_{7-x} SQUID magnetometers operated with additional positive feedback," *Appl. Phys. Lett.* **68**, 1856–1858.
- Drung, D., F. Ludwig, W. Müller, U. Steinhoff, L. Trahms, Y. Q. Shen, M. B. Jensen, P. Vase, T. Holst, T. Freltoft, and G. Curio, 1996, "Integrated YBa₂Cu₃O_{7-x} magnetometer for biomagnetic measurements," *Appl. Phys. Lett.* **68**, 1421–1423.
- Du, G., M. Mironova, S. Sathyamurthy, and K. Salama, 1998, "An investigation on high-angle grain boundaries in melt-textured YBa₂Cu₃O_{6+x} superconductors," *Physica C* **306**, 199–212.
- Early, E. A., A. F. Clark, and K. Char, 1993, "Half-integral constant voltage steps in high- T_c grain boundary junctions," *Appl. Phys. Lett.* **62**, 3357–3359.
- Early, E. A., R. L. Steiner, A. F. Clark, and K. Char, 1994, "Evidence for parallel junctions within high- T_c grain-boundary junctions," *Phys. Rev. B* **50**, 9409–9418.
- Edstam, J., P. A. Nilsson, E. A. Stepantsov, and H. K. Olsson, 1993, "100 GHz oscillations on monolithic high T_c chips," *Appl. Phys. Lett.* **62**, 896–898.
- Edwards, J. A., J. S. Satchell, N. G. Chew, R. G. Humphreys, N. N. Keene, and O. D. Dosser, 1992, "YBa₂Cu₃O₇ thin-film step junctions on MgO substrates," *Appl. Phys. Lett.* **60**, 2433–2435.
- Ekin, J. W., A. I. Braginski, A. J. Panson, M. A. Janocko, D. W. Capone II, N. J. Zaluzec, B. Flandermeyer, O. F. de Lima, M. Hong, J. Kwo, and S. H. Liou, 1987, "Evidence for weak link and anisotropy limitations on the transport critical current in bulk polycrystalline Y₁Ba₂Cu₃O_x," *J. Appl. Phys.* **62**, 4821–4828.
- Elly, J., M. G. Medici, A. Gilabert, F. Schmidl, T. Schmauder, E. Heinz, and P. Seidel, 1995, "Magnetic-field dependence of Josephson critical current in YBa₂Cu₃O_{7-x} bicrystal grain boundary junctions," *Physica C* **251**, 171–174.
- Elly, J., M. G. Medici, A. Gilabert, F. Schmidl, P. Seidel, A. Hoffmann, and I. K. Schuller, 1997, "Effect of light irradiation on Fiske resonances and the Josephson effect in high- T_c junctions," *Phys. Rev. B* **56**, 8507–8510.
- Eltsev, Y. F., K. Nakao, Y. Yamada, I. Hirabayashi, Y. Ishimaru, K. Tanabe, Y. Enomoto, J. Wen, and N. Koshizuka, 2001, "Transport properties of bicrystal Josephson junctions in Y-Ba-Cu-O films grown by liquid phase epitaxy," *IEEE Trans. Appl. Supercond.* **11**, 3784–3787.
- Enpuku, K., T. Minotani, F. Shiraishi, A. Kandori, and S. Kawakami, 1999, "High T_c dc SQUID utilizing bicrystal junctions with 30 degree misorientation angle," *IEEE Trans. Appl. Supercond.* **9**, 3109–3112.
- Enpuku, K., G. Tokita, T. Maruo, and T. Minotani, 1995, "Parameter dependencies of characteristics of a high T_c dc superconducting quantum interference device," *J. Appl. Phys.* **78**, 3498–3503.
- Eom, C. B., A. F. Marshall, S. S. Laderman, R. D. Jacowitz, and T. H. Geballe, 1990, "Epitaxial and smooth films of a-axis YBa₂Cu₃O₇," *Science* **249**, 1549–1552.
- Eom, C. B., A. F. Marshall, Y. Suzuki, B. Boyer, R. F. W. Pease, and T. H. Geballe, 1991, "Absence of weak-link behaviour in YBa₂Cu₃O₇ grains connected by 90° [010] twist boundaries," *Nature (London)* **353**, 544–547.
- Eom, C., A. F. Marshall, Y. Suzuki, T. H. Geballe, B. Boyer, R. F. W. Pease, R. B. van Dover, and J. M. Phillips, 1992, "Growth mechanisms and properties of 90° grain boundaries in YBa₂Cu₃O₇ thin films," *Phys. Rev. B* **46**, 11 902–11 913.
- Evetts, J. E., M. J. Hogg, B. A. Glowacki, N. A. Rutter, and V. N. Tsaneva, 1999, "Current percolation and the $V-I$ transition in YBa₂Cu₃O₇ bicrystals and granular coated conductors," *Supercond. Sci. Technol.* **12**, 1050–1053.
- Feldmann, D. M., J. L. Reeves, A. A. Polyanskii, G. Kozlowski, R. R. Biggers, R. M. Nekkanti, I. Maartense, M. Tomsic, P. Barnes, C. E. Oberly, T. L. Peterson, S. E. Bab-

- cock, and D. C. Larbalestier, 2000, "Influence of nickel substrate grain structure on $\text{YBa}_2\text{Cu}_3\text{O}_{7-x}$ supercurrent connectivity in deformation-textured coated conductors," *Appl. Phys. Lett.* **77**, 2906–2908.
- Feng, Y., Y. E. High, D. C. Larbalestier, Y. S. Sung, and E. E. Hellstrom, 1993, "Evidence for preferential formation of the $(\text{Bi,Pb})_2\text{Sr}_2\text{Ca}_2\text{Cu}_3\text{O}_x$ phase at the Ag interface in Ag-sheathed $(\text{Bi,Pb})_2\text{Sr}_2\text{Ca}_2\text{Cu}_3\text{O}_x$ tapes," *Appl. Phys. Lett.* **62**, 1553–1555.
- Feng, Y., D. C. Larbalestier, S. E. Babcock, and J. B. Vander Sande, 1992, "(001) faceting and $\text{Bi}_2\text{Sr}_2\text{CuO}_{6+x}$ ($T_c = 7\text{--}22\text{ K}$) phase formation at the Ag/Bi-Sr-Ca-Cu-O interface in Ag-clad $\text{Bi}_2\text{Sr}_2\text{CaCu}_2\text{O}_{8+x}$ ($T_c = 75\text{--}95\text{ K}$) superconducting tapes," *Appl. Phys. Lett.* **61**, 1234–1236.
- Field, M. B., D. C. Larbalestier, A. Parikh, and K. Salama, 1997, "Critical current properties and the nature of the electromagnetic coupling in melt-textured $\text{YBa}_2\text{Cu}_3\text{O}_{6+x}$ bicrystals of general misorientation," *Physica C* **280**, 221–233.
- Field, M. B., V. R. Todt, D. J. Miller, D. H. Kim, 2001, "The effect of grain boundary plane on transport properties of bulk scale 90° [100] grain boundaries in $\text{YBa}_2\text{Cu}_3\text{O}_{6+x}$," unpublished.
- Fischer, G. M., B. Mayer, R. Gross, T. Nissel, K. D. Husemann, R. P. Huebener, T. Freltoft, Y. Shen, and P. Vase, 1994, "Spatially resolved observation of static magnetic flux states in $\text{YBa}_2\text{Cu}_3\text{O}_{7-\delta}$," *Science* **263**, 1112–1114.
- Fischer, G. M., J. Mygind, and N. F. Pedersen, 1997, "Comparison of effective noise temperatures in $\text{YBa}_2\text{Cu}_3\text{O}_{6-\delta}$ junctions," *IEEE Trans. Appl. Supercond.* **7**, 3654–3657.
- Fletcher, J. R., P. J. King, and R. G. Ormson, 1997, "Helical current flow at the junction between two tilted anisotropic conductors," *Phys. Rev. Lett.* **79**, 2522–2525.
- Fogelström, M., D. Rainer, and J. A. Sauls, 1997, "Tunneling into current-carrying surface states of high- T_c superconductors," *Phys. Rev. Lett.* **79**, 281–284.
- Fogelström, M., and S. K. Yip, 1998, "Time-reversal symmetry-breaking states near grain boundaries between d-wave superconductors," *Phys. Rev. B* **57**, 14 060–14 063.
- Forkl, A., T. Dragon, and H. Kronmüller, 1990, "Investigation of the mixed state of $\text{YBa}_2\text{Cu}_3\text{O}_{7-\delta}$ superconductors," *J. Appl. Phys.* **67**, 3047–3053.
- Freericks, J. K., B. K. Nikolic, and P. Miller, 2001, "Tuning a Josephson junction through a quantum critical point," *Phys. Rev. B* **64**, 054511.
- Frey, T., J. Mannhart, J. G. Bednorz, and E. J. Williams, 1996a, "High- T_c superconductor-insulator-superconductor heterostructures with highly resistive insulator layers," *Jpn. J. Appl. Phys.*, Part 2 **35**, L384–L386.
- Frey, U., H. Meffert, P. Haibach, K. Üstüner, G. Jakob, and H. Adrian, 1996b, "Transport properties of $\text{Bi}_2\text{Sr}_2\text{Ca}_2\text{Cu}_3\text{O}_{10+\delta}$ bicrystal grain boundary Josephson junctions and SQUIDs," *J. Phys. IV* **6C3**, 277–282.
- Frey, U., K. Üstüner, M. Blumers, M. Basset, J. C. Martinez, and H. Adrian, 1997, in *ISEC '97, Extended Abstracts*, edited by H. Koch and S. Knappe (Physikalische Technische Bundesanstalt, Braunschweig, Germany), pp. 230–232.
- Friedl, G., B. Roas, M. Römheld, L. Schultz, and W. Jutzi, 1991, "Transport properties of epitaxial $\text{YBa}_2\text{Cu}_3\text{O}_x$ films at step edges," *Appl. Phys. Lett.* **59**, 2751–2753.
- Froehlich, O. M., A. Beck, R. Gross, H. Sato, and M. Naito, 1996, "In-plane penetration depth of high-temperature superconductors with single and double CuO layers," *Europhys. Lett.* **36**, 467–472.
- Froehlich, O. M., P. Richter, A. Beck, R. Gross, and G. Koren, 1997b, "Quasiparticle tunneling in HTS grain boundary Josephson junctions," *J. Low Temp. Phys.* **106**, 243–248.
- Froehlich, O. M., P. Richter, A. Beck, D. Koelle, and R. Gross, 1997a, "Barrier properties of grain boundary junctions in high- T_c superconductors," *IEEE Trans. Appl. Supercond.* **7**, 3189–3192.
- Froehlich, O. M., H. Schulze, A. Beck, L. Alff, R. Gross, and R. P. Huebener, 1995, "Analysis of the critical current density in grain boundary Josephson junctions on a nanometer scale," *Appl. Phys. Lett.* **66**, 2289–2291.
- Froehlich, O. M., H. Schulze, R. Gross, A. Beck, and L. Alff, 1994, "Precision measurement of the in-plane penetration depth $\lambda_{ab}(T)$ in $\text{YBa}_2\text{Cu}_3\text{O}_{7-\delta}$ using grain-boundary Josephson junctions," *Phys. Rev. B* **50**, 13 894–13 897.
- Fukumoto, Y., R. Ogawa, and Y. Kawate, 1993, "Millimeter-wave detection by YBaCuO step-edge microbridge Josephson junction," *J. Appl. Phys.* **74**, 3567–3571.
- Gao, Y., K. L. Merkle, G. Bai, H. L. M. Chang, and D. J. Lam, 1991, "Structure and composition of grain boundary dislocation cores and stacking faults in MOCVD-grown $\text{YBa}_2\text{Cu}_3\text{O}_{7-x}$ thin films," *Physica C* **174**, 1–10.
- Gayle, F. W., and D. L. Kaiser, 1991, "The nature of [001] tilt grain boundaries in $\text{YBa}_2\text{Cu}_3\text{O}_{7-x}$," *J. Mater. Res.* **6**, 908–915.
- Gerdemann, R., T. Bauch, O. M. Fröhlich, L. Alff, A. Beck, D. Koelle, and R. Gross, 1995, "Asymmetric high temperature superconducting Josephson vortex-flow transistors with high current gain," *Appl. Phys. Lett.* **67**, 1010–1012.
- Gilabert, A., A. Hoffmann, M. G. Medici, and I. Schuller, 2000, "Photodoping effects in high critical temperature superconducting films and Josephson junctions," *J. Supercond.* **13**, 1–20.
- GINLEY, D. S., E. L. Venturini, J. F. Kwak, R. J. Baughman, B. Morosin, and J. E. Schirber, 1987, "Superconducting shells in ceramic $\text{YBa}_2\text{Cu}_3\text{O}_7$," *Phys. Rev. B* **36**, 829–832.
- Glyantsev, V. N., Y. Tavrín, W. Zander, J. Schubert, and M. Siegel, 1996, "The stability of dc and rf SQUIDs in static ambient fields," *Supercond. Sci. Technol.* **9**, A105–A108.
- Goetz, B., R. R. Schulz, C. W. Schneider, A. Schmehl, H. Bielefeldt, H. Hilgenkamp, and J. Mannhart, 2001, unpublished.
- Götz, B., 2000, "Untersuchung der Transporteigenschaften von Korngrenzen in Hochtemperatur-Supraleitern," Ph.D. thesis (University of Augsburg).
- Golubov, A. A., and M. Y. Kupriyanov, 1999, "Properties of rough interfaces in superconductors with d-wave pairing," *IEEE Trans. Appl. Supercond.* **9**, 3444–3447.
- Golubov, A., and F. Tafuri, 2000, "Andreev reflection in layered structures: Implications for high- T_c grain-boundary Josephson junctions," *Phys. Rev. B* **62**, 15 200–15 203.
- Goyal, A., D. P. Norton, J. D. Budai, M. Paranthaman, E. D. Specht, D. M. Kroeger, D. K. Christen, Q. He, B. Saffian, F. A. List, D. F. Lee, P. M. Martin, C. E. Klabunde, E. Hartfield, and V. K. Sikka, 1996, "High critical current density superconducting tapes by epitaxial deposition of $\text{YBa}_2\text{Cu}_3\text{O}_x$ thick films on biaxially textured metals," *Appl. Phys. Lett.* **69**, 1795–1797.
- Goyal, A., E. D. Specht, D. M. Kroeger, and T. A. Mason, 1996, "Effect of texture on grain boundary misorientation distributions in polycrystalline high temperature superconductors," *Appl. Phys. Lett.* **68**, 711–713.

- Goyal, A., E. D. Specht, D. M. Kroeger, T. A. Mason, D. J. Dingley, G. N. Riley, Jr., and M. W. Rupich, 1995, "Grain boundary misorientations and percolative current paths in high- J_c powder-in-tube $(\text{Bi,Pb})_2\text{Sr}_3\text{Ca}_3\text{Cu}_3\text{O}_x$," *Appl. Phys. Lett.* **66**, 2903–2905.
- Grant, P. M., 2000, "Current without borders," *Nature (London)* **407**, 139–141.
- Gray, K. E., M. B. Field, and D. J. Miller, 1998, "Explanation of low critical currents in flat, bulk versus meandering, thin film [001] tilt bicrystal grain boundaries in $\text{YBa}_2\text{Cu}_3\text{O}_7$," *Phys. Rev. B* **58**, 9543–9548.
- Gray, K. E., D. J. Miller, M. B. Field, D. H. Kim, and P. Berghuis, 2000, "Grain boundary dissipation in high- T_c superconductors," *Physica C* **341-348**, 1397–1400.
- Greuter, F., and G. Blatter, 1990, "Electrical properties of grain boundaries in polycrystalline compound semiconductors," *Supercond. Sci. Technol.* **5**, 111–137.
- Grindatto, D. P., B. Hensel, G. Grasso, H. U. Nissen, and R. Flükiger, 1996, "TEM study of twist boundaries and colony boundaries in $(\text{Bi,Pb})_2\text{Sr}_2\text{Ca}_2\text{Cu}_3\text{O}_x$ silver-sheathed tapes," *Physica C* **271**, 155–163.
- Gross, R., 1994, in *Interfaces in High- T_c Superconducting Systems*, edited by S. L. Shinde and D. A. Rudman (Springer-Verlag, New York), pp. 176–209.
- Gross, R., L. Alff, A. Beck, O. M. Froehlich, R. Gerber, R. Gerdemann, A. Marx, B. Mayer, and D. Koelle, 1995, in *Proceedings of the 2nd Workshop on HTS Applications and New Materials*, edited by D. H. A. Blank (University of Twente, Enschede), pp. 8–15.
- Gross, R., L. Alff, A. Beck, O. M. Froehlich, D. Koelle, and A. Marx, 1997, "Physics and technology of high temperature superconducting Josephson junctions," *IEEE Trans. Appl. Supercond.* **7**, 2929–2935.
- Gross, R., P. Chaudhari, D. Dimos, A. Gupta, and G. Koren, 1990a, "Thermally activated phase slippage in high- T_c grain-boundary Josephson junctions," *Phys. Rev. Lett.* **64**, 228–231.
- Gross, R., P. Chaudhari, M. Kawasaki, and A. Gupta, 1990b, "Scaling behavior in electrical transport across grain boundaries in $\text{YBa}_2\text{Cu}_3\text{O}_{7-\delta}$ superconductors," *Phys. Rev. B* **42**, 10 735–10 737.
- Gross, R., P. Chaudhari, M. Kawasaki, M. B. Ketchen, and A. Gupta, 1990c, "Low-noise $\text{YBa}_2\text{Cu}_3\text{O}_{7-\delta}$ grain-boundary junction dc SQUIDS," *Appl. Phys. Lett.* **57**, 727–729.
- Gross, R., P. Chaudhari, M. Kawasaki, M. Ketchen, and A. Gupta, 1990d, "Noise characteristics of single grain-boundary junction dc SQUIDS in $\text{YBa}_2\text{Cu}_3\text{O}_{7-\delta}$ films," *Physica C* **170**, 315–318.
- Gross, R., P. Chaudhari, M. Kawasaki, and A. Gupta, 1991, "Superconducting transport characteristic of $\text{YBa}_2\text{Cu}_3\text{O}_{7-\delta}$ grain boundary junctions," *IEEE Trans. Magn.* **27**, 3227–3230.
- Gross, R., and B. Mayer, 1991, "Transport processes and noise in $\text{YBa}_2\text{Cu}_3\text{O}_{7-\delta}$ grain boundary junctions," *Physica C* **180**, 235–242.
- Grupp, D. E., and A. M. Goldman, 1997, "Indications of a $T=0$ quantum phase transition in SrTiO_3 ," *Phys. Rev. Lett.* **78**, 3511–3514; **82**, 3001(E) (1999).
- Gupta, A., J. Sun, and C. C. Tsuei, 1994, "Mercury-based cuprate high- T_c grain boundary junctions and SQUIDS operating above 110 K," *Science* **265**, 1075–1077.
- Gurevich, A., 1999, "Current-limiting mechanisms and grain boundary pinning in superconductors," *Int. Workshop on Critical Currents*, July 1999, University of Madison-Wisconsin, 2-3.
- Gurevich, A., and L. D. Cooley, 1994, "Anisotropic flux pinning in a network of planar defects," *Phys. Rev. B* **50**, 13 563–13 576.
- Gurevich, A., and E. A. Pashitskii, 1998, "Current transport through low-angle grain boundaries in high-temperature superconductors," *Phys. Rev. B* **57**, 13 878–13 893; **63**, 139901(E).
- Guth, K., H. U. Krebs, H. C. Freyhardt, and Ch. Jooss, 2001, "Modification of transport properties in low-angle grain boundaries via calcium doping of $\text{YBa}_2\text{Cu}_3\text{O}_\delta$ thin films," *Phys. Rev. B* **64**, 140508.
- Gutkin, M. Yu., and I. A. Ovid'ko, 2001, "Transformations of low-angle tilt boundaries in high- T_c superconductors," *Phys. Rev. B* **63**, 064515.
- Gyorgy, E. M., R. B. van Dover, L. F. Schneemeyer, A. E. White, H. M. O'Bryan, R. J. Felder, J. V. Waszczak, and W. W. Rhodes, 1990, "Sharp angular sensitivity of pinning due to twin boundaries in $\text{Ba}_2\text{YCu}_3\text{O}_7$," *Appl. Phys. Lett.* **56**, 2465–2467.
- Haage, T., J. Zegenhagen, J. Q. Li, H.-U. Habermeier, M. Cardona, Ch. Jooss, R. Warthmann, A. Forkl, and H. Kronmüller, 1997, "Transport properties and flux pinning by self-organization in $\text{YBa}_2\text{Cu}_3\text{O}_{7-\delta}$ films on vicinal SrTiO_3 (001)," *Phys. Rev. B* **56**, 8404–8418.
- Habib, Y. M., D. E. Oates, G. Dresselhaus, M. S. Dresselhaus, L. R. Vale, and R. H. Ono, 1998, "Microwave power handling in engineered $\text{YBa}_2\text{Cu}_3\text{O}_{7-\delta}$ grain boundaries," *Appl. Phys. Lett.* **73**, 2200–2202.
- Haensel, H., C. Hoefener, D. Koelle, and R. Gross, 1997, "Fabrication and characterization of $\text{YBa}_2\text{Cu}_3\text{O}_{7-\delta}$ / SrTiO_3 /Ag trilayer films on SrTiO_3 bicrystal substrates," *IEEE Trans. Appl. Supercond.* **7**, 2296–2299.
- Hagerhorst, J. M., J. D. Mannhart, M. M. Oprysko, M. R. Scheuermann, and C. C. Tsuei, 1989, in *Laser and Particle-Beam Modification of Chemical Processes on Surfaces*, edited by A. W. Johnson, G. L. Loper, and T. W. Sigmon, MRS Symp. Proc. No. 129 (Materials Research Society, Pittsburgh), pp. 347–352.
- Halbritter, J., 1992, "Pair weakening and tunnel channels at cuprate interfaces," *Phys. Rev. B* **46**, 14 861–14 871.
- Halbritter, J., 1993, "Extrinsic or intrinsic conduction in cuprates. Anisotropy, weak, and strong links," *Phys. Rev. B* **48**, 9735–9746.
- Hammerl, G., H. Bielefeldt, B. Goetz, A. Schmehl, C. W. Schneider, R. R. Schulz, H. Hilgenkamp, and J. Mannhart, 2001, "Doping-induced enhancement of grain boundary critical currents," *IEEE Trans. Appl. Supercond.* **11**, 2830–2837.
- Hammerl, G., H. Hilgenkamp, R. R. Schulz, C. W. Schneider, B. Goetz, H. Bielefeldt, A. Schmehl, and J. Mannhart, 2000, unpublished.
- Hammerl, G., A. Schmehl, R. R. Schulz, B. Goetz, H. Bielefeldt, C. W. Schneider, H. Hilgenkamp, and J. Mannhart, 2000, "Enhanced supercurrent density in polycrystalline $\text{YBa}_2\text{Cu}_3\text{O}_{7-\delta}$ at 77 K from calcium doping of grain boundaries," *Nature (London)* **407**, 162–164.
- Hammond, S. G., Y. He, C. M. Muirhead, P. Wu, M. S. Colclough, and K. Char, 1993, "Noise properties of bi-epitaxial HTS junctions," *IEEE Trans. Appl. Supercond.* **3**, 2319–2320.

- Hao, L., J. C. Macfarlane, and C. M. Pegrum, 1994, "Comparative noise measurements in YBCO step-edge and bicrystal grain-boundary junctions," *Physica C* **232**, 111–118.
- Hao, L., J. C. Macfarlane, and C. M. Pegrum, 1996, "Excess noise in $\text{YBa}_2\text{Cu}_3\text{O}_7$ thin film grain boundary Josephson junctions and devices," *Supercond. Sci. Technol.* **9**, 678–687.
- Hao, L., J. C. Macfarlane, C. M. Pegrum, G. J. Sloggett, and C. P. Foley, 1997, "Magnetic field and microwave effects on critical current fluctuations in HTS grain-boundary Josephson junctions," *IEEE Trans. Appl. Supercond.* **7**, 2840–2843.
- Hasegawa, K., N. Yoshida, K. Fujino, H. Mukai, K. Hayashi, K. Sato, T. Ohkuma, S. Honjyo, H. Ishii, and T. Hara, 1996, in *Proceedings of the International Cryogenic Engineering Conference (ICEC16)*, Kitakyushu, Japan, 1996, edited by T. Hasayama, T. Mitsui, and K. Yamafuji (Elsevier, Amsterdam), pp. 1413–1416.
- Häuser, B., B. B. G. Klopman, G. J. Gerritsma, J. Gao, and H. Rogalla, 1989, "Response of YBaCuO thin-film microbridges to microwave irradiation," *Appl. Phys. Lett.* **54**, 1368–1370.
- Hawley, M., 2000, in *Characterization of High- T_c Materials and Devices by Electron Microscopy*, edited by N. D. Browning and S. J. Pennycook (Cambridge University Press, Cambridge), pp. 125–160.
- Hawsey, R. A., D. M. Kroeger, and D. K. Christen, 1999, "Development of biaxially textured $\text{YBa}_2\text{Cu}_3\text{O}_7$ coated conductors in the US," *Adv. Supercond.* XII, in press.
- Hein, M. A., M. Strupp, H. Piel, A. M. Portis, and R. Gross, 1994, "Surface impedance of $\text{YBa}_2\text{Cu}_3\text{O}_{7-x}$ thin film grain boundary Josephson junctions: evaluation of the IcRn product," *J. Appl. Phys.* **75**, 4581–4587.
- Heine, K., J. Tenbrink, and M. Thöner, 1989, "High-field critical current densities in $\text{Bi}_2\text{Sr}_2\text{Ca}_1\text{Cu}_2\text{O}_{8+x}/\text{AG}$ wires," *Appl. Phys. Lett.* **55**, 2441–2443.
- Heinig, N. F., R. D. Redwing, J. E. Nordman, and D. C. Larbalestier, 1999, "Strong to weak coupling transition in low misorientation angle thin film $\text{YBa}_2\text{Cu}_3\text{O}_{7-\delta}$ bicrystals," *Phys. Rev. B* **60**, 1409–1417.
- Heinig, N. F., R. D. Redwing, I. F. Tsu, A. Gurevich, J. E. Nordman, S. E. Babcock, and D. C. Larbalestier, 1996, "Evidence for channel conduction in low misorientation angle [001] tilt $\text{YBa}_2\text{Cu}_3\text{O}_{7-\delta}$ bicrystal films," *Appl. Phys. Lett.* **69**, 577–579.
- Hensel, B., G. Grasso, and R. Flukiger, 1995, "Limits to the critical transport current in superconducting $(\text{Bi,Pb})_2\text{Sr}_2\text{Ca}_2\text{Cu}_3\text{O}_{10}$ silver-sheathed tapes: the railway-switch model," *Phys. Rev. B* **51**, 15 456–15 473.
- Hensel, B., J.-C. Grivel, A. Jeremie, A. Perin, A. Pollini, and R. Flukiger, 1993, "A model for the critical current in $(\text{Bi,Pb})_2\text{Sr}_2\text{Ca}_2\text{Cu}_3\text{O}_x$ silver-sheathed tapes," *Physica C* **205**, 329–337.
- Herbsommer, J. A., G. Nieva, and J. Luzuriaga, 2000, "Interplay between pinning energy and vortex interaction in $\text{YBa}_2\text{Cu}_3\text{O}_{7-\delta}$ with oriented twin boundaries in tilted magnetic fields: Bitter decoration and tilt-modulus measurements," *Phys. Rev. B* **62**, 3534–3541.
- Herbstritt, F., T. Kemen, L. Alff, A. Marx, and R. Gross, 2001, "Transport and noise characteristics of submicron high-temperature superconductor grain-boundary junctions," *Appl. Phys. Lett.* **78**, 955–957.
- Herd, J. S., D. Oates, and J. Halbritter, 1997, "Identification and modeling of microwave loss mechanisms in $\text{YBa}_2\text{Cu}_3\text{O}_{7-x}$," *IEEE Trans. Appl. Supercond.* **7**, 1299–1302.
- Herrmann, K., Y. Zhang, H.-M. Mück, J. Schubert, W. Zander, and A. I. Braginski, 1991, "Characterization of $\text{YBa}_2\text{Cu}_3\text{O}_7$ step edge Josephson junctions," *Supercond. Sci. Technol.* **4**, 583–586.
- Hilgenkamp, H., and J. Mannhart, 1997, "Intrinsic weak link originating from tilt in contacts $d_{x^2-y^2}$ -wave superconductors," *Appl. Phys. A: Mater. Sci. Process.* **64**, 553–554.
- Hilgenkamp, H., and J. Mannhart, 1998a, "Band-bending and d-wave symmetry at interfaces in high- T_c Superconductors," Twente-HTS Workshop on Superconducting Electronics, Enschede, Netherlands.
- Hilgenkamp, H., and J. Mannhart, 1998b, "Superconducting and normal-state properties of $\text{YBa}_2\text{Cu}_3\text{O}_{7-\delta}$ -bicrystal grain boundary junctions in thin films," *Appl. Phys. Lett.* **73**, 265–267.
- Hilgenkamp, H., and J. Mannhart, 1999, "Grain boundaries and other interfaces in cuprate high- T_c superconductors," unpublished.
- Hilgenkamp, H., J. Mannhart, and B. Mayer, 1996, "Implications of $d_{x^2-y^2}$ -symmetry and faceting for the transport properties of grain boundaries in high- T_c superconductors," *Phys. Rev. B* **53**, 14 586–14 593.
- Hilgenkamp, H., J. Mannhart, B. Mayer, and Ch. Gerber, 1997, "Influence of $d_{x^2-y^2}$ symmetry on device applications of high- T_c grain boundary junctions," *IEEE Trans. Appl. Supercond.* **7**, 3670–3673.
- Hilgenkamp, H., J. Mannhart, B. Mayer, Ch. Gerber, J. Kirtley, K. A. Moler, and M. Sgrist, 1996, "Implications of $d_{x^2-y^2}$ -symmetry for grain-boundary-based high- T_c devices," *Proceedings of the Third Twente HTS Workshop*, edited by R. Moerman (Low Temperature Division, University of Twente), pp. 66–72.
- Hilgenkamp, H., C. W. Schneider, R. R. Schulz, B. Goetz, A. Schmehl, H. Bielefeldt, and J. Mannhart, 1999, "Modifying electronic properties of interfaces in high- T_c superconductors by doping," *Physica C* **326-327**, 7–11.
- Hilgenkamp, J. W. M., G. C. S. Brons, J. G. Soldevilla, R. P. J. Ijsselsteijn, J. Flokstra, and H. Rogalla, 1994, "Four-layer monolithic integrated high- T_c dc SQUID magnetometer," *Appl. Phys. Lett.* **64**, 3497–3499.
- Hinaus, B. M., R. D. Redwing, and M. S. Rzchowski, 1997, "Flux penetration in bicrystal-substrate thin film $\text{YBa}_2\text{Cu}_3\text{O}_{7-\delta}$ Josephson junctions," *Appl. Phys. Lett.* **70**, 517–519.
- Höfener, C., J. B. Philipp, J. Klein, L. Alff, A. Marx, B. Büchner, and R. Gross, 2000, "Voltage and temperature dependence of the grain boundary magnetoresistance in manganites," *Europhys. Lett.* **50**, 681–687.
- Hoffmann, A., I. K. Schuller, A. Gilabert, M. G. Medici, F. Schmidl, and P. Seidel, 1997, "Persistent photoconductivity in high T_c grain boundary Josephson junctions," *Appl. Phys. Lett.* **70**, 2461–2463.
- Hogan-O'Neill, J. J., A. M. Martin, and J. F. Annett, 1999, "Tilt grain-boundary effects in s- and d-wave superconductors," *Phys. Rev. B* **60**, 3568–3571.
- Hogg, M. J., F. Kahlmann, E. J. Tarte, Z. H. Barber, and J. E. Evetts, 2001, "Vortex channeling and the voltage-current characteristic of $\text{YBa}_2\text{Cu}_3\text{O}_7$ low-angle grain boundaries," *Appl. Phys. Lett.* **78**, 1433–1435.
- Hohmann, H., H.-J. Krause, H. Soltner, Y. Zhang, C. A. Copetti, H. Bousack, A. I. Braginski, M. I. Faley, 1997, "HTS SQUID system with Joule-Thomson cryocooler for eddy cur-

- rent nondestructive evaluation of aircraft structures,” *IEEE Trans. Appl. Supercond.* **7**, 2860–2865.
- Holzappel, B., L. Fernandez, F. Schindler, B. de Boer, N. Reger, J. Eickemeyer, P. Berberich, and W. Prusseit, 2001, “Grain boundary networks in Y123 coated conductors: formation, properties and simulation,” *IEEE Trans. Appl. Supercond.* **11**, 3782–3785.
- Holzappel, B., D. Verebelyi, C. Cantoni, M. Paranthaman, B. Sales, R. Feenstra, D. Christen, and D. P. Norton, 2000, “Low angle grain boundary transport properties of undoped and doped Y123 thin film bicrystals,” *Physica C* **341-348**, 1431–1434.
- Hong, J. P., H. R. Fetterman, A. J. Forse, and A. H. Cardona, 1993, “Double step-edge weak links integrated with spiral antenna structure in epitaxial $Tl_2CaBa_2Cu_2O_8$ films for millimeter wave mixing,” *Appl. Phys. Lett.* **62**, 2865–2867.
- Horng, H. E., S. Y. Yang, W. L. Lee, H. C. Yang, and J. M. Wu, 1997, “Biepitaxial grain boundary $YBa_2Cu_3O_{7-\delta}$ thin-film SQUIDs,” *Appl. Supercond.* **1-2**, 683–686.
- Hu, C. R., 1994, “Midgap surface states as a novel signature for $d_{x^2-y^2}$ -wave superconductivity,” *Phys. Rev. Lett.* **72**, 1526–1529.
- Hu, Q. Y., P. V. P. S. S. Sastry, U. P. Trociewitz, and J. Schwartz, 1999, “Microstructure and critical currents in AgMg-sheathed multifilamentary $Bi_2Sr_2CaCu_2O_8$ tapes,” *IEEE Trans. Appl. Supercond.* **9**, 1876–1879.
- Huang, M. Q., L. Chen, T. Yang, J. C. Nie, P. J. Wu, G. R. Liu, and Z. X. Zhao, 1997, “Infrared detector fabricated by YBCO Josephson junctions in series,” *Physica C* **282-287**, 2545–2546.
- Huang, Y. K., B. ten Haken, and H. H. J. ten Kate, 1998, “Critical current of high T_c superconducting $Bi2223/Ag$ tapes,” *Physica C* **309**, 197–202.
- Huebener, R. P., 1988, “Scanning electron microscopy at very low temperatures,” *Adv. Electron. Electron Phys.* **70**, 1–78.
- Huebener, R. P., 2000, in *Characterization of High- T_c Materials and Devices by Electron Microscopy*, edited by N. D. Browning and S. J. Pennycook (Cambridge University Press, Cambridge), pp. 103–124.
- Humphreys, R. G., and J. A. Edwards, 1993, “ $YBa_2Cu_3O_7$ thin film grain boundary junctions in a perpendicular magnetic field,” *Physica C* **210**, 42–54.
- Humphreys, R. G., J. S. Satchell, S. W. Goodyear, N. G. Chew, M. N. Keene, J. A. Edwards, C. P. Barret, N. J. Exon, and K. Lander, 1995, in *Proceedings of the 2nd Workshop on HTS Applications and New Materials*, edited by D. H. A. Blank (University of Twente, Enschede), pp. 16–21.
- Hurd, M., 1997, “Current-voltage relation for superconducting d -wave junctions,” *Phys. Rev. B* **55**, 11 993–11 996.
- Hwang, D. M., T. S. Ravi, R. Ramesh, S. W. Chan, C. Y. Chen, L. Nazar, X. D. Wu, A. Inam, and T. Venkatesan, 1990, “Application of near coincidence site lattice theory to the orientation of grains on (001) MgO substrates,” *Appl. Phys. Lett.* **57**, 1690–1692.
- Hylton, T. L., A. Kapitulnik, M. R. Beasley, J. P. Carini, L. Drabek, and G. Grüner, 1988, “Weakly coupled grain model of high-frequency losses in high T_c superconducting thin films,” *Appl. Phys. Lett.* **53**, 1343–1435.
- Iguchi, I., K. Nukui, and K. Lee, 1994, “Dynamic Cooper-pair breaking by tunnel injection of quasiparticles into a high- T_c $YBa_2Cu_3O_7$ superconductor,” *Phys. Rev. B* **50**, 457–461.
- Iijima, Y., M. Kimura, T. Saitoh, and K. Takeda, 2000, “Development of Y-123-coated conductors by IBAD process,” *Physica C* **335**, 15–19.
- Iijima, Y., K. Onabe, N. Futaki, N. Tanabe, N. Sadakata, O. Kohno, and Y. Ikeno, 1993, “Structural and transport properties of biaxially aligned $YBa_2Cu_3O_{7-x}$ films on polycrystalline Ni-based alloy with ion-beam-modified buffer layers,” *J. Appl. Phys.* **74**, 1905–1911.
- Iijima, Y., N. Tanabe, O. Kohno, and Y. Ikeno, 1992, “In-plane aligned $YBa_2Cu_3O_{7-x}$ thin films deposited on polycrystalline metallic substrates,” *Appl. Phys. Lett.* **60**, 769–771.
- Ijsselsteijn, R. P. J., J. W. M. Hilgenkamp, M. Eisenberg, C. Vittoz, J. Flokstra, and H. Rogalla, 1993, “Biepitaxial template grain-boundaries with different in-plane angles on (100) MgO substrates,” *J. Alloys Compd.* **195**, 231–234.
- Ijsselsteijn, R. P. J., J. W. M. Hilgenkamp, D. Terpstra, J. Flokstra, and H. Rogalla, 1994, “Bi-epitaxial template grain boundary weak links on MgO: high T_c Josephson junctions,” *Adv. Cryog. Eng.* **40**, 353–360.
- Il’ichev, E., 2000, “Peculiarities of the current phase relationship for YBCO-based Josephson junctions,” presentation at the Workshop: Kryoelektronische Bauelemente, Schloß Pommersfelden, Germany, Oct. 2000.
- Il’ichev, E., M. Grajcar, R. Hlubina, R. P. J. Ijsselsteijn, H. E. Hoenig, H. G. Meyer, A. Golubov, M. H. S. Anim, A. M. Zagoskin, A. N. Omelyanchouk, and M. Y. Kupriyanov, 2001, “Degenerate ground state in a mesoscopic $YBa_2Cu_3O_{7-\delta}$ grain boundary Josephson junction,” *Phys. Rev. Lett.* **86**, 5369–5372.
- Il’ichev, E., V. Zakosarenko, R. P. J. Ijsselsteijn, H. E. Hoenig, H. G. Meyer, M. V. Fistul, and P. Müller, 1999a, “Phase dependence of the Josephson current in inhomogeneous high- T_c grain-boundary junctions,” *Phys. Rev. B* **59**, 11 502–11 505.
- Il’ichev, E., V. Zakosarenko, R. P. J. Ijsselsteijn, H. E. Hoenig, V. Schultze, H.-G. Meyer, M. Grajcar, and R. Hlubina, 1999b, “Anomalous periodicity of the current-phase relationship of grain-boundary Josephson junctions in high- T_c superconductors,” *Phys. Rev. B* **60**, 3096–3099.
- Il’ichev, E., V. Zakosarenko, R. P. J. Ijsselsteijn, V. Schultze, H.-G. Meyer, H. E. Hoenig, H. Hilgenkamp, and J. Mannhart, 1998, “Nonsinusoidal current-phase relationship of grain boundary Josephson junctions in high- T_c superconductors,” *Phys. Rev. Lett.* **81**, 894–897.
- Inoue, M., S. Imaeda, Y. Tsukino, A. Fujimaki, Y. Takai, and H. Hayakawa, 1994, “Planar-type $Ba_{1-x}K_xBiO_3$ -Josephson tunnel junctions prepared on $SrTiO_3$ bicrystal substrates,” *Appl. Phys. Lett.* **65**, 243–245.
- Inoue, N., T. Sugano, T. Utagawa, Y. Wu, S. Adachi, and K. Tanabe, 2001, “Properties of (Hg, Re)-1212 bicrystals junctions with different misorientation angles,” *Physica C* **357-360**, 1444–1446.
- Isaac, S. P., E. J. Tarte, F. J. Baudenbacher, and M. G. Blamire, 1997, “Development of 3 terminal devices based on asymmetric, long YBCO Josephson junctions,” *IEEE Trans. Appl. Supercond.* **7**, 2619–2622.
- Ishimaru, Y., K. Hayashi, and Y. Enomoto, 1995, “Properties of basal-plane-faced tilt boundary Josephson junction in YBCO films,” *Jpn. J. Appl. Phys., Part 2* **34**, L1123–L1126.
- Ishimaru, Y., J. Wen, N. Koshizuka, and Y. Enomoto, 1997, “Superconducting-gap symmetry study using a/c boundary Josephson junctions in $YBa_2Cu_3O_{7-\delta}$ films,” *Phys. Rev. B* **55**, 11 851–11 859.

- Ivanov, Z. G., N. Fogel, P. Å. Nilsson, E. A. Stepantsov, and A. Ya. Tzalenchuk, 1994, "Transport properties of submicron YBaCuO low angle grain boundary weak links," *Physica C* **235-240**, 3253–3254.
- Ivanov, Z. G., V. K. Kaplunenko, E. A. Stepantsov, E. Wikborg, and T. Claeson, 1994, "An experimental implementation of a high- T_c based RSFQ set-reset trigger at 4.2 K," *Supercond. Sci. Technol.* **7**, 239–241.
- Ivanov, Z. G., P. Å. Nilsson, D. Winkler, J. A. Alarco, T. Claeson, E. A. Stepantsov, and A. Ya. Tzalenchuk, 1991, "Weak links and dc SQUIDS on artificial nonsymmetric grain boundaries in YBa₂Cu₃O_{7- δ} ," *Appl. Phys. Lett.* **59**, 3030–3032.
- Ivanov, Z. G., E. A. Stepantsov, T. Claeson, F. Wenger, S. Y. Lin, N. Khare, and P. Chaudhari, 1996, "Impact of the symmetry of the superconducting wave function on supercurrent transport in YBa₂Cu₃O_{7- δ} Josephson junctions," *Czech. J. Phys.* **46**, 1311–1312.
- Ivanov, Z. G., E. A. Stepantsov, T. Claeson, F. Wenger, S. Y. Lin, N. Khare, and P. Chaudhari, 1998, "Highly anisotropic supercurrent transport in YBa₂Cu₃O_{7- δ} bicrystal Josephson junctions," *Phys. Rev. B* **57**, 602–607.
- Ivanov, Z. G., E. A. Stepantsov, A. Y. Tzalenchuk, and T. Claeson, 1994, "Properties of locally doped bi-crystal grain boundary junctions," *Physica B* **194-196**, 2187–2188.
- Ivanov, Z. G., E. A. Stepantsov, A. Ya. Tzalenchuk, R. I. Shekhter, and T. Claeson, 1993, "Field effect transistor based on a bi-crystal grain boundary Josephson junction," *IEEE Trans. Appl. Supercond.* **3**, 2925–2927.
- Jagannadham, K., and J. Narayan, 1992, "Depression of order parameter and effect on grain boundary critical current density," *Mater. Sci. Eng., B* **14**, 214–226.
- Jia, C. L., B. Kabius, K. Urban, K. Herrmann, G. J. Cui, J. Schubert, W. Zander, A. I. Braginski, and C. Heiden, 1991, "Microstructure of epitaxial YBa₂Cu₃O₇ films on step-edge SrTiO₃ substrates," *Physica C* **175**, 545–554.
- Jia, C. L., B. Kabius, K. Urban, K. Herrmann, J. Schubert, W. Zander, and A. I. Braginski, 1992, "The microstructure of epitaxial YBa₂Cu₃O₇ films on steep steps in LaAlO₃ substrates," *Physica C* **196**, 211–226.
- Jiang, Q. D., Z. J. Huang, A. Brazdeikis, M. Dezaneti, C. L. Chen, P. Jin, and C. W. Chu, 1998, "Nondestructive investigation of microstructures and defects at a SrTiO₃ bicrystal grain boundary," *Appl. Phys. Lett.* **72**, 3365–3367.
- Jiang, Q. D., X. Q. Pan, and J. Zegenhagen, 1997, "Atomic-scale structure of a SrTiO₃ bicrystal boundary studied by scanning tunneling microscopy," *Phys. Rev. B* **56**, 6947–6951.
- Jin, S., R. C. Sherwood, R. B. van Dover, T. H. Tiefel, and D. W. Johnson, Jr., 1987, "High T_c superconductors-composite wire fabrication," *Appl. Phys. Lett.* **51**, 203–204.
- Jooss, Ch., 2000, presentation at the Topical Workshop on Grain Boundaries and Interfaces in High Temperature Superconductors, Williamsburg (VA, USA), Sept. 2000.
- Jooss, Ch., J. Albrecht, H. Kuhn, H. Kronmüller, and S. Leonhardt, 2002, "Magneto-optical studies of current distributions in high- T_c -superconductors," *Rep. Prog. Phys.* **65**, 651–788.
- Jooss, Ch., B. Bringmann, H. Walter, A. Leenders, and H. C. Freyhardt, 2000, "Magneto-optical study of current distributions at grain boundaries in YBaCuO melt-textured monoliths," *Physica C* **341-348**, 1423–1426.
- Jooss, Ch., R. Warthmann, and H. Kronmüller, 2000, "Pinning mechanism of vortices at antiphase boundaries in YBa₂Cu₃O_{7- δ} ," *Phys. Rev. B* **61**, 12 433–12 446.
- Jooss, Ch., R. Warthmann, H. Kronmüller, T. Haage, H.-U. Habermeier, and J. Zegenhagen, 1999, "Vortex pinning due to strong quasiparticle scattering at antiphase boundaries in YBa₂Cu₃O_{7- δ} ," *Phys. Rev. Lett.* **82**, 632–635.
- Jooss, Ch., R. Warthmann, H. Kronmüller, J. Zegenhagen, and H.-U. Habermeier, 2000, "Pinning mechanism of vortices at antiphase boundaries in YBaCuO films," *Physica C* **341-348**, 1419–1422.
- Joose, K., Y. M. Boguslavskij, L. Vargas, G. J. Gerritsma, and H. Rogalla, 1995, "Transistor performance of high- T_c three terminal devices based on carrier concentration modulation," *IEEE Trans. Appl. Supercond.* **5**, 2883–2886.
- Kabius, B., J. W. Seo, T. Amrein, U. Dähne, A. Scholen, M. Siegel, K. Urban, and L. Schulz, 1994, "Grain-boundary structure of thin films of YBa₂Cu₃O₇ and Bi₂Sr₂CaCu₂O₈ on bicrystalline substrates," *Physica C* **231**, 123–130.
- Kaestner, A., M. Volk, F. Ludwig, M. Schilling, and J. Menzel, 2000, "YBa₂Cu₃O₇ Josephson junctions on LaAlO₃ bicrystals for terahertz-frequency applications," *Appl. Phys. Lett.* **77**, 3057–3059.
- Kang, K. Y., I. Song, Y. S. Ha, S. K. Han, G. Y. Sung, I. H. Song, and G. Park, 1999, "Microwave radiation and sensing of Josephson junction with the log-periodic toothed trapezoid antenna of high T_c superconducting films," *IEEE Trans. Appl. Supercond.* **9**, 3074–3076.
- Kaplan, S. B., C. C. Chi, P. Chaudhari, D. Dimos, R. Gross, A. Gupta, and G. Koren, 1991, "Response of YBa₂Cu₃O_{7- δ} grain boundary junctions to short light pulses," *Phys. Rev. B* **43**, 8627–8630.
- Kaplunenko, V. K., G. Fisher, Z. G. Ivanov, N. F. Pedersen, T. Claeson, J. Mygind, and E. Wikborg, 1994, "Microwave testing of high- T_c based direct current to a single flux quantum converter," *J. Appl. Phys.* **76**, 5996–6000.
- Kaplunenko, V. K., Z. G. Ivanov, E. A. Stepantsov, T. Claeson, and E. Wikborg, 1995, "Voltage divider based on sub-micron slits in a high T_c superconducting film and two bicrystal grain boundaries," *Appl. Phys. Lett.* **67**, 282–284.
- Kaplunenko, V. K., E. Stepantsov, H. R. Yi, T. Claeson, H. Toepfer, G. Hildebrand, F. H. Uhlmann, and E. Wikborg, 1997, "Single Flux Quantum Elements Based on a Single Layer of a High- T_c superconductor," *IEEE Trans. Appl. Supercond.* **7**, 3176–3180.
- Kasatkin, A. L., V. M. Pan, and H. C. Freyhardt, 1997, "Vortex transfer mechanism in c -oriented YBCO films with small-angle boundaries," *IEEE Trans. Appl. Supercond.* **7**, 1588–1591.
- Kashiwaya, S., and Y. Tanaka, 2000, "Tunneling effects on surface bound states in unconventional superconductors," *Rep. Prog. Phys.* **63**, 1641–1724.
- Kawano, K., J. S. Abell, A. D. Bradley, W. Lo, and A. Campbell, 2000, "Magnetic field and current distributions at an artificial grain boundary on YBa₂Cu₃O_{7- x} ," *Supercond. Sci. Technol.* **13**, 999–1004.
- Kawasaki, M., P. Chaudhari, and A. Gupta, 1992, "1/ f Noise in YBa₂Cu₃O_{7- δ} superconducting bicrystal grain-boundary junctions," *Phys. Rev. Lett.* **68**, 1065–1068.
- Kawasaki, M., P. Chaudhari, T. H. Newman, and A. Gupta, 1991, "Submicron YBa₂Cu₃O_{7- δ} grain-boundary junction dc SQUIDS," *Appl. Phys. Lett.* **58**, 2555–2557.
- Kawasaki, M., E. Sarnelli, P. Chaudhari, A. Gupta, A. Kussmaul, J. Lacey, and W. Lee, 1993, "Weak link behavior of

- grain boundaries in Nd-, Bi-, and TI-based cuprate superconductors,” *Appl. Phys. Lett.* **62**, 417–419.
- Khare, N., and A. K. Gupta, 1999, “Radio frequency-SQUID effect due to natural grain boundary junctions in $\text{ErNi}_2\text{B}_2\text{C}$ and $\text{DyNi}_2\text{B}_2\text{C}$ magnetic borocarbide superconductors,” *Appl. Phys. Lett.* **75**, 1775–1777.
- Khare, N., A. K. Gupta, S. Khare, L. C. Gupta, R. Nagarajan, Z. Hossain, and R. Vijayaraghavan, 1996, “Radio frequency-SQUID effect in $\text{YNi}_2\text{B}_2\text{C}$ due to natural grain boundary weak links,” *Appl. Phys. Lett.* **69**, 1483–1485.
- Kim, D., P. Berghuis, M. B. Field, D. J. Miller, K. E. Gray, R. Feenstra, and D. K. Christen, 2000, “Evidence for pinning of grain-boundary vortices by Abrikosov vortices in the grains of $\text{YBa}_2\text{Cu}_3\text{O}_{7-x}$,” *Phys. Rev. B* **62**, 12 505–12 508.
- Kim, Y. H., J. H. Kang, G. Y. Sung, J. H. Park, J. M. Lee, K. R. Jung, C. H. Kim, T. S. Hahn, and S. S. Choi, 1999, “Digital and analog measurements of HTS SFQ RS flip-flops and shift register circuits,” *IEEE Trans. Appl. Supercond.* **9**, 3817–3820.
- Kirtley, J. R., P. Chaudhari, M. B. Ketchen, N. Khare, S. Y. Lin, and T. Shaw, 1995, “Distribution of magnetic flux in high grain boundary junctions enclosing hexagonal and triangular areas,” *Phys. Rev. B* **51**, 12 057–12 060.
- Kirtley, J. R., M. B. Ketchen, K. G. Stawiasz, J. Z. Sun, W. J. Gallagher, S. H. Blanton, and S. J. Wind, 1994, “High-resolution scanning SQUID microscope,” *Appl. Phys. Lett.* **66**, 1138–1140.
- Kirtley, J. R., C. C. Tsuei, M. Rupp, J. Z. Sun, L. S. Yu-Jahnes, A. Gupta, M. B. Ketchen, K. A. Moler, and M. Bhushan, 1996, “Direct imaging of integer and half-integer Josephson vortices in high- T_c grain boundaries,” *Phys. Rev. Lett.* **76**, 1336–1339.
- Kirtley, J. R., C. C. Tsuei, J. Z. Sun, C. C. Chi, L. S. Yu-Jahnes, A. Gupta, M. Rupp, and M. B. Ketchen, 1995, “Symmetry of the order parameter in the high- T_c superconductor $\text{YBa}_2\text{Cu}_3\text{O}_{7-\delta}$,” *Nature (London)* **373**, 225–228.
- Kita, S., H. Tanabe, and T. Kobayashi, 1998, “Millimeter-wave detection by GBJJ using high- T_c superconducting YBaCuO films,” *IEEE Trans. Magn.* **TM-25**, 907–910.
- Kleefisch, S., L. Alff, U. Schoop, A. Marx, R. Gross, M. Naito, and H. Sato, 1998, “Superconducting $\text{Nd}_{1.85}\text{Ce}_{0.15}\text{CuO}_{4-y}$ bicrystal grain boundary Josephson junctions,” *Appl. Phys. Lett.* **9**, 2888–2890.
- Klein, J., C. Höfener, S. Uhlenbruck, L. Alff, B. Büchner, and R. Gross, 1999, “On the nature of grain boundaries in colossal magnetoresistance manganites,” *Europhys. Lett.* **47**, 371–377.
- Klushin, A. M., W. Prusseit, E. Sodtke, S. I. Borovitskii, L. E. Amatuni, and H. Kohlstedt, 1996, “Shunted bicrystal Josephson junctions for voltage standards,” *Appl. Phys. Lett.* **69**, 1634–1636.
- Klushin, A. M., C. Weber, M. Darula, H. Kohlstedt, R. Semerad, and W. Prusseit, 1997, in *ISEC '97, Extended Abstracts*, edited by H. Koch and S. Knappe (Physikalische Technische Bundesanstalt, Braunschweig, Germany), pp. 159–161.
- Knauss, L., 2000, “MAGMA-C1: Neocera’s scanning SQUID microscope,” *Superconductor and Cryoelectronics*, issue of summer 2000, 16–22.
- Koblischka, M. R., Th. Schuster, and H. Kronmüller, 1994, “Flux penetration in $\text{YBa}_2\text{Cu}_3\text{O}_{7-\delta}$ granular samples,” *Physica C* **219**, 205–212.
- Koch, R. H., C. P. Umbach, G. J. Clark, P. Chaudhari, and R. B. Laibowitz, 1987, “Quantum interference devices made from superconducting oxide thin films,” *Appl. Phys. Lett.* **51**, 200–202.
- Koch, R. H., C. P. Umbach, M. M. Oprysko, J. D. Mannhart, B. Bumble, G. J. Clark, W. J. Gallagher, A. Gupta, A. Kleinsasser, R. B. Laibowitz, R. B. Sandstrom, and M. R. Scheuermann, 1989, “DC SQUIDS made from $\text{YBa}_2\text{Cu}_3\text{O}_y$,” *Physica C* **153–155**, 1685–1689.
- Koelle, D., R. Kleiner, F. Ludwig, E. Dantsker, and J. Clarke, 1999, “High-transition-temperature superconducting quantum interference devices,” *Rev. Mod. Phys.* **71**, 631–686.
- Koelle, D., R. Kleiner, F. Ludwig, A. H. Miklich, E. Dantsker, and J. Clarke, 1995, “Asymmetric $\text{YBa}_2\text{Cu}_3\text{O}_{7-x}$ dc SQUID: A three terminal device with current gain at 77 K,” *Appl. Phys. Lett.* **66**, 640–642.
- Koelle, D., A. H. Miklich, E. Dantsker, F. Ludwig, D. T. Nemeth, J. Clarke, W. Ruby, and K. Char, 1993a, “High performance dc SQUID magnetometers with single layer $\text{YBa}_2\text{Cu}_3\text{O}_{7-x}$ flux transformers,” *Appl. Phys. Lett.* **63**, 3630–3632.
- Koelle, D., A. H. Miklich, F. Ludwig, E. Dantsker, D. T. Nemeth, and J. Clarke, 1993b, “dc SQUID magnetometers from single layers of $\text{YBa}_2\text{Cu}_3\text{O}_{7-x}$,” *Appl. Phys. Lett.* **63**, 2271–2273.
- Kogan, V. G., 1989, “Clean boundary between anisotropic superconductors as a weak link,” *Phys. Rev. Lett.* **62**, 3001–3003.
- Kogure, T., Y. Zhang, R. Levonmaa, R. Kontra, W. X. Wang, D. A. Rudman, G. J. Yurek, and J. B. Vandersande, 1988, “Grain-boundary structure of $\text{YbBa}_2\text{Cu}_3\text{O}_{7-x}$ formed by oxidation of metallic precursors,” *Physica C* **156**, 707–716.
- Korolev, K. A., P. M. Shadrin, J. S. Preston, R. A. Hughes, J. K. Nam, and V. V. Pavlovskii, 2000, “Local characterization of HTS thin films by laser scanning microscopy,” *Physica C* **341–348**, 1435–1438.
- Koshizuka, N., T. Takagi, J. G. Wen, K. Nakao, T. Usagawa, Y. Eltsev, and T. Machi, 2000, “Critical currents and microstructures of LPE grown YBCO bicrystal films with large single facet grain boundaries,” *Physica C* **337**, 1–6.
- Krause, H. J., Y. Zhang, R. Hohmann, M. Grünekle, M. I. Faley, D. Lomparski, M. Maus, H. Bousack, and A. I. Braginski, 1997, in *Proceedings of the Third European Conference on Applied Superconductivity EUCAS'97* (Veldhoven, Institute of Physics Conference Series No. 158), edited by H. Rogalla and D. H. A. Blank, pp. 775–780.
- Kreutzbruck, M. v., K. Tröll, M. Mück, C. Heiden, and Y. Zhang, 1997, “Experiments on eddy current NDE with HTS rf SQUIDS,” *IEEE Trans. Appl. Supercond.* **7**, 3279–3282.
- Kroeger, D. M., A. Choudhury, J. Brynestad, R. K. Williams, R. A. Padgett, and W. A. Coghlan, 1988, “Grain-boundary compositions in $\text{YBa}_2\text{Cu}_3\text{O}_{7-x}$ from Auger electron spectroscopy of fracture surfaces,” *J. Appl. Phys.* **64**, 331–335.
- Kroeger, D. M., A. Goyal, E. D. Specht, Z. L. Wang, J. E. Tkaczyk, J. A. Sutliff, and J. A. DeLuca, 1994, “Local texture and percolative paths for long-range conduction in high critical current density $\text{TlBa}_2\text{Ca}_2\text{Cu}_3\text{O}_{8+x}$ deposits,” *Appl. Phys. Lett.* **64**, 106–108.
- Kromann, R., J. J. Kingston, A. H. Miklich, L. T. Sagdahl, and J. Clarke, 1993, “Integrated high-transition temperature magnetometer with only two superconducting layers,” *Appl. Phys. Lett.* **63**, 559–561.

- Kumakura, H., H. Kitaguchi, K. Togano, T. Muroga, J. Sato, and M. Okada, 1999, "Influence of Ag substrates on grain alignment and critical current density of Bi-2212 tape conductors," *IEEE Trans. Appl. Supercond.* **9**, 1804–1807.
- Kumar, S., R. Matthews, S. G. Haupt, D. K. Lathrop, M. Takigawa, J. R. Rozen, S. L. Brown, and R. H. Koch, 1997, "Nuclear magnetic resonance using a high temperature superconducting quantum interference device," *Appl. Phys. Lett.* **70**, 1037–1039.
- Kume, E., I. Iguchi, and H. Takahashi, 1999, "On-chip spectroscopic detection of Terahertz radiation emitted from a quasiparticle-injected non equilibrium superconductor using a high- T_c Josephson junction," *Appl. Phys. Lett.* **75**, 2809–2811.
- Kung, H., S. R. Foltyn, P. N. Arendt, and M. P. Maley, 1999, "Characterization of the structure of Y-Ba-Cu-O coated conductors," *IEEE Trans. Appl. Supercond.* **9**, 2034–2037.
- Küpfer, H., I. Apfelstedt, R. Flükiger, C. Keller, R. Meier-Hirmer, B. Runtsch, A. Turowski, U. Wiech, and T. Wolf, 1989, "Intragrain junctions in $\text{YBa}_2\text{Cu}_3\text{O}_{7-\delta}$ ceramics and single crystals," *Cryogenics* **29**, 268–280.
- Kusmaul, A., E. S. Hellman, E. H. Hartford, Jr., and P. M. Tedrow, 1993, "Superconductor-insulator-superconductor tunneling in $\text{Ba}_{1-x}\text{K}_x\text{BiO}_3$ grain boundaries," *Appl. Phys. Lett.* **63**, 2824–2826.
- Kusmaul, A., P. M. Tedrow, and A. Gupta, 1993, "Potential of NdCeCuO thin films for electronic applications," *IEEE Trans. Appl. Supercond.* **3**, 1550–1551.
- Kusunoki, M., Y. Takano, M. Mukaida, and S. Ohshima, 1999, "The influence of in-plane 0–45° grain boundary on microwave surface resistance of c-axis $\text{YBa}_2\text{Cu}_3\text{O}_{7-\delta}$ films on MgO substrates," *Physica C* **321**, 81–85.
- Kwok, W. K., U. Welp, G. W. Crabtree, K. G. Vandervoort, R. Hulscher, and J. Z. Lie, 1990, "Direct observation of dissipative flux motion and pinning by twin boundaries in $\text{YBa}_2\text{Cu}_3\text{O}_{7-\delta}$ single crystals," *Phys. Rev. Lett.* **64**, 966–969.
- Larbalestier, D. C., 2000, presentation at the Topical Workshop on Grain Boundaries and Interfaces in High Temperature Superconductors, Williamsburg (VA, USA), Sept. 2000.
- Larbalestier, D. C., S. E. Babcock, X. Cai, M. Daeumling, D. P. Hampshire, T. F. Kelly, L. A. Lavanier, P. J. Lee, and J. Sentjens, 1988, "Weak links and the poor transport critical currents of the 123 compounds," *Physica C* **153-155**, 1580–1585.
- Larbalestier, D. C., S. E. Babcock, X. Y. Cai, M. B. Field, Y. Gao, N. F. Heinig, D. L. Kaiser, K. Merkle, L. K. Williams, and N. Zhang, 1991, "Electrical transport across grain boundaries in bicrystals of $\text{YBa}_2\text{Cu}_3\text{O}_{7-\delta}$," *Physica C* **185-189**, 315–320.
- Larbalestier, D. C., X. Y. Cai, H. Edelman, M. B. Field, Y. Feng, J. Parrell, A. Pashitski, and A. Polyanskii, 1994, "Visualizing current flow in high- T_c superconductors," *J. Met.* **46**, 20–22.
- Lathrop, D. K., B. H. Moeckly, S. E. Russek, and R. A. Buhrman, 1991, "Transport properties of high-angle grain boundary weak links in $\text{YBa}_2\text{Cu}_3\text{O}_7$ thin films," *Appl. Phys. Lett.* **58**, 1095–1097.
- Laval, J. Y., M. Drouet, W. Swiatnicki, E. Gradys, G. Schiffmacher, I. Monot, and G. Desgardin, 1996, "Low attenuation of the supercurrent by high angle grain boundaries in $\text{YBa}_2\text{Cu}_3\text{O}_{7-x}$ ceramics," *Mater. Sci. Forum* **207-209**, 637–640.
- Lee, K., I. Iguchi, T. Ishibashi, and M. Kawabe, 1996, "Josephson transport and crystallographic properties of $\text{Bi}_2\text{Sr}_2\text{CaCu}_2\text{O}_y$ junctions on (100) MgO bicrystal substrates," *Physica C* **257**, 99–104.
- Lee, S.-G. and Y. Hwang, 2000, "Gap symmetry and critical current of $\text{YBa}_2\text{Cu}_3\text{O}_7$ step edge Josephson junctions," *Appl. Phys. Lett.* **76**, 2755–2757.
- Lee, S.-G., Y. Hwang, J.-T. Kim, and G. Y. Sung, 2000, "Effects of d-wave symmetry in high T_c step-edge Josephson junctions," *Physica C* **341-348**, 1473–1474.
- Lee, S. S., D. G. Hwang, C. M. Park, and J. R. Rhee, 1999, "Magnetoresistance in $\text{La}_{(0.8)}\text{Sr}_{(0.2)}\text{MnO}_{3-\delta}$ biepitaxial grain boundary junction," *IEEE Trans. Magn.* **35**, 2871–2873.
- Lee, T. S., Y. R. Chemla, E. Dantsker, and J. Clarke, 1997, "High- T_c SQUID microscope for room temperature samples," *IEEE Trans. Appl. Supercond.* **7**, 3147–3150.
- Lee, T. S., E. Dantsker, and J. Clarke, 1996, "High-transition temperature SQUID microscope," *Rev. Sci. Instrum.* **67**, 4208–4215.
- Leenders, A., H. C. Freyhardt, M. P. Delamare, B. Bringmann, and H. Walter, 1999, in *Proceedings of the 9th International Workshop on Critical Currents*, edited by D. Larbalestier (University of Madison-Wisconsin, Madison), pp. 53–54.
- Lesueur, J., L. H. Greene, W. L. Feldmann, and A. Inam, 1992, "Zero bias anomalies in $\text{YBa}_2\text{Cu}_3\text{O}_7$ tunnel junctions," *Physica C* **191**, 325–332.
- Lew, D. J., Y. Suzuki, A. F. Marshall, T. H. Geballe, and M. R. Beasley, 1994, "Transport through 90° [010] basal-plane-faced tilt and twist grain boundaries in $\text{YBa}_2\text{Cu}_3\text{O}_{7-\delta}$ thin films," *Appl. Phys. Lett.* **65**, 1584–1586.
- Li, H. Q., R. H. Ono, L. R. Vale, D. A. Rudman, and S. H. Liou, 1997, "High temperature superconducting Josephson junctions in a stacked bicrystal geometry," *Appl. Phys. Lett.* **71**, 1121–1123.
- Li, M. Y., H. L. Kao, W. J. Chang, C. L. Lin, C. C. Chi, W. Y. Guan, and M. K. Wu, 1995, "Control of the inplane epitaxy for bi-epitaxial grain-boundary junctions using a new multilayer structure," *J. Appl. Phys.* **77**, 4584–4588.
- Li, Q., G. N. Riley, R. D. Parrella, S. Fleshler, M. W. Rupich, W. L. Carter, J. O. Willis, J. Y. Coulter, J. F. Bingert, V. K. Sikka, J. A. Parrell, and D. C. Larbalestier, 1997, "Progress in superconducting performance of rolled multifilamentary Bi-2223 HTS composite conductors," *IEEE Trans. Appl. Supercond.* **7**, 2026–2029.
- Li, Q., Y. N. Tsay, M. Suenaga, G. Wirth, G. D. Gu, and N. Koshizuka, 1999a, "Superconducting transport properties of 2.2-GeV Au-ion irradiated c-axis twist $\text{Bi}_2\text{Sr}_2\text{CaCu}_2\text{O}_{8+\delta}$ bicrystals," *Appl. Phys. Lett.* **74**, 1323–1325.
- Li, Q., Y. N. Tsay, M. Suenaga, R. A. Klemm, G. D. Gu, and N. Koshizuka, 1999b, " $\text{Bi}_2\text{Sr}_2\text{CaCu}_2\text{O}_{8+\delta}$ bicrystal c-axis twist Josephson junctions: a new phase sensitive test of order parameter symmetry," *Phys. Rev. Lett.* **83**, 4160–4163.
- Li, Q., Y. N. Tsay, Y. M. Zhu, and M. Suenaga, 1999c, "Electromagnetic and microstructural properties of grain boundaries in bulk $\text{Bi}_2\text{Sr}_2\text{CaCu}_2\text{O}_{8+\delta}$ bicrystals," 1999, in *International Workshop on Critical Currents*, July 7–12, University of Madison-Wisconsin (publisher, city), pp. 6–7.
- Likharev, K. K., and V. K. Semenov, 1991, "RSFQ logic/memory family: a new Josephson-junction technology for sub-terahertz-clock-frequency digital systems," *IEEE Trans. Appl. Supercond.* **1**, 3–28.

- Lin, C. L., W. J. Chang, M. Y. Li, C. H. Li, C. C. Chi, and M. K. Wu, 1996, "Josephson coupling behavior of $\text{YBa}_2\text{Cu}_3\text{O}_{7-x}$ bicrystal grain-boundary junctions," *Physica C* **269**, 291–296.
- Liu, H. K., R. K. Wang, and S. X. Dou, 1994, "TEM study of microstructure of longitudinal cross-section of Ag-clad Bi-based (2223) tapes," *Physica C* **229**, 39–46.
- Löfwander, T., G. Johansson, M. Hurd, and G. Wendin, 1998, "Superconducting d-wave junctions: the disappearance of the odd ac-components," *Phys. Rev. B* **57**, 3225–3228.
- Löfwander, T., V. S. Shumeiko, and G. Wendin, 1998, "Time-reversal symmetry breaking at Josephson tunnel junction of purely d-wave superconductors," *Phys. Rev. B* **62**, 14 653–14 656.
- Löfwander, T., V. S. Shumeiko, and G. Wendin, 2001, "Andreev bound states in high- T_c superconducting junctions," *Supercond. Sci. Technol.* **14**, R53–R77.
- Lombardi, F., Z. G. Ivanov, P. Komissinski, G. M. Fischer, P. Larsson, and T. Claeson, 1998, "The influence of the top and the bottom grain boundaries on the current transport in $\text{YBa}_2\text{Cu}_3\text{O}_{7-\delta}$ step-edge Josephson junctions," *Appl. Supercond.* **6**, 437–443.
- Lombardi, F., U. Scotti di Uccio, Z. Ivanov, T. Claeson, and M. Cirillo, 2000, "Flux flow in $\text{YBa}_2\text{Cu}_3\text{O}_{7-\delta}$ grain boundary Josephson junctions with a four-terminal configuration," *Appl. Phys. Lett.* **76**, 2591–2593.
- Ludwig, F., E. Dantsker, R. Kleiner, D. Koelle, J. Clarke, S. Knappe, D. Drung, H. Koch, N. McN. Alford, and T. W. Button, 1995, "Integrated high- T_c multiloop magnetometer," *Appl. Phys. Lett.* **66**, 1418–1420.
- Luine, J., J. Bulman, J. Burch, K. Daly, A. Lee, C. Pettiette-Hall, S. Schwarzbek, and D. Miller, 1992, "Characteristics of high performance $\text{YBa}_2\text{Cu}_3\text{O}_7$ step-edge junctions," *Appl. Phys. Lett.* **61**, 1128–1130.
- Luine, J. A., and V. Z. Kresin, 1998, "Critical current in high T_c grain boundary junctions," *J. Appl. Phys.* **84**, 3972–3979.
- Luine, J. A., and V. Z. Kresin, 2001, "High T_c superconductivity grain boundary junctions," preprint.
- Ma, Y., K. Watanabe, S. Awaji, and M. Motokawa, 2000, " J_c enhancement of $\text{YBa}_2\text{Cu}_3\text{O}_7$ films on polycrystalline silver substrates by metalorganic vapor deposition in high magnetic fields," *Appl. Phys. Lett.* **77**, 3633–3635.
- Macfarlane, J. C., L. Hao, C. M. Pegrum, and G. B. Donaldson, 1995, "Excess low frequency noise in YBCO grain boundary Josephson junctions," *IEEE Trans. Appl. Supercond.* **5**, 2212–2215.
- Macfarlane, J. C., E. J. Romans, D. A. Peden, C. M. Pegrum, and L. Hao, 1997, in *ISEC '97, Extended Abstracts*, edited by H. Koch and S. Knappe (Physikalische Technische Bundesanstalt, Braunschweig, Germany), pp. 10–12.
- Maggio-Aprile, I., C. Renner, A. Erb, E. Walker, and Ø. Fischer, 1997, "Critical currents approaching the depairing limit at a twin boundary in $\text{YBa}_2\text{Cu}_3\text{O}_{7-\delta}$," *Nature (London)* **390**, 487–490.
- Malozemoff, A. P., G. N. Riley, Jr., S. Fleshler, and Q. Li, 1997, "Supercurrent conduction mechanisms in BSCCO 2223 tapes," talk presented at SPA '97 Conference, Xi'an, China, March 1997, unpublished.
- Mannhart, J., 1990, in *Earlier and Recent Aspects of Superconductivity*, edited by J. G. Bednorz and K. A. Müller (Springer-Verlag, Heidelberg), pp. 208–221.
- Mannhart, J., 1996, "High- T_c transistors," *Supercond. Sci. Technol.* **9**, 49–67.
- Mannhart, J., H. Bielefeldt, B. Goetz, H. Hilgenkamp, A. Schmehl, C. W. Schneider, and R. R. Schulz, 2000a, "Doping induced enhancement of the critical currents of grain boundaries in high- T_c superconductors," *Physica C* **341–348**, 1393–1396.
- Mannhart, J., H. Bielefeldt, B. Goetz, H. Hilgenkamp, A. Schmehl, C. W. Schneider, and R. R. Schulz, 2000b, "Grain boundaries in high- T_c superconductors: insights and improvements," *Philos. Mag. B* **80**, 827–834.
- Mannhart, J., and P. Chaudhari, 2001, "The Interplay of Physics, Materials Science, and Applications: The High- T_c Bicrystals," *Phys. Today* **54** (11), 48–53.
- Mannhart, J., P. Chaudhari, D. Dimos, C. C. Tsuei, and T. R. McGuire, 1988, "Critical currents in [001] grains and across their tilt boundaries in $\text{YBa}_2\text{Cu}_3\text{O}_7$ films," *Phys. Rev. Lett.* **61**, 2476–2479.
- Mannhart, J., R. Gross, K. Hipler, R. P. Huebener, C. C. Tsuei, D. Dimos, and P. Chaudhari, 1989, "Spatially resolved observation of supercurrents across grain boundaries in YBaCuO films," *Science* **245**, 839–841.
- Mannhart, J., R. Gross, R. P. Huebener, P. Chaudhari, D. Dimos, and C. C. Tsuei, 1990, "Spatially resolved observation of charge transfer across single grain boundaries in YBaCuO films," *Cryogenics* **30**, 397–400.
- Mannhart, J., and H. Hilgenkamp, 1997, "Wavefunction symmetry and its influence on superconducting devices," *Supercond. Sci. Technol.* **10**, 880–883.
- Mannhart, J., and H. Hilgenkamp, 1998, "Possible influence of band bending on the normal state properties of grain boundaries in high- T_c superconductors," *Mater. Sci. Eng., B* **56**, 77–85.
- Mannhart, J., and H. Hilgenkamp, 1999, "Interfaces involving complex superconductors," *Physica C* **317–318**, 383–391.
- Mannhart, J., and H. Hilgenkamp, 2002, in the *Encyclopedia of Materials: Science and Technology*, edited by K. H. J. Buschow, R. W. Cahn, M. C. Flemmings, B. Ilschner, E. J. Kramer, and S. Mahajan (Elsevier Science Ltd.).
- Mannhart, J., H. Hilgenkamp, B. Mayer, Ch. Gerber, J. R. Kirtley, K. A. Moler, and M. Sigrist, 1996, "Generation of magnetic flux by single grain boundaries of $\text{YBa}_2\text{Cu}_3\text{O}_{7-x}$," *Phys. Rev. Lett.* **77**, 2782–2785.
- Mannhart, J., R. P. Huebener, F. Kober, D. Koelle, P. Chaudhari, D. Dimos, R. Gross, A. Gupta, G. Koren, and C. C. Tsuei, 1990, "Current transport across grain boundary networks in high- T_c superconductors," *Physica A* **168**, 345–352.
- Mannhart, J., B. Mayer, and H. Hilgenkamp, 1996, "Anomalous dependence of the critical current of 45° grain boundaries in $\text{YBa}_2\text{Cu}_3\text{O}_{7-x}$ on an applied magnetic field," *Z. Phys. B: Condens. Matter* **101**, 175–179.
- Mannhart, J., and C. C. Tsuei, 1989, "Limits of the critical current density of polycrystalline high-temperature superconductors based on the transport properties of single grain boundaries," *Z. Phys. B: Condens. Matter* **77**, 53–59.
- Marshall, A. F., and C. Eom, 1993, "Microfaceting of 90° [001] tilt boundaries in $\text{YBa}_2\text{Cu}_3\text{O}_{7-x}$ thin films," *Physica C* **207**, 239–246.
- Martens, J. S., V. M. Hietala, T. E. Zipperian, G. A. Vawter, D. S. Ginley, C. P. Tigges, and T. A. Plut, 1992a, "Fabrication of TiCaBaCuO step-edge Josephson junctions with hysteretic behavior," *Appl. Phys. Lett.* **60**, 1013–1015.
- Martens, J. S., T. E. Zipperian, G. A. Vawter, D. S. Ginley, V. M. Hietala, and C. P. Tigges, 1992b, " Ti-Ca-Ba-Cu-O step-edge Josephson junctions," *Appl. Phys. Lett.* **60**, 1141–1143.

- Marx, A., L. Alff, and R. Gross, 1997, "Low frequency noise in high temperature superconductor Josephson junctions," *IEEE Trans. Appl. Supercond.* **7**, 2719–2722.
- Marx, A., U. Fath, L. Alff, and R. Gross, 1995a, "Correlation of critical current and resistance fluctuations in bicrystal grain boundary Josephson junctions," *Appl. Phys. Lett.* **67**, 1929–1931.
- Marx, A., U. Fath, W. Ludwig, R. Gross, and T. Amrein, 1995b, " $1/f$ noise in $\text{Bi}_2\text{Sr}_2\text{CaCu}_2\text{O}_{8+x}$ bicrystal grain-boundary Josephson junctions," *Phys. Rev. B* **51**, 6735–6738.
- Marx, A., and R. Gross, 1997, "Scaling behavior of $1/f$ noise in high-temperature superconductor Josephson junctions," *Appl. Phys. Lett.* **70**, 120–122.
- Mashtakov, A. D., K. I. Konstantinyan, G. A. Ovsyannikov, and E. A. Stepantsov, 1999, "YBa₂Cu₃O_x Josephson junctions on a bicrystal sapphire substrate for devices in the millimeter and submillimeter wavelength ranges," *Tech. Phys. Lett.* **25**, 249–252.
- Mathai, A., D. Song, Y. Gim, and F. C. Wellstood, 1992, "One-dimensional magnetic-flux microscope based on the dc superconducting quantum interference device," *Appl. Phys. Lett.* **61**, 598–600.
- Mathai, A., D. Song, Y. Gim, and F. C. Wellstood, 1993, "High resolution magnetic microscopy using a dc SQUID," *IEEE Trans. Appl. Supercond.* **3**, 2609–2612.
- Mathur, N. D., G. Burnell, S. P. Isaac, T. J. Jackson, B. S. Teo, J. L. MacManus-Driscoll, L. F. Cohen, J. E. Evetts, and M. G. Blamire, 1997, "Large low-field magnetoresistance in $\text{La}_{0.7}\text{Ca}_{0.3}\text{MnO}_3$ induced by artificial grain boundaries," *Nature (London)* **387**, 266–268.
- Matsuda, M., S. Ono, K. Kato, K. Yokosowa, H. Oyama, and S. Kuriki, 1999, "High- T_c SQUIDs on bicrystal substrate with low permittivity," preprint.
- Matsui, T., and H. Ohta, 1993, "The AC Josephson effect and submillimeter wave mixing with a weak link array of grain boundaries formed in YBCO film," *IEEE Trans. Appl. Supercond.* **3**, 2421–2425.
- Mayer, B., L. Alff, T. Träuble, R. Gross, P. Wagner, and H. Adrian, 1993, "Superconducting transport properties of $\text{Bi}_2\text{Sr}_2\text{CaCu}_2\text{O}_{8+x}$ bicrystal grain boundary junctions," *Appl. Phys. Lett.* **63**, 996–998.
- Mayer, B., J. Mannhart, and H. Hilgenkamp, 1996, "Electric field controllable Josephson junctions of high quality in high- T_c superconductors," *Appl. Phys. Lett.* **68**, 3031–3033.
- Mayer, B., H. Schulze, G. M. Fischer, and R. Gross, 1995, "Nonlocal response of grain-boundary-type Josephson junctions to local perturbation," *Phys. Rev. B* **52**, 7727–7741.
- McBrien, P. F., R. H. Hadfield, W. E. Booij, A. Moya, M. G. Blamire, E. J. Tarte, J. Clark, and C. M. Pegrum, 1999, "Josephson junctions with hysteretic current voltage characteristic at high temperatures," *IEEE Trans. Appl. Supercond.* **9**, 3468–3471.
- McBrien, P. F., R. H. Hadfield, W. E. Booij, A. Moya, F. Kahlmann, W. E. Booij, M. G. Blamire, C. M. Pegrum, and E. J. Tarte, 2000, "The capacitance of grain boundaries in superconductor films with strontium titanate and other substrates," *Physica C* **339**, 88–92.
- McDaniel, E. B., S. C. Gausephol, C. T. Li, M. Lee, J. W. P. Hsu, R. A. Rao, and C. B. Eom, 1997, "Influence of SrTiO₃ bicrystal microstructural defects on YBa₂Cu₃O₇ grain boundary Josephson junctions," *Appl. Phys. Lett.* **70**, 1882–1884.
- Médici, M. G., J. Elly, A. Gilabert, O. Legrand, F. Schmidl, T. Schmauder, E. Heinz, and P. Seidel, 1995, in *Proceedings of the EUCAS 1995*, edited by D. Dew-Hughes, IOP Conf. Proc. No. 148 (IOP, Bristol), pp. 1331–1334.
- Médici, M. G., A. Gilabert, F. Schmidl, and P. Seidel, 2000, "Photodoping of 60 K and 90 K YBaCuO grain boundary Josephson junctions," *Physica C* **341-348**, 1461–1462.
- Meilikhov, E. Z., 1994, "Intergrain boundary asymmetry and the critical current of HTSC ceramics," *Physica C* **226**, 69–75.
- Meilikhov, E. Z., 1996, "Modified dislocation model of intergrain tilt boundaries in HTSC," *Physica C* **271**, 277–285.
- Merkle, K. L., Y. Gao, and B. C. Vuchic, in *Characterization of High- T_c Materials and Devices by Electron Microscopy*, edited by N. D. Browning and S. J. Pennycook (Cambridge University Press, Cambridge), pp. 235–262.
- Miklich, A. H., J. Clarke, M. S. Colclough, and K. Char, 1992, "Flicker ($1/f$) noise in biepitaxial grain boundary junctions of YBa₂Cu₃O_{7-x}," *Appl. Phys. Lett.* **60**, 1899–1901.
- Miklich, A. H., D. Koelle, F. Ludwig, D. T. Nemeth, E. Dantsker, and J. Clarke, 1995, "Picovoltmeter based on a high transition temperature SQUID," *Appl. Phys. Lett.* **66**, 230–232.
- Miller, D. J., T. A. Roberts, J. H. Kang, J. Talvacchio, D. B. Buchholz, and R. P. H. Chang, 1995, "Meandering grain boundaries in YBa₂Cu₃O_y bi-crystal thin films," *Appl. Phys. Lett.* **66**, 2561–2563.
- Miller, J. H., Q. Y. Ying, Z. G. Zou, N. Q. Fan, J. H. Xu, M. F. Davis, and J. C. Wolfe, 1995, "Use of tricrystal junctions to probe the pairing state symmetry of YBa₂Cu₃O_{7- δ} ," *Phys. Rev. Lett.* **74**, 2347–2350.
- Millis, A. J., 1994, "Josephson coupling between a disk of one superconductor and a surrounding superconducting film of different symmetry," *Phys. Rev. B* **49**, 15 408–15 411.
- Minotani, T., S. Kawakami, T. Kiss, Y. Kuroki, and K. Enpuhu, 1997, "High performance DC superconducting quantum interference device utilizing a bicrystal junction with a 30 degrees misorientation angle," *Jpn. J. Appl. Phys., Part 2* **36**, L1092–L1095.
- Mints, R. G., 1998, "Self-generated flux in Josephson junctions with alternating critical current density," *Phys. Rev. B* **57**, 3221–3224.
- Mints, R. G., and V. G. Kogan, 1997, "Josephson junctions with alternating critical current density," *Phys. Rev. B* **55**, 8682–8684.
- Mints, R. G., and I. Papiashvili, 2000, "Self-generated magnetic flux in YBa₂Cu₃O_{7-x} grain boundaries," *Phys. Rev. B* **62**, 15 214–15 220.
- Mints, R. G., and I. Papiashvili, 2001, "Josephson vortices with fractional quanta at YBa₂Cu₃O_{7-x} grain boundaries," *Phys. Rev. B* **64**, 134501.
- Moeckly, B. H., and R. A. Buhrman, 1994, "Josephson properties of basal-plane-faced tilt boundaries in YBa₂Cu₃O_{7- δ} thin films," *Appl. Phys. Lett.* **65**, 3126–3128.
- Moeckly, B. H., and R. H. Buhrman, 1995, "Electromagnetic properties of YBa₂Cu₃O_{7- δ} thin-film grain-boundary weak links," *IEEE Trans. Appl. Supercond.* **5**, 3414–3417.
- Moeckly, B. H., D. K. Lathrop, and R. A. Buhrman, 1993, "Electromigration study of oxygen disorder and grain-boundary effects in YBa₂Cu₃O_{7- δ} thin films," *Phys. Rev. B* **47**, 400–417.
- Moore, D. F., 1989, in *Proceedings of the 2nd Workshop on High Temperature Superconducting Electron Devices*, Shik-

- abe, Japan, 1989 (Research and Development Association for Future Electron Devices, Whistler, B.C.), p. 281.
- Mück, M., C. Heiden, and J. Clarke, 1994, "Investigation and reduction of excess low-frequency noise in rf superconducting quantum interference devices," *J. Appl. Phys.* **75**, 4588–4592.
- Mück, M., M. v. Kreutzbruck, U. Baby, J. Tröll, and C. Heiden, 1997, "Eddy current nondestructive material evaluation based on HTS SQUID," *Physica C* **282-287**, 407–410.
- Müller, K. A., M. Takashige, and J. G. Bednorz, 1987, "Flux trapping and superconductive glass state in $\text{La}_2\text{CuO}_{4-y}:\text{Ba}$," *Phys. Rev. Lett.* **58**, 1143–1146.
- Murakami, M., 1999, in *Proceedings of the Fourth European Conference on Applied Superconductivity EUCAS'99*, Sitges, Institute of Physics Conference Series No. 167, edited by X. Obrados, F. Sandiumenge, and J. Fontcuberta (IOP, Bristol), pp. 7–10.
- Muroga, T., J. Sato, H. Kitaguchi, H. Kumakura, K. Togano, and M. Okada, 1998, "Enhancement of critical current density for Bi-2212/Ag tape conductors through microstructure control," *Physica C* **309**, 236–244.
- Nabatame, T., S. Koike, O. B. Hyun, I. Hirabayashi, H. Sahara, and K. Nakamura, 1994, "Transport superconducting properties of grain boundaries in $\text{Tl}_1\text{Ba}_2\text{Ca}_2\text{Cu}_3\text{O}_x$ thin films," *Appl. Phys. Lett.* **65**, 776–778.
- Nagaishi, T., H. Kugai, H. Toyoda, and H. Itozaki, 1997, "NDT of high speed fine particles by high T_c SQUID," *IEEE Trans. Appl. Supercond.* **7**, 2886–2889.
- Nakahara, S., G. J. Fisanick, M. F. Yan, R. B. van Dover, and T. Boone, 1988, "Correlation of grain boundary defect structure with boundary misorientation in $\text{Ba}_2\text{YCu}_3\text{O}_{7-x}$," *Appl. Phys. Lett.* **53**, 2105–2107.
- Nakahara, S., G. J. Fisanick, M. F. Yan, R. B. Van Dover, T. Boone, and R. Moore, 1987, "On the defect structure of grain boundaries in $\text{Ba}_2\text{YCu}_3\text{O}_{7-x}$," *J. Cryst. Growth* **85**, 639–651.
- Nakajima, K., J. Chen, H. Myoren, T. Yamashita, and P. Wu, 1997, "Terahertz response for bicrystal YBCO Josephson junctions," *IEEE Trans. Appl. Supercond.* **7**, 2607–2610.
- Nakajima, K., K. Yokota, J. Chen, H. Myoren, and T. Yamashita, 1994, "Electric field effects on $\text{YBa}_2\text{Cu}_3\text{O}_{7-\delta}$ grain boundary Josephson junctions," *Jpn. J. Appl. Phys., Part 2* **33**, L934–L937.
- Nakajima, K., K. Yokota, H. Myoren, J. Chen, and T. Yamashita, 1993, "Electric field effect on the artificial grain boundary of bicrystal $\text{YBa}_2\text{Cu}_3\text{O}_{7-\delta}$ films," *Appl. Phys. Lett.* **63**, 684–686.
- Nakamura, N., G. D. Gu, K. Takamuku, M. Muarkami, and N. Koshizuka, 1992, "Magneto-optical observation of flux pinning at the grain boundary in a $\text{Bi}_2\text{Sr}_2\text{CaCu}_2\text{O}_x$ superconductor," *Appl. Phys. Lett.* **61**, 3044–3046.
- Navacerrada, M. A., M. L. Lucía, and F. Sánchez-Quesada, 2000, "Electromagnetic properties and He^+ irradiation effects on $\text{YBa}_2\text{Cu}_3\text{O}_{7-x}$ grain-boundary Josephson junctions," *Phys. Rev. B* **61**, 6422–6427.
- Navacerrada, M. A., M. L. Lucía, and F. Sánchez-Quesada, 2001, "A comparative analysis of $\text{YBa}_2\text{Cu}_3\text{O}_{7-x}$ grain boundary junctions modified by oxygen annealings and He^+ irradiation," *Europhys. Lett.* **54**, 387–393.
- Neils, W. K., and D. J. Van Harlingen, 2002, "Experimental test for subdominant phases with complex order parameters in cuprate grain boundary junctions," *Phys. Rev. Lett.* **88**, 047001.
- Neocera Inc., 1000 Virginia Manor Road, Beltsville, MD, USA 20705.
- Nesher, O., and E. N. Ribak, 1997, "Retrieval of critical current distribution in small Josephson junctions," *Appl. Phys. Lett.* **71**, 1249–1251.
- Nguyen, T., G. A. Daniels, J. B. Beyer, and J. E. Nordman, 1999, "A discrete HTS Josephson flux-flow structure with gain at 77 K," *IEEE Trans. Appl. Supercond.* **9**, 3945–3948.
- Nichols, C. S., and D. R. Clarke, 1991, "Critical currents in inhomogeneous triangular Josephson arrays: a model for polycrystalline superconductors," *Acta Metall. Mater.* **39**, 995–1002.
- Nicoletti, S., and J. C. Villegier, 1997a, "Electrical behavior of $\text{YBa}_2\text{Cu}_3\text{O}_{7-x}$ grain boundary junctions under low magnetic field," *J. Appl. Phys.* **82**, 303–308.
- Nicoletti, S., and J. C. Villegier, 1997b, "Artificially generated bi-epitaxial YBCO grain boundary junctions on SrTiO_3 and sapphire substrates," *IEEE Trans. Appl. Supercond.* **7**, 1399–1402.
- Nikolic, B. K., J. K. Freericks, and P. Miller, 2001, "Equilibrium properties of double-screened-dipole barrier SINIS Josephson junctions," *Phys. Rev. B* **65**, 064529.
- Nilsson-Mellbin, M., and K. Salama, 1994a, " I - V characteristics of melt-textured $\text{YBa}_2\text{Cu}_3\text{O}_{7-x}$ superconductors containing grain boundaries," *Physica C* **223**, 19–29.
- Nilsson-Mellbin, M., and K. Salama, 1994b, "Effect of applied magnetic field on the I - V characteristics of melt-textured $\text{YBa}_2\text{Cu}_3\text{O}_{7-x}$ superconductors containing grain boundaries," *Physica C* **227**, 40–48.
- Norton, D. P., A. Goyal, J. D. Budai, D. K. Christen, D. M. Kroeger, E. D. Specht, Q. He, B. Saffian, M. Paranthaman, C. E. Klabunde, D. F. Lee, B. C. Sales, and F. A. List, 1996, "Epitaxial $\text{YBa}_2\text{Cu}_3\text{O}_7$ on biaxially textured nickel (001): an approach to superconducting tapes with high critical current density," *Science* **274**, 755–757.
- Nücker, N., J. Fink, J. C. Fuggle, P. J. Durham, and W. M. Temmerman, 1988, "Evidence for holes on oxygen sites in the high- T_c superconductors $\text{La}_{2-x}\text{Sr}_x\text{CuO}_4$ and $\text{YBa}_2\text{Cu}_3\text{O}_{7-y}$," *Phys. Rev. B* **37**, 5158–5163.
- Nücker, N., H. Romberg, X. X. Xi, J. Fink, B. Gegenheimer, and Z. X. Zhao, 1989, "Symmetry of holes in high- T_c superconductors," *Phys. Rev. B* **39**, 6619–6629.
- Obara, H., A. Sawa, H. Yamasaki, and S. Kosaka, 2001, "Microwave surface resistance of $\text{YBa}_2\text{Cu}_3\text{O}_y$ films covered by overdoped $\text{Y}_{1-x}\text{Ca}_x\text{Ba}_2\text{Cu}_3\text{O}_y$ layers," *Appl. Phys. Lett.* **78**, 646–648.
- Odagawa, A., and Y. Enomoto, 1995, "Characteristics of bicrystal-type Josephson junctions of $\text{YBa}_2(\text{Cu}_{1-x}\text{Ni}_x)_3\text{O}_{7-\delta}$ films," *Physica C* **755-757**, 141–146.
- Oelze, B., B. Ruck, M. Roth, R. Dömel, M. Siegel, A. Y. Kidiyarova-Shevchenko, T. V. Filippov, M. Y. Kupriyanov, G. Hildebrandt, H. Töpfer, F. H. Ihlmann, and W. Prusseit, 1996, "Rapid single-flux-quantum balanced comparator based on high- T_c bicrystal Josephson junctions," *Appl. Phys. Lett.* **68**, 2732–2734.
- Ohbayashi, K., H. Fujii, A. Kuzuhara, T. Ohtsuki, M. Inoue, A. Fujimaki, and H. Hayakawa, 1995, "Fabrication of $\text{Bi}_2\text{Sr}_2\text{Ca}_2\text{Cu}_3\text{O}_x$ thin film grain boundary junctions," *IEEE Trans. Appl. Supercond.* **5**, 2816–2819.
- Olsson, H. K., P.-Å. Nilsson, Z. Ivanov, R. H. Koch, E. A. Stepanov, and A. Ya. Tzalenchuk, 1992, "Low 1/f noise in $\text{YBa}_2\text{Cu}_3\text{O}_7$ dc SQUIDS on (Y)ZrO₂ bicrystal substrates," *Appl. Phys. Lett.* **61**, 861–863.

- Östlund, S., 1998, "Landau Ginzburg theory of the d -wave Josephson junction," *Phys. Rev. B* **58**, 14 757–14 758.
- Ovsyannikov, G. A., I. V. Borisenko, A. D. Mashtakov, and K. Y. Constantinian, in *Proceedings of the 4th European Conference on Applied Superconductivity EUCAS '99*, Sitges, Institute of Physics Conference Series No. 167, edited by X. Obrades, F. Sandiumenge, and J. Fontcuberta (IOF, Bristol, England), pp. 253–256.
- Parikh, A. S., B. Meyer, and K. Salama, 1994, "A method to improve grain boundary current-carrying capability in melt-textured $\text{YBa}_2\text{Cu}_3\text{O}_{7-\delta}$," *Supercond. Sci. Technol.* **7**, 455–461.
- Park, C., D. P. Norton, J. D. Budai, D. K. Christen, D. Verebeyli, R. Feenstra, D. F. Lee, A. Goyal, D. M. Kroeger, and M. Paranthaman, 1998, "Bend strain tolerance of critical currents for $\text{YBa}_2\text{Cu}_3\text{O}_{7-\delta}$ deposited on rolled-textured [001] Ni," *Appl. Phys. Lett.* **73**, 1904–1906.
- Petersen, K., C. Stolz, M. Schmitt, C. Krimmer, W. Wilkens, J. Sollner, H. W. Grueninger, and H. Adrian, 1995, "Fabrication of biepitaxial YBCO Josephson junctions on different substrates," *IEEE Trans. Appl. Supercond.* **5**, 2180–2183.
- Petersen, K., I. Takeuchi, V. Talyansky, C. Doughty, X. X. Xi, and T. Venkatesan, 1995, "Electric field effect on ultrathin $\text{YBa}_2\text{Cu}_3\text{O}_{7-\delta}$ grain boundary Josephson junctions," *Appl. Phys. Lett.* **67**, 1477–1479.
- Peterson, R. L., and J. W. Ekin, 1988, "Josephson-junction model of critical current in granular $\text{Y}_1\text{Ba}_2\text{Cu}_3\text{O}_{7-\delta}$ superconductors," *Phys. Rev. B* **37**, 9848–9851.
- Pinto, R., N. Goyal, S. P. Pai, P. R. Apte, L. C. Gupta, and R. Vijayaraghavan, 1993, "Improved microwave performance of Ag-doped $\text{Y}_1\text{Ba}_2\text{Cu}_3\text{O}_{7-\delta}$ thin film microstrip resonators," *J. Appl. Phys.* **73**, 5105–5108.
- Polyanskii, A. A., A. Gurevich, A. E. Pashitski, N. F. Heinig, R. D. Redwing, J. E. Nordman, and D. C. Larbalestier, 1996, "Magneto-optical study of flux penetration and critical current densities in [001] tilt $\text{YBa}_2\text{Cu}_3\text{O}_{7-\delta}$ thin-film bicrystals," *Phys. Rev. B* **53**, 8687–8697.
- Poppe, U., Y. Y. Divin, M. I. Faley, J. S. Wu, C. L. Jia, P. Shadrin, and K. Urban, 2001, "Properties of $\text{YBa}_2\text{Cu}_3\text{O}_7$ thin films deposited on substrates and bicrystals with vicinal offset and realization of high $I_c R_n$ junctions," *IEEE Trans. Appl. Supercond.* **11**, 3768–3771.
- Quincey, P. G., 1993, "High T_c Josephson junctions combining a grain boundary and local strain using NdGaO_3 bicrystal substrates," *Appl. Phys. Lett.* **64**, 517–519.
- Ramos, J., Z. G. Ivanov, E. Olsson, S. Zarembinski, and T. Claeson, 1993, " $\text{YBa}_2\text{Cu}_3\text{O}_{7-\delta}$ Josephson junctions on directionally ion beam etched MgO substrates," *Appl. Phys. Lett.* **63**, 2141–2143.
- Ravi, T. S., D. M. Hwang, R. Ramesh, S. W. Chan, L. Nazar, C. Y. Chen, A. Inam, and T. Venkatesan, 1990, "Grain boundaries and interfaces in Y-Ba-Cu-O films laser deposited on single-crystal MgO ," *Phys. Rev. B* **42**, 10 141–10 151.
- Ravikumar, V., R. P. Rodrigues, and V. P. Dravid, 1995, "Direct imaging of spatially varying potential and charge across internal interfaces in solids," *Phys. Rev. Lett.* **75**, 4063–4066.
- Read, W. T., and W. Shockley, 1950, "Dislocation models of crystal grain boundaries," *Phys. Rev.* **78**, 275–289.
- Reade, R. P., P. Berdahl, R. E. Russo, and S. M. Garrison, 1992, "Laser deposition of biaxially textured yttria-stabilized zirconia buffer layers on polycrystalline metallic alloys for high critical current Y-Ba-Cu-O thin films," *Appl. Phys. Lett.* **61**, 2231–2233.
- Redwing, R. D., B. M. Hinaus, M. S. Rzchowski, N. F. Heinig, B. A. Davidson, and J. E. Nordman, 1999, "Observation of strong to Josephson-coupled crossover in 10° $\text{YBa}_2\text{Cu}_3\text{O}_x$ bicrystal junctions," *Appl. Phys. Lett.* **75**, 3171–3173.
- Reuter, W., M. Siegel, K. Herrmann, J. Schubert, W. Zander, and A. I. Braginski, 1993, "Fabrication and characterization of $\text{YBa}_2\text{Cu}_3\text{O}_7$ step-edge junction arrays," *Appl. Phys. Lett.* **62**, 2280–2282.
- Rhyner, J., and G. Blatter, 1989, "Limiting-path model of the critical current in textured $\text{YBa}_2\text{Cu}_3\text{O}_{7-\delta}$ film," *Phys. Rev. B* **40**, 829–832.
- Rijpma, A. P., H. J. M. ter Brake, J. Borgmann, H. J. G. Krooshoop, and H. Rogalla, 1999, in *Proceedings of the Fourth European Conference on Applied Superconductivity EUCAS'99*, Sitges, Institute of Physics Conference Series No. 167, edited by X. Obrados, F. Sandiumenge, and J. Fontcuberta (IOP, Bristol, England), pp. 561–564.
- Romans, E. J., A. Eulenburg, C. Carr, A. J. Millar, G. B. Donaldson, and C. M. Pegrum, 2001, " $\text{NdBa}_2\text{Cu}_3\text{O}_{7-\delta}$ bicrystal Josephson junctions and SQUIDS operating at 77 K," *IEEE Trans. Appl. Supercond.* **11**, 1347–1350.
- Rosenthal, P. A., M. R. Beasley, K. Char, M. S. Colclough, and G. Zaharchuk, 1991, "Flux focusing effects in planar thin-film grain-boundary Josephson junctions," *Appl. Phys. Lett.* **59**, 3482–3484; **60**, 1519(E) (1992).
- Roshchin, I., V. Stepankin, and A. Kuznetsov, 1995, "Reentrant superconducting transport behavior of single grain boundary Josephson junction in $\text{BaPb}_{1-x}\text{Bi}_x\text{O}_3$ bicrystals," *J. Low Temp. Phys.* **100**, 229–240.
- Rosner, S. J., K. Char, and G. Zaharchuk, 1992, "Microstructure of biepitaxial grain boundary junctions in $\text{YBa}_2\text{Cu}_3\text{O}_7$," *Appl. Phys. Lett.* **60**, 1010–1012.
- Ruggiero, S. T., A. Cardona, and H. R. Fetterman, 1991, "Mixing in TlCaBaCuO superconducting films at 61 GHz," *IEEE Trans. Magn.* **TM-27**, 3070–3072.
- Russek, S. E., D. K. Lathrop, B. H. Moeckly, R. A. Buhman, D. H. Shin, and J. Silcox, 1990, "Scaling behavior of $\text{YBa}_2\text{Cu}_3\text{O}_{7-\delta}$ thin-film weak links," *Appl. Phys. Lett.* **57**, 1155–1157.
- Rutter, N. A., B. A. Glowacki, and J. E. Evetts, 2000, "Percolation modeling for highly aligned polycrystalline superconducting tapes," *Supercond. Sci. Technol.* **13**, L25–L30.
- Salama, K., M. Mironova, S. Stolbov, and S. Sathyamurthy, 2000, "Grain boundaries in bulk YBCO," *Physica C* **341-348**, 1401–1405.
- Saleh, A. M., G. Schindler, C. Sarma, D. G. Haase, C. C. Koch, and A. I. Kingon, 1998, "Isolation techniques and electrical characterization of single grain boundaries of $\text{Bi}_2\text{Sr}_2\text{CaCu}_2\text{O}_8$ high-temperature superconductor," *Physica C* **285**, 225–234.
- Santiso, J., V. Laukhin, M. Doudkowski, G. Garcia, A. Figueras, L. A. Angurel, R. I. Merino, J. I. Pea, M. L. Sanjun, and V. M. Orera, 2000, "A new approach to obtain strip-structured biepitaxial $\text{YBa}_2\text{Cu}_3\text{O}_{7-\delta}$ films by using Ca-stabilized zirconia- CaZrO_3 eutectic substrates," *Adv. Mater.* **12**, 116–119.
- Sarnelli, E., 1993, "A two-channel model for transport across high- T_c bicrystal grain boundary junctions," *Interface Sci.* **1**, 287–290.

- Sarnelli, E., F. Carillo, G. Testa, F. Lombardi, F. M. Granozio, F. Ricci, U. Scotti di Uccio, and F. Tafuri, 2001, "Transport properties of [100] tilt and twist biepitaxial Y-Ba-Cu-O junctions," *IEEE Trans. Appl. Supercond.* **11**, 776–779.
- Sarnelli, E., P. Chaudhari, and J. Lacey, 1993, "Residual critical current in high T_c bicrystal grain boundary junctions," *Appl. Phys. Lett.* **62**, 777–779.
- Sarnelli, E., P. Chaudhari, W. Y. Lee, and E. Esposito, 1994, "Transport properties in TI-Ba-Ca-Cu-O grain boundary junctions on SrTiO₃ bicrystal substrates," *Appl. Phys. Lett.* **65**, 362–364.
- Sarnelli, E., and G. Testa, 2001, "Transport properties of high-temperature grain boundary Josephson junctions," *Physica C* (in press).
- Sarnelli, E., G. Testa, F. Carillo, and F. Tafuri, 1999, in *Proceedings of the Fourth European Conference on Applied Superconductivity EUCAS'99*, Sitges, Institute of Physics Conference Series No. 167, edited by X. Obrados, F. Sandiumenge, and J. Fontcuberta (IOP, Bristol, England), pp. 589–592.
- Sarnelli, E., G. Testa, and E. Esposito, 1993, "A two-channel model as a possible microscopic configuration of the 'barrier' in high- T_c grain boundary junctions," *J. Supercond.* **7**, 387–390.
- Satchell, J. S., J. A. Edwards, N. G. Chew, and R. G. Humphreys, 1992, "High temperature superconducting vortex flow transistor," *Electron. Lett.* **28**, 781–783.
- Satchell, J. S., R. G. Humphreys, J. A. Edwards, and N. G. Chew, 1993, "Arrays of high temperature superconductor Josephson junctions," *IEEE Trans. Appl. Supercond.* **3**, 2273–2276.
- Sawatzky, G., 2000, "The interplay between charge, spin, and orbital degrees of freedom in transitional metal oxides," presentation at 7th Workshop on Oxide Electronics, Les Diablerets, Switzerland.
- Schindler, G., B. Seebacher, R. Kleiner, P. Müller, and K. Andres, 1992, "Electrical characterisation of single grain boundaries in DyBa₂Cu₃O_{7- δ} ceramics," *Physica C* **196**, 1–6.
- Schlenga, K., R. McDermott, J. Clarke, R. E. de Souza, A. Wong-Foy, and A. Pines, 1999, "Low-field magnetic resonance imaging with a high- T_c dc superconducting quantum interference device," *Appl. Phys. Lett.* **75**, 3695–3697.
- Schlom, D. G., E. S. Hellman, E. H. Hartford, C. B. Eom, J. C. Clark, and J. Mannhart, 1996, "Origin of the $\phi \approx \pm 9^\circ$ peaks in YBa₂Cu₃O_{7- δ} films grown on cubic zirconia substrates," *J. Mater. Res.* **11**, 1336–1348.
- Schlom, D. G., and J. Mannhart, 2002, in *Encyclopedia of Materials: Science and Technology*, edited by K. H. J. Buschow, R. W. Cahn, M. C. Flemings, B. Ilshner, E. J. Kramer, and S. Mahajan (Elsevier Science, Amsterdam), pp. 3806–3820.
- Schmehl, A., B. Goetz, R. R. Schulz, C. W. Schneider, H. Bielefeldt, H. Hilgenkamp, and J. Mannhart, 1999, "Doping-induced enhancement of the critical currents of grain boundaries in YBa₂Cu₃O_{7- δ} ," *Europhys. Lett.* **47**, 110–115.
- Schmidl, F., S. Linzen, S. Wunderlich, and P. Seidel, 1998, "High- T_c direct current SQUIDs on silicon bicrystal substrates operating at 77 K," *Appl. Phys. Lett.* **72**, 602–604.
- Schneider, C. W., R. R. Schulz, B. Goetz, A. Schmehl, H. Bielefeldt, H. Hilgenkamp, and J. Mannhart, 1999, "Tailoring of high- T_c Josephson junctions by doping their electrodes," *Appl. Phys. Lett.* **75**, 850–852.
- Scholl, A., J. Stöhr, J. Lüning, J. W. Seo, J. Fompeyrine, H. Siegwart, J.-P. Locquet, F. Nolting, S. Anders, E. E. Fullerton, M. R. Scheinfein, and H. A. Padmore, 2000, "Observation of antiferromagnetic domains in epitaxial thin films," *Science* **287**, 1014–1016.
- Schoop, U., S. Kleefisch, S. Meyer, A. Marx, L. Alff, R. Gross, M. Naito, and H. Sato, 1999, "Nd_{1.85}Ce_{0.15}CuO_{4- y} bicrystal grain boundary Josephson junctions," *IEEE Trans. Appl. Supercond.* **9**, 3409–3412.
- Schulz, R. R., B. Chesca, B. Goetz, C. W. Schneider, A. Schmehl, H. Bielefeldt, H. Hilgenkamp, J. Mannhart, and C. C. Tsuei, 2000, "Design and realization of an all d-wave dc π -SQUID," *Appl. Phys. Lett.* **76**, 912–914.
- Schuster, Th., M. R. Koblishka, H. Kuhn, H. Kronmüller, G. Friedl, B. Roas, and L. Schultz, 1993, "Flux penetration into YBa₂Cu₃O _{x} thin films covering substrate step edges," *Appl. Phys. Lett.* **62**, 768–770.
- Selvam, P., E. W. Seibt, D. Kumar, R. Pinto, and P. R. Apte, 1997, "Enhanced J_c and improved grain-boundary properties in Ag-doped YBa₂Cu₃O_{7- δ} films," *Appl. Phys. Lett.* **71**, 137–139.
- Seo, J. W., B. Kabius, U. Dähne, A. Scholen, and K. Urban, 1995, "TEM investigation of grain boundaries in YBa₂Cu₃O₇ thin films grown on SrTiO₃ bicrystal substrates," *Physica C* **245**, 25–35.
- Shadrin, P. M., and Y. Y. Divin, 1998, "Submicrometer electrical imaging of grain boundaries in high- T_c thin film junctions by laser scanning microscopy," *Physica C* **297**, 69–74.
- Shadrin, P. M., Y. Y. Divin, S. Keil, J. Martin, and R. P. Huebener, 1999, "Comparative study of electron and laser beam scanning for local electrical characterization of high- T_c thin films and junctions," *IEEE Trans. Appl. Supercond.* **9**, 3925–3928.
- Shadrin, P., C. L. Jia, and Y. Divin, 2001, "Spread of critical currents in thin-film YBa₂Cu₃O_{7- x} bicrystal junctions and faceting of grain boundary," *Physica C* (in press).
- Shimakage, H., J. C. Booth, L. R. Vale, and R. H. Ono, 1999, in *ISEC '99, Extended Abstracts*, edited by J. Clarke (University of California, Berkeley), pp. 191–193.
- Sigrist, M., D. B. Bailey, and R. B. Laughlin, 1995, "Fractional vortices as evidence of time-reversal symmetry breaking in high-temperature superconductors," *Phys. Rev. Lett.* **74**, 3249–3252.
- Sigrist, M., and T. M. Rice, 1995, "Unusual paramagnetic phenomena in granular high-temperature superconductors—a consequence of d -wave pairing?" *Rev. Mod. Phys.* **67**, 503–513.
- Singh, A., N. Chandrasekhar, and A. H. King, 1990, "Coincidence orientations of crystals in tetragonal systems, with applications to YBa₂Cu₃O_{7- δ} ," *Acta Crystallogr., Sect. B: Struct. Sci.* **B46**, 117–125.
- Smith, D. A., M. F. Chisholm, and J. Clabes, 1988, "Special grain boundaries in YBa₂Cu₃O₇," *Appl. Phys. Lett.* **53**, 2344–2345.
- St. Louis-Weber, M., V. P. Dravid, V. R. Todt, X. F. Zhang, D. J. Miller, and U. Balachandran, 1996, "Transport properties of an engineered [001] tilt series in bulk YBa₂Cu₃O_{7- x} bicrystals," *Phys. Rev. B* **54**, 16 238–16 245.
- Steel, D. G., J. D. Hettinger, F. Yuan, D. J. Miller, K. E. Gray, J. H. Kang, and J. Talvacchio, 1996, "Electrical transport properties of [001] tilt bicrystal grain boundaries in YBa₂Cu₃O₇," *Appl. Phys. Lett.* **68**, 120–122.

- Steenbeck, K., T. Eick, K. Kirsch, K. O'Donnell, and E. Steinbeiß, 1997, "Influence of a 36.8 degrees grain boundary on the magnetoresistance of $\text{La}_{0.8}\text{Sr}_{0.2}\text{MnO}_{3-\delta}$ single crystal films," *Appl. Phys. Lett.* **71**, 968–970.
- Stepankin, V. N., E. A. Protasov, A. V. Kuznetsov, and S. V. Zaitsev-Zotov, 1985, "Josephson and single-particle tunneling in superconducting bicrystals $\text{BaPb}_{1-x}\text{Bi}_x\text{O}_3$," *JETP Lett.* **41**, 27–29.
- Stolbov, S. V., M. K. Mironova, and K. Salama, 2001, "Microscopic description of grain boundaries in superconducting copper oxides. II. Method to determine superconducting properties," unpublished.
- Strikovsky, M., G. Linker, S. Gapanov, L. Mazo, and O. Meyer, 1992, "Grain-misorientation control of the critical current in high- J_c epitaxial $\text{YBa}_2\text{Cu}_3\text{O}_7/\text{SrTiO}_3$ films," *Phys. Rev. B* **45**, 12 522–12 527.
- Stucki, F., P. Bruesch, and T. Baumann, 1988, "XPS study of the grain-boundary phase in $\text{YBa}_2\text{Cu}_3\text{O}_{7-\delta}$," *Physica C* **156**, 461–466.
- Sugimoto, A., T. Yamaguchi, and I. Iguchi, 2001, "Temperature dependence of the half flux quantum in $\text{YBa}_2\text{Cu}_3\text{O}_{7-\delta}$ tricrystal thin film by scanning SQUID microscopy," presented at the International Symposium Superconducting Device Physics Year 2001, June 2001, Tokyo.
- Suh, J. D., G. Y. Sung, and D. K. Kim, 1997, "Superconductivity and electric field effect of 90 degree grain boundaries in $\text{YBa}_2\text{Cu}_3\text{O}_{7-x}$ thin films," *IEEE Trans. Appl. Supercond.* **7**, 2184–2187.
- Sung, G. Y., J. D. Suh, K. Y. Kang, J. S. Hwang, S. G. Yoon, M. C. Lee, and S. G. Lee, 1999, "Characteristics of bi-crystal grain boundary junctions with different tilt angles for digital circuit applications," *IEEE Trans. Appl. Supercond.* **9**, 3921–3924.
- Sung, G. Y., J. D. Suh, and S. G. Lee, 1997, "Properties of doped-YBCO bicrystal grain-boundary junctions for Josephson field effect transistor," *Physica C* **282-287**, 2475–2476.
- Sutton, A. P., and R. W. Balluffi, 1995, *Interfaces in Crystalline Materials* (Oxford University Press, New York).
- Suzuki, K., Y. Honami, Y. Li, T. Utagawa, H. Tano, and K. Tanabe, 2000, in *Extended Abstracts of the International Workshop on Superconductivity* (ISTEC, Tokyo).
- Swartzendruber, L. J., A. Roitburd, D. L. Kaiser, F. W. Gayle, and L. H. Bennett, 1990, "Direct evidence for an effect of twin boundaries on flux pinning in single-crystal $\text{YBa}_2\text{Cu}_3\text{O}_{6+x}$," *Phys. Rev. Lett.* **64**, 483–486.
- Sydow, J. P., M. Berninger, R. A. Buhrman, and B. H. Moeckly, 1999a, "Effects of oxygen content on YBCO Josephson junction structures," *IEEE Trans. Appl. Supercond.* **9**, 2993–2996.
- Sydow, J. P., M. Berninger, R. A. Buhrman, and B. H. Moeckly, 1999b, in *ISEC'99, Extended Abstracts*, edited by J. Clarke (University of California, Berkeley), pp. 288–290.
- Tachiki, M., Y. Takano, and T. Hatano, 2002, "Critical current in cross-whiskers Josephson junctions and mechanism of cuprate superconductivity," *Physica C* **367**, 343–347.
- Tafuri, F., F. Carillo, F. Lombardi, F. Mileto Granozio, F. Ricci, U. Scotti di Uccio, A. Barone, G. Testa, E. Sarnelli, and J. R. Kirtley, 2000, "Feasibility of biepitaxial $\text{YBa}_2\text{Cu}_3\text{O}_{7-x}$ Josephson junctions for fundamental studies and potential circuit implementation," *Phys. Rev. B* **62**, 14 431–14 438.
- Tafuri, F., F. Mileto Granozio, F. Carillo, A. Di Chiara, K. Verbist, and G. Van Tendeloo, 1999, "Microstructure and Josephson phenomenology in 45 degrees tilt and twist $\text{YBa}_2\text{Cu}_3\text{O}_{7-\delta}$ artificial grain boundaries," *Phys. Rev. B* **59**, 11 523–11 531.
- Tafuri, F., B. Nadgorny, S. Shokhor, M. Gurvitch, F. Lombardi, F. Carillo, A. Di Chiara, and E. Sarnelli, 1998, "Barrier properties in $\text{YBa}_2\text{Cu}_3\text{O}_{7-x}$ grain-boundary Josephson junctions using electron-beam irradiation," *Phys. Rev. B* **57**, 14 076–14 079.
- Tafuri, F., S. Shokhor, B. Nadgoorny, M. Gurvitch, F. Lombardi, and A. Di Chiara, 1997, "Electron beam irradiation of $\text{Y}_1\text{Ba}_2\text{Cu}_3\text{O}_{7-x}$ grain boundary Josephson junctions," *Appl. Phys. Lett.* **71**, 125–127.
- Takagi, T., J. G. Wen, T. Machi, K. Hashimoto, Y. Takahashi, T. Morishita, I. Hirabayashi, and N. Koshizuka, 1999, "Inter-grain critical current density of Y123 bicrystal films grown by LPE method," *IEEE Trans. Appl. Supercond.* **9**, 2328–2331.
- Takami, T., K. Kuroda, M. Kataoka, Y. Wada, K. Terada, J. Tanimura, K. Kojima, and M. Nunoshita, 1994, "Hysteretic Josephson-junction behavior of $\text{Ba}_{1-x}\text{K}_x\text{BiO}_3$ grain boundary junctions using SrTiO_3 bicrystal substrates," *Jpn. J. Appl. Phys., Part 2* **33**, L1004–L1006.
- Takami, T., K. Kuroda, K. Kojima, M. Kataoka, J. Tanimura, O. Wada, and T. Ogama, 1993, "45-Degrees grain-boundary junctions in (001)-oriented BiSrCaCuO films," *Jpn. J. Appl. Phys., Part 2* **32**, L583–L585.
- Takami, T., K. Kuroda, J. Tanimura, K. Kojima, M. Nunoshita, and M. Hirota, 1996, "DC superconducting quantum interference devices with BiSrCaCuO bicrystal grain boundary junctions at 77 K," *Jpn. J. Appl. Phys., Part 2* **35**, L391–L392.
- Tallon, J. L., G. V. M. Williams, and J. W. Loram, 2000, "Factors affecting the optimal design of high- T_c superconductors—the pseudogap and critical currents," *Physica C* **338**, 9–17.
- Tanabe, K., F. H. Teherani, S. Kubo, H. Asano, and M. Suzuki, 1994, "Effects of photoinduced hole doping on transport properties of $\text{YBa}_2\text{Cu}_3\text{O}_y$ grain boundary junctions," *J. Appl. Phys.* **76**, 3679–3683.
- Tanaka, S., H. Itozaki, H. Toyoda, N. Harada, A. Adachi, K. Okajima, and H. Kado, 1994, "Four-channel $\text{YBa}_2\text{Cu}_3\text{O}_{7-y}$ dc SQUID magnetometer for biomagnetic measurements," *Appl. Phys. Lett.* **64**, 514–516.
- Tanaka, S., H. Kado, T. Matura, and H. Itozaki, 1993, "Step-edge junction of YBCO thin films on MgO substrates," *IEEE Trans. Appl. Supercond.* **3**, 2365–2368.
- Tanaka, Y., and S. Kashiwaya, 1995, "Theory of tunneling spectroscopy of d-wave superconductors," *Phys. Rev. Lett.* **74**, 3451–3454.
- Tanaka, Y., and S. Kashiwaya, 1996, "Theory of the Josephson effect in d-wave superconductors," *Phys. Rev. B* **53**, 11 957–11 960.
- Tang, H. X., Z. D. Wang, and J. X. Zhu, 1996, "Supercurrent and quasiparticle interference between two d-wave superconductors coupled by a normal metal or insulator," *Phys. Rev. B* **54**, 12 509–12 516.
- Tanimura, J., T. Takami, K. Kuroda, O. Wada, M. Kataoka, K. Kojima, and T. Ogama, 1993, "Microscopic study of an artificial grain boundary Josephson junction in a BiSrCaCuO thin film formed on a SrTiO_3 (110) substrate using a MgO buffer layer," *Jpn. J. Appl. Phys., Part 2* **32**, L51–L53.
- Tarasov, M., E. Stepantsov, D. Golubev, Z. Ivanov, T. Claeson, O. Harnack, M. Darula, S. Beuven, and H. Kohlstedt, 1999,

- “Submillimeter-wave mixing and noise in HTS Josephson junctions,” *IEEE Trans. Appl. Supercond.* **9**, 3761–3764.
- Tarte, E. J., P. F. McBrien, J. T. H. Ransley, R. H. Hadfield, E. Inglessi, W. Booij, G. Burnell, M. Blamire, and J. E. Evetts, 2001, “Capacitance as a probe of high angle grain boundary transport in oxide superconductors,” preprint.
- Tarte, E. J., G. A. Wagner, R. E. Somekh, F. J. Baudenbacher, P. Berghuis, and J. E. Evetts, 1997, “The capacitance of bicrystal Josephson junctions deposited on SrTiO₃ substrates,” *IEEE Trans. Appl. Supercond.* **7**, 3662–3665.
- Tavares, P. A. C., E. J. Romans, and C. M. Pegrum, 1999, “High current gain HTS Josephson vortex flow transistors,” *IEEE Trans. Appl. Supercond.* **9**, 3941–3944.
- Taylor, W. E., N. H. Odell, and H. Y. Fan, 1952, “Grain boundary barriers in germanium,” *Phys. Rev.* **88**, 867–875.
- Terpstra, D., R. P. J. Ijsselstein, and H. Rogalla, 1995, “Subharmonic Shapiro steps in high- T_c Josephson junctions,” *Appl. Phys. Lett.* **66**, 2286–2288.
- Terzioglu, E., and M. R. Beasley, 1998, “Complementary Josephson junction devices and circuits: a possible new approach to superconducting electronics,” *IEEE Trans. Appl. Supercond.* **8**, 48–53.
- Testa, G., E. Sarnelli, F. Carillo, and F. Tafuri, 1999, “a-axis tilt grain boundaries for YBa₂Cu₃O_{7-x} superconducting quantum interference devices,” *Appl. Phys. Lett.* **75**, 3542–3544.
- Thiele, K., Ch. Jooss, J. Hoffmann, L.-O. Kautschor, J. Dzick, and H. C. Freyhardt, 2001, “Grain boundaries in YBa₂Cu₃O_{7-δ} films grown on bicrystalline Ni substrates,” *Physica C* **355**, 203–210.
- Tietz, L. A., and C. B. Carter, 1991, “Special grain boundaries in YBa₂Cu₃O_{7-x} thin films,” *Physica C* **182**, 241–251.
- Tinkham, M., 1989, in *Proceedings of the ISTEK Workshop on Critical Currents in High- T_c Superconductors* (ISTEK, Tokyo).
- Todd, N. K., N. D. Mathur, S. P. Isaac, J. E. Evetts, and M. G. Blamire, 1999, “Current-voltage characteristics and electrical transport properties of grain boundaries in La_{1-x}(Sr/Ca)_xMnO₃,” *J. Appl. Phys.* **85**, 7263–7266.
- Todt, V. R., X. F. Zhang, D. J. Miller, M. St Louis-Weber, and V. P. Dravid, 1996, “Controlled growth of bulk bicrystals and the investigation of microstructure-property relations of YBa₂Cu₃O_x grain boundaries,” *Appl. Phys. Lett.* **69**, 3746–3748.
- Tomita, N., Y. Takahashi, and Y. Ishida, 1990, “Preparation of bicrystal in a Bi-Sr-Ca-Cu-O superconductor,” *Jpn. J. Appl. Phys.*, Part 2 **29**, L30–L32.
- Tönies, S., H. W. Weber, Y. C. Guo, S. X. Dou, R. Sawh, and R. Weinstein, 2001, “On the current transport limitations in Bi-based high temperature superconducting tapes,” *Appl. Phys. Lett.* **78**, 3851–3853.
- Træholt, C., J. G. Wen, H. W. Zandbergen, Y. Shen, and J. W. M. Hilgenkamp, 1994, “TEM investigation of YBa₂Cu₃O₇ thin films on SrTiO₃ bicrystals,” *Physica C* **230**, 425–434.
- Tsai, J. W. H., S.-W. Chan, J. R. Kirtley, S. C. Tidrow, and Q. Jiang, 2001, “The variation of J_{cgb} with GB misorientation and inclination measured using the scanning SQUID microscope,” *IEEE Trans. Appl. Supercond.* **11**, 3880–3883.
- Tsai, S. H., J. R. Chiou, C. C. Chi, and M. K. Wu, 1998, “A new method of growing YBa₂Cu₃O_y 45 degrees bi-epitaxial thin films on MgO substrates,” *Chin. J. Phys. (Taipei)* **36**, 355–359.
- Tsu, I. F., J. L. Wang, D. L. Kaiser, and S. E. Babcock, 1998, “A comparison of grain boundary topography and dislocation network structure in bulk-scale [001] tilt bicrystals of Bi₂Sr₂CaCu₂O_{8+x} and YBa₂Cu₃O_{7-δ},” *Physica C* **306**, 163–187.
- Tsuei, C. C., and J. R. Kirtley, 2000, “Pairing symmetry in cuprate superconductors,” *Rev. Mod. Phys.* **72**, 969–1016.
- Tsuei, C. C., J. R. Kirtley, C. C. Chi, L. S. Yu-Jahnes, A. Gupta, T. Shaw, J. Z. Sun, and M. B. Ketchen, 1994, “Pairing symmetry and flux quantization in a tricrystal superconducting ring of YBa₂Cu₃O_{7-δ},” *Phys. Rev. Lett.* **73**, 593–596.
- Tsuei, C. C., J. R. Kirtley, Z. F. Ren, J. H. Wang, H. Raffy, and Z. Z. Li, 1997, “Pure $d_{x^2-y^2}$ order-parameter symmetry in the tetragonal superconductor Tl₂Ba₂CuO_{6+δ},” *Nature (London)* **387**, 481–483.
- Tsuei, C. C., J. R. Kirtley, M. Rupp, J. Z. Sun, A. Gupta, M. B. Ketchen, C. A. Wang, Z. F. Ren, J. H. Wang, and M. Bhusan, 1996, “Pairing symmetry in single-layer Tl₂Ba₂CuO_{6+δ} superconductors,” *Science* **271**, 329–332.
- Tsuei, C. C., J. Mannhart, and D. Dimos, 1989, in *Proceedings of the Topical Conference on High- T_c Superconducting Films, Devices and Applications*, Atlanta, 1989, edited by G. Marariondo, R. Joint, and M. Onellion, pp. 194–207.
- Tsukamoto, A., K. Takagi, Y. Moriwaki, T. Sugano, S. Adachi, and K. Tanabe, 1998, “High-performance (Hg,Re)Ba₂CaCu₂O_y grain-boundary Josephson junctions and dc superconducting quantum interference devices,” *Appl. Phys. Lett.* **73**, 990–992.
- Tuohimaa, A. H., and J. A. J. Paasi, 1999, “Magnetic flux pinning in high- T_c grain boundary junctions in low magnetic fields,” *Physica C* **319**, 73–78.
- Tuohimaa, A., J. Paasi, and T. Di Matteo, 1999, in *Proceedings of the 4th European Conference on Applied Superconductivity*, Sitges, edited by X. Obrados, F. Sandiumenge, and J. Fontcuberta, Institute of Physics Conference Series No. 167 (IOP, Bristol, England), pp. 771–774.
- Turchinskaya, M., D. L. Kaiser, F. W. Gayle, A. J. Shapiro, A. Roytburd, L. A. Dorosinskii, V. I. Nikitenko, A. A. Polyanskii, and V. K. Vlasko-Vlasov, 1994, “Real-time observation of the effect of grain boundaries on magnetization of YBa₂Cu₃O_{7-δ} polycrystals,” *Physica C* **221**, 62–70.
- Usoskin, A., F. Garcia-Moreno, J. Knoke, S. Sievers, J. Dzick, and H. C. Freyhardt, 2000, in *Proceedings of the 4th European Conference on Applied Superconductivity*, Sitges, edited by X. Obrados, F. Sandiumenge, and J. Fontcuberta, Institute of Physics Conference Series No. 167 (IOP, Bristol, England), pp. 447–450.
- Van Harlingen, D. J., 1995, “Phase-sensitive tests of the symmetry of the pairing state in the high-temperature superconductors—evidence for $d_{x^2-y^2}$ symmetry,” *Rev. Mod. Phys.* **67**, 515–535.
- Vargas, J. L., Na Zhang, D. L. Kaiser, and S. E. Babcock, 1997, “Systematic copper concentration variations along grain boundaries in bulk-scale YBa₂Cu₃O_{7-δ} bicrystals,” *Physica C* **292**, 1–16.
- Vase, P., R. Flükiger, M. Leghissa, and B. Glowacki, 2000, “Current status of high- T_c wire,” *Supercond. Sci. Technol.* **13**, R71–R84.
- Vengrus, I. I., A. M. Balbashov, A. V. Mozhaev, E. K. Kov’ev, S. I. Krasnosvobodtsev, M. Y. Kupriyanov, S. N. Polyakov, I. Y. Pavloskii, and O. V. Snigirev, 1997, in *ISEC’97, Extended Abstracts*, edited by H. Koch and S. Knappe (Physikalische Technische Bundesanstalt, Braunschweig, Germany), pp. 46–48.

- Verbist, K., O. I. Lebedev, G. Van Tendeloo, F. Tafuri, F. Miletto Granozio, A. Di Chiara, and H. Bender, 1999, "A potential method to correlate electrical properties and microstructure of a unique high- T_c superconducting Josephson junction," *Appl. Phys. Lett.* **74**, 1024–1026.
- Verebelyi, D. T., D. K. Christen, R. Feenstra, C. Cantoni, A. Goyal, D. F. Lee, M. Paranthaman, P. N. Arendt, R. F. DePaula, J. R. Groves, and C. Prouteau, 2000, "Low angle grain boundary transport in $\text{YBa}_2\text{Cu}_3\text{O}_{7-\delta}$ coated conductors," *Appl. Phys. Lett.* **76**, 1755–1757.
- Verebelyi, D. T., C. Prouteau, R. Feenstra, and D. K. Christen, 1999, "Critical current of YBCO grain boundaries in large magnetic fields," *IEEE Trans. Appl. Supercond.* **9**, 2655–2658.
- Vlasko-Vlasov, V. K., L. A. Dorosinskii, A. A. Polyanskii, V. I. Nikitenko, U. Welp, B. W. Veal, and G. W. Crabtree, 1994, "Study of the influence of individual twin boundaries on the magnetic flux penetration in $\text{YBa}_2\text{Cu}_3\text{O}_{7-\delta}$," *Phys. Rev. Lett.* **72**, 3246–3249.
- Vollmann, M., R. Hagenbeck, and R. Waser, 1997, "Grain-boundary defect chemistry of acceptor-doped titanates: Inversion layer and low-field conduction," *J. Am. Ceram. Soc.* **80**, 2301–2314.
- Vollnhals, G., H. Kinder, H. Schmidt, W. Wersing, B. Daalman, and M. Seitz, 1994, "A system of epitaxial buffer layers on (100) SrTiO_3 substrates for the preparation of bi-epitaxial grain-boundaries in $\text{YBa}_2\text{Cu}_3\text{O}_x$ for magnetometers," *Supercond. Sci. Technol.* **7**, 364–366.
- Vuchic, B. V., K. L. Merkle, P. M. Baldo, K. A. Dean, D. B. Buchholz, R. P. H. Chang, H. Zhang, and L. D. Marks, 1996, "The formation, transport properties and microstructure of 45° [001] grain boundaries induced by epitaxy modification in $\text{YBa}_2\text{Cu}_3\text{O}_{7-x}$ thin films," *Physica C* **270**, 75–90.
- Vuchic, B. V., K. L. Merkle, K. A. Dean, D. B. Buchholz, R. P. H. Chang, and L. D. Marks, 1995, "Sputter-induced grain boundary junctions in $\text{YBa}_2\text{Cu}_3\text{O}_{7-x}$ thin films on MgO ," *J. Appl. Phys.* **77**, 2591–2594.
- Wakao, K., T. Ohta, H. Terai, M. Inoue, A. Fujimaki, and H. Hayakawa, 1995, in *ISEC '95 Extended Abstracts* (Nagoya University, Nagoya, Japan), pp. 126–128.
- Walker, M. B., 1996, "Mechanism for magnetic-flux generation in grain boundaries of in phase-sensitive tetracystal pairing-symmetry measurements and broken time-reversal symmetry states of $\text{YBa}_2\text{Cu}_3\text{O}_{7-x}$," *Phys. Rev. B* **54**, 13 269–13 274.
- Walker, M. B., 2000, "Phase-sensitive tetracystal pairing-symmetry measurements and broken time-reversal symmetry states of high- T_c superconductors," *Phys. Rev. B* **62**, 11 854–11 858.
- Walker, M. B., and J. Luettmmer-Strathmann, 1996, "Josephson tunneling in high- T_c superconductors," *Phys. Rev. B* **54**, 588–601.
- Wang, J.-L., X. Y. Cai, R. J. Kelley, M. D. Vaudin, S. E. Babcock, and D. C. Larbalestier, 1994, "Electromagnetic coupling character of [001] twist boundaries in sintered $\text{Bi}_2\text{Sr}_2\text{CaCu}_2\text{O}_{8+x}$ bicrystals," *Physica C* **230**, 189–198.
- Wang, J. L., I. F. Tsu, X. Y. Cai, R. J. Kelly, M. D. Vaudin, S. E. Babcock, and D. C. Larbalestier, 1996, "Electromagnetic and microstructural investigations of a naturally grown [001] tilt bicrystal of $\text{Bi}_2\text{Sr}_2\text{CaCu}_2\text{O}_{8+x}$," *J. Mater. Res.* **11**, 868–877.
- Wang, Z. L., J. Brynestad, D. M. Kroeger, Y. R. Sun, J. R. Thompson, and R. K. Williams, 1993, "Grain-boundary chemistry and weak-link behavior of polycrystalline $\text{YBa}_2\text{Cu}_4\text{O}_8$," *Phys. Rev. B* **48**, 9726–9734.
- Weaver, B. D., and E. M. Jackson, 1996, "Temperature dependence of critical current and normal-state resistance in bicrystal $\text{Tl}_2\text{Ba}_2\text{CaCu}_2\text{O}_y$ Josephson junctions," *Physica C* **266**, 210–214.
- Wen, J. G., T. Takagi, and N. Koshizuka, 2000, "Microstructural studies of YBCO film bicrystals with large single facet grain boundaries grown by liquid phase epitaxy," *Supercond. Sci. Technol.* **13**, 820–826.
- Wen, J. G., T. Usagawa, T. Takagi, Y. Ishimaru, Y. Enomoto, and N. Koshizuka, 1999, "Microstructural studies of high- T_c superconducting Josephson junctions to understand junction properties," *IEEE Trans. Appl. Supercond.* **9**, 2046–2049.
- Wen, Z., and H. Abe, 1996, " $\text{YBa}_2\text{Cu}_3\text{O}_{7-\delta}/\text{Ag}$ bi-epitaxial grain boundary junctions for flux-flow devices," *Supercond. Sci. Technol.* **9**, A76–A78.
- Werner, J., 1985, in *Polycrystalline Semiconductors*, edited by G. Harbeke (Springer Verlag, Berlin), pp. 76–94.
- Westerburg, W., G. Jakob, F. Martin, S. Friedrich, M. Maier, and H. Adrian, 1999, "Current dependence of grain boundary magnetoresistance in $\text{La}_{0.67}\text{Ca}_{0.33}\text{MnO}_3$ films," *J. Appl. Phys.* **86**, 2173–2177.
- Willis, J. O., P. N. Arendt, S. R. Foltyn, Q. X. Jia, J. R. Groves, R. F. DePaula, P. C. Dowden, E. J. Peterson, T. G. Holesinger, J. Y. Coulter, M. Ma, M. P. Maley, and D. E. Peterson, 2000, "Advances in YBCO-coated conductor technology," *Physica C* **335**, 73–77.
- Windt, M., H. Haensel, D. Koelle, and R. Gross, 1999, "On the nature of the electric-field effect on $\text{YBa}_2\text{Cu}_3\text{O}_{7-\delta}$ grain boundary junctions employing epitaxial SrTiO_3 gate insulators," *Appl. Phys. Lett.* **74**, 1027–1029.
- Winkler, D., Y. M. Zhang, P. Å. Nilsson, E. A. Stepanov, and T. Claeson, 1994, "Electromagnetic properties at the grain boundary interface of a $\text{YBa}_2\text{Cu}_3\text{O}_{7-\delta}$ bicrystal Josephson junction," *Phys. Rev. Lett.* **72**, 1260–1263.
- Woods, S. I., A. S. Katz, T. L. Kirk, M. C. de Andrade, M. B. Maple, and R. C. Dynes, 1999, "Investigation of Nd-Ce-Cu-O planar tunnel junctions and bicrystal grain boundary junctions," *IEEE Trans. Appl. Supercond.* **9**, 3917–3920.
- Wosik, J., L.-M. Xie, M. F. Davis, N. Tralshawala, P. Gierlowski, and J. H. Miller, 1995, "Microwave characterization of bicrystal grain boundary Josephson junctions," *Proc. SPIE* **2559**, 76.
- Wu, M. K., J. R. Ashburn, C. J. Torng, P. H. Hor, R. L. Meng, L. Gao, Z. J. Huang, Y. Q. Wang, and C. W. Chu, 1987, "Superconductivity at 93 K in a new mixed-phase Y-Ba-Cu-O compound system at ambient pressure," *Phys. Rev. Lett.* **58**, 908–912.
- Wu, X. D., S. R. Foltyn, P. N. Arendt, W. R. Blumenthal, I. H. Campbell, J. D. Cotton, J. Y. Coulter, W. L. Hulst, M. P. Maley, H. F. Safar, and J. L. Smith, 1995, "Properties of $\text{YBa}_2\text{Cu}_3\text{O}_{7-\delta}$ -thick films on flexible buffered metallic substrates," *Appl. Phys. Lett.* **67**, 2397–2399.
- Wu, X. D., S. R. Foltyn, P. N. Arendt, J. Townsend, C. Adams, I. H. Campbell, P. Tiwari, Y. Coulter, and D. E. Peterson, 1994, "High current $\text{YBa}_2\text{Cu}_3\text{O}_{7-\delta}$ -thick films on flexible nickel substrates with textured buffer layers," *Appl. Phys. Lett.* **65**, 1961–1963.
- Wu, X. D., L. Luo, R. E. Muenchausen, K. N. Springer, and S. Foltyn, 1992, "Creation of 45 grain-boundary junctions by lattice engineering," *Appl. Phys. Lett.* **60**, 1381–1383.

- Xie, Y. Y., T. Aytug, J. Z. Wu, D. Verebelyi, M. Paranthaman, A. Goyal, and D. K. Christen, 2000, "Epitaxy of $\text{HgBa}_2\text{CaCu}_2\text{O}_6$ superconducting films on biaxially textured Ni substrates," *Appl. Phys. Lett.* **77**, 4193–4195.
- Xin, H., D. E. Oates, S. Sridhar, G. Dresselhaus, and M. S. Dresselhaus, 2000, "Observation of individual Josephson vortices in $\text{YBa}_2\text{Cu}_3\text{O}_{7-\delta}$ bicrystal grain-boundary junctions," *Phys. Rev. B* **61**, 14 952–14 955.
- Yamamoto, T., S. Suzuki, K. Takahashi, Y. Yoshisato, and S. Maekawa, 1995, "Superconductor-insulator-superconductor quasiparticle tunneling current in $\text{Ba}_{1-x}\text{K}_x\text{BiO}_3$ grain-boundary junctions on SrTiO_3 bicrystal substrates," *Appl. Phys. Lett.* **66**, 1000–1002.
- Yan, X. Z., and C. R. Hu, 1999, "Magnetic-field effect in Josephson tunneling between d-wave superconductors," *Phys. Rev. Lett.* **83**, 1656–1659.
- Yan, Y., W. Lo, J. E. Evetts, A. M. Campbell, and W. M. Stobbs, 1995, "Lower T_c barriers at high angle boundaries in the $(\text{BiPb})_2\text{Sr}_2\text{Ca}_2\text{Cu}_3\text{O}_x$ system," *Appl. Phys. Lett.* **67**, 2554–2557.
- Yang, I. S., B. Y. Chang, and G. Y. Sung, 1999, "Raman Study of the 90° grain boundaries in $\text{YBa}_2\text{Cu}_3\text{O}_{7-\delta}$ thin films," *Physica C* **311**, 75–80.
- Yi, H. R., M. Gustafsson, D. Winkler, E. Olsson, and T. Claesson, 1996, "Electromagnetic and microstructural characterization of $\text{YBa}_2\text{Cu}_3\text{O}_7$ step edge junctions on (001) LaAlO_3 substrates," *J. Appl. Phys.* **79**, 9213–9220.
- Yi, H. R., Z. G. Ivanov, D. Winkler, Y. M. Zhang, H. Olin, P. Larsson, and T. Claesson, 1994, "Improved step edges on LaAlO_3 substrates by using amorphous carbon etch masks," *Appl. Phys. Lett.* **65**, 1177–1179.
- Yi, H. R., D. Winkler, and T. Claesson, 1995, "Junction parameters of $\text{YBa}_2\text{Cu}_3\text{O}_7$ step edge junctions on LaAlO_3 substrates from Fiske resonances," *Appl. Phys. Lett.* **66**, 1677–1679.
- Yoshida, Y., T. Takami, K. Kuroda, and T. Ozeki, 1997, in *ISEC'97, Extended Abstracts*, edited by H. Koch and S. Knappe (Physikalische Technische Bundesanstalt, Braunschweig, Germany), pp. 10–12.
- Youn, D., and J. H. Kim, 1995, "Low-angle biepitaxial Josephson-junction fabricated on obliquely cut SrTiO_3 substrate," *Physica C* **251**, 399–404.
- Yu, D. P., X. D. Hu, Y. Z. Wang, Y. D. Dai, S. G. Wang, L. P. You, Z. Q. Liu, and Z. Zhang, 1997, "TEM study of microstructure of $\text{YBa}_2\text{Cu}_3\text{O}_y$ bicrystal grain boundary junctions on Y_2O_3 stabilized ZrO_2 bicrystal," *Physica C* **282-287**, 2473–2474.
- Yu, H.-W., M.-J. Chen, H. C. Yang, S. Y. Yang, and H. E. Horng, 2000, "Effect of the grooved SrTiO_3 bicrystal line on the $\text{YBa}_2\text{Cu}_3\text{O}_7$ grain boundary," *Physica C* **333**, 163–169.
- Yu, Y., S. L. Yan, L. Fang, Y. Y. Xie, J. Z. Wu, S. Y. Han, H. Shimakage, and Z. Wang, 1999, "Fabrication of $\text{HgBa}_2\text{CaCu}_2\text{O}_y$ grain boundary junctions with cation exchange method," *Supercond. Sci. Technol.* **12**, 1020–1022.
- Zakharov, N. D., D. Hesse, H. Frank, R. Stollmann, and G. Güntherodt, 1998, "HRTEM study on the structure of boundaries between grains of different phases in BSCCO-type ceramics," *Phys. Status Solidi A* **168**, 381–388.
- Zandbergen, H. W., R. Gronsky, and G. Thomas, 1988, "High resolution electron microscopy study of grain boundaries in sintered $\text{YBa}_2\text{Cu}_3\text{O}_{7-\delta}$," *Physica C* **153-155**, 1002–1003.
- Zandbergen, H. W., and G. Thomas, 1988, "Grain-boundaries in sintered $\text{YBa}_2\text{Cu}_3\text{O}_{7-\delta}$," *Acta Crystallogr., Sect. A: Found. Crystallogr.* **A44**, 772–775.
- Zhang, X. F., D. J. Miller, and J. Talvacchio, 1996, "Control of meandering grain boundary configurations in $\text{YBa}_2\text{Cu}_3\text{O}_y$ bicrystal thin films based on deposition rate," *J. Mater. Res.* **11**, 2440–2449.
- Zhang, Y. M., E. Carlsson, D. Winkler, G. Brorsson, H. Zirath, and E. Wikborg, 1995, "RF characterization of Josephson flux-flow transistors: design, modeling and on-wafer measurement," *IEEE Trans. Appl. Supercond.* **5**, 3385–3388.
- Zhang, Y. M., N. Dubash, U. Goshal, and K. Char, 1997, "High- T_c superconductor oversampled delta modulator for analog-to-digital converters," *IEEE Trans. Appl. Supercond.* **7**, 2292–2295.
- Zhang, Y., H. M. Mück, K. Herrmann, J. Schubert, W. Zander, A. I. Braginski, and C. Heiden, 1992, "Low-noise $\text{YBa}_2\text{Cu}_3\text{O}_7$ rf SQUID magnetometer," *Appl. Phys. Lett.* **60**, 645–647.
- Zhang, Y. M., D. Winkler, P. Å. Nilsson, and T. Claesson, 1994, "Flux-flow transistors based on long $\text{YBa}_2\text{Cu}_3\text{O}_{7-\delta}$ bicrystal grain boundary junctions," *Appl. Phys. Lett.* **64**, 1153–1155.
- Zhang, Y. M., D. Winkler, P. Å. Nilsson, and T. Claesson, 1996, "Josephson flux-flow resonances in overdamped long $\text{YBa}_2\text{Cu}_3\text{O}_7$ grain-boundary junctions," *Phys. Rev. B* **51**, 8684–8687.
- Zhu, J.-X., and C. S. Ting, 1999, "Spontaneous flux in a d-wave superconductor with time-reversal-symmetry-broken pairing state at $\{110\}$ -oriented boundaries," *Phys. Rev. B* **60**, R3739–R3742.
- Zhu, Y., Q. Li, Y. N. Tsay, M. Suenaga, G. D. Gu, and N. Koshizuka, 1998, "Structural origin of misorientation-independent superconducting behavior at $[001]$ twist boundaries in $\text{Bi}_2\text{Sr}_2\text{Ca}_1\text{Cu}_2\text{O}_{8+\delta}$," *Phys. Rev. B* **57**, 8601–8607.
- Zhu, Y., and M. Suenaga, 1995, "Nano-scale electron energy-loss spectroscopy of the oxygen K edge in $\text{Bi}_2\text{Sr}_2\text{Ca}_1\text{Cu}_2\text{O}_{8+\delta}$," *Physica C* **252**, 117–124.
- Zhu, Y., J. M. Zuo, A. R. Moodenbaugh, and M. Suenaga, 1994, "Grain-boundary constraint and oxygen deficiency in $\text{YBa}_2\text{Cu}_3\text{O}_{7-\delta}$: application of the coincidence site lattice model to a non-cubic system," *Philos. Mag. A* **70**, 969–984.